



UNIVERSITEIT VAN PRETORIA
UNIVERSITY OF PRETORIA
YUNIBESITHI YA PRETORIA

Chemical characterization and development of anti-aging ingredients from *Sclerocarya birrea* and *Ficus sycomorus*

By

Tinotenda Shoko

Submitted in partial fulfilment of the requirements of the degree

Philosophiae Doctor Chemistry

In the Faculty of Natural and Agricultural Sciences
Department of Chemistry
University of Pretoria
Pretoria
South Africa

February 2018

Submission declaration

I, Tinotenda Shoko, declare that the thesis, which I hereby submit for the degree of *Philosophiae Doctor* in the Department of Chemistry, at the University of Pretoria, is my own work and has not previously been submitted by me for a degree at this or any other tertiary institution.

Signature: ... 

Date:.....16 February 2018.....

Plagiarism declaration

Full names of student: Tinotenda Shoko Student number: 11058642

Title of work: Chemical characterization and development of anti-aging ingredients from *Sclerocarya birrea* and *Ficus sycomorus*

Declaration

1. I understand what plagiarism is and I am aware of the University's policy in this regard.
2. I declare that this thesis is my own original work. Where other people's work has been used (either from a printed source, internet or any other source), due acknowledgement was given and reference was made according to departmental requirements.
3. I did not make use of another student's previous work and submit it as my own.
4. I did not allow and will not allow anyone to copy my work with the intention of presenting it as his or her own work.

Signature:



Date: 16 February 2018

Acknowledgements

I acknowledge with gratitude the guidance and support from my supervisors Professor V. J. Maharaj (Main supervisor), Dr D. Naidoo (co-supervisor) and Professor Z. Apostolides (co-supervisor). I appreciate their significant scientific contributions, ideas, patience and wisdom which have made this work a success.

I want to thank the Council for Scientific and Industrial Research (CSIR) for the collaboration which helped us to access their valuable instruments and expertise. Special thanks to Rudzani Nthambeleni, Eric Khorombi, Gugulethu Ndlovu, the formulation team under Phatheka Mbambiso for the opportunity to benefit from their skills and knowledge and Dr Malefa Tselanyane for bioassays. I want to thank members of the Chemistry Department at the University of Pretoria, special thanks to Felix Katele-Zongwe, Severin Muyisa and Dr Mamoalosi Selepe for help with structure elucidation and the rest of the Bioprospecting group under Prof Maharaj for the valuable scientific discussions. I am grateful for help given by Mr Jason Sampson the curator at the University of Pretoria in collecting plant samples from the University of Pretoria botanic gardens. Thanks to Dr Mamoalosi Selepe and Madelien Wooding for running samples on the UPLC-Q-TOF-MS.

This work would not have been successful without funding from the Carnegie Regional Initiative for Science Education (Carnegie-RISE) through the Southern Africa Biochemistry and Informatics Network (SABINA). In addition, we acknowledge the Department of Science and Technology (South Africa) for funding the project under which this work was done at the CSIR.

I am grateful for emotional support, love and encouragement from my wife Placidia, my sister Tinomuda and my daughter Tumelo. Above all I want to thank God for the opportunity to pursue my PhD studies and the strength to bring this work to completion.

Summary

Degradation of elastin and collagen in the extracellular matrix by elastase and collagenase accelerates skin aging. Phytochemicals that inhibit these enzymes can be developed as anti-aging ingredients. The anti-aging properties of *Sclerocarya birrea* (A. Rich.) Hochst (Marula) and *Ficus sycomorus* Linn (Sycamore) were investigated with the aim of developing chemically characterized anti-aging ingredients. The two plants were selected from the CSIR repository of extracts linked to traditional cosmetic use, extracts which had not been previously reported to have scientific data linked to anti-aging activity were selected. Young Marula soft wood stems, leaves and fruits collected from Kwazulu Natal and leaves of the Sycamore tree collected from Sodwana Nature Reserve were extracted using methanol:dichloromethane (DCM) (1:1). Results from the anti-collagenase and anti-elastase assays showed that Marula stems and leaves of the Sycamore were the most active. Extracts of the stems of Marula and leaves of the Sycamore tree have for the first time been scientifically proven to exhibit anti-elastase and anti-collagenase activities.

Marula stems and Sycamore leaves harvested from the University of Pretoria experimental farm were extracted using acetone, ethanol, methanol:DCM (1:1) and sequentially using hexane, DCM, ethyl acetate and methanol and were screened in the anti-elastase and anti-collagenase assays. The results revealed that the ethanolic extract of both plants was the most appropriate for further research and development. The chemical profile of crude ethanol extracts of Marula stems and Sycamore leaves were determined using UPLC-Q-TOF-MS with MassLynx software. Eleven compounds have been tentatively identified in the ethanol extract of Marula stems of which four; quinic acid, catechin, epigallocatechin gallate (EGCg) and epicatechin gallate (ECg) have been confirmed using pure standards. Eight compounds were tentatively identified in the ethanol extract of leaves of the Sycamore tree of which five; palatinose, quinic acid, chlorogenic acid, rutin and isoquercetin have been confirmed using pure standards and four; vicianin-2, biflorin and isobiflorin have been confirmed through isolation, purification and structure elucidation using NMR. Palatinose, quinic acid, isobiflorin, chlorogenic acid, biflorin, vicianin-2 and quercetin-3-glucuronide have been identified for the first time in leaves of the Sycamore tree. Chemical profiles of ethanol extracts of Marula stems and leaves of the Sycamore tree were developed for quality control purposes allowing these to be used for further development with a potential for commercialization.

The Marula stem ethanol extract was separately defatted, concentrated and then defatted-concentrated and the extract of Sycamore leaves was defatted by liquid-liquid partitioning. Screening of these extracts and Marula oil (purchased from a commercial supplier) in the anti-elastase and anti-collagenase assays revealed that the defatting-concentration step improved the anti-collagenase activity of the Marula extract. Further, the concentration and defatting-concentration steps lowered the colour intensity of the Marula stem ethanol extract and defatting lowered the colour intensity of the Sycamore leaf extract. Marula oil although traded as a cosmetic ingredient did not have any anti-collagenase or anti-elastase activity when bioassayed, anti-aging claims on products containing the oil are thus due to a different mode of action.

The Marula stem ethanol extract was fractionated using a prep HPLC-UV to produce 23 fractions and leaves of the Sycamore tree produced 17 fractions after fractionation followed by screening of the fractions in the anti-elastase and anti-collagenase assays. Five Marula stem fractions exhibited good anti-collagenase activities (>80%) in the similar range as the positive control, EDTA. Chemical analysis of the active fractions using UPLC-MS revealed that EGCg and ECg were present in the fractions and may have contributed to their anti-collagenase activities. Upon screening the pure compounds in the collagenase assay, EGCg and ECg were as potent ($p < 0.05$) as EDTA at 5 $\mu\text{g/ml}$. Thus, for the first-time EGCg and ECg have been shown to be the major compounds contributing to the collagenase inhibition activity of Marula stems and could be potentially developed into anti-aging ingredients. Similarly, three Sycamore fractions exhibited collagenase inhibition activity (>70%), chemical analysis of the active fractions revealed that isoquercetin contributed to the collagenase inhibition activities of the fractions. Screening of pure compounds at 10 $\mu\text{g/ml}$ confirmed that isoquercetin exhibits anti-collagenase activity. This is the first report of anti-collagenase activity of isoquercetin, this report justifies further development of the compound as a cosmetic ingredient. In the anti-elastase assay, the ethanol extract of Marula stems and leaves of the Sycamore and their fractions showed activity. Upon screening of pure compounds from both plants, none of the compounds showed activity revealing that activity in the extracts and the fractions was due to synergistic effects.

In conclusion, stable formulations of an anti-aging day cream and nourishing night cream were developed from combinations of the active, chemically characterized ethanol extracts of Marula stems and leaves of *F. sycamorus* for proof of concept. Further studies will be carried out beyond the scope of this study to evaluate the formulations for shelf life, compatibility, microbiology and dermal safety studies

Table of contents

Submission declaration	i
Plagiarism declaration	ii
Acknowledgements	iii
Summary	iv
List of Figures	xii
List of Tables	xvi
Abbreviations	xvii
Supplementary data	xix

CHAPTER 1: INTRODUCTION	1
1.1 SKIN STRUCTURE	1
1.1.1 Epidermis.....	1
1.1.2 Dermis (corium)	2
1.1.2.1 Collagen and elastin fibres	3
1.1.3 The hypodermis (subcutaneous fat, panniculus adiposus).....	3
1.2 SKIN AGING.....	4
1.2.1 Role of elastase and collagenase in skin aging.....	6
1.2.2 Existing anti-aging products and their side effects	7
1.2.2.1 Sunscreens	7
1.2.2.2 Hydroquinones	7
1.2.2.4 Hormones.....	8
1.2.2.5 Alpha hydroxy acids and alpha keto acids.....	8
1.3 NATURAL PRODUCTS AS ANTI-AGING INGREDIENTS.....	9
1.3.1 Natural antioxidants	9
1.3.2 Retinoids.....	10
1.3.3 Vitamin D.....	11
1.3.4 Vitamin C.....	11
1.4 TRADITIONAL USES OF PLANTS FOR CURING SKIN AILMENTS AND FOR COSMETIC PURPOSES.....	12
1.5 PHYTOCHEMICALS AS INHIBITORS OF COLLAGENASE AND ELASTASE.....	14
1.6 PHYTOCHEMICALS AS POTENTIAL GROWTH PROMOTERS OF ELASTIN AND COLLAGEN	17
1.7 PROBLEM STATEMENT AND JUSTIFICATION.....	17
1.8 GOALS AND OBJECTIVES.....	21
1.9 REFERENCES.....	22

CHAPTER 2: <i>Sclerocarya birrea</i> (MARULA)	28
2.1 BOTANY AND SPATIAL DISTRIBUTION.....	28
2.2 TRADITIONAL USES OF THE PLANT.....	30
2.3 COSMETIC APPLICATIONS.....	31
2.4 PREVIOUSLY REPORTED BIOASSAYING OF MARULA.....	31
2.5 PHYTOCHEMISTRY.....	34
2.5.1 Marula stems.....	34
2.5.2 Marula fruit and seed.....	35
2.5.3 Marula leaves.....	36
2.6 METHODOLOGY.....	37
2.6.1 Collection and extraction of Marula stems, leaves and fruits.....	37
2.6.2 Collection and extraction of Marula stems.....	38
2.6.3 Sequential extraction of Marula stems.....	39
2.6.4 Marula oil production.....	40
2.6.5 Bioassay of crude extracts and fractions.....	41
2.6.6 Chemical Profiling.....	41
2.6.7 Bioassay-guided fractionation.....	42
2.6.8 Defatting of Marula stem ethanol extract.....	43
2.6.9 Concentration of actives of Marula stem extract.....	44
2.6.10 Defatting-concentration of actives of Marula stem extract.....	45
2.7 RESULTS AND DISCUSSION.....	46
2.7.1 Selection of the most appropriate solvent.....	47
2.7.2 Sequential extraction using polar and non-polar solvents and bioassaying.....	47
2.7.3 UPLC-QTOF-MS analysis of Marula stems extracted sequentially using polar and non-polar solvents.....	48
2.7.4 Separate extraction using different polar solvents and their bioassaying.....	51
2.7.5 UPLC-QTOF-MS analysis of Marula stems extracted separately with different solvents.....	52
2.7.6 Chemical profiling and phytochemical analysis of the ethanol extract of Marula stems.....	55
2.7.7 Improving the quality of the ethanol extract as a cosmetic ingredient.....	72
2.7.8 Comparison of chemical profiles of the Marula extract, and fractions obtained through defatting and concentration.....	77
2.7.9 Bioassay-guided fractionation.....	79
2.7.10 Collagenase inhibition activity of fractions of <i>S. birrea</i>	79

2.7.11 UPLC-QTOF-MS analysis of active fractions.....	80
2.7.12 Collagenase inhibition assaying of pure compounds.....	82
2.7.13 Elastase inhibition activity of fractions of <i>S. birrea</i>	84
2.7.13.1 UPLC-QTOF-MS analysis of active fractions.....	85
2.7.14 Elastase inhibition of pure compounds.....	89
2.8 CONCLUSIONS.....	91
2.9 REFERENCES.....	93
Chapter 3: <i>Ficus sycomorus</i> (SYCAMORE).....	98
3.1 BOTANY AND GEOGRAPHICAL DISTRIBUTION.....	98
3.2 TRADITIONAL USES OF THE PLANT.....	99
3.3 PREVIOUS RESEARCH ON <i>F. SYCOMORUS</i>	100
3.3.1 Leaves.....	100
3.3.2 Stem bark.....	102
3.3.3 Roots.....	104
3.3.4 Fruits.....	104
3.5 PHYTOCHEMISTRY.....	105
3.5.1 Stems.....	105
3.5.2 Leaves.....	105
3.5.3 Roots.....	107
3.6 METHODOLOGY.....	107
3.6.1 Collection and extraction of plant material from KwaZulu Natal.....	107
3.6.2 Collection of plant material from the University of Pretoria garden and experimental farm.....	108
3.6.3 Separate extraction of leaf material using polar solvents.....	108
3.6.4 Sequential extraction of leaf material.....	109
3.6.5 Bioassaying of crude extracts and fractions.....	111
3.6.6 Chemical profiling using UPLC MS and NMR.....	111
3.6.7 Bioassay guided fractionation.....	113
3.6.8 Defatting the crude ethanol extract of leaves of <i>F. sycomorus</i>	114
3.7 RESULTS AND DISCUSSION.....	114
3.7.1 Sequential extraction using polar and non-polar solvents and bio-assaying.....	115
3.7.2 UPLC-QTOF-MS analysis of <i>F. sycomorus</i> leaves extracted sequentially with polar and non-polar solvents.....	116

3.7.3	Separate extraction using different polar solvents and their bioassaying.....	118
3.7.4	UPLC-QTOF-MS analysis of <i>F. sycomorus</i> leaves extracted separately with polar solvents.....	120
3.7.5	Chemical marker identification and phytochemical analysis.....	123
3.7.6	Fractionation of ethanol extract of leaves of <i>F. sycomorus</i>	144
3.7.7	Structure elucidation using NMR.....	144
3.7.8	Improving the quality of the ethanol extract as a cosmetic ingredient.....	156
3.7.9	Comparison of chemical profiles of the <i>F. sycomorus</i> crude extract and its defatted fraction.....	158
3.7.10	Bioassay guided fractionation.....	161
3.7.11	Collagenase inhibition activity of fractions of <i>F. sycomorus</i>	161
3.7.12	UPLC-QTOF-MS analysis of active fractions.....	162
3.7.13	Collagenase inhibition assay of pure compounds.....	164
3.7.14	Elastase inhibition activity of fractions of <i>F. sycomorus</i>	166
3.7.15	UPLC-QTOF-MS analysis of active fractions.....	167
3.7.16	Elastase inhibition activity of pure compounds.....	168
3.8	CONCLUSIONS.....	169
3.9	REFERENCES.....	171
CHAPTER 4: COMBINATION AND FORMULATION STUDIES.....		175
4.1	INTRODUCTION.....	175
4.2	COMBINATION STUDIES.....	175
4.3	FORMULATION STUDIES.....	176
4.4	METHODOLOGY.....	176
4.4.1	Preparation of mixtures.....	176
4.4.2	Bioassay of the combinations/mixtures.....	176
4.4.3	Formulation of the anti-aging day cream at lab scale.....	177
4.4.4	Formulation of the nourishing night cream at lab scale.....	177
4.4.5	Formulation of the anti-aging day cream at kilogram scale.....	178
4.4.6	Formulation of nourishing night cream at kilogram scale.....	178
4.5	RESULTS AND DISCUSSION.....	178
4.5.1	Bioassay of the combinations/mixtures.....	178
4.5.1.1	Collagenase inhibition activity.....	178

4.5.1.2	Elastase inhibition activity.....	180
4.5.2	Anti-aging day cream-SPF 20.....	181
4.5.3	Nourishing night cream.....	182
4.6	CONCLUSION.....	183
4.7	REFERENCES.....	184
CHAPTER 5: METHODOLOGY		185
5.1	INTRODUCTION.....	185
5.2	CHAPTERS 2 AND 3.....	185
5.2.1	Chemicals and reagents.....	185
5.2.2	Extraction procedures.....	186
5.2.2.1	Extraction of plant material at CSIR.....	186
5.2.2.2	Separate extraction of plant material.....	186
5.2.2.3	Sequential extraction of plant material.....	187
5.2.3	Defatting of extracts.....	188
5.2.4	Concentration of actives.....	188
5.2.5	Defatting-concentration of actives.....	188
5.2.6	Determination of anti-elastase activity.....	189
5.2.7	Determination of anti-collagenase activity.....	190
5.2.8	Statistical Analysis.....	191
5.2.9	UPLC-Q-TOF-MS analysis.....	191
5.2.9.1	MS Conditions.....	192
5.2.9.2	Acquisition.....	192
5.2.10	Column and thin layer chromatography.....	192
5.2.11	Purification of compounds 1, 2 and 3 using preparative HPLC-MS.....	193
5.2.12	NMR.....	194
5.2.13	Chemical profiling.....	195
5.2.14	Semi Prep HPLC fractionation.....	195
5.3	CHAPTER 4.....	196
5.3.1	Combination studies.....	196
5.3.1.1	Combination of Marula and Sycamore extracts.....	196
5.3.1.2	Combination of Sycamore extract and active compounds from Marula.....	196
5.3.2	Formulation studies.....	196
5.3.2.1	Formulation of the antiaging day cream (200.00 g batch).....	196

5.3.2	Formulation of the nourishing night cream (200.00 g batch).....	197
5.3.3	Formulation of the antiaging day cream (2 kg batch).....	198
5.3.4	Formulation of the nourishing night cream (2 kg batch).....	198
5.4	REFERENCES.....	199
	CHAPTER 6: CONCLUSIONS	200

List of figures

Chapter 1

- Figure 1.1.** The skin diagram showing the layers of the epidermis and the main structures of the dermis..... 4
- Figure 1.2.** Natural compounds β -amyrin and syringic acid isolated from *T. erecta* flower.....16
- Figure 1.3.** Plant extracts containing the anti-aging ingredient lupeol have been developed.....16

Chapter 2

- Figure 2.1** Picture A showing the Marula tree and picture B shows a stem with leaves and fruits from the Marula plant.....29
- Figure 2.2.** Flow diagram for the extraction of Marula stems, fruits and leaves separately using methanol:DCM (1:1).....38
- Figure 2.3.** Flow diagram for the extraction of Marula stems separately using ethanol, acetone, and methanol:DCM (1:1)..... 39
- Figure 2.4.** Flow diagram for sequential extraction of *S. birrea* stems..... 40
- Figure 2.5.** Flow diagram for bioassay-guided fractionation of Marula stems ethanol extract using prep-HPLC..... 43
- Figure 2.6.** Flow diagram for the defatting of Marula stem ethanol extract through liquid liquid partitioning..... 44
- Figure 2.7.** Flow diagram for concentration of active ingredients of Marula stem ethanol extract.....45
- Figure 2.8.** Flow diagram for defatting-concentration of Marula stem ethanol extract..... 46
- Figure 2.9.** ESI negative mode BPI chromatograms (0 to 18 minutes) of Marula stems extracted sequentially..... 50
- Figure 2.10.** ESI negative mode BPI chromatograms of Marula stems extracted separately using different solvents..... 54
- Figure 2.11.** ESI negative mode BPI chromatogram of Marula stem ethanol extracts..... 56
- Figure 2.12.** Chemical structures of compounds identified.....62
- Figure 2.13.** Fragmentation pathways of B-type trimeric procyanidins: loss of neutral molecules by HRF(heterocyclic ring fission), RDA (retro-Diels-Alder) and QM (quinone methide) mechanisms.....63
- Figure 2.14.** ESI negative mode BPI chromatogram of Marula stems extracted with ethanol overlaid with quinic acid pure standard.....64
- Figure 2.15.** ESI negative mode BPI chromatogram of Marula stems extracted with ethanol overlaid with catechin pure standard..... 67
- Figure 2.16.** ESI negative mode BPI chromatogram of Marula stems extracted with ethanol overlaid with epigallocatechin gallate pure standard..... 69

Figure 2.17. ESI negative mode BPI chromatogram of Marula stems extracted with ethanol overlaid with epigallocatechin gallate pure standard.....	71
Figure 2.18. Picture A shows the dark-brown colour of Marula crude extract, picture B shows a slightly lower intensity of the dark brown colour produced by defatting. In pictures C and D the brown intensity was significantly lowered. Picture C is the concentrated extract and picture D is the defatted-concentrated fraction.....	74
Figure 2.19. Elastase inhibition of the improved quality samples and Marula oil at 100 and 10 µg/ml.....	75
Figure 2.20. Collagenase inhibition of the fractions with improved quality and Marula oil tested at 100 and 10 µg/ml.....	77
Figure 2.21. Negative mode BPI chromatograms of Marula stem ethanol extract and its fractions.....	78
Figure 2.22. Collagenase inhibition activity of Marula fractions at 200 µg/ml and positive control EDTA at test concentration 143 µg/ml.....	80
Figure 2.23. ESI negative mode BPI chromatograms of fractions S5, S6, S7 and S8 from Marula stem ethanol extract.....	82
Figure 2.24. Collagenase inhibition activities of major compounds identified in Marula stem ethanol extract at 20, 10 and 5 µg/ml.....	84
Figure 2.25. % Elastase inhibition activity of Marula stem fractions at 25 µg/ml, in comparison to the positive control elafin, tested at a concentration of 1.43 µg/ml.....	85
Figure 2.26. Chemical profiles of fractions S1 and S2 overlaid.....	87
Figure 2.27. Chemical profiles of active fractions S18, S19 and S20.....	88
Figure 2.28. Chemical profiles of active fractions S23, S22 and inactive fraction S21.....	89
Figure 2.29. Elastase inhibition activities of major compounds identified in Marula stem ethanol extract at 20, 10 and 5 µg/ml.....	91

Chapter 3

Figure 3.1. Picture A showing the <i>F. sycomorus</i> tree and picture B shows a stem and leaves from the <i>F. sycomorus</i> plant.....	99
Figure 3.2. Flow diagram for the separate extraction of leaves of <i>F. sycomorus</i> plant using methanol : DCM (1:1).....	108
Figure 3.3. Flow diagram for the extraction of dried ground leaves of <i>F. sycomorus</i> separately using ethanol, acetone, and methanol:DCM (1:1).....	109
Figure 3.4. Flow diagram for the sequential extraction of dried ground leaf material of <i>F. sycomorus</i>	110
Figure 3.5. Flow diagram for the fractionation of crude ethanol extract of leaves of <i>F. sycomorus</i> using column chromatography followed by mass directed fractionation using preparatory HPLC-MS.....	112
Figure 3.6. Flow diagram for bioassay guided fractionation of crude ethanol extract of leaves of <i>F. sycomorus</i>	113

Figure 3.7. Flow diagram for the defatting of crude ethanol extract of leaves of <i>F. sycomorus</i>	114
Figure 3.8. ESI negative mode BPI chromatograms of leaves of <i>F. sycomorus</i> extracted sequentially.	118
Figure 3.9. ESI negative mode BPI chromatograms of leaves of <i>F. sycomorus</i> extracted sequentially.....	122
Figure 3.10. ESI negative mode BPI chromatogram of crude ethanol extract of leaves of <i>F. sycomorus</i>	125
Figure 3.11. Chemical structures of compounds identified from <i>F. sycomorus</i> leaves.....	130
Figure 3.12. Negative mode ESI mass spectrum of peak 1 showing a mixture of palatinose and quinic acid.....	132
Figure 3.13. ESI negative mode BPI chromatogram of the ethanolic extract of leaves of <i>F. sycomorus</i> overlaid with quinic acid and palatinose pure standards.....	132
Figure 3.14. ESI negative mode BPI chromatogram of leaves of <i>F. sycomorus</i> extracted with ethanol overlaid with purified isobiflorin.....	134
Figure 3.15. ESI negative mode BPI chromatogram of leaves of <i>F. sycomorus</i> extracted with ethanol overlaid with purified biflorin.....	135
Figure 3.16. ESI negative mode BPI chromatogram of leaves of <i>F. sycomorus</i> extracted with ethanol overlaid with chlorogenic acid pure standard.....	136
Figure 3.17. ESI negative mode BPI chromatogram of leaves of <i>F. sycomorus</i> extracted with ethanol overlaid with purified peak 6.....	138
Figure 3.18. ESI negative mode BPI chromatogram of <i>F. sycomorus</i> leaf ethanol extract overlaid with rutin pure standard.....	140
Figure 3.19. Fragmentation of quercetin-3-glucoronide.....	142
Figure 3.20. ESI negative mode BPI chromatogram of leaves of <i>F. sycomorus</i> extracted with ethanol overlaid with isoquercetin pure standard.....	144
Figure 3.21. Structure of compound 1 (biflorin).....	146
Figure 3.22. Key HMBC and COSY correlations of compound 1 (biflorin).....	147
Figure 3.23. Structure of compound 2 (isobiflorin).....	150
Figure 3.24. Key HMBC and COSY correlations of compound 2 (isobiflorin).....	151
Figure 3.25. Structure of compound 3 (vicenin-2).....	153
Figure 3.26. Key HMBC and COSY correlations of compound 3 (vicenin-2).....	155
Figure 3.27. Picture A shows the dark-green colour of the ethanol extract of leaves of <i>F. sycomorus</i> , picture B shows the defatted leaf extract with the dark-green colour removed. Picture C is the hexane layer showing the green colour of chlorophyll removed from the crude extract.....	156
Figure 3.28. Collagenase inhibition activities of <i>F. sycomorus</i> crude extract and its fractions produced by defatting.....	158
Figure 3.29. Elastase inhibition activities of <i>F. sycomorus</i> crude extract and its fractions produced by defatting.....	159

Figure 3.30. Negative mode BPI chromatograms of crude <i>F. sycamor</i> ethanol extract and its defatted fraction.....	160
Figure 3.31. Collagenase inhibition activity of <i>F. sycamor</i> fractions at 25 µg/ml. Fractions F5, F8 and F13 showed inhibition activity (>70%) in the same range as EDTA the positive control.....	162
Figure 3.32. ESI negative mode BPI chromatograms of the four active fractions from <i>F. sycamor</i> leaf ethanol extract overlaid with a mix of standards.....	164
Figure 3.33. Collagenase inhibition activities of major compounds identified in leaves of <i>F. sycamor</i> ethanol extract at 20, 10 and 5 µg/ml.....	166
Figure 3.34. % Elastase inhibition activity of <i>F. sycamor</i> fractions at 25 µg/ml.....	167
Figure 3.35. ESI negative mode BPI chromatograms of fraction F4.....	168
Figure 3.36. Elastase inhibition activities of major compounds identified in <i>F. sycamor</i> ethanol extract at 20, 10 and 5 µg/ml.....	169

Chapter 4

Figure 4.1. Collagenase inhibition of combinations of defatted <i>F. sycamor</i> and Marula defatted and concentrated fractions screened at 100 and 10 µg/ml.....	179
Figure 4.2. Elastase inhibition of combinations of defatted <i>F. sycamor</i> and Marula defatted and concentrated fractions screened at 100 and 10 µg/ml.....	181
Figure 4.3. Anti-aging day cream SPF-20 prototype.....	182
Figure 4.4. Nourishing night cream prototype.....	183

List of tables

Chapter 2

- Table 2.1.** Comparison of inhibition of the elastase and collagenase activities for extracts of different parts of *S. birrea* tested at 200 µg/ml and the positive controls at EDTA at 143 µg/ml and elafin 1.43 µg/ml..... 47
- Table 2.2.** Extraction yields of Marula stems sequentially extracted and their inhibition of the elastase and collagenase enzymes at 200 µg/ml and the positive controls EDTA at 143 µg/ml and elafin at 1.43 µg/ml.....48
- Table 2.3.** Extraction yields of Marula stems extracted using different solvents and their inhibition of the elastase and collagenase enzymes at 200 µg/ml and the positive controls EDTA at 143 µg/ml and elafin 1.43 µg/ml.....52
- Table 2.4.** Chemical profile of Marula stems extracted with ethanol.....57
- Table 2.5.** A comparison of major compounds identified in the Marula fractions after liquid-liquid partitioning..... 78

Chapter 3

- Table 3.1.** Inhibition of the elastase and collagenase activities for leaves of *F. sycomorus* tested at 200 µg/ml and the positive controls at EDTA at 143 µg/ml and elafin 1.43 µg/ml.....115
- Table 3.2.** Extraction yields, elastase and collagenase inhibition activities of leaves of *F. sycomorus* extracted using different solvents and tested at 200 µg/ml and the positive controls EDTA at 143 µg/ml and elafin at 1.43 µg/ml.....116
- Table 3.3.** Extraction yields, elastase and collagenase inhibition activities of leaves of *F. sycomorus* extracted using different solvents..... 120
- Table 3.4.** Chemical profile of ethanol extract of leaves of *F. sycomorus* extracted with ethanol..... 126
- Table 3.5.** Comparison of ¹H and ¹³C NMR data of biflorin in MeOD-*d*4 and the published ¹H and ¹³C data of biflorin in DMSO-*d*6 and ¹H data of biflorin in MeOD-*d*4..... 146
- Table 3.6.** ¹H and ¹³C-NMR data of isobiflorin in MeOD-*d*4 as compared with ¹H and ¹³C data of isobiflorin in DMSO-*d*6 and ¹H data of isobiflorin in MeOD-*d*4 from literature..... 149
- Table 3.7.** ¹H and ¹³C-NMR data of vicenin-2 in MeOD-*d*4 as compared with ¹H and ¹³C data of vicenin-2 in DMSO-*d*6..... 153

Abbreviations

^{13}C NMR	Carbon-13 nuclear magnetic resonance
^1H NMR	Proton NMR
9,10,13 TriHOME	9,10,13-Trihydroxy-11-octadecenoic acid
ATCC	American type culture collection
<i>A. niger</i>	<i>Aspergillus niger</i>
BPI	Base peak ion
BFF	Benzofuran-forming fission
CD_3CN	Deuterated acetonitrile
CD_3OD	Deuterated methanol
CE	Catechin equivalent
COSY	Correlation spectroscopy
DCM	Dichloromethane
DEPT	Distortionless enhancement by polarisation transfer
DMSO	Dimethyl sulfoxide
DPPH	2,2-diphenyl-1-picrylhydrazyl
ECg	Epicatechin gallate
EGCg	Epigallocatechin gallate
<i>E. coli</i>	<i>Escherichia coli</i>
EDTA	Ethylenediaminetetraacetic acid
EtOAc	Ethyl acetate
ESI	Electron spray ionisation
FA	Formic acid
FALGPA	N-[3-(2-Furyl)acryloyl]-Leu-Gly-Pro-Ala
FD extract	<i>F. sycomorus</i> defatted extract
<i>F. sycomorus</i>	<i>Ficus sycomorus</i>
GAE	Gallic acid equivalent
HEPES	4-(2-hydroxyethyl)-1-piperazinethanesulfonic acid
HLE	Human Leucocyte Elastase
HPLC QTOF MS	High-performance-liquid chromatography/quadrupole-time-of-flight mass spectrometry
HMBC	Heteronuclear multiple bond correlation
HRF	Heterocyclic ring fission
HSQC	Heteronuclear single quantum correlation
iFit	Isotopic fit value
MBC	Minimum Bacterial concentration
MDC extract	Marula defatted and concentrated extract
MeOH	Methanol
MeOD	Deuterated methanol
MIC	Minimum inhibitory concentration
min	Minute
ml	millilitre
MS	Mass spectrophotometry
<i>m/z</i>	Mass to charge ratio
ng	nanogram
NMR	Nuclear magnetic resonance
ppm	Parts per million
Prep HPLC-MS	Preparatory High-performance- liquid- chromatography coupled to a Mass spectrometer
Prep-HPLC-UV	Preparatory High Performance-liquid chromatography with an Ultra Violet detector
PTFE	Polytetrafluoroethylene (Teflon)

QM	Quinone -methide
RDA	Retro Dials Alder
ROS	Reactive oxygen species
RP-HPLC-ESI-QTOF/MS ²	Reverse Phase High performance liquid chromatography Electrospray ionization quadrupole-time of flight mass spectrometry
RPM	Revolutions per minute
RT	Retention time
SD	Standard deviation
SEM	Standard error of the mean
<i>S. aureus</i>	<i>Staphylococcus aurius</i>
<i>S. birrea</i>	<i>Sclerocarya birrea</i>
<i>S. typhimurium</i>	<i>Salmonella typhimurium</i>
TES	tris(hydroxymethyl)-methyl-2-aminoethane sulfonate
TLC	Thin layer chromatography
μl	microliter
μg	microgram
μM	micromolar
UPLC	Ultra-perfomance-liquid-chromatography
UPLC QTOF MS	Ultra-perfomance-liquid chromatography/quadrupole-time-of- flight mass spectrometry
UV-VIS	Ultra violet visible spectroscopy

SUPPLEMENTARY DATA

Supplementary Data 1. ESI positive mode BPI chromatogram of crude ethanol extract of Marula stems.....	205
Supplementary Data 2. MS/MS fragmentation pattern of peak 1 (quinic acid) in Marula stem ethanol extract.....	205
Supplementary Data 3. MS/MS fragmentation pattern of peak 1 (quinic acid) in Marula stems overlaid with MS/MS fragmentation pattern of quinic acid pure standard.....	206
Supplementary Data 4. iFit value quinic acid.....	206
Supplementary Data 5. MS/MS fragmentation pattern of peak 3 (gallo catechin) in Marula stem ethanol extract.....	207
Supplementary Data 6. iFit value for peak 2 (gallo catechin) in Marula stem ethanol extract.....	207
Supplementary Data 7. MS and MS/MS data of peak 3 (procyanidin B2).....	208
Supplementary Data 8. iFit value peak 4 (procyanidin B2).....	208
Supplementary Data 9. MS and MS/MS data for peak 5 (catechin) in Marula stem ethanol extract.....	209
Supplementary Data 10. iFit value for peak 5 (catechin) in Marula stem ethanol extract.....	209
Supplementary Data 11. MS/MS fragmentation pattern of peak 4 (catechin) in Marula stems overlaid with MS/MS fragmentation pattern of quinic acid pure standard.....	210
Supplementary Data 12. MS and MS/MS data for peak 7 showing fragments for epicatechin-epicatechin-3'-O-gallate) in Marula stem ethanol extract.....	210
Supplementary Data 13. iFit value for peak 6 (epicatechin-epicatechin-3'-gallate).....	211
Supplementary Data 14. MS and MS/MS fragmentation pattern of peak 8 (epigallocatechin gallate) in Marula stem ethanol extract.....	211
Supplementary Data 15. iFit value for peak 7 (epigallocatechin gallate) in Marula stem ethanol extract.....	212
Supplementary Data 16. MS/MS fragmentation pattern of peak 7 (epicatechin gallate) in Marula stems overlaid with MS/MS fragmentation pattern of epicatechin gallate pure standard.....	212
Supplementary Data 17. MS and MS/ MS data for peak 8 (epicatechin-3-O-gallate-epicatechin) in Marula stem ethanol extract.....	213
Supplementary Data 18. iFit value for peak 8 (epicatechin-3-O-gallate-epicatechin) in Marula stem ethanol extract.....	213

Supplementary Data 19. MS and MS/MS fragmentation pattern of peak 9 (procyanidin B2-3'3 di-O-gallate) in Marula stem ethanol extract.....	214
Supplementary Data 20. iFit value peak 9 (procyanidin B2-3'3 di-O-gallate) in Marula stem ethanol extract.....	214
Supplementary Data 21. MS fragmentation pattern overlaid with MS/MS fragmentation pattern of peak 10 (epicatechin gallate) in Marula stem ethanol extract.....	215
Supplementary Data 22. iFit value epicatechin gallate peak 10 (epicatechin gallate) in Marula stem ethanol extract.....	215
Supplementary Data 23. MS/MS fragmentation pattern of peak 10 (epicatechin gallate) in Marula stems overlaid with MS/MS fragmentation pattern of epicatechin gallate pure standard.....	216
Supplementary Data 24. MS fragmentation pattern of peak 11 (undecanedioic acid) overlaid with MS/MS fragmentation pattern of peak 11 (undecanedioic acid) in Marula stem ethanol extract.....	216
Supplementary Data 25. iFit value for undecanedioic acid.....	217
Supplementary Data 26. MS fragmentation pattern of 9,10,13 TriHOME (peak 12) overlaid with its MS/MS fragmentation pattern.....	217
Supplementary Data 27. iFit value of 9,10,13 TriHOME (peak 12).....	218
Supplementary Data 28. Expansion of ESI negative mode BPI chromatograms of leaves of <i>F. sycomorus</i> extracted sequentially showing retention times 2.20 minutes to 3.80 minutes.....	218
Supplementary Data 29. ESI negative mode BPI chromatogram of crude ethanol extract of leaves of <i>F. sycomorus</i>	219
Supplementary Data 30. iFit value chloride adduct of palatinose.....	219
Supplementary Data 31. iFit value of palatinose in <i>F. sycomorus</i> leaves extracted with ethanol.....	220
Supplementary Data 32. MS/MS fragmentation pattern peak of 1 (palatinose and chlorogenic acid) in leaves of <i>F. sycomorus</i> extracted with ethanol.....	220
Supplementary Data 33. iFit value for quinic acid.....	221
Supplementary Data 34. MS and MS/MS fragmentation pattern of peak 2 (Isobiflorin) in the ethanol extract of leaves of <i>F. sycomorus</i>	221
Supplementary Data 35. MS and MS/MS fragmentation pattern for Biflorin (peak 4) in <i>F. sycomorus</i> ethanol extract.....	222
Supplementary Data 36. iFit value Peak 2 (isobiflorin) in leaves of <i>F. sycomorus</i> extracted with ethanol.....	222
Supplementary Data 37. iFit value biflorin peak 5 in leaves of <i>F. sycomorus</i> extracted with ethanol.....	223

Supplementary Data 38. MS/MS fragmentation pattern of biflorin overlaid with MS/MS fragmentation pattern of isobiflorin.....	223
Supplementary Data 39. MS/MS fragmentation pattern of peak 2 (isobiflorin) in <i>F. sycomorus</i> ethanol extract overlaid with MS/MS fragmentation pattern of purified isobiflorin from <i>F. sycomorus</i>	224
Supplementary Data 40. MS/MS fragmentation pattern of peak 4 (biflorin) in <i>F. sycomorus</i> ethanol extract overlaid with MS/MS fragmentation pattern of purified biflorin from <i>F. sycomorus</i>	224
Supplementary Data 41. MS and MS/MS data of peak 3 (chlorogenic acid) in the ethanol extract of leaves of <i>F. sycomorus</i>	225
Supplementary Data 42. iFit value for peak 3 (Chlorogenic acid) in the ethanol extract of the leaves of <i>F. sycomorus</i>	225
Supplementary Data 43. MS/MS fragmentation pattern of peak 3 (chlorogenic acid) overlaid with MS/MS fragmentation pattern of chlorogenic acid pure standard.....	226
Supplementary Data 44. MS and MS/MS fragmentation pattern of peak 5 in the ethanol extract of leaves of <i>F. sycomorus</i>	226
Supplementary Data 45. iFit value for peak 5 (vicenin-2) in the ethanol extract of leaves of <i>F. sycomorus</i>	227
Supplementary Data 46. MS/MS peak 5 (vicenin-2) in <i>F. sycomorus</i> crude extract overlaid with the MS/MS of vicenin-2 pure standard.....	227
Supplementary Data 47. MS and MS/MS fragmentation pattern of peak 6 (rutin) in the ethanol extract of leaves of <i>F. sycomorus</i>	228
Supplementary Data 48. iFit value for peak 6 (rutin) in the ethanol extract of <i>F. sycomorus</i>	228
Supplementary Data 49. MS/MS peak 6 (rutin) in <i>F. sycomorus</i> crude extract overlaid with the MS/MS of rutin pure standard.....	229
Supplementary Data 50. MS and MS/MS fragmentation pattern of peak 7 (quercetin 3 glucuronide) in the ethanol extract of leaves of <i>F. sycomorus</i>	229
Supplementary Data 51. iFit value for peak 7 (quercetin 3 glucuronide) in the ethanol extract of leaves of <i>F. sycomorus</i>	230
Supplementary Data 52. MS and MS MS data of peak 8 (isoquercetin) in the ethanol extract of leaves of <i>F. sycomorus</i>	230
Supplementary Data 53. iFit value for peak 8 (isoquercetin) in the ethanol extract of leaves of <i>F. sycomorus</i>	231
Supplementary Data 54. MS/MS peak 8 (isoquercetin) in <i>F. sycomorus</i> crude extract overlaid with the MS/MS of isoquercetin pure standard.....	231
Supplementary Data 55. Expanded chromatograms of the <i>F. sycomorus</i> crude ethanol extract overlaid with the defatted fraction.....	232

Supplementary Data 56. 1H NMR of compound 1 (biflorin) in MeOD-d4.....	233
Supplementary Data 57. 13C NMR of compound 1 (biflorin) in MeOD-d4.....	234
Supplementary Data 58. DEPT 135 for compound 1 (biflorin) in MeOD-d4.....	235
Supplementary Data 59. HSQC spectrum for compound 1 (biflorin) in MeOD-d4	236
Supplementary Data 60. COSY spectrum for compound 1 (biflorin) in MeOD-d4.....	237
Supplementary Data 61. HMBC spectrum of compound 1 (biflorin) in MeOD-d4.....	238
Supplementary Data 62. 1H spectrum for compound 2 (isobiflorin) in MeOD-d4.....	239
Supplementary Data 63. 1H spectrum for compound 2 (isobiflorin) in CD3CN-d3.....	240
Supplementary Data 64. 13C spectrum for compound 2 (isobiflorin) in MeOD-d4.....	241
Supplementary Data 65. DEPT 135 spectrum for compound 2 (isobiflorin) in MeOD- d4.....	242
Supplementary Data 66. HSQC spectrum for compound 2 (isobiflorin) in MeOD-d4.....	243
Supplementary Data 67. COSY spectrum for compound 2 (isobiflorin) in MeOD-d4.....	244
Supplementary Data 68. HMBC spectrum for compound 2 (isobiflorin) in MeOD-d4.....	245
Supplementary Data 69. 1H NMR spectrum for compound 3 (vicenin 2) in MeOD-d6....	246
Supplementary Data 70. 1H NMR of compound 2 (vicenin 2) in DMSO-d6.....	247
Supplementary Data 71. 13C NMR of compound 3 (vicenin 2) in MeOD d4.....	248
Supplementary Data 72. DEPT 135 spectrum for compound 3 (vicenin- 2) in MeOD-d4.....	249
Supplementary Data 73. HSQC spectrum of compound 3 (vicenin- 2) in MeOD d4.....	250
Supplementary Data 74. COSY spectrum of compound 3 (vicenin-2) in MeOD d4.....	251
Supplementary Data 75. HMBC spectrum for compound 3 (vicenin 2) in MeOD d4.....	252

CHAPTER 1: INTRODUCTION

1.1 SKIN STRUCTURE

The skin is the largest and most extensive organ of our body by surface area [1-3]. It accounts for about 15% of the total body by weight and covers the entire surface of the body [1, 4]. It serves as a physical barrier between the internal and the external environment [4, 5]. Further, it is part of the integumentary system maintaining an internal homeostatic balance [6]. It is our first line of defence against pathogens, irritants, trauma and ultraviolet radiation [2, 4, 7]. The skin synthesises vitamin D, provides temperature regulation and immunological protection, it is pivotal in the reception of physical stimuli from the outside environment [7]. Further, it enhances our body image and augments outward beauty which leads to a higher self-esteem [4, 8]. A healthy and beautiful skin is a major factor in the perception of general health and well-being of the body [2, 8, 9]. Consequently, it greatly contributes to the comfort and psychological well-being of an individual [6, 8]. The skin is made up of three major layers, which are the epidermis, dermis and hypodermis [1, 5, 10]. There is considerable regional variations in thickness of the human skin according to function and anatomic location [4, 6]. The skin ranges from about 0.5 mm in the eyelids and 3-4 mm in the soles of the feet with an average thickness of 1-2 mm in most parts of the body [1, 6].

1.1.1 Epidermis

The epidermis is the external skin surface, it is the thinner outer layer and is mainly made up of keratinocytes which constitute (90-95%), the remaining 5-10% is made up of Langerhans cells, Melanocytes and Merkel cells [1, 2, 4]. Melanin the pigment which protects the inner skin from UV radiation is produced in the epidermis by Melanocytes [6, 10]. Langerhans cells participate in immune response and Merkel cells function in the sensation of touch [6]. The epidermis is made up of five layers which are the stratum basale, stratum spinosum, stratum granulosum, stratum lucidum and the stratum corneum with each layer representing a stage

in the life of an epidermal cell [6]. The structure and thickness of the epidermis varies according to anatomic location [3]. Its average thickness is 0.1 mm, but in acral areas (peripheral skin parts including palms, soles, elbows, knuckles, knees, toes, heels) it can go up to 1.6 mm thick [1, 3, 11]. The normal epidermis continuously undergoes renewal with keratinocytes on the skin surface being replaced after about 30 days [1, 4]. The epidermis is joined to the dermis through the dermal-epidermal junction which provides mechanical support for adhesion of the dermis to the epidermis [4, 5]. The dermal-epidermal junction is synthesised by dermal fibroblasts and basal keratinocytes [1, 4].

1.1.2 Dermis (corium)

The dermis is mainly made up of connective tissue and blood vessels, it is about 1 to 3 mm thick [5, 11]. Like the epidermis, the thickness of the dermis varies with anatomic location with the thickest layers being located in soles and palms and the thinner layers found in the eyelids [1, 11]. It has two layers the papillary (superficial dermis) and the reticular (deep) dermis [4, 6]. The papillary dermis contains nerves and capillaries used to nourish the epidermis, it provides adhesion between the dermis and the epidermis [1, 6]. The dermis is constituted of many cells (fibroblasts, dermal dendrocytes, mast cells), vessels and nerve endings [1, 4]. Fibroblasts are the most important cells found in the dermis and in all connective tissues because they synthesise all fibres and the ground substance of the dermis [1, 4]. The space between fibres and dermal cells is filled up by a ground substance which is made up of macromolecules which include proteoglycans (hyaluronic acid, dermatan sulphate, chondroitin-4-sulphate, fibronectin, tenascin, epimorphin) and glycoproteins [1, 4]. The ground substance is abundant in the papillary dermis [4]. The dermis contains two main types of sweat glands which are eccrine and apocrine glands, these release sweat into hair follicles on the skin surface through pores [1, 6]. Further, the superficial dermis is constituted of collagen fibres in loose bundles and thin elastic fibres which stretch to the dermal-epidermal junction [1, 4]. In contrast, the reticular dermis has coarser collagen bundles arranged parallel to the

skin surface and a thicker elastic network, additionally it contains the deep part of cutaneous appendages, vascular and nerve plexuses [1, 4].

1.1.2.1 Collagen and elastin fibres

Collagen fibers which are produced from fibroblasts in the skin dermis are the major constituent of the skin dermis constituting more than 90% wet weight and 98% of total mass of dried dermis [1, 10, 12]. The fibres are made up of mainly type I and type III collagen [4]. Collagen fibres are arranged in loose bundles in the papillary dermis and become thicker in the deep dermis [1]. The protein is the chief structural unit responsible for tensile strength, mechanical resistance and rigidity of the skin [1, 2, 13, 14]. It ensures cohesion and regeneration of the skin, cartilage and bone [15]. It is important in controlling cell shape and differentiation, migration, synthesis of some proteins and acts as a base on which other cells can proliferate [15].

Elastin fibres like collagen fibres are produced in the skin dermis by connective tissue cells known as fibroblasts [10]. Elastin is responsible for elasticity and retractile properties, in addition it provides resilience of the skin [8]. The protein is most abundant in organs providing elasticity to the connective tissues [10]. Elastin fibres are thin in the papillary dermis, they become thicker and are arranged horizontally in the reticular dermis [4].

1.1.3 The hypodermis (subcutaneous fat, panniculus adiposus)

The hypodermis is a connective tissue binding the skin to internal organs and is the thickest layer of the skin [3, 5]. It is an adipose tissue which is important in regulating temperature, insulation, protection from mechanical injuries and it acts as a store of energy [1, 3]. Adipocytes are the major cells in this tissue, they are large, rounded cells whose cytoplasm is composed of triglycerides and fatty acids [1]. These cells are arranged in lobules separated

by connective tissue septae, the thickness of the hypodermis shows anatomic variation between individuals and is reflective of nutritional status of an individual [3].

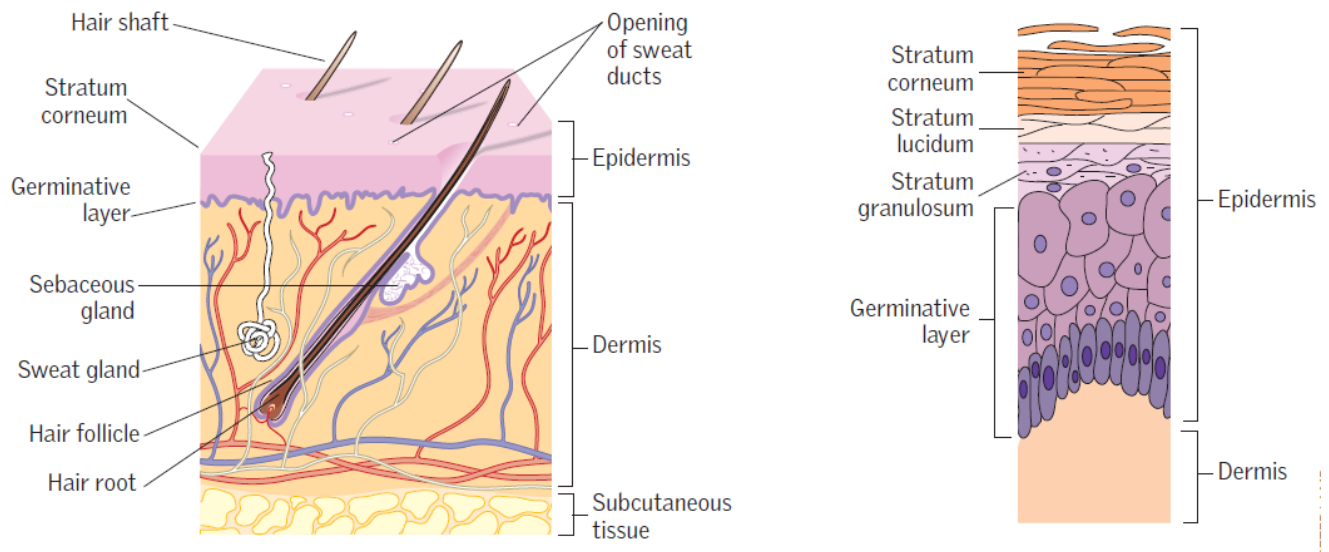


Figure 1.1. The skin diagram showing the layers of the epidermis and the main structures of the dermis McLafferty *et al.*[6].

1.2 SKIN AGING

The skin provides the most visible indicator of age [5, 7, 9]. Skin aging is a result of intrinsic and extrinsic processes [4]. Intrinsic also known as chronologic or cellular or natural aging is genetically determined and is inevitable [4, 16]. As a result, chronologic skin aging cannot be altered by changes in human behaviour [16]. On the other hand, extrinsic or photoaging is caused by external factors of which exposure to the sun is the main contributing factor [4, 16]. Other factors contributing to extrinsic aging include smoking, excessive alcohol consumption and poor nutrition [16]. The causes of photoaging can be controlled by altering human behaviour and they represent premature skin aging [16]. Exposed areas of the skin such as the face, chest, exterior surfaces of the arm show the majority of extrinsically aged skin [16]. Photoaging is characterised by dryness, rhytids, irregular pigmentation, loss of skin elasticity, epidermal atrophy and degradation of collagen and elastic fibres [4]. The loss of skin elasticity and skin tone is a characteristic of photo-aged skin. In addition, marked degradation of collagen and elastic fibres was observed in photo aged skin [16]. The formation of reactive

oxygen species (ROS) or free radicals influences both intrinsic and extrinsic ageing [16, 17]. In a study by El-Domyati et al.[18], it was observed that in different decades the thickness of the epidermis in sun-exposed skin was the same as the thickness of the epidermis in protected skin which suggests that the epidermis is not affected by age-related changes. On the contrary, a few other studies noticed some changes in the epidermis [19]. In their analysis of age-related changes to the skin, Baumer et al.[16] concluded that although the epidermis manifests important changes related to ageing, the age-related changes in the dermis are more pronounced than those in the epidermis. It has, however, been observed in other studies [20] that aged skin was characterised by a thinner epidermis in all anatomic sites investigated.

With age, the lifespan of fibroblasts which produce collagen fibres and their capacity to regenerate and produce collagen is diminished as a result of a reduction in metabolism of the fibroblasts [21]. Further, Finch [7] explained that in aged skin, dermal cells are replaced at a slower rate thus slowing the healing process. El-domyati et al.[18] observed that both extrinsic and intrinsic ageing have quantitative and qualitative effects on collagen and elastic fibres. These effects are characterised by loss of skin elasticity and strength which are a direct result of degradation of elastin and collagen [16]. In addition, elastin and collagen fibres become loosely connected which results in the skin losing elasticity and become more vulnerable to trauma and shearing forces. A reduction in elastin in the skin leads to decreased skin elasticity [10]. As a result, during skin aging, degradation of elastin and collagen fibres leads to sagging [16]. The dermis wastes away due to collagen degradation, this significantly contributes to wrinkle formation [21].

Kuwazuru et al.[8] explained that wrinkle reduction especially in facial skin leads to a youthful skin, a youthful appearance and a youthful mind. On the other hand, aged skin characterised by wrinkles may lead to psychological pain. Consequently, there are many anti-wrinkle

surgical, non-surgical and dermatological therapies [4]. This reveals that skin aging has the potential to affect an individual's lifestyle. In a review of structural characteristics of the aging skin, Farage et al.[5] explains that changes which are a result of skin aging lead to an increase in fragility, an increase in the risk for toxicological injuries, promotes development of several cutaneous disorders and produces wrinkling and uneven pigmentation.

1.2.1 Role of elastase and collagenase in skin aging

The main types of collagen types I and III in the dermal area of the skin are degraded by the enzyme matrix metalloproteinase-1 (MMP-1) a collagenase (collagenase-1, interstitial collagenase, EC 3.4.24.7) [22, 23]. Expression of this enzyme increases with age [23]. Further, there is a decrease in the synthesis of the protein collagen with age [12]. Consequently, this leads to an accelerated reduction of collagen levels and skin aging which is associated with collagen deficiency [24]. Collagen is responsible for rigidity of the connective tissue [10]. Its depletion significantly contributes to a decrease in tissue supporting the epidermis thus accelerating skin aging [25]. As such, the activity of collagenase has to be inhibited to retain skin elasticity and tensile strength [26].

Elastase (EC 3.4.4.7) is the only proteinase capable of degenerating dermal elastin, its activity is consequently believed to contribute to wrinkling and ageing [27]. The enzyme is non-specific, it hydrolyses all major proteins responsible for connectivity including collagen, proteoglycans and keratins [28]. Expression of elastase is induced by exposure to free radicals (ROS) and UV radiation [29] thus accelerating degeneration of elastin fibers. It has also been revealed that both chronological aging and photo aging lead to an increase in elastase type activity [30]. The breakdown of elastin fibres results in a decrease in the resilience of the skin [26]. As the elastic fibre network is important in skin elasticity, its reduction leads to wrinkle formation [28].

The activities of the enzymes elastase and collagenase lead to a higher rate of degradation of the extracellular matrix, thus accelerating the aging process. As a result, compounds which inhibit the activity of elastase and collagenase enzymes can be used to slow down or delay the ageing process [31]. Further, growth promoters of the proteins elastin and collagen can be used to revive aged skin and maintain healthy skin [22].

1.2.2 Existing anti-aging products and their side effects

1.2.2.1 Sunscreens

Several anti-aging products are available on the market and these have different mode of actions. Sunscreens are used for preventive measures, they protect against sunlight by blocking UVA and UVB, they reduce irritations linked to exposure to the sun and prevent pigment change [32, 33]. Additionally, efficient sunscreens may contribute to an overall decrease in ROS load thus minimising induced photoaging [34]. ROS activate collagenase and elastase to breakdown collagen and elastin, thus a decrease in ROS load contributes to prevention of collagen and elastin degradation [32, 33]. Sunscreens are, however, not desirable due to the chalky opaque appearance which they give [33]. Further, some sunscreens have been reported to cause adverse reactions including burning sensations, erythema and dermatitis [35].

1.2.2.2 Hydroquinones

Hydroquinones are applied to reverse skin aging, treat photodamaged and hyperpigmented skin, they give the skin an even tone and lighten the skin through suppression of melanocyte metabolic processes and pigment production [32]. Hydroquinones are mostly used in combination with retinoids and other treatments [36-38]. The use of hydroquinones in cosmetics was banned due to side effects which include occupational vitiligo, exogenous

onchronosis and carcinogenesis [39]. Additionally, hydroquinones have been reported to have the adverse effects of skin irritation and contact dermatitis [40].

1.2.2.4 Hormones

Hormonal levels decrease with time, treatment with hormones has been used for anti-aging purposes [41]. The effects of estrogen are evident especially in the post-menopausal period through receptors in the epidermis and the dermis [33]. Estrogen-progestin hormone replacement therapy was found to maintain skin firmness, reduce wrinkles and increase skin thickness in postmenopausal women [42, 43]. In addition, hormone replacement therapy was found to increase skin elasticity [43, 44], skin collagen content [45] and to improve the appearance of photo-aged skin [33]. Further, there was a significant improvement in the water-holding capacity of the skin following estrogen hormone replacement therapy [45]. Estrogen was also found to increase the surface lipid content in the epidermis [33]. Side effects of hormone replacement therapy include increased risk of invasive cancer, heart attack, stroke and blood clotting [46]. In men the side effects of testosterone use in hormone replacement therapy include higher risk of prostate cancer, benign prostatic hyperplasia and increased risk of cardiovascular disease and obesity [47].

1.2.2.5 Alpha hydroxy acids and alpha keto acids

Alpha hydroxy acids (glycolic and lactic acid, their common salts and their esters) were declared to be safe for use in formulating cosmetic ingredients at concentrations below 10% and at low a pH [48]. These are applied on the skin to reduce the thickness of the stratum corneum which will allow for control of dry skin, ichthyosis, follicular hyperkeratosis and other related conditions [49]. Alpha hydroxy acids are also used in salon products and can be used to reduce facial wrinkles [48, 49]. These acids are applied in low concentrations, use in high concentrations result in epidermolysis. The use of alpha hydroxy acids poses the threat of increasing skin sensitivity to the sun and may cause sunburns [48].

1.3 NATURAL PRODUCTS AS ANTI-AGING INGREDIENTS

The myriad of compounds in natural products present a potential solution to the challenge of delaying aging. Several phytochemicals have anti-aging properties with a number exhibiting rejuvenating effects [50]. Anti-aging agents function through a variety of mechanisms which include antioxidant activity, improved collagen synthesis and protection from collagen breakdown [51]. Anti-aging mediations can interfere with the biochemical and molecular processes which cause aging, reverse signs and symptoms of aging and decrease susceptibility to aging related diseases [41].

1.3.1 Natural antioxidants

Oxidative stress occurs when the levels of ROS overwhelms the antioxidant capacity [52, 53]. Generation of ROS leads to the activation and overproduction of collagenase and elastase thus accelerating the process of aging [17]. Additionally, ROS contribute to the process of aging through oxidative damage to various cell components [54]. Antioxidants interfere with free radical and ROS formation terminating the chain reaction and neutralising it [53]. As a result, they offer protection against photo-damage, skin cancer and they curb inflammation [55].

Antioxidants from plants have been reported to protect against oxidative stress and can be used effectively through topical application [50, 53]. Plant antioxidants can be classified into carotenoids, flavonoids and polyphenols which can be further subdivided into anthocyanins, bioflavonoids, proanthocyanidins, catechins, hydroxycinnamic acids and hydroxybenzoic acids [14]. Natural antioxidants in cells come in different forms which include enzymatic, high molecular weight, non-enzymatic, or low molecular weight antioxidants [54]. Vitamin E (tocopherol) and vitamin C are low molecular weight antioxidants used in cosmetic formulations and cannot be synthesised by the human body [55]. Further, α -tocopherol has

been shown to inhibit protein kinase and hence prevent age dependant collagenase (MMP-1) expression [23]. Additionally, tocopherol has a moisturising effect a characteristic rendering it valuable in cosmetic formulations [55]. Thus, tocopherol is the most popular vitamin used for topical application [56]. It is the most biologically active form of vitamin E, and its mode of action is through the termination of lipid radical chain reactions [56]. Vitamin B3 is another antioxidant commonly used in cosmetics which reduces trans-epidermal water loss [55].

Several phytochemicals have antioxidant activity and can scavenge ROS due to their phenolic hydroxyl groups [57]. Phytochemicals were found to increase the manufacture of antioxidants in rats, additionally phytochemicals with more hydroxyl groups exhibit stronger antioxidant activity [57]. Fruits and vegetables can be used to provide low molecular weight antioxidants so as to protect the skin against ROS initiated aging [54]. Quercetin the flavonoid which is abundant in fruits and vegetables and its derivative quercetin caprylate have been shown to possess antioxidant properties which influence cellular lifespan [50]. Topical application of an amino acid derivative N-acetyl cysteine (NAC) increases levels of potent antioxidant glutathione [33]. In addition it prevents the breakdown of collagen by blocking UV induced protein kinase activation [33].

1.3.2 Retinoids

Retinoids are natural and synthetic vitamin A derivatives, they interfere with some harmful effects of UV radiation through their ability to absorb wavelengths in the UV-visible range because of their long conjugated double bond system thus acting as sunfilters [52]. Vitamin A cannot be synthesised by the body, naturally it occurs as retinyl esters and beta-carotene [58]. Unlike systemic retinoids, topical retinoids are able to add to the skin high amounts of retinol and retinyl esters [52]. Tretinoin (retinoic acid) is a retinoid widely researched on due to its association with treatment of intrinsic and photo aging [58]. Retinoic acid is used to treat signs

of aging which include wrinkle lines [33]. Short term studies revealed that tretinoin was potent against skin aging [58]. Tretinoin activates synthesis of collagen 1 and prevents its loss from the papillary dermis of sun-exposed skin [33]. Topical retinol was found to improve the fine wrinkles associated with aging [24]. It functions in chronically aged skin the same way it does in photo-aged skin through a reduction of matrix metalloproteinase expression and stimulation of collagen synthesis [12]. Additionally, topical retinoid inhibits dermal collagen breakdown [59]. Vitamin A occurs naturally as retinol in red, yellow, and orange fruits and vegetables, further, retinol can be oxidised to retinaldehyde which can subsequently be converted to retinoic acid through oxidation as well [56]. Application of topical retinoids may, however, cause itching, burning, erythema and skin peeling, this limits its use in some patients [59].

1.3.3 Vitamin D

Vitamin D is applied to the skin and can be taken orally, it maintains the bony architecture over which the skin is wrapped [56]. It is applied topically mainly to increase the capacity of the skin to hold water [56]. Vitamin D is important for maintenance of calcium homeostasis [41]. Consequently, it plays a critical role in maintenance of facial bones, improper mineralisation leads to bone loss which subsequently results in wrinkling of the skin covering the mouth and inward turning of the lips [56]. Vitamin D is synthesised when the body is exposed to sunlight [56]. There have been controversies over the sunscreens and protection from the sun as this may have the effect of inhibiting formation of vitamin D by the body resulting in vitamin D deficiency [60]. The effects of vitamin D deficiency which include osteopenia, osteoporosis and osteomalacia increase the risk of fracture [41, 60].

1.3.4 Vitamin C

Ascorbic acid commonly known as vitamin C is abundant in citrus fruits and dark green leafy vegetables [51]. Ascorbic acid is involved in a myriad of reactions as a cofactor supplying

electrons which reduce molecular oxygen [61]. The vitamin stimulates the synthesis of collagen but it cannot be synthesised by the human body, as a result its deficiency results in scurvy a disease associated with a malfunctioning in synthesis of collagen [55, 62]. Topically applied vitamin C on dermal cells increased the messenger RNA levels of collagen type I, type III and that of three procollagen processing enzymes [51]. Ascorbic acid has many functions in skin health and in combating skin ageing [62]. Nevertheless, ascorbic acid is innately unstable, product instability and insufficient skin penetration limit its use in topical products [61, 62]. On the other hand L-ascorbic acid has no reported adverse effects and can be safely used in the treatment of photo aging [61]. As a result, L-ascorbic acid and its ester form ascorbyl palmitate are commonly used in cosmetic formulations instead of ascorbic acid [51].

1.4 TRADITIONAL USES OF PLANTS FOR CURING SKIN AILMENTS AND FOR COSMETIC PURPOSES

Plants have been used for cosmetic purposes since ancient times and are still relevant to date, forming the basis for the development of modern day herbal cosmetics and inspiring synthesis of compounds for use in new cosmetics [14]. Due to the diversity of compounds present in plants, traditional herbal medicines possess huge potential for discovery of new extracts, fractions or pure compounds which can be developed into novel cosmetic ingredients. Plants have been traditionally used in different parts of the world for curing skin diseases and for cosmetic purposes. According to a review by Samuelsen et al.[63], the plant *Plantago major* L. has been used in folkloric medicine in various countries for curing skin related ailments. Its leaves were used in Hawaii, Norway, Turkey, Guatemala for the treatment of abscesses, in Guatemala and Norway, the plant has been used to treat dermatitis.

In Traditional Chinese medicine, plants have been used to treat skin conditions like hyperpigmentation. This condition is a skin disorder in which melanin is overproduced, it is

usually linked to too much exposure to the sun and overactivity of tyrosinase which catalyses the synthesis of melanin, inhibitors of tyrosinase are therefore used to stop the production of melanin and hence are used in skin whitening [64, 65]. The herbs *Pharbitis nil*, *Sophora japonica*, *Spatholobus suberectus* and *Morus alba* traditionally used in Chinese medicine for skin-care were shown to be potent tyrosinase inhibitors thus validating their traditional use in skin care [64]. In another study, 50 herbal extracts prepared from 32 herbs used in traditional Chinese medicine for skin whitening were screened for tyrosinase activity. Extracts from the plants *Ampelopsis japonica*, *Lindera aggregate* and *Polygonatum odoratum* showed inhibition against mushroom and cellular tyrosinase activity [63].

The flower *Tagetes erecta* is traditionally used in India for the treatment of several skin ailments including sores, burns wounds, eczema [31]. Saikia et al.[66] investigated the plants used by communities in India for treatment of skin diseases and for cosmetics. Wrinkled skin is treated by drinking *Mangifera indica* and *Citrus medica* fruit juice, topical application of crushed leaves of *Melia azedarach*, *Lawsonia inermis* and *Embllica officinalis* fruit paste. To attain a fair and beautiful face, juice from *Lycopersicon esculentum* fruit is taken orally and *Citrus odorata* fruit juice is applied to the face. For a smooth and fair skin ripe *Mangifera indica* is taken with cow `s milk, *Curcuma longa* roots are pulverised and applied to the skin, *Citrus odorata* fruit juice is applied to the skin and powdered *Pterocarpus santalinus* wood is applied to the face. To soften dry skin, *Citrus Limon* fruit juice is applied topically, *Sesbania grandiflora* crushed flower is applied to the skin and crushed *Melia azedach* leaves are applied onto the skin. Scabies is treated by taking a drink made from crushed *Foeniculum vulgare* seeds, topically applying *Lycopersicon esculentum* fruit juice, washing infected area with boiled *Melia azedarach* leaves and applying crushed *Cajanus cajan* seeds on to infected area. In order to cure leprosy, a paste of roots of *Thevetia nerifolia* is applied on the infected area, the juice from leaves of *Osbeckia napalensis* is applied on to the infected area and an aqueous extract of *Justicia adhatoda* leaves is taken orally. Several other skin conditions including ringworms,

pimples, skin burns, eczema, urticaria, measles, toe cracks and cellulites have traditional treatments from plants in Assam state.

In the African communities, plants have also been traditionally used in a variety of cosmetic applications and in treatment of a wide range of skin diseases. The plant *Schotia brachypetala* is traditionally used in South African communities for cosmetic purposes, it is used for washing the body, applied to the face for treatment of pimples and *Peltophorum africanum* is applied on to wounds [17]. Lall and Kishore. [67] reported on South African plants used for cosmetic purposes which include *Sideroxylon inerme* plant is traditionally used for skin lightening by the Zulu and Xhosa tribes of South Africa; oil from the Marula kernel is used as a massage and body lotion and to protect against dry and cracked skin; oil from the rosemary plant is used for aromatherapy, for cosmetic purposes and as a perfume and *Citrus lanatus* is used to make soap and face masks from the fruit are used a cosmetic. Mapunya et al.[65] also reported of several South African plants which are traditionally used for cosmetic purposes; from the Aloe genus *Aloe aculeata* and *Aloe pretoriensis* are used as skin lighteners; *Aloe vera* is used to treat minor burns and scars from sunburn; *Calodendrum capensis* is used as a facial mask, for making soap and as a skin lightener; *Harpephyllum caffrum* is used as a face mask and further for treatment of acne and eczema and it is used as a facial sauna; *Ximenia americana* seed oil is used as a cosmetic and skin ointment [65]. Further, Mapunya et al.[65] investigated the tyrosinase inhibition activity of these plants at 500 µg/ml and the results revealed that *Aloe ferox*, *Harpephyllum caffrum* leaves and bark had above 60% inhibition activity thus scientifically validating the use of these plants in skin lightening.

1.5 PHYTOCHEMICALS AS INHIBITORS OF COLLAGENASE AND ELASTASE

Prevention of skin aging is the most effective anti-wrinkle therapy [8]. In order to evade skin aging, it is essential to stop the breakdown of the proteins elastin and collagen which are the

major constituents of the extracellular matrix [9]. Cosmetics have been used to protect the skin from wrinkling, however, some synthetic cosmetics have adverse effects, the most common being allergic and irritant contact dermatitis, phototoxic and photo-allergic reactions [14]. As a result, there has been a growing demand towards herbal cosmeceutical products as they are perceived to be safer and having less known side effects in comparison to synthetic alternatives [68, 69]. Consequently, demand has been shifting from synthetic anti-aging products towards anti-aging ingredients formulated from natural ingredients [68]. This creates a gap for research to be directed towards the discovery and development of phytochemicals with capacity to be formulated into new anti-aging ingredients.

Several studies have shown that plant extracts exhibit elastase and collagenase inhibition activity [17, 31, 70]. Plants have been screened in search of extracts having anti-elastase and anti-collagenase activity [28, 71]. Plant polyphenols including flavonoids, tocopherols, phenolic acids and tannins have exhibited collagenase and elastase inhibition [22, 23, 72]. Further, natural compounds with collagenase and elastase inhibitory activity have been purified for potential application in cosmetic formulation [31]. Maity et al.[31] investigated the *Tagetes erecta* Linn flower for elastase and collagenase inhibition activities. In their study, a methanol extract of fresh *T. erecta* was fractionated and purified using column chromatography with silica gel to produce β -amyrin and syringic acid. The two compounds were screened in the elastase and collagenase inhibition assays. Results revealed that both compounds inhibited collagenase enzyme with the same potency as oleanolic acid the positive control but had lower elastase inhibition activities than oleanolic acid [31].

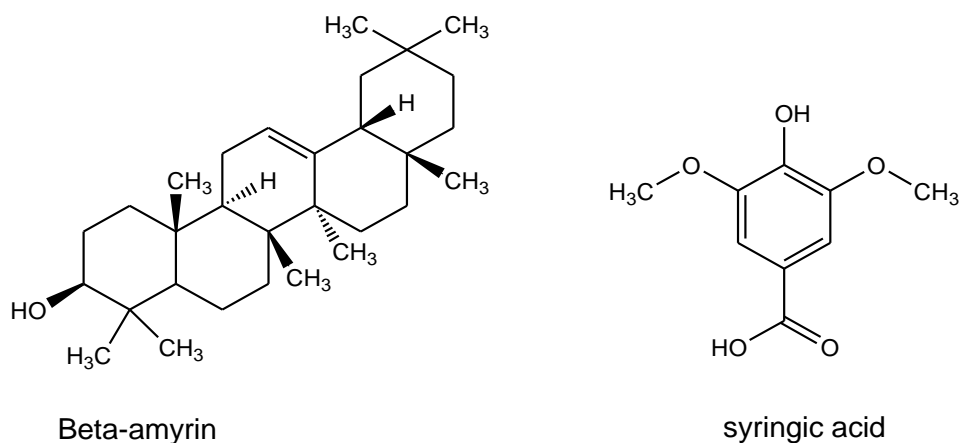


Figure 1.2. Natural compounds β -amyrin and syringic acid isolated from *T. erecta* flower exhibited collagenase inhibition and elastase inhibition activities

Pure active compounds of plant origin showing potential are being formulated into new organic cosmetics [73, 74]. This includes lupeol a triterpenoid (Figure 1.2) which is a secondary metabolite produced by a variety of plant species [10, 75-78]. The triterpenoid has been shown to exhibit elastase inhibition activity [10, 70]. Further lupeol and its esters were shown to promote proliferation of keratinocytes thus verifying the ability of lupeol to promote regeneration of epidermal cells [79]. Studies have also demonstrated the antioxidant activity of lupeol [80]. Based on its anti-aging potential, plant extracts containing lupeol are formulated into anti-aging creams, lotions, gels, lip balms and other products [73]. Generally, products formulated from natural compounds as active ingredients have lower incidence of adverse effects and are thus perceived to be safer than those of synthetic origin [68, 69, 81].

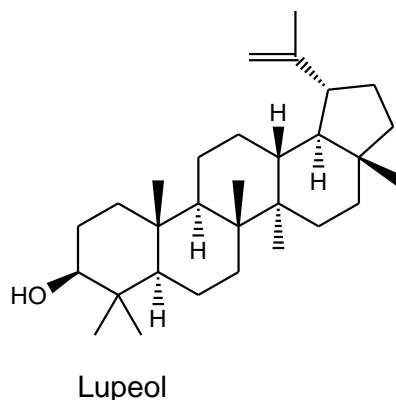


Figure 1.3. Plant extracts containing the anti-aging ingredient lupeol have been developed

1.6 PHYTOCHEMICALS AS POTENTIAL GROWTH PROMOTERS OF ELASTIN AND COLLAGEN

Anti-aging active compounds do not only help to prevent skin damage but they also regenerate new skin components [82]. Degradation of metallo-protein networks with aging leads to hypoactive changes in the skin [83]. The promotion of growth of these metallo-proteins has a renewal effect on the skin [82]. The revival of collagen synthesis has the potential to protect dermal homeostasis against aging [83]. Plant extracts have been shown to promote growth of elastase and collagen [72]. Studies done in the absence of growth factors suggest that bioactive molecules promote synthesis of metallo-proteins through mimicking growth factors in the dermis [83]. Collagen is also involved in wound repair and the growth promoters have been also shown to promote the healing process in wounds. Cinnamaldehyde was identified as the major active component of cinnamon extract which promotes type-1 collagen biosynthesis and as such it can be used to prevent formation of wrinkles [83]. The compound retinol which enhances the growth of dermal collagen production was also revealed to exert its anti-aging properties through enhancing elastin fibre growth [82].

1.7 PROBLEM STATEMENT AND JUSTIFICATION

Plants have been used since medieval times in different communities as sources of food, medicines, cosmeceuticals, religious and other purposes [84, 85]. Natural products from plants have been used traditionally to protect against skin aging, sunburns, to act as skin moisturisers and lighteners [17, 28]. In addition, studies have revealed the anti-aging potential of plant extracts [31, 86]. As such, these have proven to be a potential source of potent, readily available and versatile means of providing skincare. Several local plants in South Africa including *Sclerocarya birrea* (Marula) and *Ficus sycomorus* (Sycamore) have been traditionally used for cosmetic purposes and some of these uses have been reported in literature [67, 87-89]. Further, cosmetic products from the Marula plant have been

commercialised and are on the market with some of the products containing Marula oil having claims to possess anti-aging activities with its use being justified based on its enhanced antioxidant properties [87-89].

Despite the traditional uses of the Sycamore and Marula plants and claims on products on the market, it is surprising that no studies have been carried out to investigate the elastase and collagenase inhibition activities of the *S. birrea* (Marula) and *F. sycomorus* (Sycamore). Elastase and collagenase inhibition activities are critical in determining the anti-aging properties of extracts. Studies to validate traditional uses and claims on commercialised products are necessary to bring confidence to the consumer, protect the consumer and deliver to the consumer the product with properties scientifically proven to be present in the product. Scientific validation will also give confidence which will help to promote utilisation local plant resources in the communities in which the plants are found and create a basis for sustainable utilisation and commercialisation of these plant resources for the benefit of the community and the society at large. Further, it provides a basis for engagements with the industrial community for commercialisation.

In addition to validation of traditional uses of the plants, it is critical that studies be carried out to investigate the phytochemistry and identify ingredients responsible for activity of the plant extracts thus generating new knowledge on these plants. Pure compounds may be more potent in their anti-aging activity and may possess in their pure form potential to be formulated into a wider variety of products for the benefit of the consumer and the society at large. Additionally, there is the possibility of isolating novel compounds with the potential of curbing wider variety ailments. Thus, the reported uses of these plants may be an underestimation of their potential. Purification may optimise the benefits obtainable from these plants. Furthermore, new knowledge on these plants is necessary to boost local production, utilisation

and commercialisation of these indigenous resources. It is thus critical to identify specific components in the Marula and *F. sycomorus* plant extracts which show the biological activities of collagenase and elastase inhibition.

Synthetic cosmetics are used to protect the skin but their demand is lowering due to their potential toxicity and carcinogenic nature [14]. Cosmeceuticals derived from natural products are perceived to be generally safer, more gentle, less toxic, healthier and ecological than synthetically derived ones [68, 69]. Consequently, plant extracts may be better choices for formulating cosmetics due to a lower incidence of adverse effects associated with them [71]. In addition, the trend is going towards more organic products, the shift towards green economy and due to the increase in consumer environmental awareness, it is also critical to develop products which are environmentally friendly while meeting the consumer's needs. A combination of these factors has led to an increase in demand for plant derived cosmeceuticals [68]. This demand creates a need for a wider range of natural cosmetic products to cater for different preferences and requirements. Novel organic cosmetics carry with them the potential to cure skin conditions to which no solutions have yet been found. As such, research to develop new cosmeceuticals from the Marula and *F. sycomorus* plant is required.

With rising demand and growth of use of herbal cosmeceuticals, it is critical to monitor and regulate the quality of herbal products so as to provide standardised botanical cosmeceuticals [90]. Quality control is thus required to guarantee safe use of herbal products. Chemical profiling has been shown to be a useful technique in quality control of herbal medicines [91]. A chemical profile or fingerprint is a unique pattern indicating the presence of various chemical markers in a sample [91]. Chemical profiling can be used for the purpose of authenticating a plant sample to identify if it is the genuine species [91]. If authentication is not done properly,

in trying to meet the growing demand for herbal cosmeceuticals, there may be a risk of intoxication. Nortier et al.[92] reported of kidney failure and kidney cancer in Belgium which was traced back to the mixing of species of Chinese herbs during manufacture. Instead of the herb *Stephaniae tetrandrae radix* which contains tetrandine, the nephrotoxic herb *Aristolochia fangchi* which contains the carcinogenic and mutagenic aristolochic acids was substituted in manufacturing Chinese weight reducing pills. This resulted in 43 patients having end-stage renal failure commonly known as Chinese-herb nephropathy or aristolochia nephropathy. In a review of evidence, Cosyns [93] reported that aristolochia nephropathy was not only restricted to Belgian cases but other cases were observed in other parts of the world. These kidney intoxications in Belgium and other parts of the world could have been prevented by proper quality control in authenticating the plant *S. tetrandrae*. Further, quality control of extracts for formulation of cosmeceuticals is important to ensure that there are no residual solvents which may have adverse effects in the product. Quality control of herbal medicines can also be used to guarantee reliable efficacy through confirmation of the presence of active constituents in the herbal medicine. Consequently, chemical profiles of the Marula and *F. sycomorus* extracts exhibiting anti-aging activities will be developed in this study for quality control purposes.

Due to the harsh African sun a lot of individuals are exposed to UV radiation, however, not many can afford the cost of skin protecting agents [17]. Exploitation of locally available natural products may reduce the cost of producing anti-aging agents making it accessible to more people. Further, utilisation of locally available natural resources provides opportunities for development of the local community through creation of opportunities for employment and business for the local population thus creating local centres of economic growth.

1.8 GOALS AND OBJECTIVES

The goal of this study is to evaluate the potential to develop *Sclerocarya birrea* and *Ficus sycomorus* plant extracts as natural anti-aging ingredients through biological screening against elastase and collagenase enzyme, chemical finger printing of the most suitable extracts for quality control purposes, identification of possible active ingredients and early formulation studies.

The specific objectives of **Chapter 2** were to;

- Determine the most suitable solvents for extraction of anti-aging ingredients from *S. birrea* stems.
- Develop chemical profiles of the most suitable and active extract from *S. birrea* stems for quality control purposes using UPLC-QTOF-MS.
- Bioassay guided fractionation to identify active ingredients from *S. birrea* stems based on elastase and collagenase inhibition activities.
- Process optimisation to produce concentrates of the active ingredients from *S. birrea* stems.

The specific objectives of **Chapter 3** were to;

- Determine the most suitable solvents for extraction of anti-aging ingredients from *F. sycomorus* leaves.
- Develop chemical profiles of the most suitable and active extract from *F. sycomorus* leaves for quality control purposes using UPLC-QTOF-MS.
- Bioassay guided fractionation to identify active ingredients from *F. sycomorus* leaves based on elastase and collagenase inhibition activities.
- Process optimisation to produce concentrates of the active ingredients from *F. sycomorus* leaves.

The specific objective of **Chapter 4** was to;

- Develop stable formulations of an anti-aging day cream and a nourishing night cream using the most suitable anti-aging ingredients identified.

Chapter 5 gives a detailed account of the materials and methods used in the study.

The concluding remarks of the study are discussed in **Chapter 6**.

1.9 REFERENCES

1. Kanitakis J: **Anatomy, histology and immunohistochemistry of normal human skin**. *European Journal of Dermatology* 2002, **12**(4):390-399; quiz 400-391.
2. Raine-Fenning NJ, Brincat MP, Muscat-Baron Y: **Skin aging and menopause**. *American Journal of Clinical Dermatology* 2003, **4**(6):371-378.
3. Slominski A, Wortsman J: **Neuroendocrinology of the Skin**. *Endocrine Reviews* 2000, **21**(5):457-487.
4. Khavkin J, Ellis DA: **Aging skin: histology, physiology, and pathology**. *Facial plastic surgery clinics of North America* 2011, **19**(2):229-234.
5. Farage MA, Miller KW, Elsner P, Maibach HI: **Structural characteristics of the aging skin: a review**. *Cutaneous and ocular toxicology* 2007, **26**(4):343-357.
6. McLafferty E, Hendry C, Farley A: **The integumentary system: anatomy, physiology and function of skin**. *Nursing standard* 2012, **27**(3):35-42.
7. Finch M: **Assessment of skin in older people: As the largest organ in the body, the skin can offer valuable information about the general health of an older person. Mary Finch explains how**. *Nursing older people* 2003, **15**(2):29-30.
8. Kuwazuru O, Saothong J, Yoshikawa N: **Mechanical approach to aging and wrinkling of human facial skin based on the multistage buckling theory**. *Medical Engineering & Physics* 2008, **30**(4):516-522.
9. Ganceviciene R, Liakou AI, Theodoridis A, Makrantonaki E, Zouboulis CC: **Skin anti-aging strategies**. *Dermato-endocrinology* 2012, **4**(3):308-319.
10. Ko RK, Kim GO, Hyun CG, Jung DS, Lee NH: **Compounds with tyrosinase inhibition, elastase inhibition and DPPH radical scavenging activities from the branches of *Distylium racemosum* Sieb. et Zucc.** *Phytotherapy Research* 2011, **25**(10):1451-1456.
11. Rees JL: **The genetics of sun sensitivity in humans**. *The American Journal of Human Genetics* 2004, **75**(5):739-751.
12. Varani J, Warner RL, Gharaee-Kermani M, Phan SH, Kang S, Chung J, Wang Z, Datta SC, Fisher GJ, Voorhees JJ: **Vitamin A antagonizes decreased cell growth and elevated collagen-degrading matrix metalloproteinases and stimulates collagen accumulation in naturally aged human skin**. *Journal of Investigative Dermatology* 2000, **114**(3):480-486.
13. Sahasrabudhe A, Deodhar M: **Anti-hyaluroiüdase, Anti-elastase Activity of *Garcinia indica***. *International Journal of Botany* 2010, **6**(3):299-303.
14. Mukherjee PK, Maity N, Nema NK, Sarkar BK: **Bioactive compounds from natural resources against skin aging**. *Phytomedicine* 2011, **19**(1):64-73.

15. Madhan B, Krishnamoorthy G, Rao JR, Nair BU: **Role of green tea polyphenols in the inhibition of collagenolytic activity by collagenase.** *International Journal of Biological Macromolecules* 2007, **41**(1):16-22.
16. Baumann L: **Skin ageing and its treatment.** *The Journal of pathology* 2007, **211**(2):241-251.
17. Ndlovu G, Fouché G, Tselanyane M: **In vitro determination of the anti-aging potential of four southern Africa medicinal plants: Poster.** *BMC Complementary and Alternative Medicine* 2013, **13**(304):1-7.
18. El-Domyati M, Attia S, Saleh F, Brown D, Birk D, Gasparro F, Ahmad H, Uitto J: **Intrinsic aging vs. photoaging: a comparative histopathological, immunohistochemical, and ultrastructural study of skin.** *Experimental dermatology* 2002, **11**(5):398-405.
19. Branchet M, Boisnic S, Frances C, Robert A: **Skin thickness changes in normal aging skin.** *Gerontology* 1990, **36**(1):28-35.
20. Gambichler T, Matip R, Moussa G, Altmeyer P, Hoffmann K: **In vivo data of epidermal thickness evaluated by optical coherence tomography: effects of age, gender, skin type, and anatomic site.** *Journal of Dermatological Science* 2006, **44**(3):145-152.
21. Levakov A, Vučković N, Đolai M, Mocko-Kačanski M, Božanić S: **Age-related skin changes.** *Medicinski Pregled* 2012, **65**(5-6):191-195.
22. Lim H, Kim HP: **Inhibition of mammalian collagenase, matrix metalloproteinase-1, by naturally-occurring flavonoids.** *Planta Medica* 2007, **73**(12):1267-1274.
23. Ricciarelli R, Maroni P, Özer N, Zingg J-M, Azzi A: **Age-dependent increase of collagenase expression can be reduced by α -tocopherol via protein kinase C inhibition.** *Free Radical Biology and Medicine* 1999, **27**(7):729-737.
24. Kafi R, Kwak HSR, Schumacher WE, Cho S, Hanft VN, Hamilton TA, King AL, Neal JD, Varani J, Fisher GJ: **Improvement of naturally aged skin with vitamin a (retinol).** *Archives of Dermatology* 2007, **143**(5):606-612.
25. Danhof IE: **Potential reversal of chronological and photo-aging of the skin by topical application of natural substances.** *Phytotherapy Research* 1993, **7**(7):S53-S56.
26. Roy A, Sahu RK, Matlam M, Deshmukh VK, Dwivedi J, Jha AK: **In vitro techniques to assess the proficiency of skin care cosmetic formulations.** *Pharmacognosy Reviews* 2013, **7**(14):97.
27. Zhi-ying Y, Guo-xiong G, Wei-qin Z, Zhe-fu L: **Elastolytic activity from *Flavobacterium odoratum*. Microbial screening and cultivation, enzyme production and purification.** *Process biochemistry* 1994, **29**(6):427-436.
28. Lee KK, Kim JH, Cho JJ, Choi JD: **Inhibitory Effects of 150 Plant Extracts on Elastase Activity, and Their Anti-inflammatory Effects.** *International Journal of Cosmetic Science* 1999, **21**(2):71-82.
29. Manosroi A, Jantrawut P, Akihisa T, Manosroi W, Manosroi J: **In vitro and in vivo skin anti-aging evaluation of gel containing niosomes loaded with a semi-purified fraction containing gallic acid from *Terminalia chebula* galls.** *Pharmaceutical biology* 2011, **49**(11):1190-1203.
30. Labat-Robert J, Fourtanier A, Boyer-Lafargue B, Robert L: **Age dependent increase of elastase type protease activity in mouse skin: Effect of UV-irradiation.** *Journal of Photochemistry and Photobiology B: Biology* 2000, **57**(2):113-118.
31. Maity N, Nema NK, Abedy MK, Sarkar BK, Mukherjee PK: **Exploring *Tagetes erecta* Linn flower for the elastase, hyaluronidase and MMP-1 inhibitory activity.** *Journal of Ethnopharmacology* 2011, **137**(3):1300-1305.
32. Bruce S: **Cosmeceuticals for the attenuation of extrinsic and intrinsic dermal aging.** *Journal of Drugs in Dermatology* 2008, **7**(2 Suppl):s17-22.
33. Konda D, Thappa DM: **Age reversing modalities: An overview.** *Indian Journal of Dermatology, Venereology, and Leprology* 2013, **79**(1):3.

34. Scharffetter–Kochanek K, Brenneisen P, Wenk J, Herrmann G, Ma W, Kuhr L, Meewes C, Wlaschek M: **Photoaging of the skin from phenotype to mechanisms.** *Experimental Gerontology* 2000, **35**(3):307-316.
35. Fischer T, Bergström K: **Evaluation of customers' complaints about sunscreen cosmetics sold by the Swedish pharmaceutical company.** *Contact dermatitis* 1991, **25**(5):319-322.
36. Lowe N, Horwitz S, Tanghetti E, Draelos Z, Menter A: **Tazarotene versus tazarotene plus hydroquinone in the treatment of photodamaged facial skin: A multicenter, double-blind, randomized study.** *Journal of Cosmetic and Laser Therapy* 2006, **8**(3):121-127.
37. Gladstone HB, Nguyen SL, Williams R, Ottomeyer T, Wortzman M, Jeffers M, Moy RL: **Efficacy of hydroquinone cream (USP 4%) used alone or in combination with salicylic acid peels in improving photodamage on the neck and upper chest.** *Dermatologic surgery* 2000, **26**(4):333-337.
38. Draelos ZD: **Novel approach to the treatment of hyperpigmented photodamaged skin: 4% hydroquinone/0.3% retinol versus tretinoin 0.05% emollient cream.** *Dermatologic surgery* 2005, **31**(s1):799-805.
39. Westerhof W, Kooyers T: **Hydroquinone and its analogues in dermatology—a potential health risk.** *Journal of cosmetic dermatology* 2005, **4**(2):55-59.
40. Zhu W, Gao J: **The use of botanical extracts as topical skin-lightening agents for the improvement of skin pigmentation disorders.** In: *Journal of Investigative Dermatology Symposium Proceedings: 2008*; Elsevier; 2008: 20-24.
41. Gammack J, Cepeda OF, Joseph H: **Antioxidants and hormones as antiaging therapies: high hopes, disappointing results.** *Cleveland Clinic Journal of Medicine* 2006, **73**(12):1049.
42. Chotnopparatpattara P, Panyakhamlerd K, Taechakraichana N, Tantivatana J, Chaikittisilpa S, Limpaphayom KK: **An effect of hormone replacement therapy on skin thickness in early postmenopausal women.** *Journal of the Medical Association of Thailand* 2001, **84**(9):1275-1280.
43. Wolff EF, Narayan D, Taylor HS: **Long-term effects of hormone therapy on skin rigidity and wrinkles.** *Fertility and sterility* 2005, **84**(2):285-288.
44. Sumino H, Ichikawa S, Abe M, Endo Y, Ishikawa O, Kurabayashi M: **Effects of aging, menopause, and hormone replacement therapy on forearm skin elasticity in women.** *Journal of the American Geriatrics Society* 2004, **52**(6):945-949.
45. Sauerbronn A, Fonseca A, Bagnoli V, Saldiva P, Pinotti J: **The effects of systemic hormonal replacement therapy on the skin of postmenopausal women.** *International Journal of Gynecology & Obstetrics* 2000, **68**(1):35-41.
46. Brower V: **A second chance for hormone replacement therapy?** *EMBO reports* 2003, **4**(12):1112-1115.
47. Rinaldi A: **Hormone therapy for the ageing.** *EMBO reports* 2004, **5**(10):938-941.
48. Fiume MM: **Alpha Hydroxy Acids.** *International Journal of Toxicology* 2017, **36**(5_suppl2):15S-21S.
49. Van Scott E, Yu R: **Alpha hydroxy acids: procedures for use in clinical practice.** *Cutis* 1989, **43**(3):222-228.
50. Chondrogianni N, Kapeta S, Chinou I, Vassilatou K, Papassideri I, Gonos ES: **Anti-ageing and rejuvenating effects of quercetin.** *Experimental gerontology* 2010, **45**(10):763-771.
51. Chiu A, Kimball A: **Topical vitamins, minerals and botanical ingredients as modulators of environmental and chronological skin damage.** *British Journal of Dermatology* 2003, **149**(4):681-691.
52. Sorg O, Saurat J-H: **Topical retinoids in skin ageing: a focused update with reference to sun-induced epidermal vitamin A deficiency.** *Dermatology* 2014, **228**(4):314-325.
53. Lopez-Torres M, Thiele J, Shindo Y, Han D, Packer L: **Topical application of -tocopherol modulates the antioxidant network and diminishes ultraviolet-**

- induced oxidative damage in murine skin.** *British Journal of Dermatology* 1998, **138**(2):207-215.
54. Podda M, Grundmann-Kollmann M: **Low molecular weight antioxidants and their role in skin ageing.** *Clinical and experimental dermatology* 2001, **26**(7):578-582.
 55. Ramos-e-Silva M, Celem LR, Ramos-e-Silva S, Fucci-da-Costa AP: **Anti-aging cosmetics: Facts and controversies.** *Clinics in Dermatology* 2013, **31**(6):750-758.
 56. Draelos ZD: **Nutrition and enhancing youthful-appearing skin.** *Clinics in Dermatology* 2010, **28**(4):400-408.
 57. Si H, Liu D: **Dietary antiaging phytochemicals and mechanisms associated with prolonged survival.** *The Journal of nutritional biochemistry* 2014, **25**(6):581-591.
 58. Mukherjee S, Date A, Patravale V, Korting HC, Roeder A, Weindl G: **Retinoids in the treatment of skin aging: an overview of clinical efficacy and safety.** *Clinical interventions in aging* 2006, **1**(4):327.
 59. Darlenski R, Surber C, Fluhr J: **Topical retinoids in the management of photodamaged skin: from theory to evidence-based practical approach.** *British Journal of Dermatology* 2010, **163**(6):1157-1165.
 60. Holick MF: **Optimal vitamin D status for the prevention and treatment of osteoporosis.** *Drugs and aging* 2007, **24**(12):1017-1029.
 61. Zussman J, Ahdout J, Kim J: **Vitamins and photoaging: Do scientific data support their use?** *Journal of the American Academy of Dermatology* 2010, **63**(3):507-525.
 62. Nusgens BV, Colige AC, Lambert CA, Lapière CM, Humbert P, Rougier A, Haftek M, Richard A, Creidi P: **Topically applied vitamin C enhances the mRNA level of collagens I and III, their processing enzymes and tissue inhibitor of matrix metalloproteinase 1 in the human dermis.** *Journal of Investigative Dermatology* 2001, **116**(6):853-859.
 63. Ye Y, Chou G-X, Mu D-D, Wang H, Chu J-H, Leung AK-M, Fong W-f, Yu Z-L: **Screening of Chinese herbal medicines for antityrosinase activity in a cell free system and B16 cells.** *Journal of Ethnopharmacology* 2010, **129**(3):387-390.
 64. Wang K-H, Lin R-D, Hsu F-L, Huang Y-H, Chang H-C, Huang C-Y, Lee M-H: **Cosmetic applications of selected traditional Chinese herbal medicines.** *Journal of ethnopharmacology* 2006, **106**(3):353-359.
 65. Mapunya MB, Nikolova RV, Lall N: **Melanogenesis and antityrosinase activity of selected South African plants.** *Evidence-Based Complementary and Alternative Medicine* 2012, **2012**.
 66. Saikia AP, Ryakala VK, Sharma P, Goswami P, Bora U: **Ethnobotany of medicinal plants used by Assamese people for various skin ailments and cosmetics.** *Journal of Ethnopharmacology* 2006, **106**(2):149-157.
 67. Lall N, Kishore N: **Are plants used for skin care in South Africa fully explored?** *Journal of Ethnopharmacology* 2014, **153**(1):61-84.
 68. Chermahini SH, Majid FAA, Sarmidi MR: **Cosmeceutical value of herbal extracts as natural ingredients and novel technologies in anti-aging.** *Journal of Medicinal Plants Research* 2011, **5**(14):3074-3077.
 69. Mondal SC, Singh P, Kumar B, Singh SK, Gupta SK, Verma A: **Ageing and potential anti-aging phytochemicals: an overview.** *World Journal of Pharmacy and Pharmaceutical Sciences* 2014, **4**(1):426-454.
 70. Mitaine-Offer A-C, Hornebeck W, Sauvain M, Zèches-Hanrot M: **Triterpenes and phytosterols as human leucocyte elastase inhibitors.** *Planta Medica* 2002, **68**(10):930-932.
 71. Moon J-Y, Yim E-Y, Song G, Lee NH, Hyun C-G: **Screening of elastase and tyrosinase inhibitory activity from Jeju Island plants.** *Eurasian Journal of Biosciences* 2010, **4**:41-53.
 72. Takeshi D, Sansei N, Yoshihisa N: **Constituents and pharmacological effects of Eucommia and Siberian Ginseng.** *Acta Pharmacologica Sinica* 2001, **22**:1057-1070.
 73. Majeed M, Prakash L: **Novel natural approaches to anti-aging skin care.** *Cosmetics & Toiletries Manufacture Worldwide* 2005:11-15.

74. Alander J, Andersson A-C: **The shea butter family—the complete emollient range for skin care Formulations.** *Cosmetics and Toiletries Manufacture Worldwide* 2002, **1**:28-32.
75. Shirwaikar A, Setty MM, Bommu P, Krishnanand B: **Effect of lupeol isolated from Crataeva nurvala Buch.-Ham. stem bark extract against free radical induced nephrotoxicity in rats.** *Indian Journal of Experimental Biology* 2004, **42**:686-690.
76. Saratha V, Pillai SI, Subramanian S: **Isolation and characterization of lupeol, a triterpenoid from Calotropis gigantea latex.** *International Journal of Pharmaceutical Sciences Review and Research* 2011, **10**(2):54-56.
77. Harish B, Krishna V, Kumar HS, Ahamed BK, Sharath R, Swamy HK: **Wound healing activity and docking of glycogen-synthase-kinase-3- β -protein with isolated triterpenoid lupeol in rats.** *Phytomedicine* 2008, **15**(9):763-767.
78. Agarwal R, Rangari V: **Antiinflammatory and antiarthritic activities of lupeol and 19 alpha-H lupeol isolated from Strobilanthus callosus and Strobilanthus ixiocephala roots.** *Indian Journal of Pharmacology* 2003, **35**(6):384-387.
79. Nikiema J, Vanhaelen-Fastré R, Vanhaelen M, Fontaine J, De Graef C, Heenen M: **Effects of antiinflammatory triterpenes isolated from Leptadenia hastata latex on keratinocyte proliferation.** *Phytotherapy Research* 2001, **15**(2):131-134.
80. Gupta R, Sharma AK, Sharma M, Dobhal M, Gupta R: **Evaluation of antidiabetic and antioxidant potential of lupeol in experimental hyperglycaemia.** *Natural Product Research* 2012, **26**(12):1125-1129.
81. Deyama T, Nishibe S, Nakazawa Y: **Constituents and pharmacological effects of Eucommia and Siberian ginseng.** *Acta Pharmacologica Sinica* 2001, **22**(12):1057-1070.
82. Rossetti D, Kielmanowicz M, Vigodman S, Hu Y, Chen N, Nkengne A, Oddos T, Fischer D, Seiberg M, Lin C: **A novel anti-ageing mechanism for retinol: induction of dermal elastin synthesis and elastin fibre formation.** *International Journal of Cosmetic Science* 2011, **33**(1):62-69.
83. Takasao N, Tsuji-Naito K, Ishikura S, Tamura A, Akagawa M: **Cinnamon extract promotes type I collagen biosynthesis via activation of IGF-I signaling in human dermal fibroblasts.** *Journal of Agricultural and Food chemistry* 2012, **60**(5):1193-1200.
84. Lansky EP, Paavilainen HM, Pawlus AD, Newman RA: **Ficus spp.(fig): Ethnobotany and potential as anticancer and anti-inflammatory agents.** *Journal of Ethnopharmacology* 2008, **119**(2):195-213.
85. Galil J, Eisikowitch D: **On the pollination ecology of Ficus sycomorus in East Africa.** *Ecology* 1968, **49**(2):259-269.
86. Süntar I, Akkol EK, Keles H, Yesilada E, Sarker SD, Baykal T: **Comparative evaluation of traditional prescriptions from Cichorium intybus L. for wound healing: stepwise isolation of an active component by in vivo bioassay and its mode of activity.** *Journal of Ethnopharmacology* 2012, **143**(1):299-309.
87. Komane B, Vermaak I, Summers B, Viljoen A: **Safety and efficacy of Sclerocarya birrea (A. Rich.) Hochst (Marula) oil: A clinical perspective.** *Journal of Ethnopharmacology* 2015, **176**:327-335.
88. Mckenzie LP: **Topical composition for the treatment of scar tissue.** In.: Patent WO 03/092634 A2; 2003.
89. Charlier DCP, Raynard M, Lombard CN: **Antioxidants based on Anacardiaceae species, methods for obtaining same and uses thereof.** In.: Patent WO2006097806A1; 2006.
90. Patwardhan B, Warude D, Pushpangadan P, Bhatt N: **Ayurveda and traditional Chinese medicine: a comparative overview.** *Evidence-Based Complementary and Alternative Medicine* 2005, **2**(4):465-473.
91. Li S, Han Q, Qiao C, Song J, Cheng CL, Xu H: **Chemical markers for the quality control of herbal medicines: an overview.** *Chinese Medicine* 2008, **3**(1):7.

92. Nortier JL, Martinez M-CM, Schmeiser HH, Arlt VM, Bieler CA, Petein M, Depierreux MF, De Pauw L, Abramowicz D, Vereerstraeten P: **Urothelial carcinoma associated with the use of a Chinese herb (Aristolochia fangchi)**. *New England Journal of Medicine* 2000, **342**(23):1686-1692.
93. Cosyns J-P: **Aristolochic acid and 'Chinese herbs nephropathy'**. *Drug Safety* 2003, **26**(1):33-48.

CHAPTER 2: *Sclerocarya birrea* (MARULA)

2.1 BOTANY AND SPATIAL DISTRIBUTION

Sclerocarya birrea (A. Rich.) Hochst commonly known as Marula is member of Anacardiaceae, the Mango family (Figure 2.1). The tree is known as Marula or Cider tree in English; Morula in Pedi and Tswana; Umganu in siNdebele, Zulu and siSwati; Mupfura in Shona; Mpfula in Chichewa, Muua in Kikamba, Mngongo in KiSwahili and Maroela in Afrikaans [1, 2]. It is a tree with a spreading crown which can reach a height of between 7 m and 18 m and has a trunk of an average diameter of 80 cm [2-5]. The Marula tree is mainly dioecious, however, monoecious trees have been reported to occur [2]. This deciduous, mammal dispersed plant can thrive in areas with an annual rainfall of as low as 500 to 600 mm and exists in altitudes ranging from sea level to 1800 m [4, 5]. Well drained soils are desirable for the tree although it can survive in a wide variety of soils [5]. Its alternate and compound leaves are divided into 10 or more leaflet pairs of 60 mm in length and are concentrated near the ends of the branches [6-9]. The top part of the ovate to elliptic shaped leaflets is characterized by a dark green colour and a lighter blue-green colour is found below the leaflets [5]. Its flowers have red sepals and yellow petals and are in small oblong clusters [6-8]. Its large rounded, slightly flattened fruits of about 30 mm diameter weigh approximately 20-25 g [7, 10]. The fruits have a dull to light yellow colour when ripe and a leathery skin covering a white fibrous fleshy pulp [10]. Its bark is flaky with a mottled appearance [7].

The genus *Sclerocarya* is restricted to Africa and Madagascar, its large distribution and associated genera in Africa suggests that it originates from the African continent [11, 12]. There are three documented subspecies of *S. birrea* which are subsp. *birrea*, subsp. *caffra* and subsp. *multifoliolata* [12]. Subspecies *caffra* is mainly distributed in the southern parts of Africa in countries including South Africa, Namibia, Swaziland, Botswana, Angola, Zimbabwe, Zambia, Mozambique and Malawi [2-4, 12-14]. In the northern, western and east tropical

parts of Africa, there is subspecies *birrea* which mainly distributed from Senegal to Ethiopia and south of Tanzania Sudan and Eritrea [3, 4, 11, 12]. Subspecies *multifoliolata* is restricted to Tanzania and probably some parts of neighboring Kenya [11, 12]. Marula plant is a widespread species throughout the semiarid, deciduous savannas of much of sub-Saharan Africa [2].

A. Marula tree



B. Marula stem, leaves and fruits



C. Young Marula softwood stems



Figure 2.1 Picture A showing the Marula tree, picture B shows a stem with leaves and fruits from the Marula plant and Picture C shows young Marula softwood stems used in this study.

2.2 TRADITIONAL USES OF THE PLANT

Marula fruits are some of the most commonly used fruits in Africa (Figure 2.1) [15]. They are used to make beer, consumed as whole fresh fruit and is processed into jam, juice or jelly [10, 13]. Dried skin from the fruits are reportedly used as a substitute for coffee [10]. Its kernels are eaten as a snack, taken with spinaches and are enjoyed with the main meal [2, 16]. Cooking oil is also extracted from the kernel [17] while the kernel is also used for flavoring and preserving foods [2]. The fruit and its kernel are also sold to generate household income [10]. Further, communities in Sudan use the fruits for medicinal purposes, fresh fruit juice is rubbed on to the body to stop itching or insect bite [11]. Marula stem bark is traditionally used in communities of South Africa in the management of pain, inflammatory conditions, type-2 diabetes mellitus and proctitis [7, 18]. Other South African communities use the stem-bark to control childhood convulsions and epilepsy [19]. Several African communities use the bark to treat a variety of bacterial related infections and dysentery [18]. The bark is also used in the treatment of dysentery and diarrhea [20]. In Sudan, dried ground Marula bark is sprinkled on wounds for wound healing, the bark is also soaked in cold water or boiled and the infusion is taken as a drink for the treatment of Malaria, stomach-ache, diarrhea, haemorrhoids, cough and tuberculosis [11]. Gathirwa et al. [21] reported the traditional use of *S. birrea* plant for the treatment of malaria and as a febrifuge. Sudanese communities use the roots for the treatment of swelling and gonococci healing [11]. Leaves and roots of the plant are reported to be used by some Tanzanian communities as an antidote for snake poisons [22]. In Sudan communities, the sap from young leaves is used to treat sore eyes, the leaves are used to stimulate milk production for lactating mothers and as livestock feed [11]. Marula leaf essence is to treat boils, burns and spider bites [2]. Further, leaves from the plant are cooked and taken as a relish [16]. Wood from the plant is used for fencing, carving and fuel [10].

2.3 COSMETIC APPLICATIONS

Several southern African communities, extract oil from the kernel of the Marula seed and use it for a wide range of cosmetic purposes such as skin moisturising, maintenance of healthy skin, soap production and to wash dry, damaged and fragile hair [2, 10, 23]. Oil from *S. birrea* kernels was formulated for application in the area around wounds or scars for their treatment and prevention of formation of scar tissue [24]. In another report, a French company Aldivia working with Phytotrade Africa developed and patented a Marula oil product possessing high antioxidant properties [25]. Leaves from the *S. birrea* plant are also reported to have been used in folkloric medicine for acne and other skin conditions [26]. The leaves and roots are used by some communities in Tanzania and South Africa to prepare a topical application for the treatment of skin fungal infections [22]. Similarly, the plant is used in traditional South African medicine for treatment of skin fungal infections [17]. The pressed oil extracted from Marula peel was reported to have been used in cosmetic applications [27]. A recent clinical study evaluated the irritancy potential, occlusivity properties, moisturizing and hydrating effects of Marula oil [23]. The study revealed that the oil provides moisturising, hydrating and occlusive effects after topical application. Although reports of traditional use of Marula oil and other parts of the plant for cosmetic purposes have been made [26], a detailed scientific analysis of the Marula plant for its anti-aging potential has not yet been reported.

2.4 PREVIOUSLY REPORTED BIOASSAYING OF MARULA

Traditional use of different parts of the Marula plant for medicinal purposes have led the scientific community to seek to validate claims and explore opportunities for development of new drugs for the market. Eloff et al. [18] showed that acetone extracts of inner bark, outer bark and leaf extracts of Marula exhibited antibacterial activity towards *Staphylococcus aureus*, *Pseudomonas aeruginosa*, *Escherichia coli* and *Enterococcus faecalis*. The three extracts had minimum inhibitory concentrations from 0.15 to 3 mg/ml with the inner bark extract exhibiting the highest potency [18]. These results provide scientific validation of the

traditional use of Marula bark in the treatment of bacteria-related diseases by African communities and further revealed that the leaves which also possess antibacterial activity can be used as a replacement for the bark as continued use of the bark may be detrimental to the plant [18]. A study was undertaken by Ojewole et al. [7] to scientifically validate traditional claims of the analgesic, anti-inflammatory and anti-diabetic properties of the aqueous extract of Marula stem bark using mice and rat as models. Results revealed that the extract produced a dose-dependent protection against electrical induced pain and a dose-dependent reduction in the fresh egg albumin induced acute inflammation in the rat [7]. Further, moderate-high doses of the aqueous extract produced dose-dependent reductions in blood glucose concentrations of fasted and diabetic rats. The study validates the traditional use of the stem bark in control of pain, inflammation, adult onset and type 2 diabetes mellitus [7]. The traditional use of *S. birrea* bark in the treatment of diarrhea was investigated in a rat model by Galvez et al. [28]. A decoction of the Marula bark demonstrated antidiarrheal activity through inhibition of a net secretion of fluid and electrolytes induced by magnesium sulphate and sodium picosulphate thus justifying the traditional claims of the antidiarrheal activity of Marula bark [28]. Masoko et al. [17] investigated the use of Marula bark in traditional South African medicine as a treatment for skin fungal diseases. Hexane, DCM, chloroform, ethyl acetate, acetone, methanol and ethanol were used to prepare extracts of Marula bark and the results revealed that the polar acetone, ethanol and methanol extracts of *S. birrea* stem bark exhibited antifungal activity against *Candida parapsilosis* thus verifying the traditional claims and further demonstrating the potential for application of Marula stem bark in skin fungal treatments [17]. The anti-biofilm properties of a methanolic extract of Marula bark were investigated to explore the possibility of fighting antimicrobial resistance of bacterial biofilms [20]. The study revealed that the extract had an antibiofilm activity of about 75% at 100 µg/ml and further inhibited swarming ability of the cells. The study also validated the traditional use of the bark in treatment of dysentery and diarrhea. The traditional use of Marula stem-bark for control of convulsions was investigated by Ojewole et al. [19]. The aqueous extract of the stem bark was found to inhibit pentylentetrazole, picrotoxin and bicuculline induced seizures and further

delayed the onset of pentylenetetrazole induced convulsions [19]. The study provided scientific evidence validating the traditional medicinal use of the Marula bark in controlling convulsions.

Moyo et al. [29] studied the antioxidant, acetylcholinesterase on parts of *S. birrea* Marula which revealed that extracts from the plant possessed higher antioxidant activity than butylated hydroxytoluene and the dichloromethane and methanol extracts inhibited acetylcholinesterase in a dose dependent manner [29]. The study concluded that the bark and leaves have potential to be developed into food additives with antioxidant properties. The aqueous extract of Marula stem bark was investigated for vasorelaxant and hypotensive effects using a rat model [8]. Addition of *S. birrea* stem bark aqueous extract from 12.5 to 200 mg/ml to bath fluid resulted in concentration dependent relaxations and reduction in heart rates of anaesthetized and hypersensitive rats [8]. Gondwe et al. [30] investigated the hypoglycemic properties of the ethanolic extract of Marula stem bark on major complications of diabetic mellitus, blood glucose, renal function, and mean arterial blood pressure in non-diabetic and streptozotocin-induced diabetic rats. The extract showed a dose-dependent reduction in blood glucose concentration. It had no effect on the secretion of plasma insulin in non-diabetic rats and chronic administration of the stem extract lowered plasma urea and creatinine concentrations of streptozotocin-induced diabetic rats accompanied by an increase in the glomerular filtration rate. Further, the stem extract lowered blood pressure in all animals tested [30]. Gathirwa et al. [21] showed that the aqueous extract of *S. birrea* stem bark extract has anti-plasmodial activity.

2.5 PHYTOCHEMISTRY

2.5.1 Marula stems

Phytochemical analysis of Marula leaf and bark extracts was done using standard phytochemical screening reagents with the aim of determining the classes of compounds present in these plant parts [31]. Results obtained revealed that the bark and leaf extracts contained alkaloids, flavonoids, phenol, tannins, terpenoids and saponins [31]. Moyo et al. [29] evaluated the phenolic composition of *S. birrea* young stems, leaves and operculum (well defined part of the endocarp). The young stems had the highest total phenolic content of 14.15 ± 0.03 mg gallic acid equivalent (GAE/g), flavonoid content of 1.21 ± 0.01 mg catechin equivalent (CE/g) and gallotannins (0.24 ± 0.00 mg GAE/g) and proanthocyanidins (1.25%). The abundance of a wide range of compounds in the Marula stems explain the several reported traditional and scientifically validated medicinal applications of Marula stems. The compound (-)-epicatechin-3-galloyl ester promoting secretion of fluids and electrolytes in rat colon was isolated from a methanol extract of the bark of the Marula [32]. The extract was partitioned into an aqueous and ethyl acetate fraction, column chromatography of the ethyl acetate fraction on a silica gel column resulted in isolation of the epicatechin derivative. A condensed tannin was isolated from a methanolic extract of the bark of *S. birrea* collected in Burkina Fasso. The compound was identified as procyanidin using TLC, UV-VIS and HPLC by comparison with a pure standard [28] and was shown to have anti-aging effects through attenuation of oxidative stress [33].

The chemical profile of Marula bark, roots and leaves extracted using hexane, chloroform, methanol, ethyl acetate and water and their antioxidant activity was reported by Russo et al. [34]. Chemical analysis was done using high performance liquid chromatography-tandem mass spectrometry (HPLC-MS/MS). A total of 36 compounds were identified with flavonoid glycosides abundant in leaf extracts and galloylated tannins prominent in bark and root extracts. In another study reverse-phase HPLC coupled to a Q-TOF-MS was used to evaluate

the chemical profile of extracts of Marula bark which led to the identification of a total of 95 compounds classified mainly into organic acids, polyphenols and fatty acid derivatives [35]. Identification of many different types of compounds from the Marula stem bark is essential in explaining the myriad of traditional medicinal applications of the Marula stem bark.

2.5.2 Marula fruit and seed

The composition of *S. birrea* fruit juice grown in Israel was studied, minerals sodium and potassium were determined using flame photometer, calcium, magnesium, iron, zinc, and manganese were analysed using atomic absorption spectrometer, chloride ions were measured using a chloride analyser [36]. Total soluble solids were determined using a refractometer, pH and titratable acidity were determined using a food electrode, protein content was measured spectrophotometrically, total soluble phenolic content was determined using the Folin Ciocalteu method, sugar and vitamin C content were determined using HPLC method [36]. The results revealed that Marula juice had high vitamin C (267 mg/dL) and potassium (328 mg/dL) and low sugar concentration (7.3 g/dL), significant levels of phenolics (56 mg of pyrogallol equiv/dL) and vitamin C (383 mg/dL). Analysis of a methanolic extract of *S. birrea* fruit pulp and peel from Zimbabwe was done using colorimetric as well as HPLC methods. Results revealed that there was a higher concentration of flavonoids, total phenolics and condensed tannins in the pulp as compared to the peel. The compounds, caffeic acid, vanillic acid, p-hydroxybenzaldehyde, ferulic acid, p-hydroxybenzoic acid and p-coumaric acid were identified in the peel. In comparison the pulp contained caffeic acid, ferulic acid and p-coumaric acid [14]. In another study done by Song et al. [37] caffeic acid was found to stimulate collagen-like polymer production. Saija et al. [38] showed that caffeic and ferulic acid may be used as topical protective agents against UV-radiation-induced skin damage.

Ogboke et al. [39] studied the physicochemical composition of the Marula seed using standard methods and characterized the seed oil using GC-MS analysis. The oil extracted from ground seeds using the Soxhlet method was evaluated for fatty acid distribution. Their results revealed that the seed was constituted of oil (11%), crude protein (36.70%), carbohydrate (17.20%), saponins (0.90%), fibre (3.40%), ash content (11.70%) and moisture (2.50%). The oil was constituted of the fatty acids; butyric acid (0.35%), caproic acid (1.41%), myristic acid (2.12%), palmitic acid (22.56%), stearic acid (50.76%), arachidonic acid (8.46%), behenic acid (5.14%), oleic acid (4.13%) and lignoceric acid (4.13%). In another study, the oil content, fatty acid and sterol composition of oil from Marula seed was determined using capillary gas chromatography, the tocopherols were analysed using HPLC and the oxidative stability investigated using the Rancimat method [1]. The seed was found to have a total oil content of (53.5%). The oil was made up of saturated fatty acids (25.19%) and unsaturated fatty acids (73.81%). Major fatty acids in the oil were oleic acid (67.2%), linoleic acid (5.9%) and palmitic acid (14.1%). The total tocopherol content was 13.7 mg/100g oil and sterols content was 287 mg/100g oil with gamma tocopherol (94.89%) being the major tocopherol and beta-sitosterol (62.8%) as the predominant sterol. The main phyto-constituents of Marula oilcake were studied by Hilou et al. [40]. Their results revealed that total polyphenols, catechol tannins, saponins and sterols were present in the oil cake while gallic tannins, flavonoid aglycons, coumarins, anthraquinones and anthocyanins were not detected in the oil seed sample [40].

2.5.3 Marula leaves

Phytochemical analysis of the methanol extract of leaves of *S. birrea* was achieved by fractionation on Sephadex LH-20 and purification by chromatography on RP-HPLC and elucidation of structures of purified compounds using data obtained from a 600 MHz NMR [41]. A flavonol glycoside, quercetin 3-O- α -L-(5''-galloyl)-arabinofuranoside was identified as a novel compound. Eight other phenolic compounds were isolated. The isolated compounds included four quercetin glycosides; quercetin 3-O- β -D-(6''-galloyl) glucopyranoside, quercetin

3-O- β -D-(6"-galloyl) galactopyranoside, quercetin 3-O- α -L-rhamnopyranoside and quercetin 3-O- β -D-glucopyranoside. Two epicatechin derivatives (-)-epicatechin 3-O-galloyl ester and (-)-epigallocatechin 3-O-galloyl ester were also isolated. The other isolated compounds were kaempferol 3-O- β -D-(6"-galloyl) glucopyranoside and myricetin 3-O- α -L-rhamnopyranoside, and kaempferol 3-O- α -L-rhamnopyranoside and gallic acid [41].

Several researchers have done work to validate the traditional medicinal uses of the Marula plant and to identify its active ingredients. Despite the commercial and folkloric applications of the Marula plant for anti-aging purposes, very few studies have been conducted to scientifically validate anti-aging claims on the Marula plant, to identify the active ingredients and a chemical analysis of any anti-aging Marula extracts for quality control purposes. Further, no reports have been made on the inhibition of collagenase and elastase activity of this plant, these enzymes are important in determining the anti-aging potential of ingredients.

2.6 METHODOLOGY

2.6.1 Collection and extraction of Marula stems, leaves and fruits

Marula leaves, softwood side stems or twigs and fruits (Figure 2.1) were collected from Hluhluwe river in Kwazulu Natal, South Africa as part of the Council for Scientific and Industrial Research (CSIR) programme to collect and test plants for their anti-aging potential. The plants were identified at the South African National Biodiversity Institute (SANBI, Tshwane) where the voucher specimens were deposited (PRE 0864882). The collected plant materials were separately oven-dried at 30-60 °C. Dried plant material was ground to a coarse powder using a hammer mill and stored at ambient temperature prior to extraction. Dried and ground plant material (100 g) was separately extracted with methanol:DCM (1:1) for 24 hours at room temperature. The solvent was evaporated using a rotary evaporator at 50-60 °C and then further dried in a desiccator for 24 hours. The extracts were stored in a cold room (Figure 2.2).

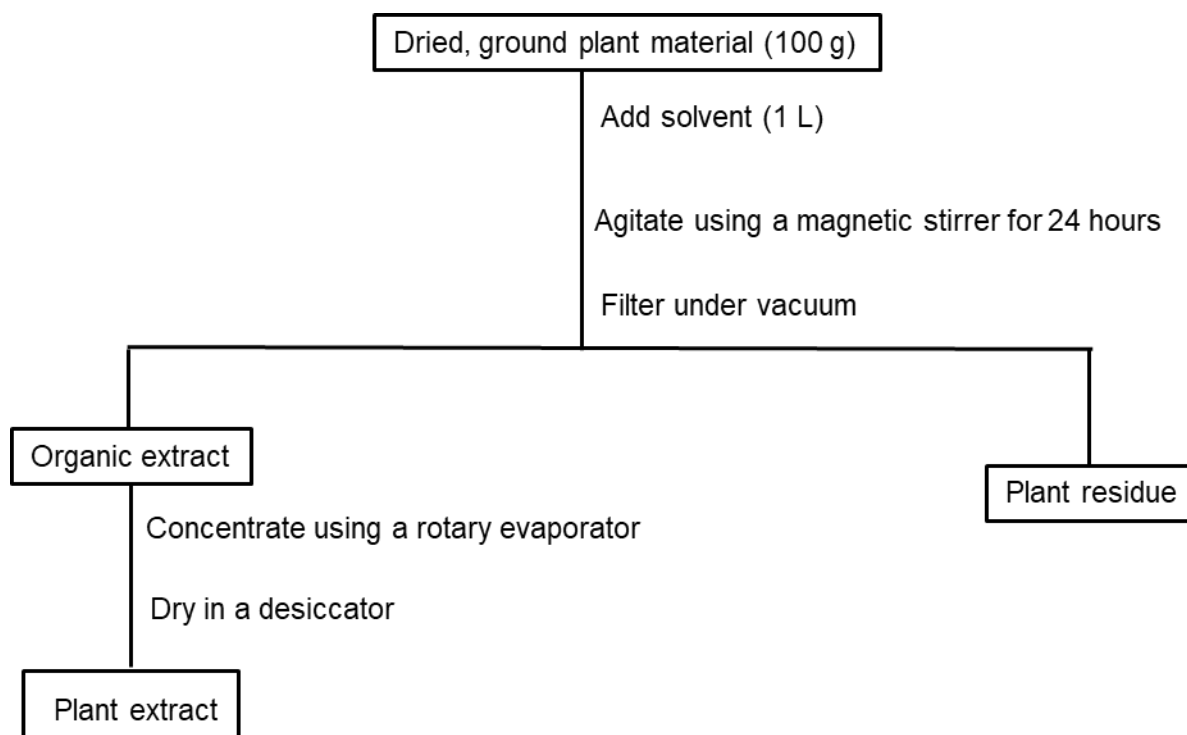


Figure 2.2. Flow diagram for the extraction of Marula stems, fruits and leaves separately using methanol:DCM (1:1)

2.6.2 Collection and extraction of Marula stems

Sclerocarya birrea (A. Rich.) Hochst (Marula) softwood stems were harvested from the University of Pretoria experimental farm with the help of the curator Jason Sampson. The identity of the plant was confirmed at the H.G.W.J Schweickerdt herbarium at the University of Pretoria (voucher number PRU 123535). The plant material was diced into small pieces and air dried in the lab. Dried plant material was ground to a coarse powder using a hammer mill and stored in the dark. The dried and ground Marula stems (100 g) were extracted separately using ethanol, acetone and methanol:DCM (1:1) by adding each solvent (1 L) and agitating for 3 hours using a magnetic stirrer. The mixture was filtered under vacuum and the organic extract was concentrated and dried using a rotary evaporator (Figure 2.3).

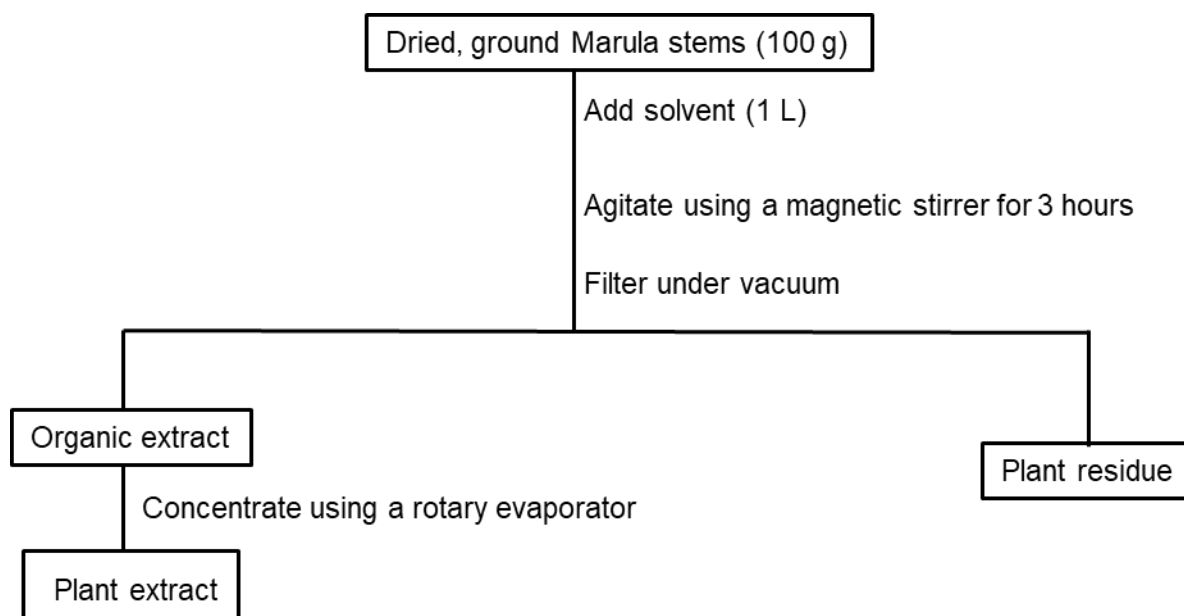


Figure 2.3. Flow diagram for the extraction of Marula stems separately using ethanol, acetone, and methanol:DCM (1:1)

2.6.3 Sequential extraction of Marula stems

The dried and ground *S. birrea* stems (100 g) were sequentially extracted using hexane, DCM, ethyl acetate and methanol. Extraction was done by agitation with each solvent (1 L) using a magnetic stirrer once for 2 hours followed by filtration under vacuum. The plant residue from the hexane extraction was extracted using DCM, the residue from the DCM extraction was extracted using ethyl acetate (EtOAc) and the residue from the EtOAc extraction was extracted using methanol. The organic extract from each stage was evaporated to dryness using a rotary evaporator. The extracts were stored in a cold room at 4 °C (Figure 2.4).

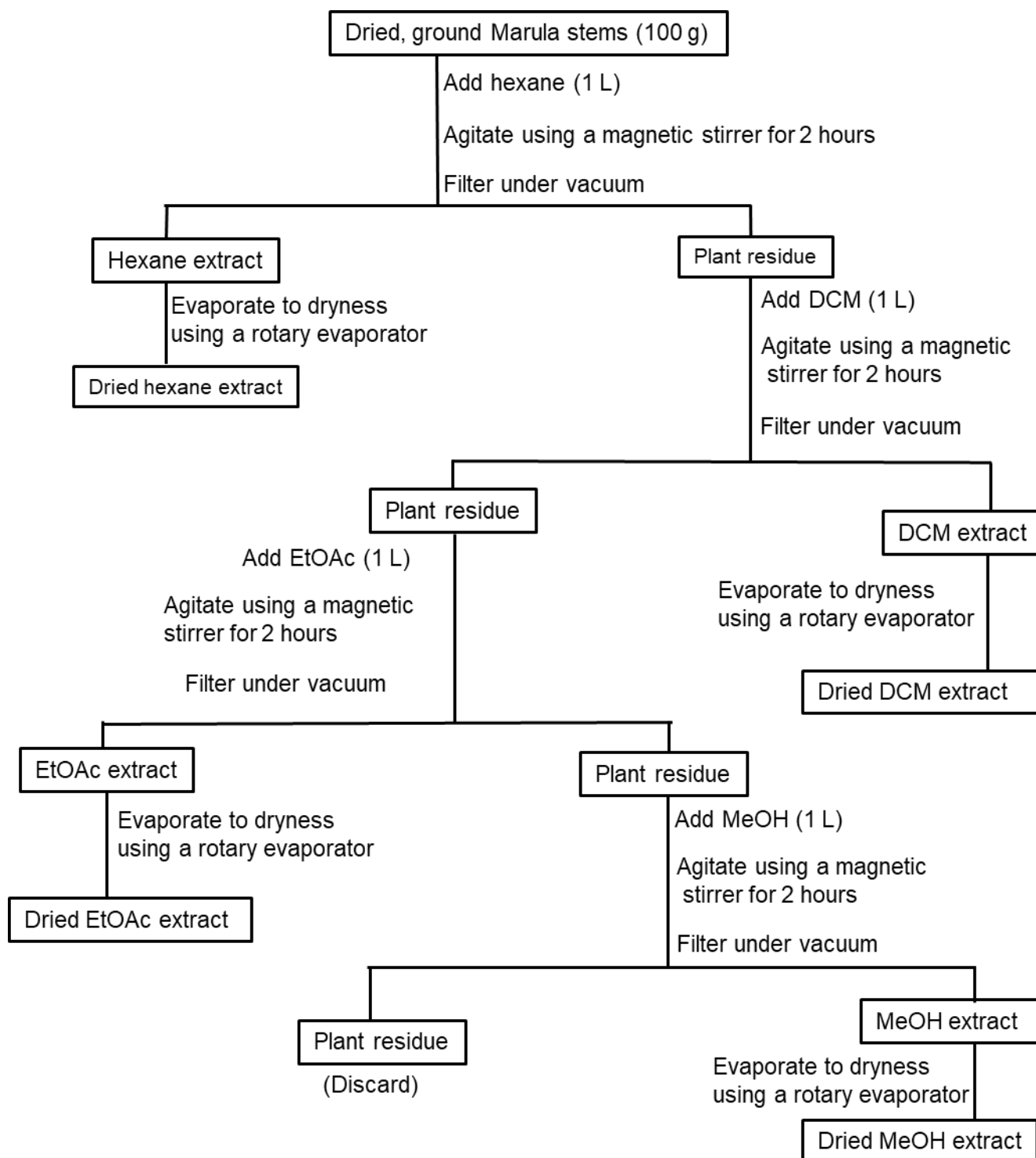


Figure 2.4. Flow diagram for sequential extraction of *S. birrea* stems

2.6.4 Marula oil production

Marula oil was obtained from a commercial supplier Phepisa Natural Resources Institute through the CSIR where it was produced through cold press.

2.6.5 Bioassay of crude extracts and fractions

The method according to Kraunsoe et al. [42] with a few modifications was used to determine anti-elastase inhibition activity. The elastase substrate N-Methoxysuccinyl-Ala-Ala-Pro-Val-*p*-nitroaniline is catalysed by the human leucocyte elastase (HLE) to give a yellow coloured product, *p*-nitroaniline which is detected by absorbance at 405 nm on a Tecan infinite 500 spectrophotometer. In this assay, in the presence of an inhibitor, the enzyme HLE is inhibited and the breakdown of the substrate proceeds at its natural rate of reaction, as a result the yellow coloured product *p*-nitroaniline is not formed, hence there will be no colour change.

Anti-collagenase inhibition was determined according to Moore and Stein's method [43] incorporating modifications by Mandl et al. [44]. Collagen is degraded by the enzyme collagenase to produce peptides which react with ninhydrin to give a blue coloured product detected by absorbance at 540 nm on a Tecan Infinite 500 spectrophotometer. In the presence of an inhibitor the enzyme collagenase will not catalyse the reaction, hence the breakdown of collagenase will proceed at its natural rate of reaction and there will be no colour change.

All enzyme assays were done in triplicate but the assays were not replicated as there was good reproducibility in the screening results of the pure compounds/standards in all the assays. MS Excel was used to analyse the enzyme assay results which were presented as percentage inhibition. The results in Tables 2.1 and 2.2 are given as mean \pm standard deviation (SD), while the results in Figure 2.19, 2.20, 2.22, 2.24, 2.25 and 2.26 are shown as mean \pm standard error of the mean (SEM). The Student's t-test function in Excel was used to compare the significance of the differences between the activity of the positive controls, the crude extracts and the pure standards.

2.6.6 Chemical Profiling

Compounds were tentatively identified by generating molecular formulas from MassLynx V 4.1 based on their isotopic fit value (iFit value), and by comparison of MS/MS fragmentation pattern with that of matching compounds from Metlin, Metfusion, ChemSpider, Massbank

libraries and Dictionary of Natural products. The iFit value is an indication of how well the measured isotopic ion ratio compares to the theoretical ion ratio [45]. Additionally, acquired accurate masses were compared with those of known compounds in compound databases. Pure standards were used to confirm the presence of selected compounds.

2.6.7 Bioassay-guided fractionation

Fractionation of the ethanol extract of Marula ground stems was done with the aim of confirming the presence of active compounds in selected fractions. The extract (100 mg) dissolved in DMSO (1 ml) was fractionated on prep HPLC-UV using a gradient elution method on a reverse phase column. The solvents water with 1% formic acid and acetonitrile were used. The sample (100 mg) dissolved in DMSO (4 ml) was fractionated using a prep HPLC-UV to produce 23 fractions using the time-based collection. The fractions were screened for collagenase and elastase inhibition activities. The active fractions were analysed by UPLC-QTOF-MS to determine the active compounds responsible for elastase and collagenase inhibition activities (Figure 2.5).

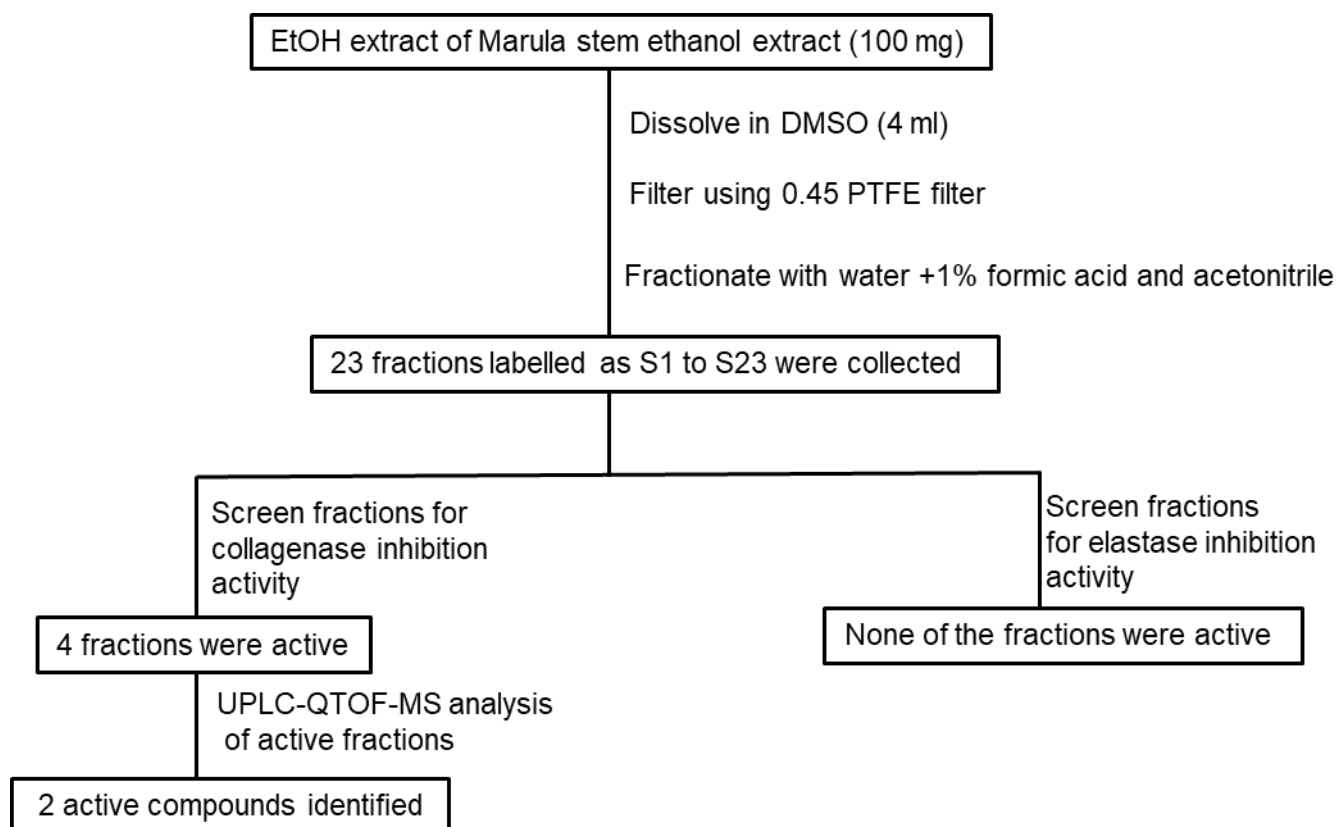


Figure 2.5. Flow diagram for bioassay-guided fractionation of Marula stems ethanol extract using prep-HPLC.

2.6.8 Defatting of Marula stem ethanol extract

In order to remove the intense dark-brown colour in the ethanol extract, the Marula stem ethanol extract (500 mg) was defatted by partitioning between 50 ml of water: ethanol (20:80) and hexane (50 ml). After separation of the two layers, the water/ethanol was evaporated to dryness using a rotary evaporator (Figure 2.6). The defatted fraction was screened for its anti-aging properties.

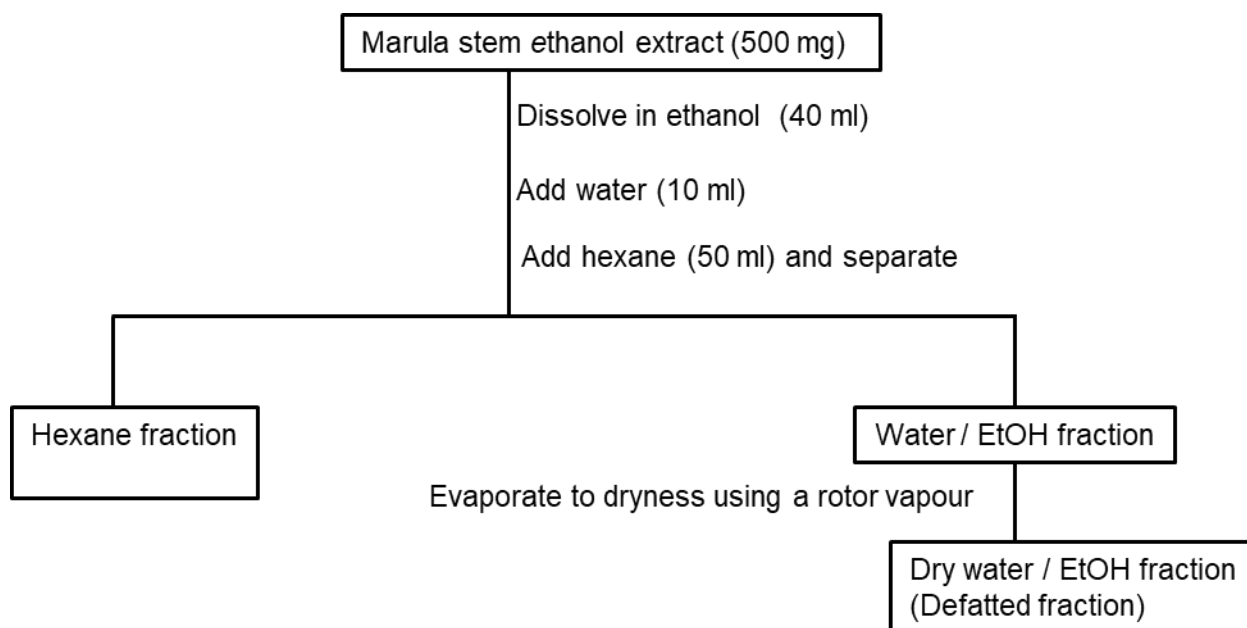


Figure 2.6. Flow diagram for the defatting of Marula stem ethanol extract through liquid-liquid partitioning

2.6.9 Concentration of actives of Marula stem extract

In order to improve the bioactivity of the Marula ethanol stem extract, the method used by Row and Jin. [46] to extract catechins from tea was modified. Marula stem ethanol extract (1 g) was dissolved in distilled water (100 ml) at 80 °C by shaking in a sonicator for 10 minutes. The solution was extracted three times with ethyl acetate (100 ml). The combined organic extract was evaporated to dryness using a rotary evaporator to produce the concentrated fraction (Figure 2.7). The concentrated fraction was screened for anti-aging activity.

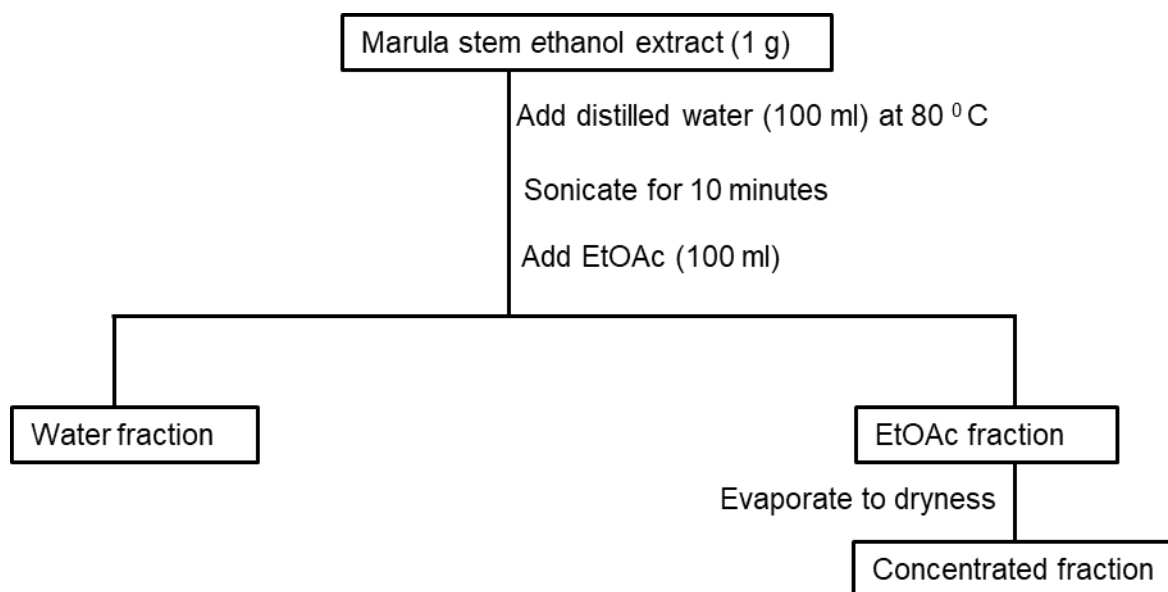


Figure 2.7. Flow diagram for concentration of active ingredients of Marula stem ethanol extract

2.6.10 Defatting-concentration of actives of Marula stem extract

In order to remove the intense dark brown colour and to improve the bio-activity of the Marula stem ethanol extract, the method used by Row and Jin [46] to extract catechins from tea was modified. Marula stem ethanol extract (1 g) was dissolved in distilled water (100 ml) at 80 °C by shaking in a sonicator for 10 minutes. The solution was defatted with hexane (100 ml) three times then extracted three times with ethyl acetate (100 ml). The ethyl acetate fraction was evaporated to dryness using a rotary evaporator and screened for anti-aging activity (Figure 2.8).

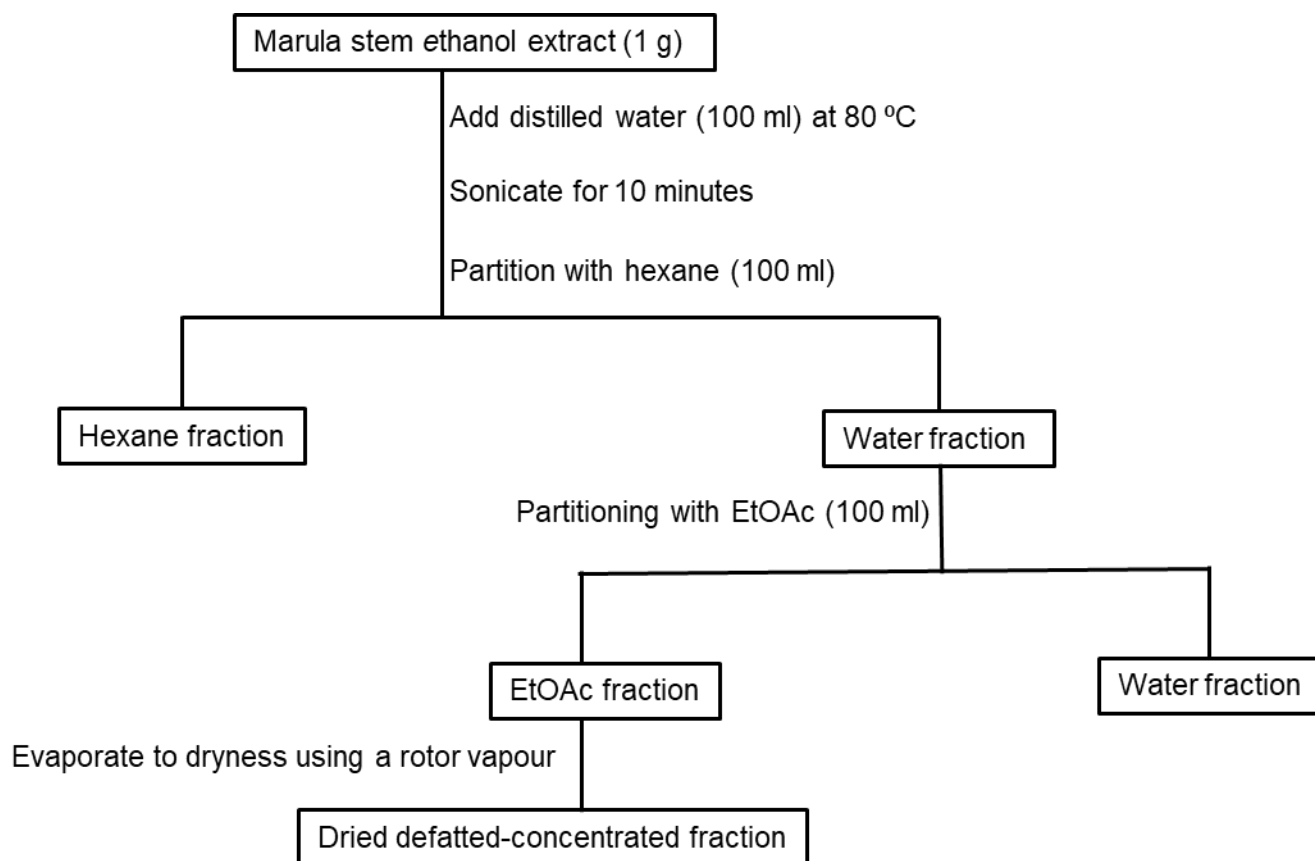


Figure 2.8. Flow diagram for defatting-concentration of Marula stem ethanol extract

2.7 RESULTS AND DISCUSSION

The results from the screening the extracts of Marula stems, leaves and fruits at 200 µg/ml and the positive controls are shown in Table 2.1. The extract of Marula stems exhibited good anti-collagenase activity of $76.92\% \pm 8.92$ and compared favourably to that of EDTA the positive control which had an inhibition activity of $79.88\% \pm 9.10$. In contrast, the extracts of Marula fruits and leaves exhibited limited collagenase inhibition activities of $25.89\% \pm 8.69$ and $21.23\% \pm 7.74$, respectively. Similarly, extracts of the Marula stems had very good elastase inhibition activity of $88.07\% \pm 2.26$ equivalent to that of the positive control (elafin) which had $93.09\% \pm 4.10$ inhibition. In comparison, moderate activity was observed for the leaf extract which had an anti-elastase activity of $53.60\% \pm 1.06$ and very limited anti-collagenase activity of $25.89\% \pm 8.69$ for the extract of the fruits.

Table 2.1. Comparison of inhibition of the elastase and collagenase activities for extracts of different parts of *S. birrea* tested at 200 µg/ml and the positive controls at EDTA at 143 µg/ml and elafin 1.43 µg/ml

Plant part	Elastase assay (% Inhibition ±SD)	Collagenase assay (% Inhibition ±SD)
Stems	88.07 ± 2.26	76.92 ± 8.92
Leaves	53.60 ± 1.06	21.23 ± 7.74
Fruits	26.79 ± 6.61	25.89 ± 8.69
Controls		
10% MeOH	1.45 ± 1.50	1.32 ± 0.73
EDTA		79.88 ± 9.10
Elafin	93.09 ± 4.10	

2.7.1 Selection of the most appropriate solvent

The development of herbal extracts as ingredients for the cosmetic industry has stringent criteria for the use of approved extraction solvents [47] for which a suitable extraction solvent that retained inhibition activity was investigated. The freshly collected Marula stems from the University of Pretoria experimental farm which were sequentially and separately extracted using different solvents were evaluated for anti-aging activity in the elastase and collagenase inhibition assays.

2.7.2 Sequential extraction using polar and non-polar solvents and bioassaying

Sequential extraction using polar and non-polar solvents was undertaken to separately extract compounds based on their polarity. In sequential extraction, the less polar hexane, DCM and ethyl acetate had below 1% extraction yield. In contrast, the more polar methanol had 8.01% yield, suggesting that in Marula stems there is a higher abundance of polar compounds in comparison to non-polar compounds (Table 2.2). The extracts were screened in the elastase and collagenase assays. Screening results revealed that the hexane extract (0%), DCM (6.69% ± 1.36) and ethyl acetate (65.02% ± 1.57) sequential extracts exhibited statistically lower elastase inhibition activities ($p < 0.01$) than elafin (99.21% ± 0.05). In contrast, the methanol sequential extract (99.19% ± 0.18) had the same level of potency with elafin (99.21% ± 0.05, $p > 0.05$). The sequential extraction therefore produced the methanol extract which

exhibited potency equivalent to the positive control in the elastase assay. The good elastase inhibition activity of this methanol extract can be attributed to sequential extraction which would have concentrated the constituents responsible for elastase inhibition thereby producing the most potent extract. Similarly, in the collagenase assay, the hexane (11.14% ± 2.51) and DCM (19.62% ± 2.78) sequential extracts exhibited significantly lower activities ($p < 0.01$) in comparison to EDTA (95.66% ± 2.11). On the other hand, the ethyl acetate (95.56% ± 1.68), and methanol (94.46% ± 2.31) sequential extracts showed similar potencies ($p > 0.05$) to EDTA (95.66% ± 2.11). The results from sequential extraction indicated that active constituents are concentrated in the more polar extracts for the elastase and collagenase inhibition.

Table 2.2. Extraction yields of Marula stems sequentially extracted and their inhibition of the elastase and collagenase enzymes at 200 µg/ml and the positive controls EDTA at 143 µg/ml and elafin at 1.43 µg/ml

Extraction solvent used for the stems	Extraction yield (calculated from dry plant material)	Elastase assay (% Inhibition ± SD)	Collagenase assay (% Inhibition ± SD)
Sequential extraction with hexane	0.38%	** 0	** 11.14 ± 2.51
Sequential extraction with DCM	0.22%	** 6.69 ± 1.36	** 19.62 ± 2.78
Sequential extraction with ethyl acetate	0.87%	** 65.02 ± 1.57	95.56 ± 1.68
Sequential extraction with methanol	8.01%	99.19 ± 0.18	94.46 ± 2.31
		Controls	
10% MeOH		3.28 ± 0.34	0
10% DMSO		4.70 ± 0.53	1.58 ± 0.60
Elafin		99.21 ± 0.05	
EDTA			95.66 ± 2.11

** showing a significant difference of $p < 0.01$ compared to EDTA

** showing a significant difference of $p < 0.01$ compared to elafin

2.7.3 UPLC-QTOF-MS analysis of Marula stems extracted sequentially using polar and non-polar solvents

The chemical profile of the hexane extract was not analysed on the UPLC-QTOF-MS since it showed no enzyme inhibition. The DCM sequential extract showed peaks mainly within the 9 to 18-minute range of the 20-minute chromatogram with a few peaks in the 0 to 9-minute

region. This distribution of peaks reveals that the extract is composed mainly of non-polar constituents. In comparison, the ethyl acetate sequential extract was constituted of both polar and non-polar constituents as shown by the retention times of the peaks distributed in the 2 to 15-minute region. The limited elastase activity exhibited by the ethyl acetate extract can be attributed to the active compounds in the polar-region of the extract having been diluted by non-polar inactive compounds in the extract. The methanol sequential extract had peaks mainly distributed in the 0 to 4-minute region, revealing that the extract is mainly composed of polar compounds. Based on the distribution of peaks in the chemical profiles of the sequential extracts it is evident that sequential extraction successfully separated compounds based on polarity (Figure 2.9).

An analysis of peaks common to the chemical profile of the active methanol and ethyl acetate sequential extracts should reveal peaks corresponding to compounds which are likely to contribute to the anti-aging activity of the two extracts. The major peak in the ethyl acetate sequential extract at m/z 289.0725 and retention time 2.30 minutes was also present in the methanol sequential extract at m/z 289.0723 retention time 2.29 minutes. The structure of the corresponding compound is catechin, its identification is described in section 2.7.6. An intense peak observed at m/z 441.0822 retention time 3.54 minutes in the ethyl acetate sequential extract was also present in the methanol sequential extract at m/z 441.0833 retention time 3.54 minutes. The structure of the compound corresponding to this peak was identified as epicatechin gallate, identification of this compound is described in section 2.7.6. This compound is likely to be one of the compounds contributing to the anti-aging activity of the methanol and the ethyl acetate extracts. The major peak in the methanol sequential extract observed at m/z 191.0556 retention time 0.66 minutes was absent in the active ethyl acetate extract but was present in the inactive DCM extract at m/z 191.0562 retention time 0.66 minutes indicating that the compound does not contribute either to the collagenase or elastase inhibition activity of the extracts. The structure of this compound was established as quinic acid and its identification is described in section 2.7.6. The intense peak at m/z 381.1743

retention time 14.69 minutes in the ethyl acetate extract is unlikely to correspond to an active compound as it is absent from the active methanol extract but present in the inactive DCM sequential extract at m/z 381.1744 retention time 14.71 minutes. The identity of this inactive compound was not established. Based on an analysis of chemical profiles, catechin and epicatechin gallate are some of the compounds likely to be contributing to the anti-aging activity of the methanol and ethyl acetate sequential extracts. Screening of these pure compounds is thus necessary to confirm if indeed these compounds contribute to the elastase and collagenase activities of the methanol and ethyl acetate sequential extracts.

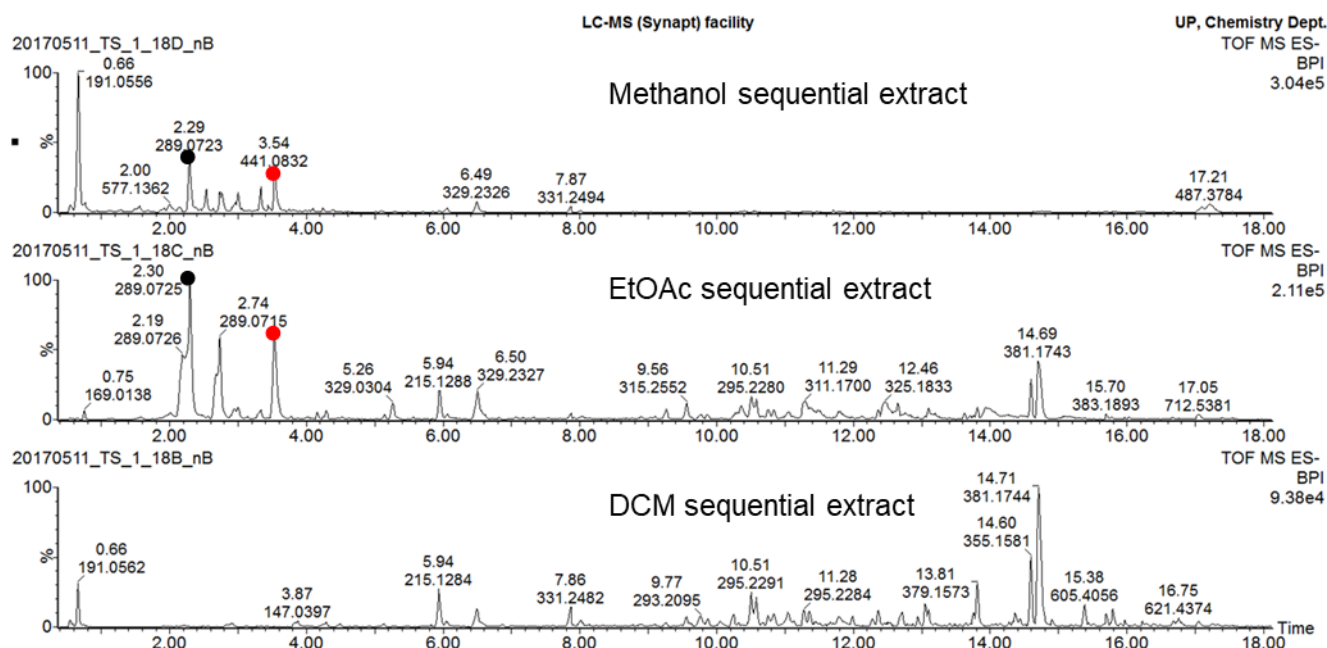


Figure 2.9. ESI negative mode BPI chromatograms (0 to 18 minutes) of Marula stems extracted sequentially. ●Catechin (m/z 441.0832 retention time 3.54 minutes) and ●epicatechin gallate (m/z 289.0723 retention time 2.29 minutes) present in the methanol sequential and ethyl acetate sequential extracts are likely to contribute to collagenase inhibition activities of these extracts.

2.7.4 Separate extraction using different polar solvents and their bioassaying

Sequential extraction revealed that the more polar solvents extracted the active anti-aging ingredients from Marula stems. Consequently, it was necessary to select a suitable polar solvent for extraction of the most active ingredients from the stems. To achieve this, the polar acetone and ethanol solvents were selected from the list of solvents acceptable in the cosmetic industry for the purposes of extraction of cosmetic ingredients. To facilitate comparison of the activities of extracts analysed with the activity of the original extracts prepared at CSIR, the solvent combination methanol:DCM (1:1) was selected as one of the extraction solvents. Dried and ground Marula stems were thus extracted separately using the solvents acetone, methanol:DCM (1:1) and ethanol.

The extraction yields obtained reflect that the methanol:DCM (1:1) solvent combination gave a 5.39% extraction yield which was higher than that of the acetone (3.36%) and the ethanol (3.09%) extraction. This clearly indicates that combining a polar and a non-polar solvent improves the capacity of the solvent system to extract compounds in matrices containing both polar and non-polar compounds. The extracts were screened in the elastase and collagenase assays. Results obtained revealed that the acetone ($91.25\% \pm 0.11$), methanol:DCM (1:1) ($89.74\% \pm 0.32$) and ethanol ($93.35\% \pm 0.89$) extracts had biologically high elastase inhibition activities, however, these elastase inhibition activities were statistically lower ($p < 0.01$) than elafin ($99.21\% \pm 0.05$). In the collagenase assay the acetone ($91.17\% \pm 3.59$), methanol:DCM (1:1) ($89.74\% \pm 0.32$) and the ethanol ($99.08\% \pm 3.57$) extracts were as potent ($p > 0.05$) as EDTA ($95.66\% \pm 2.11$). The result confirms the conclusions obtained from section 2.7.2 that active constituents are likely polar compounds for both elastase and collagenase inhibition (Table 2.3). The elastase inhibition activity of the methanol:DCM (1:1) extract ($89.74\% \pm 0.32$) of the recollected Marula stems from the University of Pretoria gardens was similar to earlier collections from Kwazulu Natal which had ($88.07\% \pm 2.26$) elastase inhibition. Similarly, the collagenase inhibition activity of the recollected Marula stems ($93.75\% \pm 3.32$) extracted with methanol:DCM (1:1) showed potency in the same range as the collections from KwaZulu Natal

which had 76.92% ± 8.92 inhibition activity. This result indicated that the geographical location does not appear to influence the active ingredients.

Table 2.3. Extraction yields of Marula stems extracted using different solvents and their inhibition of the elastase and collagenase enzymes at 200 µg/ml and the positive controls EDTA at 143 µg/ml and elafin 1.43 µg/ml

Extraction solvent used for the stems	Extraction yield ±SD (calculated from dry plant material) as w/w %	Elastase assay (% Inhibition ± SD)	Collagenase assay (% Inhibition ± SD)
Acetone	3.36	**91.25 ± 0.11	91.17 ± 3.59
Methanol: DCM (1:1)	5.39	**89.74 ± 0.32	93.75 ± 3.32
Ethanol	3.09	**93.35 ± 0.89	99.08 ± 3.57
		Controls	
10% MeOH		3.28 ± 0.34	0
10% DMSO		4.70 ± 0.53	1.58 ± 0.60
Elafin		99.21 ± 0.05	
EDTA			95.66 ± 2.11

** Showing a significant difference of $p < 0.01$ compared to Elafin

2.7.5 UPLC-QTOF-MS analysis of Marula stems extracted separately with different solvents

A chemical analysis of extracts made from acetone, methanol:DCM (1:1) and ethanol was undertaken to identify common peaks in the various extracts and compounds which could be responsible for the observed biological activity. The ethanol extract showed major peaks in the 0 to 4-minute (polar) region and a few minor peaks in the 6 to 8 minutes (medium polarity region). The methanol:DCM (1:1) extract had major peaks distributed within the 0 to 15 minutes (polar and non-polar regions) confirming that the solvent combination successfully extracted compounds from both the polar and the non-polar regions. The acetone extract showed major peaks in the 0 to 4-minute (polar) region and a few minor peaks in the 6 to 12 minutes (medium to non-polar region). A comparison revealed the presence of peaks common to the three chemical profiles.

The most intense peak in the ethanol extract was observed at m/z 191.0568 retention time 0.66 minutes. This peak was also present in the acetone extract at m/z 191.0562 retention time 0.66 minutes but however was absent from the active methanol:DCM (1:1) extract. The structure of the compound corresponding to this peak was identified as quinic acid as described in section 2.7.6. Due to its absence in the active methanol:DCM (1:1) extract, the compound quinic acid is unlikely to be one of the compounds responsible for the collagenase or elastase inhibition activities of these extracts. The most intense peak in the methanol:DCM (1:1) extract was observed at m/z 441.0828 retention time 3.51 minutes. This peak was also of high intensity in the acetone extract at m/z 441.0833 retention time 3.54 minutes and in the ethanol extract at m/z 441.0817 retention time 3.57 minutes. The structure of the compound corresponding to the peak is epicatechin gallate and its identification is described in section 2.7.6. This compound is likely to be one of the compounds contributing to the anti-aging activity of the three extracts.

The most intense peak in the acetone extract was at m/z 289.0737 retention time 2.29 minutes. This peak had high intensity in the methanol:DCM (1:1) extract where it was observed at m/z 289.0715 retention time 2.28 minutes as well as the ethanol extract at m/z 289.0712 retention time 2.32 minutes. The structure of the compound corresponding to this peak was identified as catechin and its identification is described in section 2.7.6. The compound is likely to contribute to the anti-aging activity of the extracts. Another peak observed in the ethanol extract at m/z 457.0766 retention time 2.93 minutes was also present in the acetone extract, at m/z 457.0770 retention time 2.76 minutes and in the methanol:DCM (1:1) extract at m/z 457.0770 retention time 2.75 minutes. The peak was identified as epigallocatechin gallate and its elucidation is described in section 2.7.6 and is likely to be one of the compounds contributing to the anti-aging activity of the extracts.

The methanol:DCM (1:1) extract had some additional peaks which were not present in the acetone and ethanol extracts. These include the intense molecular ions at m/z 557.2383

retention time 6.26 minutes and m/z 381.1745 retention time 14.70 minutes. In addition, less intense peaks at m/z 377.1588 retention time 4.81 minutes, m/z 311.1682 retention time 11.28 minutes and m/z 325.1841 retention time 12.42 minutes, m/z 265.1460 retention time 10.35 minutes and at m/z 339.1999 retention time 13.95 minutes were observed (Figure 2.10). The compounds corresponding to these peaks are unlikely to be active as they were absent from the active acetone and ethanol extracts showing that they are not part of the peaks contributing to activity. The identity of these inactive compounds was not established. An analysis of chemical profiles of separately extracted Marula stems revealed that catechin, epicatechin gallate and epigallocatechin gallate are some of the compounds likely to be contributing to the anti-aging activity of the ethanol, methanol:DCM (1:1) and acetone extracts. Based on the anti-aging activity, chemical profile analysis and acceptability to the cosmetic industry [48], the polar ethanolic extract was selected as the most suitable extract for development as a cosmetic ingredient.

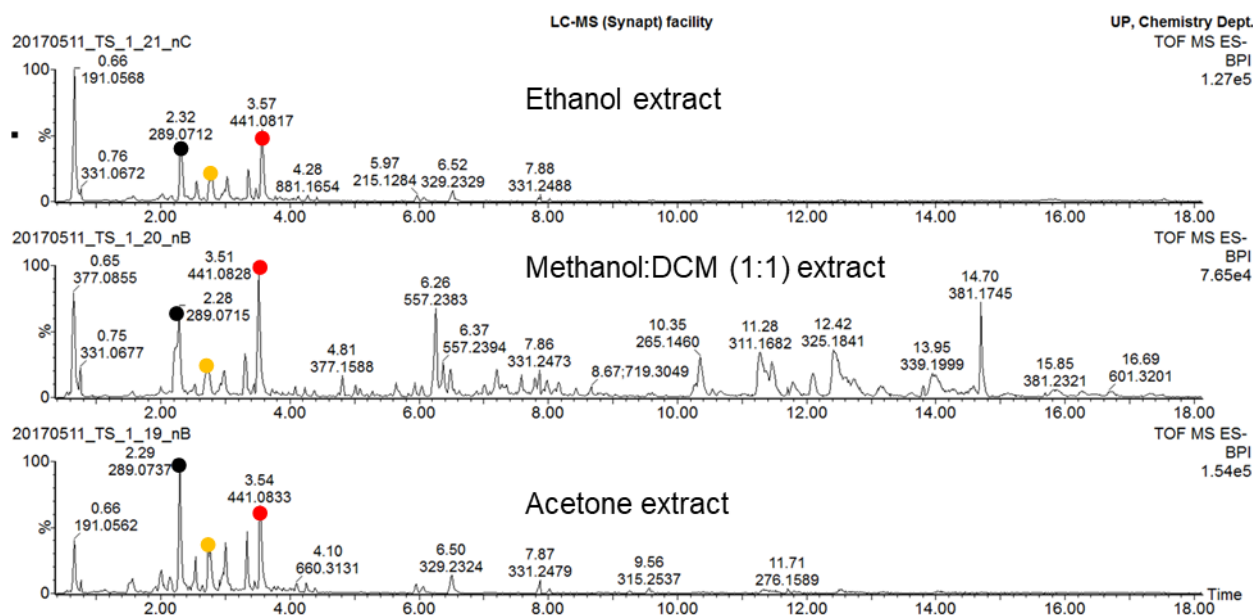


Figure 2.10. ESI negative mode BPI chromatograms of Marula stems extracted separately using different solvents. Compounds common to the three extracts identified as • epicatechin gallate (m/z 441.0817 retention time 3.57 minutes) and • catechin (m/z 289.0712 retention time 2.32 minutes) and • epigallocatechin gallate (m/z 457.0766 retention time 2.93 minutes) are likely to contribute to the anti-aging activity of these extracts.

2.7.6 Chemical profiling and phytochemical analysis of the ethanol extract of Marula stems

The guarantee of quality is the basis for reliable efficacy and safety of herbal products. The use of hyphenated chromatographic techniques such as UPLC-QTOF-MS is strongly recommended for quality control of herbal medicines as they appropriately represent the chemical constituents of herbal medicines. Chemical profiling of the ethanol extract of the stems of Marula was done for quality control purposes. The chemical fingerprint of the extract generated using UPLC-QTOF-MS operating in the ESI negative mode is shown in Figure 2.11 and the identification of the major compounds with well-resolved peaks and those identified using pure compounds is shown in Table 2.4 and their chemical structures in Figure 2.12. Using both the ESI negative and positive modes, a total of eleven known compounds were identified in the extract which included one organic acid, four flavonoids, four proanthocyanidins, two fatty acid derivatives and one unidentified compound. The structures of four of these compounds were confirmed using pure standards purchased from commercial suppliers. Supplementary data 1 shows the ESI positive mode Base Peak Ion (BPI) chromatogram of the ethanol extract of the Marula stems.

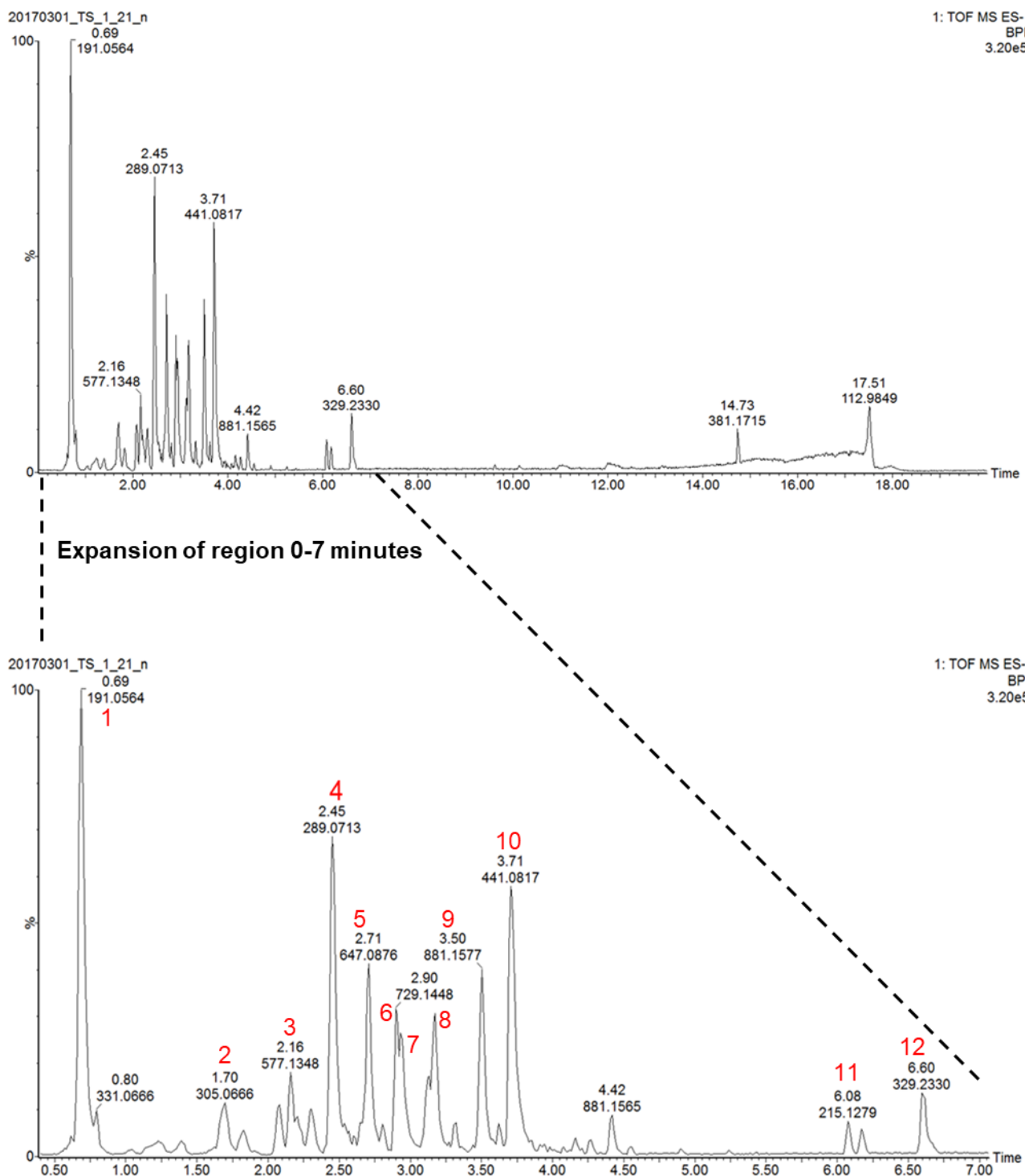


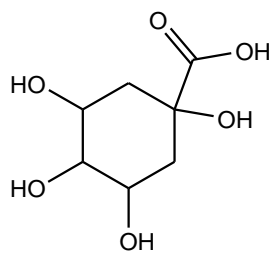
Figure 2.11. ESI negative mode BPI chromatogram of Marula stem ethanol extracts. A total of eleven compounds were identified, the presence of five of these; quinic acid (peak 1), catechin (peak 4), epigallocatechin-3-gallate (peak 7), and epicatechin gallate (peak 10) was confirmed using pure standards on UPLC-QTOF-MS. Galocatechin (peak 2), procyanidin B2 (peak 3), epicatechin-epicatechin-3'-O-gallate (peak 6) and epicatechin-3-O-gallate-epicatechin (peak 8), procyanidin B2-3'3 di-O-gallate (peak 9), undecanedioic acid (peak 11) and 9,10,13 TriHOME (peak 12) were tentatively identified while peak 5 was unidentified.

Table 2.4. Chemical profile of Marula stems extracted with ethanol

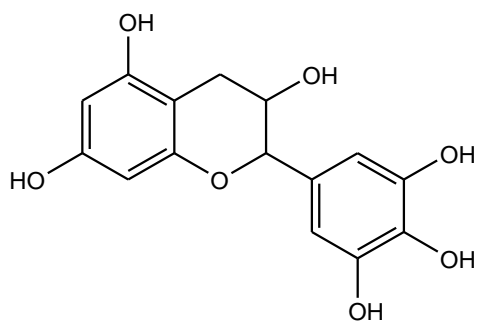
Peak #	RT (min)	Acquired [M-H] ⁻ m/z	Formula of possible structure	Theoretical [M-H] ⁻ m/z	Calculated accurate mass (Da)	Possible structure	Mass error (ppm)	MS/MS Data (fragments)		Confirmation with a standard		Ref
								RT	[M-H] ⁻ m/z	RT	[M-H] ⁻ m/z	
1	0.69	191.0564	C ₇ H ₁₂ O ₆	191.0561	192.0634	Quinic acid (Organic acid)	-1.57	173.0344	[M-H] ⁻ -H ₂ O	0.69	191.0555	[49]
								127.0338	[M-H] ⁻ - CO-2H ₂ O			
								85.0298	[M-H] ⁻ - CO ₂ -H ₂ O- C ₂ H ₆ O ₂			
								59.0125	[M-H] ⁻ - C ₅ H ₈ O ₄ ⁻			
								123.0037	[M-H] ⁻ -CHO ₂			
2	1.70	305.0666	C ₁₅ H ₁₄ O ₇	305.0667	306.0740	Gallocatechin (Flavonoid)	0.33	167.0030	[M-H] ⁻ - C ₇ H ₆ O ₃ ⁻			[50]
								137.0245	[M-H] ⁻ -C ₈ H ₈ O ₄ ⁻			
								125.0226	[M-H] ⁻ -C ₉ H ₈ O ₄ ⁻			
								109.0343	[M-H] ⁻ -C ₉ H ₈ O ₄ ⁻ -H ₂ O			
3	2.16	577.1348	C ₃₀ H ₂₆ O ₁₂	577.1351	578.1351	Procyanidin B2 (Proanthocyanidin)	0.52	451.0586	[M-H] ⁻ -C ₆ H ₅ O ₃ ⁻			[34, 35]
								425.0818	[M-H] ⁻ - C ₈ H ₈ O ₃ ⁻			
								407.0773	[M-H] ⁻ - C ₈ H ₈ O ₃ ⁻ -H ₂ O			
								289.0707	[M-H] ⁻ - C ₁₅ H ₁₂ O ₆ ⁻			
								245.0701	[M-H] ⁻ - C ₁₇ H ₁₅ O ₇ ⁻			
								137.0222	[M-H] ⁻ -C ₂₂ H ₁₇ O ₉ ⁻ - H ₂ O			
								125.0234	[M-H] ⁻ - C ₂₄ H ₂₁ O ₉			
4	2.45	289.0713	C ₁₅ H ₁₄ O ₆	289.0717	290.0790	Catechin (Flavonoid)	1.38	245.0706	[M-H] ⁻ - C ₂ H ₄ O ⁻	2.45	289.0716	[51, 52]
								151.0362	[M-H] ⁻ - C ₇ H ₆ O ₃ ⁻			
								137.0238	[M-H] ⁻ - C ₈ H ₈ O ₃ ⁻			
								125.0241	[M-H] ⁻ - C ₉ H ₈ O ₃ ⁻			
								123.0423	[M-H] ⁻ - C ₈ H ₈ O ₃ ⁻ -H ₂ O			
								109.0281	[M-H] ⁻ -C ₉ H ₈ O ₄ ⁻			
5	2.71	647.0876	C ₂₈ H ₂₄ O ₁₈	647.0890	647.0963	Unidentified	2.16	495.0740				
								343.0630				
								325.0517				
								169.0133				

							151.0038					
6	2.90	729.1448	C ₃₇ H ₃₀ O ₁₆	729.1461	730.1534	Epicatechin-epicatechin-3'-O-gallate (Proanthocyanidin)	1.78	577.1335	[M-H] ⁻ - C ₇ H ₄ O ₄	2.93	457.0749	[35]
								559.1229	[M-H] ⁻ - C ₇ H ₄ O ₄ ⁻ -H ₂ O			
								425.0851	[M-H] ⁻ - C ₁₅ H ₁₂ O ₇ ⁻			
								407.0777	[M-H] ⁻ - C ₁₅ H ₁₂ O ₇ ⁻ H ₂ O			
								289.0703	[M-H] ⁻ - C ₇ H ₅ O ₄ ⁻ - C ₁₅ H ₁₂ O ₆ ⁻			
								245.0607	[M-H] ⁻ - C ₇ H ₅ O ₄ ⁻ - C ₁₅ H ₁₂ O ₆ ⁻ - C ₂ H ₄ O ⁻			
								169.0145	[M-H] ⁻ - C ₁₅ H ₁₃ O ₆ ⁻ - C ₁₅ H ₁₃ O ₅ ⁻			
								137.0224	[M-H] ⁻ - C ₇ H ₅ O ₄ ⁻ - C ₁₅ H ₁₂ O ₆ ⁻ - C ₈ H ₈ O ₃ ⁻			
								125.0245	[M-H] ⁻ - C ₇ H ₅ O ₄ ⁻ - C ₁₅ H ₁₂ O ₆ ⁻ - C ₉ H ₁₀ O ₃ ⁻			
								109.0299	[M-H] ⁻ - C ₇ H ₅ O ₄ ⁻ - C ₁₅ H ₁₂ O ₆ ⁻			
7	2.93	457.0766	C ₂₂ H ₁₈ O ₁₁	457.0776	458.0849	Epigallocatechin-3-gallate (Flavonoid)	2.19	305.0673	[M-H] ⁻ - C ₇ H ₄ O ₄ ⁻	2.93	457.0749	[35]
								289.0708	[M-H] ⁻ - C ₇ H ₄ O ₅ ⁻			
								169.0142	[M-H] ⁻ - C ₁₅ H ₁₂ O ₆ ⁻			
								125.0244	[M-H] ⁻ - C ₁₅ H ₁₂ O ₆ ⁻ - CO ₂			
8	3.17	729.1460	C ₃₇ H ₃₀ O ₁₆	729.1461	730.1534	epicatechin-3-O-gallate-epicatechin (Proanthocyanidin)	0.14	577.1276	[M-H] ⁻ - C ₇ H ₄ O ₄ ⁻			[34, 35]
								451.0983	[M-H] ⁻ - C ₇ H ₅ O ₅ ⁻ - C ₆ H ₅ O ₂ ⁻			
								407.0798	[M-H] ⁻ - C ₁₅ H ₁₂ O ₆ ⁻ - 2H ₂ O			
								289.0717	[M-H] ⁻ - C ₇ H ₄ O ₄ ⁻ - C ₁₅ H ₁₂ O ₆ ⁻			
								245.0623	[M-H] ⁻ - C ₂₄ H ₂₀ O ₁₁ ⁻			
								169.0147	[M-H] ⁻ - C ₁₅ H ₁₂ O ₆ ⁻ - C ₁₅ H ₁₃ O ₅ ⁻			
								125.0240	[M-H] ⁻ - C ₁₅ H ₁₂ O ₆ ⁻ - C ₁₅ H ₁₃ O ₅ ⁻ - CO ₂			
9	3.50	881.1577	C ₄₄ H ₃₄ O ₂₀	881.1571	882.1644	procyanidin B2-3'3 di-O-gallate (Proanthocyanidin)	-0.68	729.1445	[M-H] ⁻ - C ₇ H ₄ O ₄ ⁻			[34, 35]
								559.1211	[M-H] ⁻ - C ₇ H ₄ O ₄ ⁻ - C ₇ H ₆ O ₅ ⁻			
								407.0759	[M-H] ⁻ - C ₇ H ₅ O ₅ ⁻ - C ₇ H ₄ O ₄ ⁻ - C ₈ H ₈ O ₈ ⁻ - H ₂ O			
								169.0145	[M-H] ⁻ - C ₂₂ H ₁₆ O ₁₀ ⁻ - C ₁₅ H ₁₃ O ₅ ⁻			
								125.0223	[M-H] ⁻ - C ₂₂ H ₁₆ O ₁₀ ⁻ - C ₁₅ H ₁₃ O ₅ ⁻ - CO ₂			
10	3.71	441.0817	C ₂₂ H ₁₈ O ₁₀	441.0827	442.0900	epicatechin gallate	2.27	289.0710	[M-H] ⁻ - C ₇ H ₄ O ₄ ⁻	3.74	441.0842	[34]

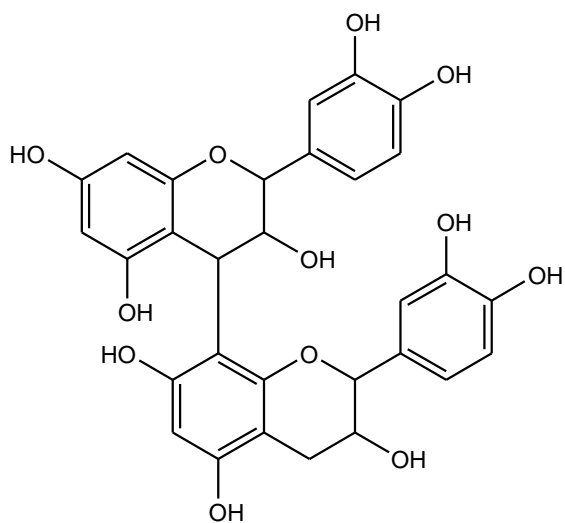
						(Flavonoid)		169.0139	[M-H] ⁻ - C ₁₅ H ₁₂ O ₅ ⁻			
								125.0241	[M-H] ⁻ - C ₁₅ H ₁₂ O ₅ ⁻ -CO ₂			
11	6.08	215.1279	C ₁₁ H ₂₀ O ₄	215.1289	216.1362	Undecanedioic acid (Fatty acid derivative)	4.65	197.1155	[M-H] ⁻ - H ₂ O			[35]
								153.1117	[M-H] ⁻ - H ₂ O - CO ₂			
12	6.60	329.2330	C ₁₈ H ₃₄ O ₅	329.2333	330.2406	9,10,13-TriHOME (Fatty acid derivative)	0.91	283.0503	[M-H] ⁻ - C ₂ H ₅ ⁻ - H ₂ O			[53]
								233.1124	[M-H] ⁻ - COOH- C ₄ H ₉ ⁻			
								211.1227	[M-H] ⁻ - COOH ⁻ - C ₄ H ₉ ⁻ - H ₂ O			
								171.0814	[M-H] ⁻ - C ₅ H ₁₁ - C ₄ H ₇ O ₂ ⁻			



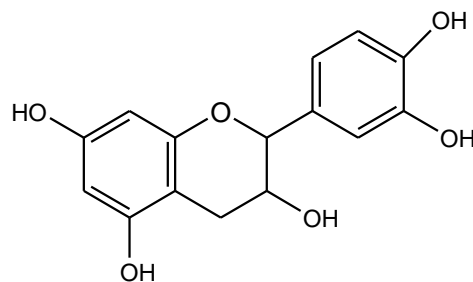
Peak 1: quinic acid



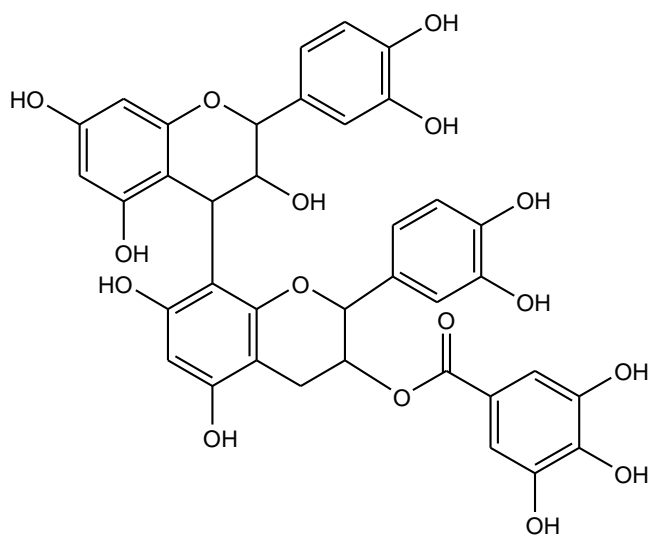
Peak 2: gallocatechin



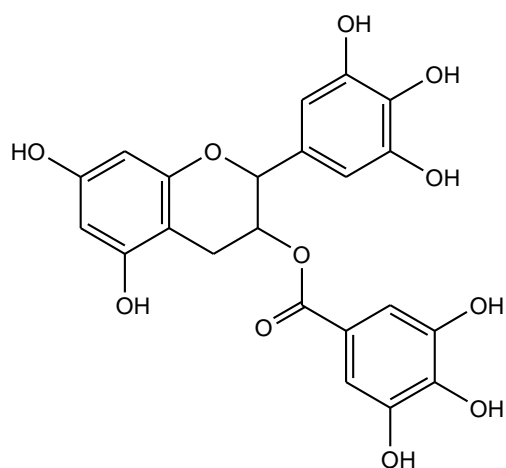
Peak 3: procyanidin B2



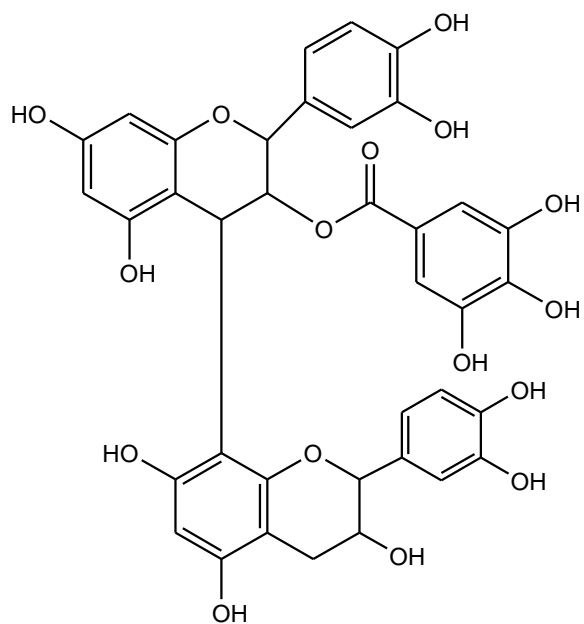
Peak 4: catechin



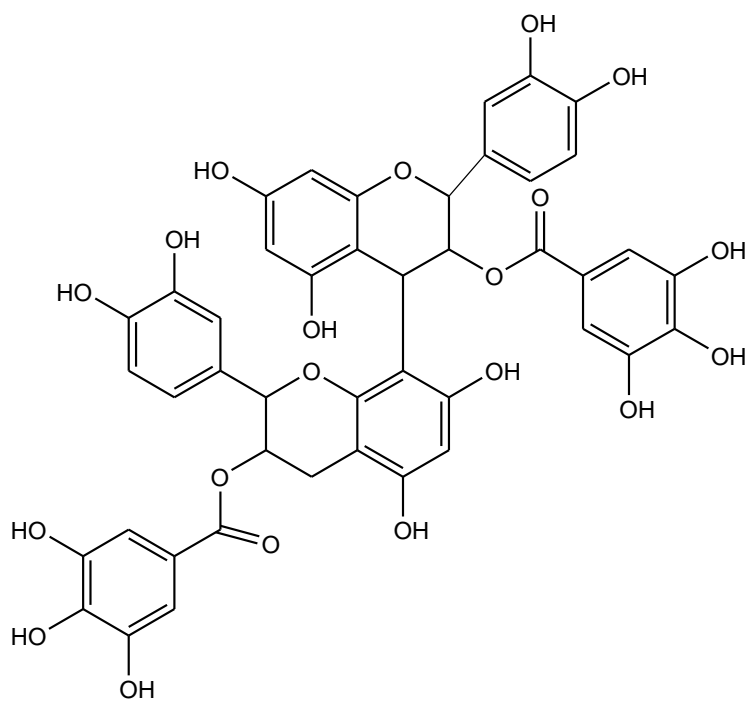
Peak 6: epicatechin-epicatechin-3'-O-gallate



Peak 7: epigallocatechin gallate



Peak 8: epicatechin-3-O-gallate-epicatechin



Peak 9: procyanidin B2-3,3''-di-O-gallate

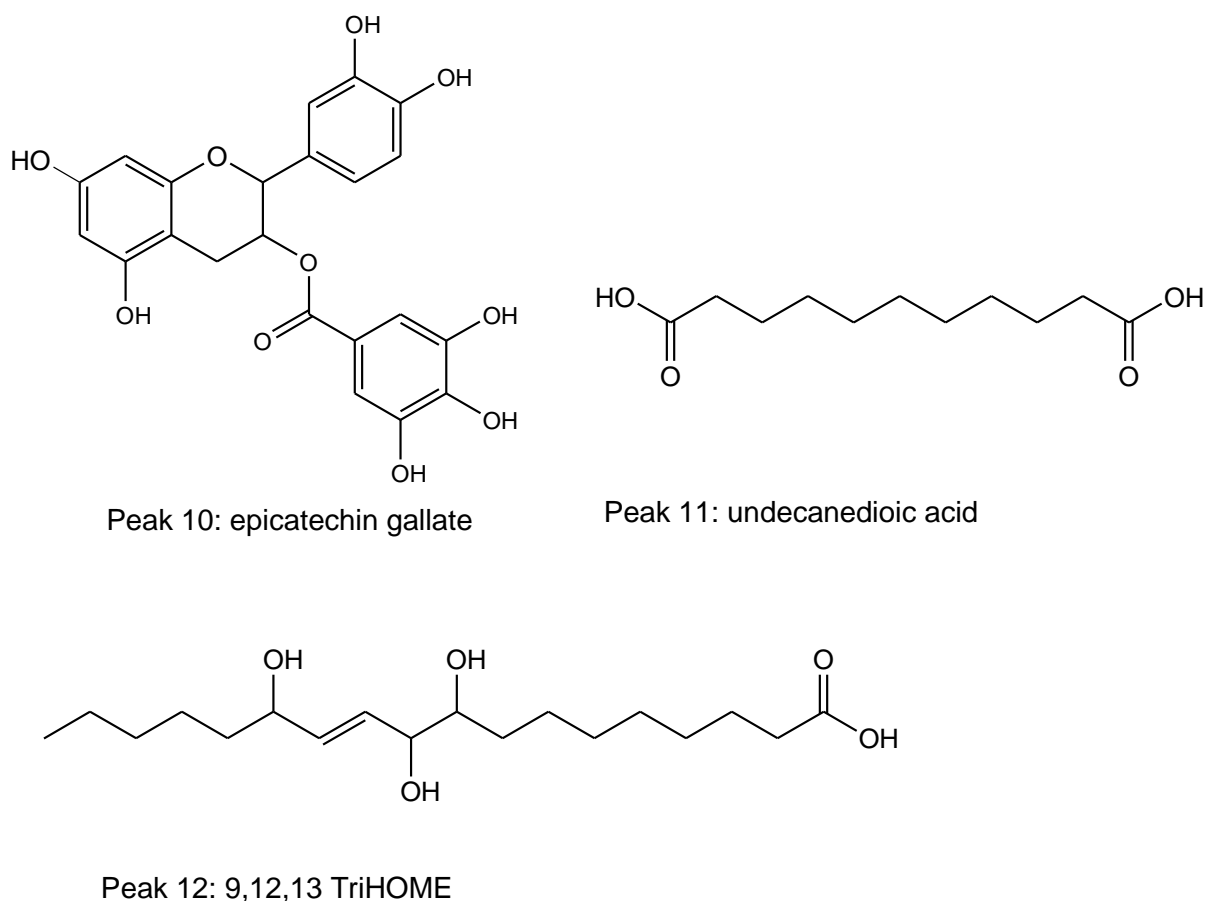


Figure 2.12. Chemical structures of compounds identified

The chemical profile of Marula stem ethanol extract included several proanthocyanidin dimers, trimers and their flavonoid monomers catechin and gallocatechin. The structures were firstly tentatively identified through accurate mass determination and fragmentation patterns. The mechanisms of fragmentation of nongalloylated proanthocyanidins according to Rohr et al. [54] and Jimenez-Sanchez et al. [35] are through retro-Diels-Alder fission (RDA) of the pyran ring of catechin, the quinone -methide (QM) mechanism, heterocyclic ring (HRF) fission and the benzofuran-forming (BFF) fission. Fecka et al. [52] illustrated the fragmentation pathways of B-type trimeric procyanidins (Figure 2.13).

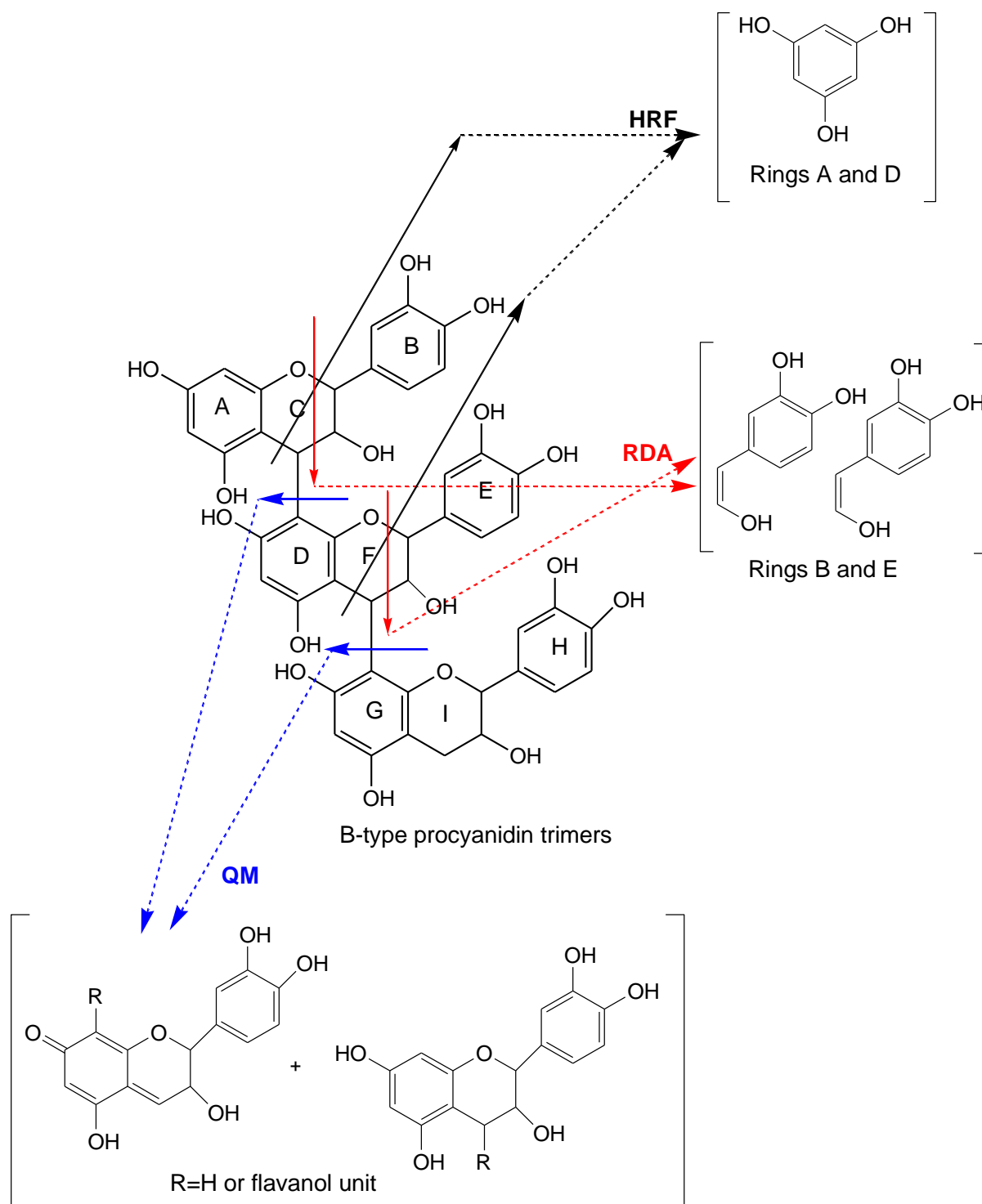


Figure 2.13. Fragmentation pathways of B-type trimeric procyanidins: loss of neutral molecules by HRF(heterocyclic ring fission), RDA (retro-Diels-Alder) and QM (quinone methide) mechanisms (Adapted from Fecka et al. [52] with permission from the authors).

In the first order mass spectrum of peak 1, the $[M-H]^-$ ion was observed at m/z 191.0571 (supplementary data 2). The MassLynx software algorithm for elemental composition determination was used to establish a molecular formula ($C_7H_{11}O_6$) with a normalised iFit value of 0.607 (supplementary data 4). The compound was tentatively identified as quinic acid, its structure is shown in Figure 2.12. The second order mass spectrum (supplementary data 2) showed fragments at m/z 173.0344 $[M-H-18]^-$ due to the loss of a water molecule, at m/z 127.0338 $[M-H-28-18-18]^-$ from the subsequent loss of carbon monoxide and two water molecules, m/z 85.0298 $[M-H-44-18-62]^-$ from the consecutive loss of a carbon dioxide molecule, a water molecule and RDA fragmentation of the ring, and at m/z 59.0125 $[M-H-132]^-$ from the RDA fragmentation of the ring. This fragmentation pattern is characteristic of quinic acid [49]. A pure standard of quinic acid analysed under the same conditions as the crude Marula stem ethanol extract had a retention time of 0.69 minutes and an m/z of 191.0555 which corresponded peak 1 retention time 0.69 minutes and m/z 191.0564 in the extract (Figure 2.14). Further, a comparison of the MS/MS fragmentation pattern of the quinic acid pure standard and that of peak 1 in Marula crude ethanol extract (supplementary data 3) showed they were almost identical and confirmed the presence of quinic acid in the extract.

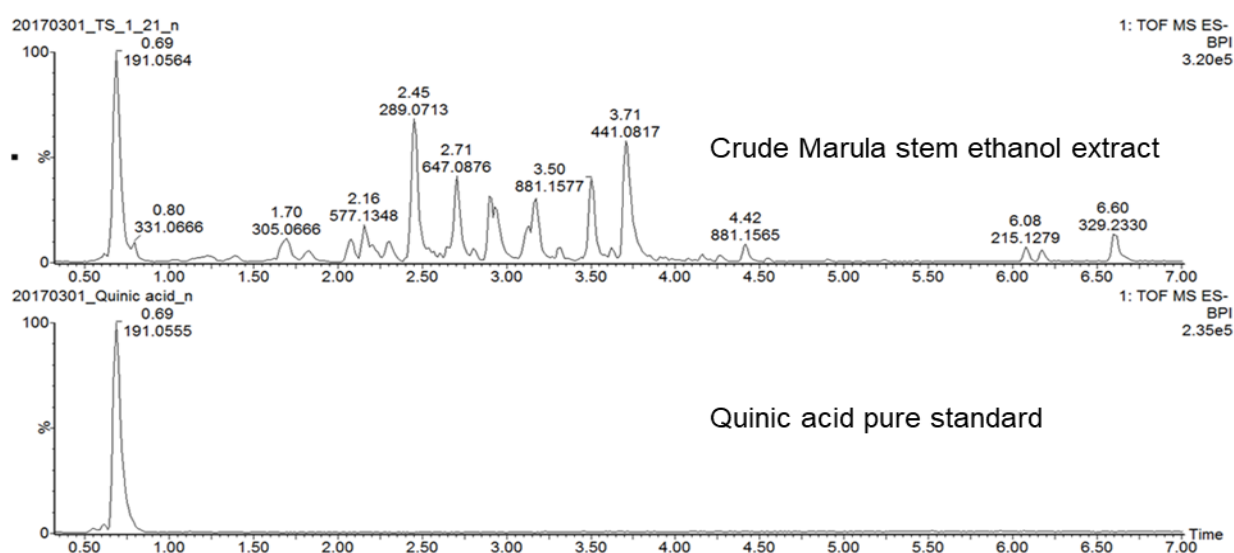


Figure 2.14. ESI negative mode BPI chromatogram of Marula stems extracted with ethanol overlaid with quinic acid pure standard. The pure standard had a retention time of 0.69 minutes and an m/z of 191.0555 which corresponded to the peak at retention time 0.69 minutes and m/z 191.0564 in the extract.

The ESI MS spectrum of peak 2 showed an [M-H]⁻ ion at m/z 305.0662 (supplementary data 5). Masslynx software was used to determine its molecular formula as (C₁₅H₁₃O₇) with an iFit value of 0.163 (supplementary data 6). Accurate mass measurement was used to confirm the molecular formula. In addition to the [M-H]⁻ ion, the first order mass spectrum exhibited an ion at m/z 593.1293 which was identified as a dimer of gallicocatechin. In the MS/MS spectrum (supplementary data 5), the base peak ion was observed at m/z 125.0226 [M-H-180]⁻ from the loss of the chromone moiety. The secondary fragments were observed at m/z 109.0343 [M-H-180-18]⁻ from the subsequent loss of the chromone moiety and loss of a water molecule confirming the presence of hydroxyl groups. Other secondary fragments were observed at m/z 167.0030 [M-H-138]⁻ from the loss of a RDA fragment and at m/z 137.0245 [M-H-168]⁻ from loss of a RDA fragment. Comparison of the theoretical and observed accurate masses tentatively confirmed the presence of gallicocatechin.

The first order mass spectrum of peak 3 showed an [M-H]⁻ ion at m/z 577.1346 (supplementary data 7). Masslynx was used to determine its elemental composition as (C₃₀H₂₅O₁₂) with a normalised iFit value of 0.545 (supplementary data 8). The MS/MS spectrum (supplementary data 7) showed a base peak ion at m/z 125.0234 [M-H-453]⁻ through the loss of a HRF fragment. Secondary ions were observed at m/z 289.0707 [M-H-288]⁻ from loss of a QM fragment; at m/z 425.0818 [M-H-152]⁻ through the loss of an RDA fragment, at m/z 137.0222 from the subsequent loss of an RDA fragment and a water molecule; 407.0773 [M-H-152-18]⁻ due to subsequent loss of an RDA fragment followed by loss of a water molecule; 451.0586 [M-H-125]⁻ from the loss of an HRF fragment and at m/z 245.0701 [M-H-331]⁻ from loss of a catechin residue. This fragmentation pattern is similar to the pattern which was observed by Jimenez-Sanchez et al. [35] and Russo et al. [34] for procyanidin B2 although in their studies they did not identify the fragments at m/z 137.0222 and m/z 245.0701. Fecka et al. [52] reported a similar fragmentation pattern for a dimer of catechin. In this study, peak 3 was tentatively identified as procyanidin B2.

In the first order mass spectrum, peak 4 exhibited an $[M-H]^-$ ion at m/z 289.0717 (supplementary data 9). Using MassLynx software, its elemental composition was determined to be $(C_{15}H_{13}O_6)$ with a normalised iFit value of 0.265 (supplementary data 10). The compound was tentatively identified as catechin, its structure shown in Figure 2.12. The second order mass spectrum (supplementary data 9) showed a base peak ion at m/z 123.0423 $[M-H-152-18]^-$ due to subsequent loss of a HRF fragment and a water molecule indicating the presence of a hydroxyl group. The secondary fragment observed at m/z 151.0362 $[M-H-138]^-$ was due to RDA fragmentation of the catechin ring. Another fragment observed at m/z 137.0238 $[M-H-152]^-$ was also due to RDA fragmentation of the catechin ring. Other fragments were observed at m/z 109.0281 $[M-H-180]^-$ due to loss of the benzo-pyrano (chromano) moiety; m/z 125.0242 $[M-H-165]^-$ due to loss of a HRF fragment and at m/z 245.0607 $[M-H-44]^-$ due to fragmentation of the flavonoid ring. Chua et al. [51] also observed the fragments at m/z 151, m/z 137 and m/z 123 upon fragmentation of catechin. UPLC-MS-QTOF analysis of a catechin pure standard and peak 4 in Marula ethanol extract under the same conditions revealed that the pure standard had a retention time of 2.45 minutes and an m/z of 289.0716 which corresponded to the peak at retention time 2.45 minutes and m/z 289.0717 in the extract (Figure 2.15). Further, a comparison of the MS/MS fragmentation patterns of the catechin pure standard with that of peak 4 (supplementary data 11) in the extract showed these to be similar and confirmed that peak 4 is indeed catechin.

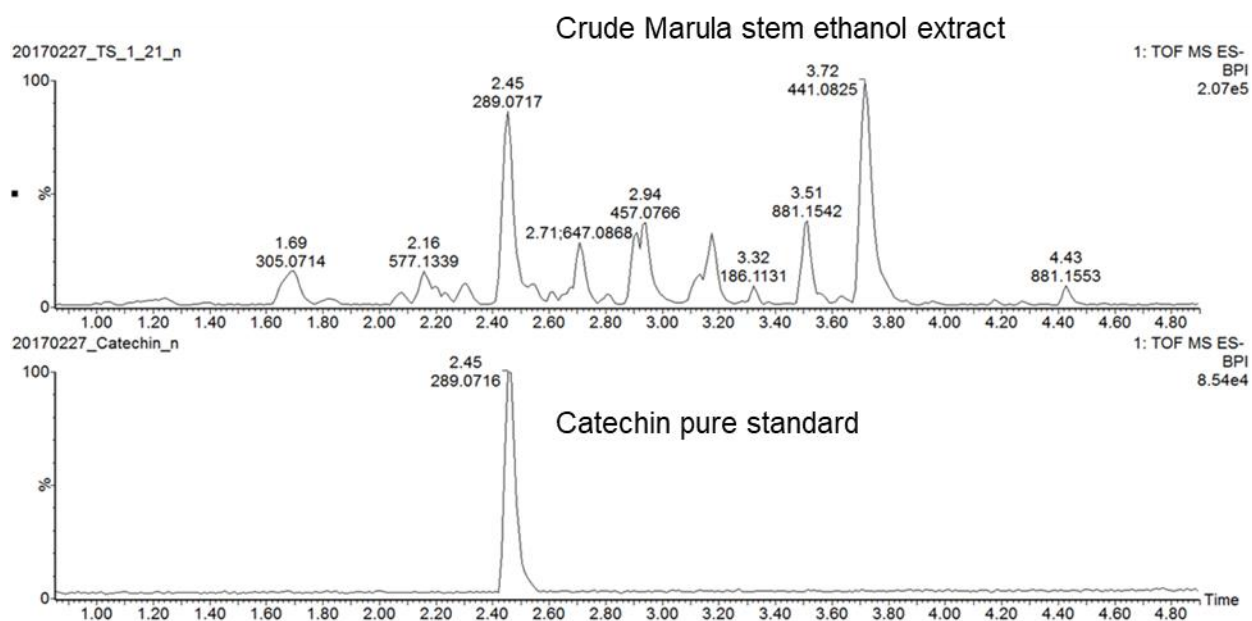


Figure 2.15. ESI negative mode BPI chromatogram of Marula stems extracted with ethanol overlaid with catechin pure standard. The pure standard had a retention time of 2.45 minutes and an m/z of 289.0716 which corresponded to the peak at retention time 2.45 minutes and m/z 289.0717 in the extract.

In the first order mass spectrum, peak 6 exhibited the major $[M-H]^-$ ion at m/z 729.1447 (supplementary data 12). Using MassLynx, the elemental composition was determined to be $C_{37}H_{29}O_{16}$ with a normalised iFit value of 0.000 (supplementary data 13). The compound was tentatively identified as epicatechin-epicatechin-3'-gallate, its structure is shown in Figure 2.12. Its base peak ion was observed at m/z 169.0145 $[M-H-289-272]^-$ from a QM fragmentation leading to loss of a catechin unit subsequently followed by cleavage of a catechin residue (supplementary data 12). Secondary fragments were identified at m/z 425.0851 $[M-H-304]^-$ due to a RDA fragmentation, at m/z 407.0777 $[M-H-304-18]^-$ due to subsequent loss of a RDA fragment and a water molecule, at m/z 577.1335 $[M-H-152]^-$ due to loss of a galloyl residue, at m/z 559.1229 $[M-H-152-18]^-$ due to subsequent loss of a galloyl residue and a water molecule. Another fragment was observed m/z 289.0717 $[M-H-152-288]^-$ due to loss of a gallic acid unit followed by QM fragmentation leading to loss of a catechin residue. The remaining fragments observed were a result of fragmentation of the catechin unit. These included a fragment at m/z 109.0299 $[M-H-152]^-$ due to loss of the benzo-pyrano

(chromano) moiety of catechin at m/z 125.0245 [M-H-165]⁻ due to loss of an HRF fragment, at m/z 137.0224 [M-H-152]⁻ due to RDA fragmentation, at m/z 245.0607 [M-H-44]⁻ due to fragmentation of the flavonoid ring. The fragmentation pattern of epicatechin-epicatechin-3'-gallate obtained in this study was similar to that obtained by Jimenez-Sanchez et al. [35] for the same compound.

Peak 7 had an [M-H]⁻ ion at m/z 457.0782 in the ESI MS (supplementary data 14). Elemental composition analysis using MassLynx provided the molecular formula (C₂₂H₁₇O₁₁) with a normalised iFit value of 0.000 (supplementary data 15). The compound was tentatively identified as epigallocatechin gallate, its structure is shown in Figure 2.12. In the MS/MS spectrum (supplementary data 14), the compound fragmented to produce the base peak ion with m/z 169.0142 [M-H-288]⁻ due to the loss of a catechin residue. Secondary fragments were obtained at m/z 305.0673 [M-H-152]⁻ due to the loss of a galloyl residue, m/z 289.0708 [M-H-168]⁻ from the loss of a gallic acid unit; m/z 125.0244 [M-H-288-44]⁻ due to subsequent loss of a catechin residue and carbon dioxide molecule indicating the presence of a carboxylic acid group. Additional minor ions were observed at m/z 407.0745 and m/z 161.0257. UPLC MS analysis of the pure epigallocatechin gallate standard and peak 8 in the extract under the same conditions showed a m/z of 457.0749 and a retention time of 2.93 minutes for the pure standard and a m/z 457.0766, retention time of 2.94 minutes for peak 8 in the Marula ethanol extract (Figure 2.16). Further, a comparison of the MS/MS fragmentation patterns of the pure standard and peak 7 showed them to be similar and (supplementary data 16) confirmed that peak 7 in Marula ethanol extract is epigallocatechin gallate.

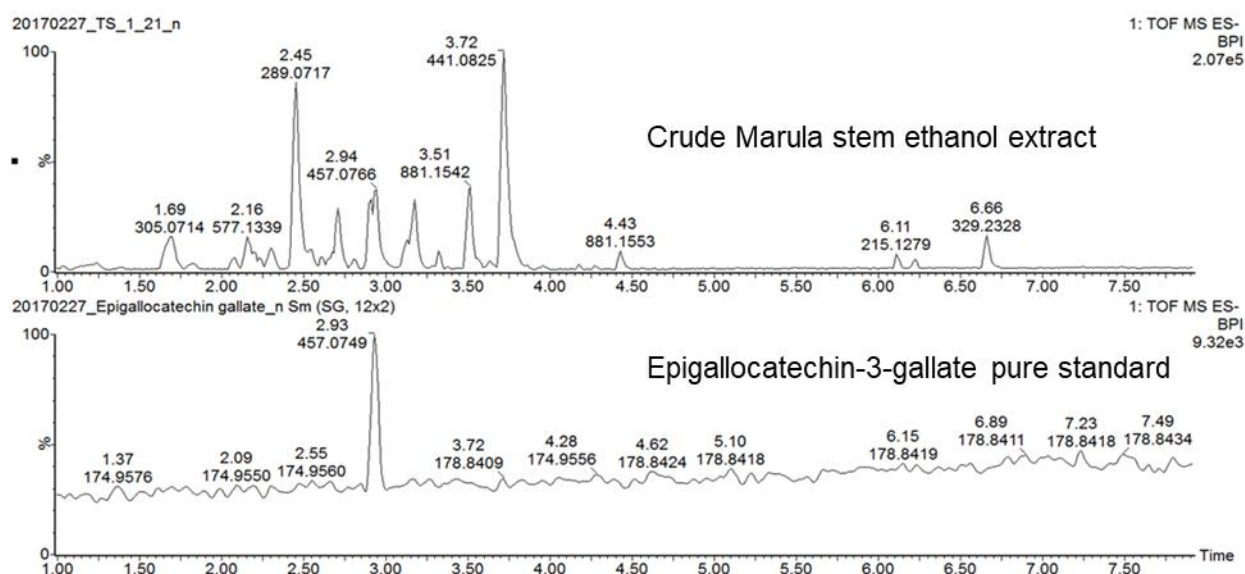


Figure 2.16. ESI negative mode BPI chromatogram of Marula stems extracted with ethanol overlaid with epigallocatechin gallate pure standard. The pure standard had a retention time of 2.93 minutes and an m/z of 457.0749 which corresponded to the peak at retention time 2.94 minutes and m/z 457.0766 in the extract.

In the first order mass spectrum, peak 8 exhibited an $[M-H]^-$ ion at m/z 729.1465 (supplementary data 17). MassLynx software was used to assign a molecular formula of ($C_{37}H_{29}O_{16}$) with a normalised iFit value of 0.009 (supplementary data 18). The peak was tentatively identified as epicatechin-3-O-gallate-epicatechin and its structure is shown in Figure 2.12. The second order mass spectrum (supplementary data 17) of this peak exhibited a base peak ion at m/z 407.0768 $[M-H-152-152-H_2O]^-$ due to successive loss of a galloyl unit, a RDA fragment and a water molecule suggesting the presence of hydroxy groups. Secondary peaks were produced at m/z 577.1276 $[M-H-152]^-$ due to loss of a galloyl residue, m/z 289.0717 $[M-H-152-288]^-$ from subsequent loss of a galloyl residue and a catechin residue. Other secondary fragments were observed at m/z 245.0623 $[M-H-484]^-$ due to loss of a catechin residue, m/z 169.0147 $[M-H-288-273]^-$ from the subsequent loss of a catechin unit via QM fragmentation and followed by loss of another catechin residue, and at m/z 125.0240 $[M-H-288-273-44]^-$ due to subsequent loss of a QM fragment followed by a catechin residue and a molecule of carbon dioxide showing the presence of a carboxylic acid group. This

fragmentation pattern is similar to that which was obtained by Jimenez-Sanchez et al. [35] for epicatechin-3-O-gallate-epicatechin. A comparison of the theoretical and the experimental accurate masses confirmed the structure. In the study of plant tissues of *S. birrea* by Russo et al. [34] only one monogalloylated procyanidin dimer was identified while in this study two monogalloylated procyanidin dimers were identified from Marula stems. Jimenez-Sanchez et al. [35] identified three monogalloylated procyanidin dimers from Marula stem bark.

In the ESI MS spectrum, peak 9 had an $[M-H]^-$ ion observed at m/z 881.1564 (supplementary data 19). MassLynx was used to establish its molecular formula as $(C_{44}H_{33}O_{20})$ with a normalised iFit value of 0.008 (supplementary data 20). Accurate mass measurement was used to confirm the molecular formula. The compound was tentatively identified as procyanidin B2-3'3 di-O-gallate, and its structure is shown in Figure 2.12. The second order mass spectrum (secondary data 19) showed a base peak ion m/z 407.0759 $[M-H-169-152-136-18]^-$ due to subsequent loss of a gallic acid unit, a galloyl residue and a RDA fragment. Secondary fragments were observed at m/z 729.1445 $[M-H-152]^-$ due to loss of a galloyl residue, m/z 559.1211 $[M-H-152-170]^-$ due to successive loss of a galloyl residue and a gallic acid unit. Other fragments were observed at m/z 169.0145 $[M-H-440-273]^-$ due to consecutive loss of a QM fragment followed by a catechin residue. This fragment at m/z 169.0145 lost a carbon dioxide molecule to give another fragment at m/z 125.0223 typical of loss of the carbonyl ester. The compound was tentatively identified as procyanidin B2-3'3 di-O-gallate. Studies by Russo et al. [34] and Jimenez et al. [35] identified procyanidin B2-3'3 di-O-gallate in the stem bark of Marula. The fragmentation pattern observed by Russo et al. [34] and Jimenez et al. [35] for procyanidin B2-3'3 di-O-gallate was similar to that identified in our study.

In the ESI MS spectrum, peak 10 showed an $[M-H]^-$ ion at m/z 441.0820 (supplementary data 21). Elemental composition analysis using MassLynx software provided the formula

(C₂₂H₁₇O₁₀) with a near perfect normalised iFit value of 0.047 (supplementary data 22). In addition to the [M-H]⁻ ion, the first order mass spectrum showed a [2M-H]⁻ ion at *m/z* 883.1716. The peak was tentatively identified as epicatechin gallate, its structure is shown in Figure 2.12. The MS/MS spectrum (supplementary data 22) displayed a base peak ion at *m/z* 169.0139 [M-H-272]⁻ due to loss of a catechin residue. Secondary peaks were at *m/z* 289.0710 [M-H-152]⁻ due to loss of a galloyl residue, *m/z* 125.0241 [M-H-272-44]⁻ from subsequent loss of a catechin residue and carbon dioxide. UPLC QTOF MS analysis of a pure standard of epicatechin gallate and peak 10 in Marula ethanol extract revealed that the pure standard had an *m/z* of 441.0842 and a retention time of 3.74 minutes while peak 10 had a *m/z* 441.0825 and retention time of 3.72 minutes (Figure 2.17). Further, a comparison of the MS/MS fragmentation pattern of epicatechin gallate pure standard and that of peak 10 (supplementary data 23) confirmed that peak 10 is indeed epicatechin gallate.

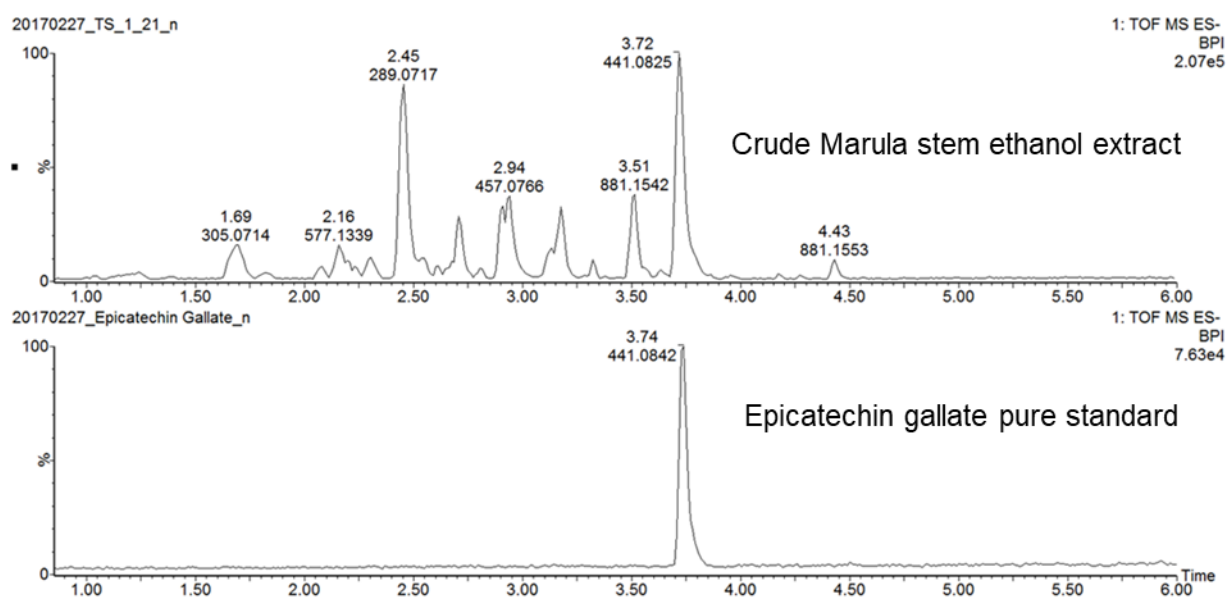


Figure 2.17. ESI negative mode BPI chromatogram of Marula stems extracted with ethanol overlaid with epigallocatechin gallate pure standard. The pure standard had a retention time of 2.93 minutes and an *m/z* of 457.0749 which corresponded to the peak at retention time 2.94 minutes and *m/z* 457.0766 in the extract.

The ESI-MS spectrum of peak 11 showed an [M-H]⁻ ion at *m/z* 215.1279 (supplementary data 24). Elemental composition analysis using MassLynx gave the formula of the ion to be

$C_{11}H_{19}O_4$ with a normalised ifit value of 0.076 (supplementary data 25). Accurate mass measurement was used to confirm the molecular formula. The compound was tentatively identified as undecanedioic acid, its structure is shown in Figure 2.12. In the MS/MS spectrum, fragments were observed at m/z 197.1155 [M-H-18]⁻ from the loss of a water molecule and at m/z 153.1117 [M-H-18-44]⁻ from the subsequent loss of a water molecule and a carbon dioxide molecule. These fragments are similar to the fragments identified by Jimenez-Sanchez et al. [35] in undecanedioic acid.

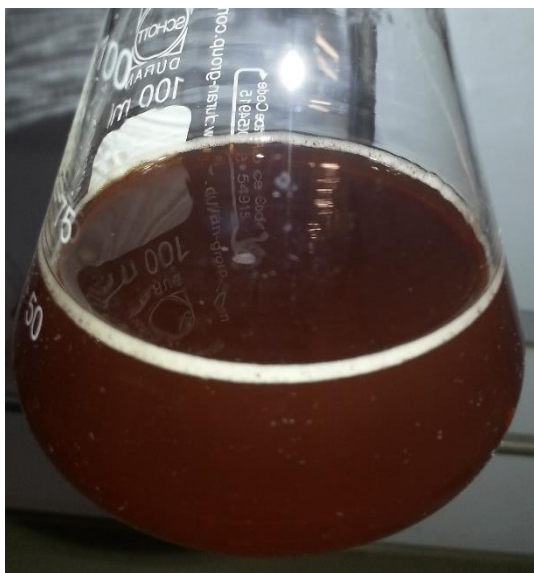
In the ESI MS spectrum, peak 12 had an [M-H]⁻ ion at m/z 329.2330 (supplementary data 26). Elemental composition analysis using MassLynx provided the molecular formula ($C_{18}H_{33}O_5$) with a normalised iFit value of 0.053 (supplementary data 27). Accurate mass measurement was used to confirm the molecular formula. The compound was tentatively identified as 9,10,13 TriHOME, its structure is shown in Figure 2.12. The MS/MS (supplementary data 26) fragments showed a base peak ion at m/z 211.1227 [M-H-45-57-18]⁻ from the consecutive loss of a carboxylic acid group, a butyl fragment and a water molecule. Secondary fragments were observed at m/z 233.1124 [M-H-45-57]⁻ from the subsequent loss of a carboxylic acid group and a butyl fragment and at m/z 171.0814 [M-H-71-87]⁻ from the consecutive loss of a pentyl group and a butene diol fragment. Other secondary fragments were observed at m/z 283.0403 [M-H-29-18]⁻ from the subsequent loss of an ethyl fragment and a water molecule. Nording et al. [53] observed the fragments at m/z 329.2 and m/z 171.1 in an analysis of a pure standard of a pure standard of 9,10,13 TriHOME.

2.7.7 Improving the quality of the ethanol extract as a cosmetic ingredient

In order to improve the quality of the Marula crude ethanol extract by lowering the intensity of the brown colour and to improve the anti-aging activity, the extracts was separately defatted, concentrated and then defatted-concentrated (three separate samples/fractions). Yields

obtained after each process were 81.66% for the defatted fraction, 42.16% for the concentrated fraction and 34.60% for the defatted-concentrated fraction. The fractions and the Marula oil were screened for collagenase and elastase inhibition activities. Defatting reduced the colour intensity but the difference in colour between the defatted fraction and the original crude extract was not highly significant. This could be due to the fact that in Marula stems there is limited chlorophyll and that other polar compounds like tannins, proanthocyanidins previously confirmed to be present in Marula stems and bark may be responsible for the brown colour in the Marula extract [9, 31, 34, 35]. The intensity of the brown colour was significantly lowered in the concentrated fraction and the defatted-concentrated fraction (Figure 2.18). This is due to the concentration step which successfully extracted active ingredients into the ethyl acetate fraction thus separating them from compounds responsible for the dark-brown pigment which remained in the water fraction.

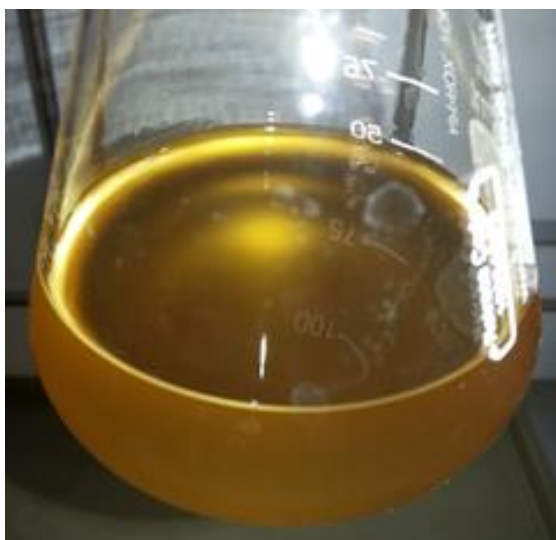
A. Crude Marula extract



B. Defatted Marula fraction



B. Concentrated Marula fraction



D. Defatted and concentrated Marula fraction



Figure 2.18. Picture A shows the dark-brown colour of Marula crude extract, picture B shows a slightly lower intensity of the dark brown colour produced by defatting. In pictures C and D the brown intensity was significantly lowered. Picture C is the concentrated extract and picture D is the defatted-concentrated fraction.

The bioassay results shown in Figure 2.19 revealed that at test concentration 10 µg/ml, the anti-elastase activities of Marula oil ($22.35\% \pm 7.60$), Marula crude extract ($29.60\% \pm 6.42$), Marula defatted fraction ($5.28\% \pm 7.74$) were significantly ($p < 0.01$) lower than that of the positive control elafin ($99.45\% \pm 0.06$). The Marula concentrated fraction and the Marula defatted- concentrated fraction showed no collagenase inhibition activities at this concentration. A similar trend was observed at 100 µg/ml. Although biologically high elastase activities were exhibited by the Marula crude extract ($88.61\% \pm 0.12$), Marula defatted fraction ($86.54\% \pm 0.21$), Marula concentrated fraction ($88.70\% \pm 0.52$) and the Marula defatted-concentrated fraction ($88.46\% \pm 0.52$), statistically, these fractions and Marula oil ($7.63\% \pm 0.65$) exhibited significantly ($p < 0.01$) lower potency than the positive control elafin ($99.79\% \pm 0.02$).

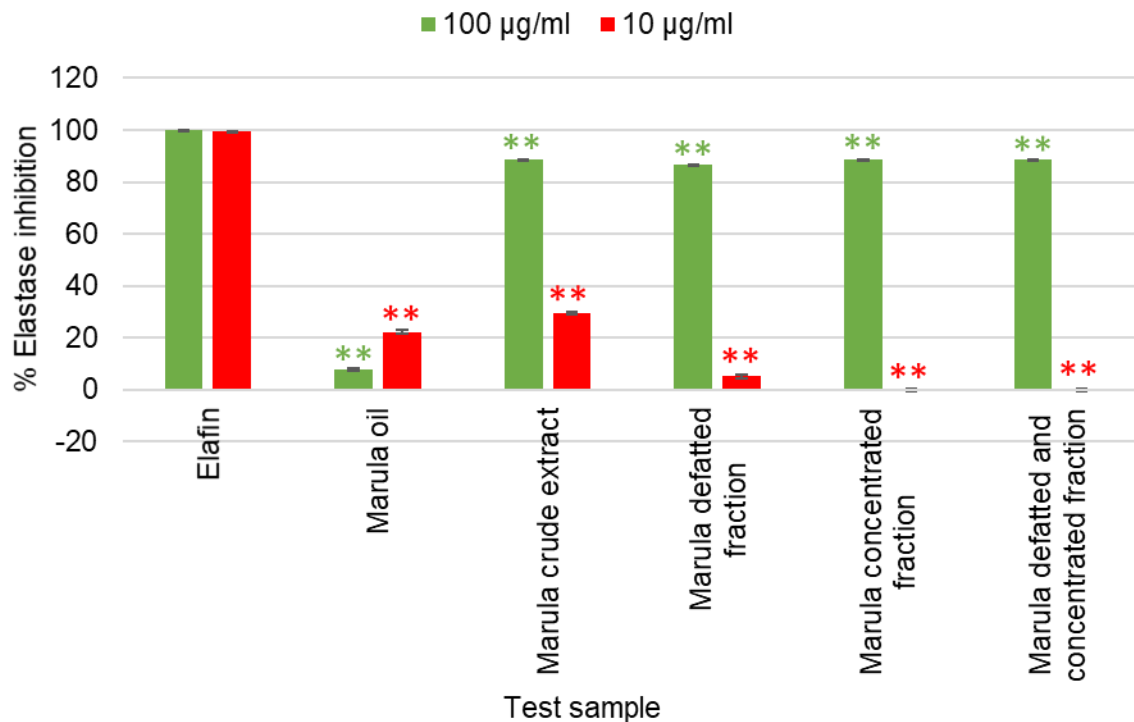


Figure 2.19. Elastase inhibition of the improved quality samples and Marula oil at 100 and 10 µg/ml (Error bars represent SEM, with n=3). * = P<0.05, ** = P<0.01 represent a significant difference compared to elafin at 10 µg/ml and * = P<0.05, ** = P<0.01 represent a significant difference compared to elafin at 100 µg/ml.

At test concentration 10 µg/ml, the collagenase inhibition activities of Marula oil (14.29% ± 1.48), Marula crude extract (45.95% ± 3.73), Marula defatted fraction (26.88% ± 0.28), were significantly (p<0.01) lower than that of EDTA (84.81% ± 0.73) (Figure 2.20). The Marula concentrated extract and Marula defatted-concentrated extract showed no collagenase inhibition activity. At the higher concentration of 100 µg/ml, Marula oil (27.88% ± 0.30), Marula crude extract (79.95% ± 0.15) and Marula defatted extract (78.96% ± 0.38) exhibited significantly (p<0.01) lower potency than EDTA (84.81% ± 0.73). However, the Marula concentrated fraction (89.26% ± 1.95) was as potent (p=0.04) as EDTA while the Marula defatted-concentrated fraction (94.34% ± 0.09) was significantly (p<0.01) more potent than EDTA. A comparison of the elastase (Figure 2.19) and collagenase inhibition activities of the defatted and the Marula crude stem ethanol extracts to the positive controls (Figure 2.20), revealed that these two extracts did not show significant activities at all concentrations tested.

Consequently, defatting did not statistically improve the elastase and collagenase inhibition activities of the Marula crude extract.

A significant improvement in collagenase inhibition activity was observed at 100 µg/ml following concentration of the Marula stem ethanol extract. At this concentration, defatting-concentration produced an extract exhibiting more potency than that of the original Marula stem ethanol extract, the concentrated extract and the positive control. The high potency observed in this extract is a result of the removal of inactive compounds through both the defatting and concentration steps. The defatted components contribute to the dilution of the active compounds in the separately concentrated extract explaining its lower activity. Due to the high potency, the defatted and concentrated ethanol extract of Marula stems (coded MDC extract) was selected for combination and formulation studies in Chapter 4.

Marula oil, an ingredient in a variety of cosmetic formulations was also evaluated for its enzyme inhibition for comparative purposes. Our results revealed that Marula oil, although traded as a cosmetic ingredient does not have any anti-collagenase activity contributing to anti-aging claims on products containing the oil. Clinical studies conducted by Komane et al. [23] showed that Marula oil is a non-irritant which provides hydrating and moisturising properties to xerotic skin and gives occlusive effects to normal skin. Another study by Mariod et al. [55] showed that Marula kernel oil cake had the highest antioxidant activity in comparison to other parts of Marula. These findings justify the traditional use of Marula oil in cosmetics although it may not be beneficial as an anti-aging ingredient. The fractions of Marula showed good inhibition at the higher concentrations while limited at the low 10 µg/ml. While activity has been seen in the fractions at different concentrations to varying degrees, the chemical compounds in these complex mixtures contribute to efficacy either as single chemical entities or through a combination of synergistic and additive effects [56-58].

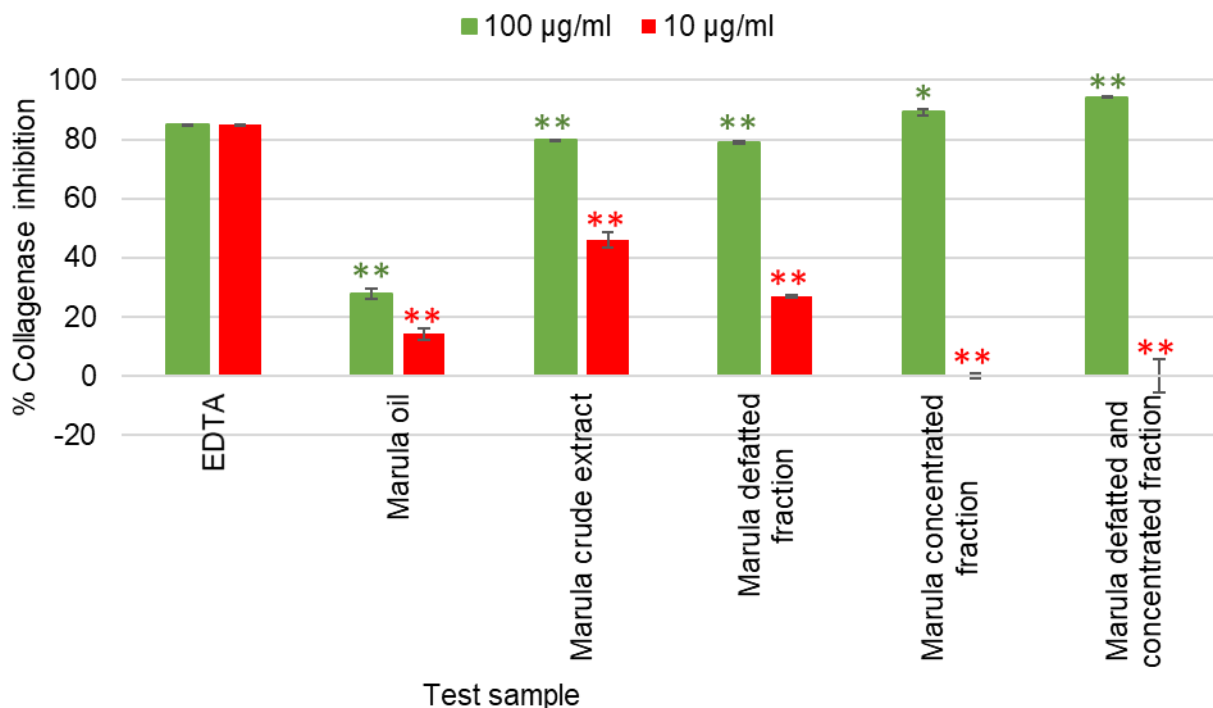


Figure 2.20. Collagenase inhibition of the fractions with improved quality and Marula oil tested at 100 and 10 µg/ml (Error bars represent SEM, with n=3). * = P<0.05, ** = P<0.01 represent a significant difference with EDTA at 10µg/ml and * = P<0.05, ** = P<0.01 represent a significant difference with EDTA at 100µg/ml.

2.7.8 Comparison of chemical profiles of the Marula extract, and fractions obtained through defatting and concentration

The chemical profiles of the crude Marula extract, and the three fractions obtained through defatting, concentration and their combination were analysed using UPLC-QTOF-MS. The comparison of the BPI chromatograms of the Marula extract, defatted and concentrated fractions showed that the major compound corresponding to quinic acid was removed from the crude extract during the concentration steps of the process (Figure 2.21 and Table 2.5). In sections 2.7.12 and 2.7.14 quinic acid was found to be inactive in both the anti-elastase and anti-collagenase assays. Thus, the concentration step was successful as it removed this major inactive compound. Epigallocatechin gallate and epicatechin gallate were retained in the concentrated, defatted, and the defatted-concentrated fractions thereby contributing to the anti-aging activity. However, the inactivity of the concentrated extracts at 10 µg/ml may be

attributed to the samples being tested at too low a concentration. A comparison of the Marula crude extract with Marula defatted extract revealed that these profiles were similar, which substantiates the lack of improvement in elastase and collagenase activities observed in section 2.7.7 upon defatting the Marula stem ethanol extract.

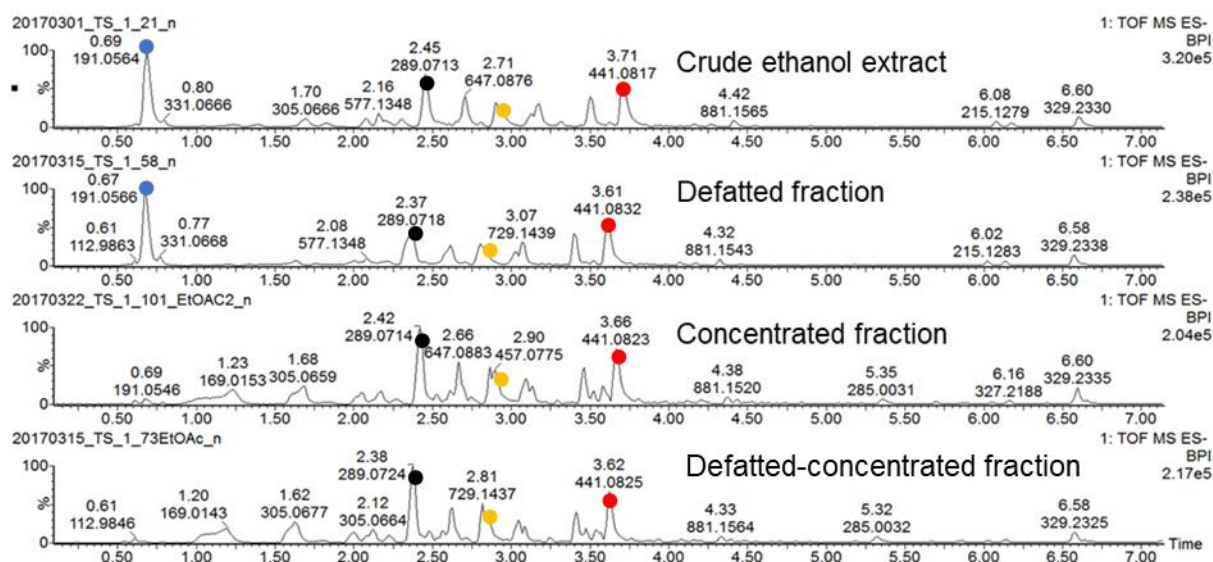


Figure 2.21. Negative mode BPI chromatograms of Marula stem ethanol extract and its fractions showing the presence of •catechin (m/z 289.0718 retention time 2.45 minutes), ●epigallocatechin gallate (m/z 457.0775 retention time 2.90 minutes) and ●epicatechin gallate (m/z 441.0817 retention time 3.71 minutes) in all samples. ●Quinic acid was present in the crude ethanol extract and in the defatted fraction but was absent in the concentrated and defatted-concentrated fraction.

Table 2.5

A comparison of major compounds identified in the Marula fractions after liquid-liquid partitioning

Compound	RT (minutes)	[M-H] m/z	Crude Ethanol extract	Defatted extract	Concentrated extract	Defatted and Concentrated fraction
Quinic acid	0.69	191.0564	present	present	absent	absent
Catechin	2.45	289.0713	present	present	present	present
Epigallocatechin gallate	2.93	457.0782	present	present	present	present
Epicatechin gallate	3.71	441.0817	present	present	present	present

2.7.9 Bioassay-guided fractionation

Fractionation of Marula stem ethanol extract was undertaken with the aim of identifying the active compounds and hence establish the correlation between the anti-aging activity of the extract and the active compounds. Using a prep HPLC UV for fractionation, twenty-three time-based fractions labelled as S1-S23 were collected. Each fraction was dried down using a speed vacuum and a sample (1 mg) of each fraction was accurately weighed for bio-assaying.

2.7.10 Collagenase inhibition activity of fractions of *S. birrea*

The crude Marula ethanol extract, the positive control EDTA and fractions S1 to S23 were screened in the collagenase assay and the results are shown in Figure 2.22. The positive control EDTA ($82.54\% \pm 0.92$) exhibited a good collagenase inhibition activity and was used as a benchmark to select the active fraction hence test samples exhibiting activity above 80% were regarded as active. The crude extract ($56.64\% \pm 4.18$) exhibited a lower collagenase inhibition activity in comparison with the positive control EDTA. Most fractions exhibited higher biological activities above that of the crude extract. This could be attributed to fractionation resulting in concentration of the active ingredients. There was generally very limited selectivity as most of the fractions showed good activity above 60%. Five of the fractions had very good collagenase activity ($>80\%$) in the similar range as EDTA. These active fractions S5 ($83.25\% \pm 0.81$), S6 ($80.46\% \pm 1.33$), S7 ($84.54\% \pm 1.62$) and S8 ($87.30\% \pm 1.25$) were thus selected for chemical analysis.

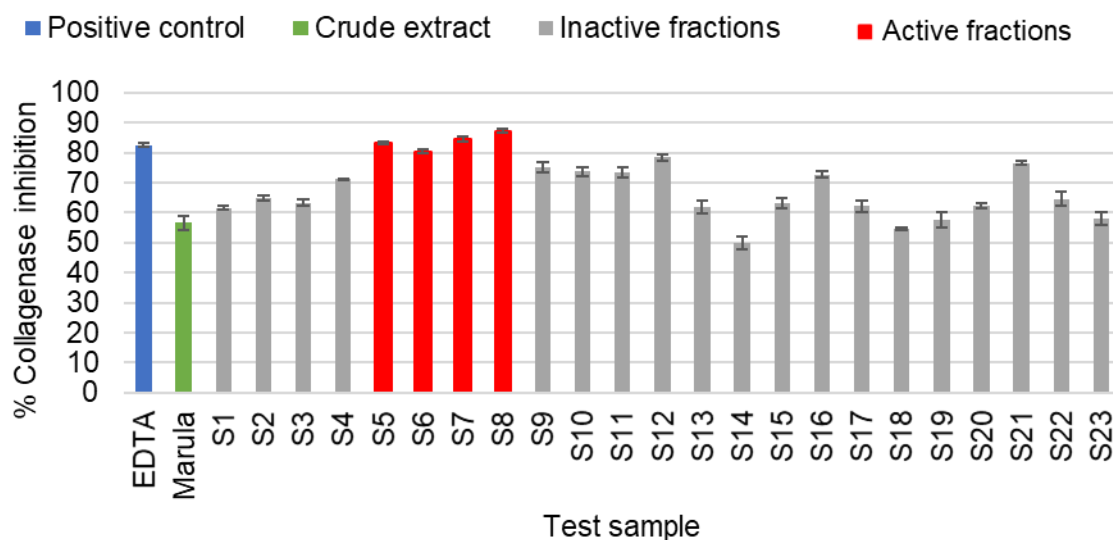


Figure 2.22. Collagenase inhibition activity of Marula fractions at 200 $\mu\text{g/ml}$ and positive control EDTA at test concentration 143 $\mu\text{g/ml}$. Active fractions S5, S6, S7 and S8 exhibited similar potency to EDTA. (Error bars represent SEM, with $n=3$).

2.7.11 UPLC-QTOF-MS analysis of active fractions

The active fractions S5, S6, S7 and S8 were analysed on UPLC-QTOF-MS in order to identify the compounds responsible for collagenase inhibition activity in these fractions (Figure 2.23). The peak at m/z 457.0775 retention time 2.90 minutes in fraction S5 was also observed in fraction S6 at m/z 457.0759 retention time 2.90 minutes, the $[2M-H]^-$ ion was observed in fraction S7 at m/z 915.1595 retention time 2.91 minutes and in fraction S8 at m/z 457.0742. The identity of the compound corresponding to this peak was confirmed to be epigallocatechin gallate in section 2.7.6. Epigallocatechin gallate was identified in section 2.7.5 as one of the compounds common to the Marula extracts which were showing collagenase inhibition activity and hence the flavonoid contributes to the anti-aging activity of the extracts. The presence of epigallocatechin gallate in active fractions S5 to S8 provides evidence which substantiates the contribution of this compound to the anti-aging activity of Marula stem extracts. The peak at m/z 441.0814 retention time 3.59 minutes in fraction S5 was present in fraction S6 at m/z 441.0811 retention time 3.59 minutes, fraction S7 at m/z 441.0823 retention time 3.60 minutes and in fraction S8 at m/z 441.0804 retention time 3.60 minutes. The compound corresponding

to this peak was identified in section 2.7.6 as epicatechin gallate. The compound has been identified in section 2.7.6 as one of the compounds contributing to the anti-aging activity of different extracts of Marula stems. The presence of this compound in active fractions S5 to S8 corroborates the results and conclusions obtained earlier in this study.

The most intense peak in fraction S5 was at m/z 647.0863 retention time 2.70 minutes, this peak was also present in fraction S6 at m/z 647.0865 retention time 2.69 minutes but was absent from fractions S7 and S8. It is therefore unlikely that the compound corresponding to this peak is contributing to the collagenase activity of these fractions. The compound corresponding to this peak remains unidentified. A peak of low intensity was observed in fraction S8 at m/z 289.0711 retention time 2.50 minutes the peak was also present in fractions S7 at m/z 289.0703 retention time 2.50 minutes, S6 at m/z 289.0707 retention time 2.50 minutes and S5 at m/z 289.0175 retention time 2.50 minutes. The compound corresponding to this peak was identified in section 2.7.6 as catechin. The compound was common to the active extracts of Marula in sections 2.7.2 and 2.7.4 and may be one of the compounds contributing to collagenase inhibition activity in this fraction. Another peak of low intensity was observed in fractions S8 at m/z 881.1548 retention time 3.40 minutes, S7 at m/z 881.1526, S6 at m/z 881.1506 retention time 3.39 minutes but was not present in fraction S5 so the compound corresponding to this peak is not likely to contribute to the anti-aging activity of the fractions. The peak at m/z 411.0231 retention time 0.81 minutes was present only in fraction S8 at m/z 411.0231 retention time 0.81 minutes. As such the compound corresponding to this peak is not likely to be contributing to the collagenase inhibition activity of the fractions. The compounds epicatechin gallate, epigallocatechin gallate and catechin were common to active fractions S5, S6, S7 and S8 and are likely to contribute to the anti-collagenase inhibition activity of Marula stem ethanol extract. It is, therefore, necessary to screen these compounds in the collagenase inhibition activity assay to confirm if they inhibit this enzyme.

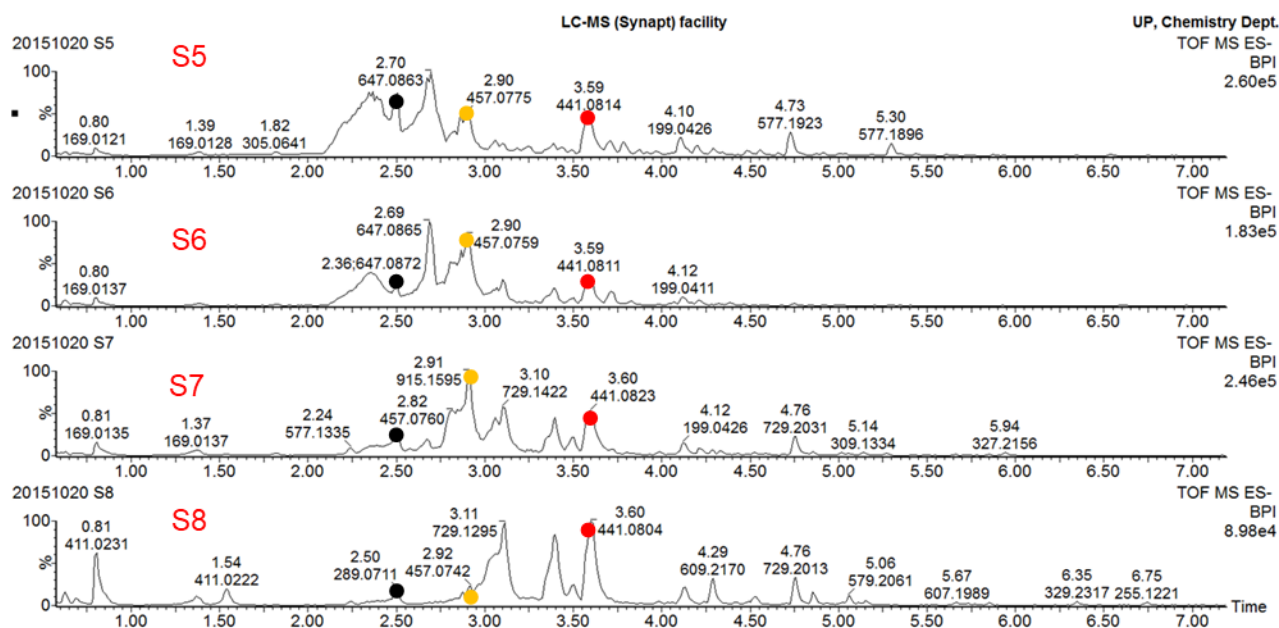


Figure 2.23. ESI negative mode BPI chromatograms of fractions S5, S6, S7 and S8 from Marula stem ethanol extract. ● Epigallocatechin gallate (at m/z 457.0775 $[M-H]^-$ retention time 2.90 minutes, ● epicatechin gallate (at m/z 441.0814 $[M-H]^-$ ion) retention time 3.59 minutes) and ● catechin (at m/z 289.0175 retention time 2.50 minutes) are likely to contribute to the collagenase inhibition activities of the four fractions.

2.7.12 Collagenase inhibition assaying of pure compounds

The compounds catechin, quinic acid, epigallocatechin gallate and epicatechin gallate confirmed to be present in Marula stem ethanol extract were screened for collagenase inhibition activity and the screening results are given in Figure 2.24. Quinic acid and catechin exhibited very low collagenase inhibition activities (<15%) at all test concentrations. Previous studies confirmed our findings of the inactivity of quinic acid [59] and catechin [57, 60] in the collagenase inhibition test. At 20 $\mu\text{g/ml}$ epigallocatechin gallate (calculated 44 μM) exhibited good anti-collagenase activity of $71.59\% \pm 1.59$ which was statistically ($p > 0.05$) as potent as EDTA ($72.09\% \pm 0.66$). Similarly, at the same test concentration of 20 $\mu\text{g/ml}$, epicatechin gallate (calculated 45 μM) showed good collagenase inhibition activity of $71.57\% \pm 1.26$ with potency statistically ($p > 0.05$) equivalent to EDTA. Upon lowering the test concentration to 10 $\mu\text{g/ml}$, epigallocatechin gallate (calculated 22 μM) exhibited good anti-collagenase inhibition

activity of $78.63\% \pm 0.96$ which remained in the same ($p > 0.05$) potency range as EDTA ($83.51\% \pm 2.84$). Similarly, at $10 \mu\text{g/ml}$ epicatechin gallate (calculated $23 \mu\text{M}$) showed good collagenase inhibition activity ($81.93\% \pm 0.40$) with potency statistically ($p > 0.05$) equivalent to EDTA. At the lower test concentration of $5 \mu\text{g/ml}$ (calculated $11 \mu\text{M}$), epicatechin gallate ($75.40\% \pm 1.66$) and epigallocatechin gallate ($67.75\% \pm 3.54$) remained in the same potency range ($0.01 < p < 0.05$) as EDTA ($81.91\% \pm 0.46$). Consequently, epigallocatechin gallate and epicatechin gallate have been confirmed to be some of the compounds contributing to the collagenase inhibition activities of Marula fractions and extracts.

A study by Madhan et al. [60] found epigallocatechin gallate to exhibit potent collagenase inhibition activity of 70% at $20 \mu\text{M}$ which was similar to our results in which epigallocatechin gallate showed $71.59\% \pm 1.59$ collagenase inhibition at $22 \mu\text{M}$. A number of studies use epigallocatechin gallate as a positive control in tests for collagenase inhibition and in one of such study it was shown to have an IC_{50} of $12.9 \mu\text{M}$ [61]. Makimura et al. [57] found epicatechin gallate to be a potent anti-collagenase inhibitor at $113 \mu\text{M}$. Our results have shown that epigallocatechin gallate with ($>65\%$ inhibition at $11 \mu\text{M}$) and epicatechin gallate ($>75\%$ inhibition at $11 \mu\text{M}$) have more potent anti-collagenase activities. The study conducted by Makimura et al. [57] revealed that the steric structure of 3-galloyl radical is important for inhibition of collagenase activity positive control gave the inhibitory activity as expected indicating the validity of the assay.

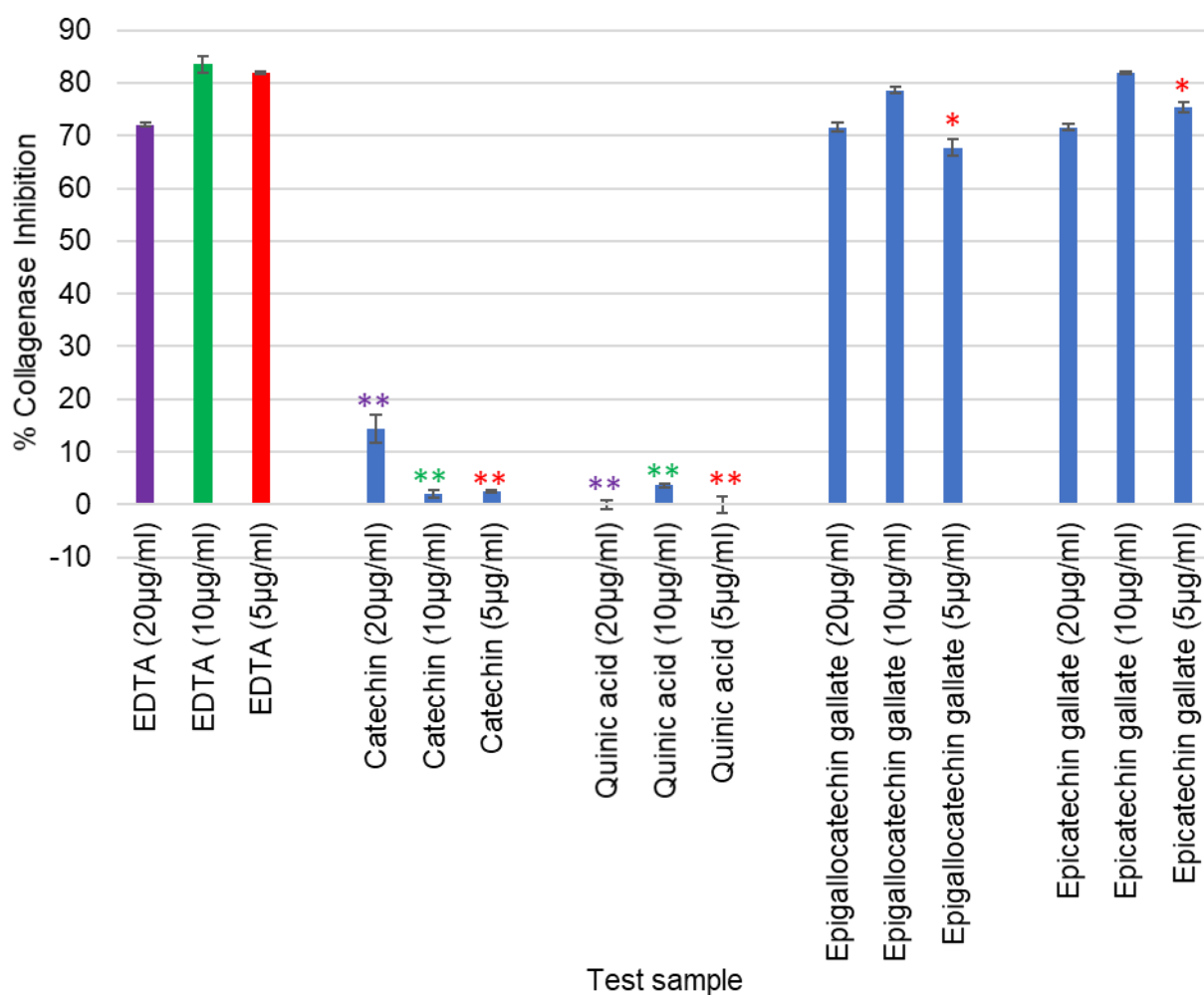


Figure 2.24. Collagenase inhibition activities of major compounds identified in Marula stem ethanol extract at 20, 10 and 5 µg/ml. (Error bars represent SEM, with n=3). * = P<0.05, ** = P<0.01 represent a significant difference with EDTA at 5 µg/ml, * = P<0.05, ** = P<0.01 represent a significant difference with EDTA at 10 µg/ml, * = P<0.05, ** = P <0.01 represent a significant difference with EDTA at 20 µg/ml.

2.7.13 Elastase inhibition activity of fractions of *S. birrea*

Fractions from Marula stem ethanol extract were also screened for elastase inhibition activity. At a test concentration of 200 µg/ml, elastase inhibition activity was >80% for most fractions showing limited selectivity. To address this lack of selectivity, fractions were screened at lower concentrations of 100 µg/ml and 25 µg/ml. The results obtained at 25 µg/ml showed greater selectivity between active and non-active fractions. At this concentration, the positive control elafin (99.15% ± 0.079) exhibited very good elastase inhibition activity. Fractions exhibiting

(>65%) elastase inhibition activity were considered to be active. Thus, fractions S1 (79.42% ± 0.57), S18 (71.38% ± 0.62), S19 (67.26% ± 1.23), S20 (72.72% ± 0.73), S22 (65.31% ± 1.57) and S23 (76.65% ± 0.69) which exhibited good elastase inhibition activities with respect to elafin (99.15% ± 0.079) (Figure 2.25) were selected for chemical analysis.

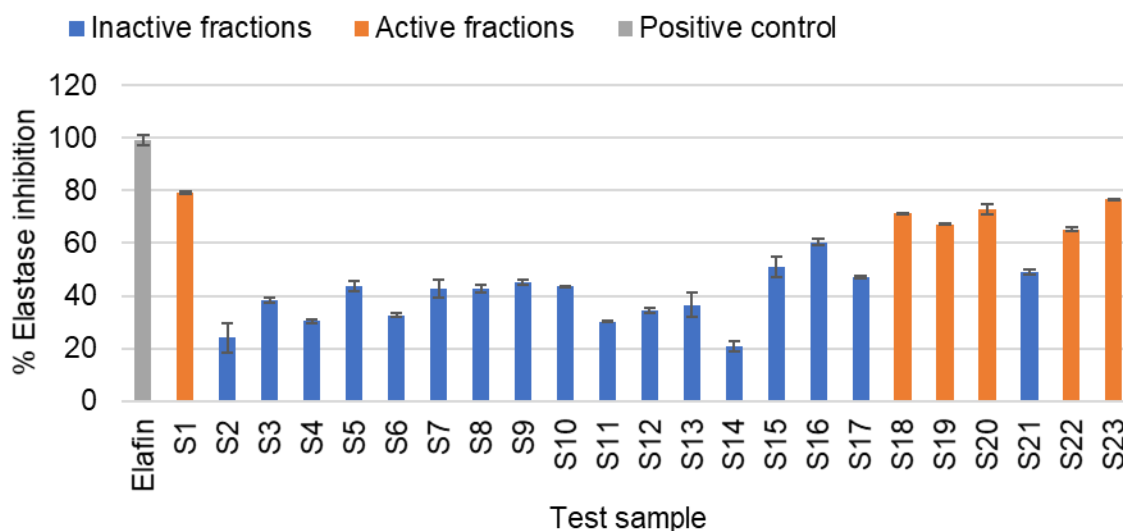


Figure 2.25. % Elastase inhibition activity of Marula stem fractions at 25 µg/ml, in comparison to the positive control elafin, tested at a concentration of 1.43 µg/ml. Active fractions S1, S18, S19, S20, S22 and S23 showed good elastase inhibition activity (>65%) which was as good as the positive control EDTA.

2.7.13.1 UPLC-QTOF-MS analysis of active fractions

An overlay of the chemical profile of fraction S1 and fraction S2 is shown in Figure 2.26. Fraction S1 was active and fraction S2 was inactive in the elastase inhibition assay. A comparison of the chemical profiles of these fractions was needed to check the presence of compounds which are present in fraction S1 but absent from fraction S2. These compounds are likely to contribute to the elastase inhibition activity of fraction S1. Analysis of the chemical profiles revealed the presence of an intense peak in fraction S1 at m/z 191.0541 retention time 0.71 minutes which was absent in fraction S2. The identity of the compound corresponding to this peak was confirmed in section 2.7.6 to be quinic acid. This organic acid is likely to be one of the compounds responsible for the elastase inhibition activity of fraction S1. The pure

compound quinic acid should be screened to confirm if it is one of the compounds contributing to the elastase inhibition activity of S1 (see section 2.7.14).

Apart from quinic acid, peaks of lower intensity were observed in fraction S1 at m/z 441.0840 retention time 3.59 minutes, in section 2.7.6 this peak was found to correspond to epicatechin gallate. This peak was also observed in inactive fraction S2 at m/z 441.0803 retention time 3.59 minutes. Other peaks of low intensity in fraction S1 were observed at m/z 289.0693 retention time 2.50 minutes and at m/z 305.0649 retention time 1.82 minutes, these peaks were previously identified in section 2.7.6 as catechin and gallic acid respectively. Peaks corresponding to catechin and gallic acid were also observed in inactive fraction S2 at m/z 289.0693 retention time 2.50 minutes and at m/z 305.0649 retention time 1.82 minutes respectively. The identity of a minor peak observed in fraction S1 at m/z 169.0134 retention time 1.38 minutes and in fraction S2 at m/z 169.0130 retention time 1.30 minutes was not determined in this study. These common compounds in fractions S1 and S2 are not likely to contribute to the elastase inhibition activity of fraction S1. As a result, the compounds tentatively identified to be inactive were screened for elastase inhibition activity in section 2.7.14 to confirm their lack of activity.

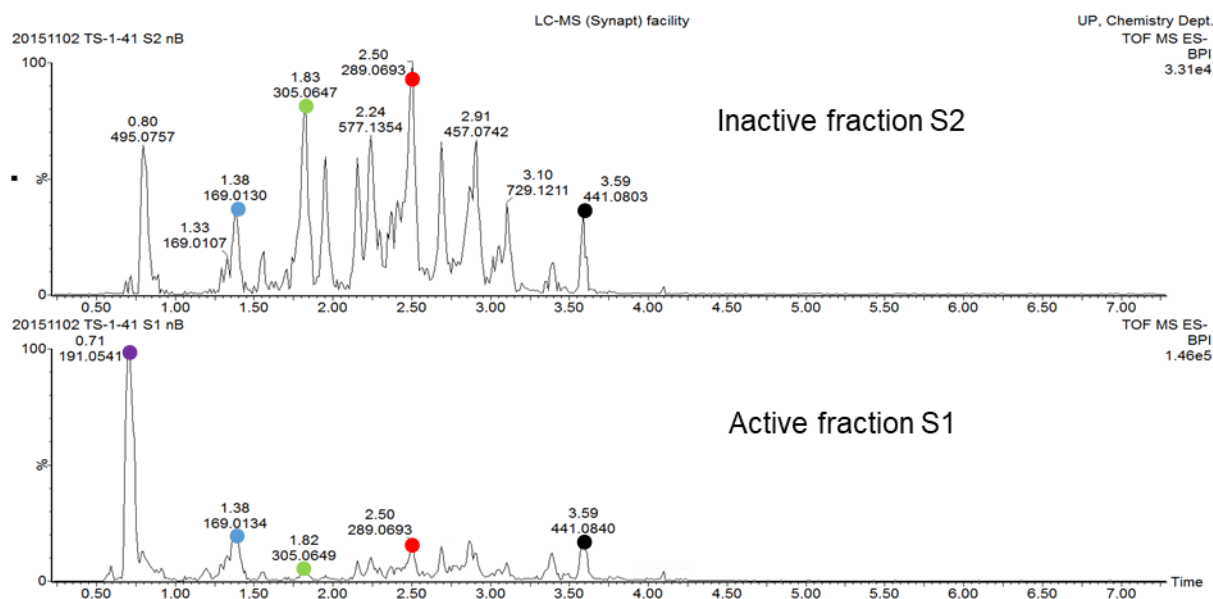


Figure 2.26. Chemical profiles of fractions S1 and S2 overlaid. The most intense peak in fraction S1 at m/z 191.0541 retention time 0.71 minutes previously identified as \bullet quinic acid was not present in fraction S2 and is likely to be one of the compounds corresponding to elastase activity of fraction S1. Peaks of lower intensity corresponding to \bullet epicatechin gallate (m/z 441.0840 retention time 3.59 minutes), \bullet catechin (m/z 289.0693 retention time 2.50 minutes), galocatechin (m/z 305.0649 retention time 1.82 minutes) and peak at \bullet m/z 169.0134 retention time 1.38 minutes were also present in inactive fraction 2 thus are not likely to contribute to elastase inhibition activity of fraction S2.

The chemical profiles of active fractions S18, S19 and S20 were also analysed to identify common peaks between the fractions which are likely to be responsible for the elastase inhibition activity of these fractions (Figure 2.27). The analysis revealed the presence of a peak in fraction S18 at m/z 199.0423 retention time 4.12 minutes. The peak was present in fraction S19 at m/z 199.0425 retention time 4.13 minutes and in fraction S20 at m/z 199.0450 retention time 4.13 minutes. This compound is likely to be one of the compounds contributing to the elastase inhibition activity of fractions S18, S19 and S20. The identity of the peak corresponding to this compound was not identified as it was a minor compound. A prominent peak was observed in fraction S18 at m/z 169.0137 retention time 0.80 minutes and in fraction S19 at m/z 169.0139 retention time 0.80 minutes. The compound corresponding to this peak is not likely to be one of the compounds responsible for activity as it was not observed in active

fraction S20. In fraction S20, the major peak was observed at m/z 167.0211 retention time 0.80 minutes. Although the retention time of this peak is the same as that of the compound in fraction S19 at m/z 169.0139, the accurate masses of these compounds differ by far greater than the 5ppm, hence, these are different compounds.

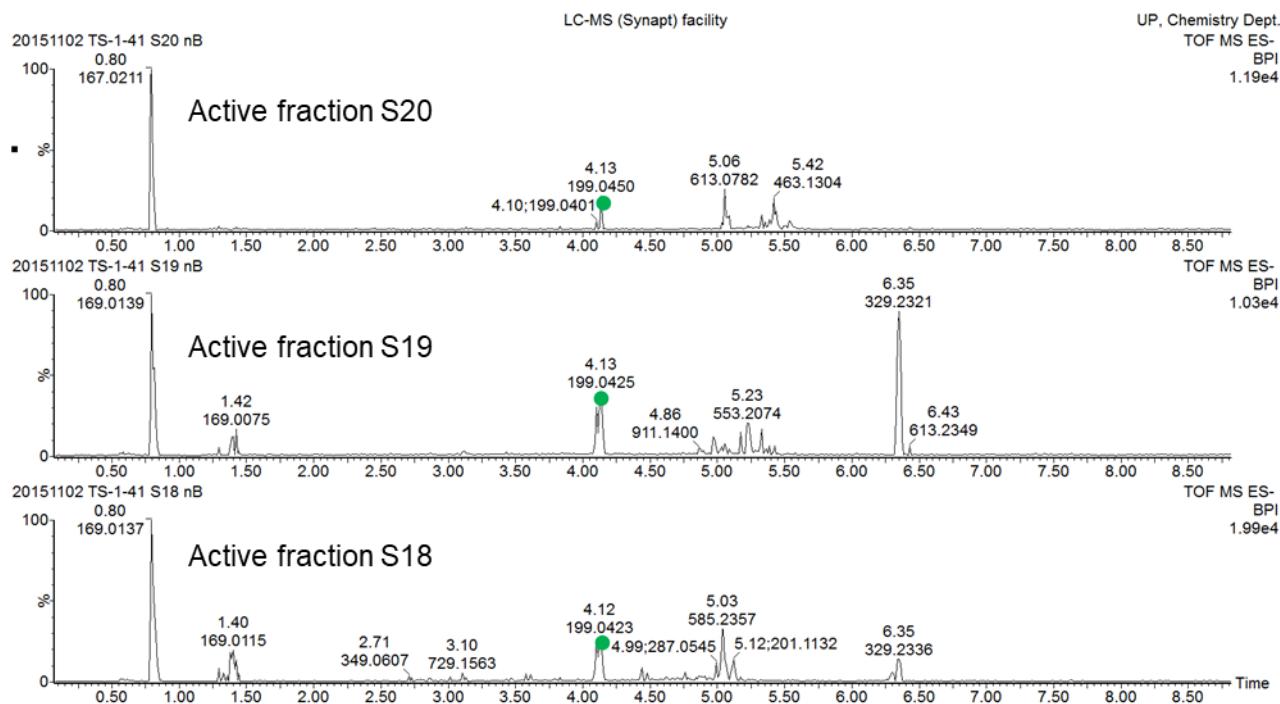


Figure 2.27. Chemical profiles of active fractions S18, S19 and S20, the compound at m/z 199.0450 at retention time 4.13 minutes is likely to be one of the compounds corresponding to the elastase inhibition activity of fractions S18, S19 and S20.

An analysis of the chemical profile of active fractions S23, S22 and inactive fraction S21 was done to identify peaks corresponding to compounds responsible for elastase inhibition activity of the extracts (Figure 2.28). The analysis targeted identifying peaks which were common to the active fractions S23 and S22 but absent from inactive fraction S21. The peak in active fraction S23 at m/z 215.1285 retention time 5.86 minutes was also present in active fraction S22 at m/z 215.1286 retention time 5.86 minutes but was absent from inactive fraction S21. The identity of the compound corresponding to this peak was tentatively identified in section

2.7.6 as undecanedioic acid. This compound is likely to be one of the compounds contributing to the activity of fractions S23 and S22.

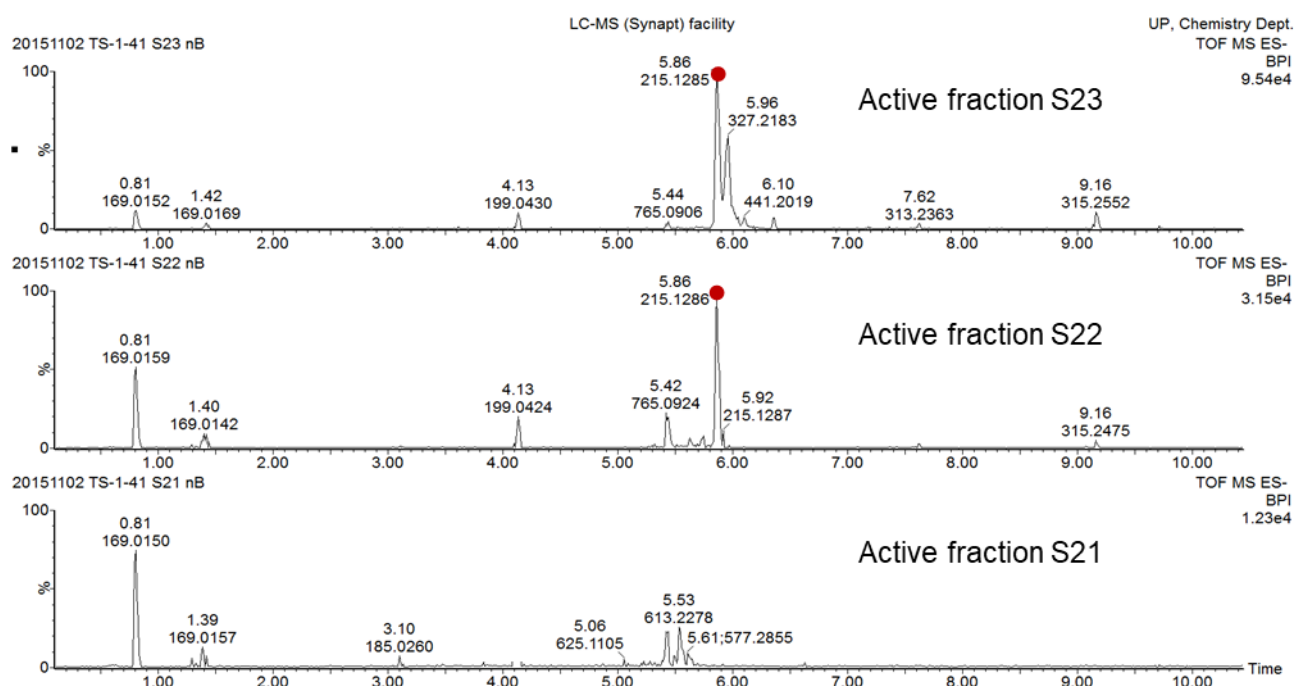


Figure 2.28. Chemical profiles of active fractions S23, S22 and inactive fraction S21.

● Undecanedioic acid at m/z 215.1285 retention time 5.86 minutes was common to fractions S23 and S22 but absent from fraction S21 is likely to be one of the compounds corresponding to the elastase inhibition activity of the active fractions S23 and S21.

2.7.14 Elastase inhibition of pure compounds

To confirm if the compounds tentatively identified in section 2.7.13 are contributing to the elastase inhibition activity of Marula extract, the inhibition activity of pure compounds identified to be present in Marula stem ethanol extract were screened for elastase inhibition activity. The compounds undecanedioic acid and the unidentified compound at m/z 199.0450 retention time 4.13 minutes in fractions S18,19 and 20 were not screened for activity as their intensity was very small in the active ethanol extract. The compounds catechin, quinic acid, epigallocatechin gallate and epicatechin gallate confirmed to be present in Marula stem ethanol extract were screened and the screening results are given in Figure 2.29. At all test concentrations, epigallocatechin gallate, epicatechin gallate, catechin and quinic acid exhibited very limited

elastase inhibition activity (< 35%). These results reveal that none of the screened compounds are responsible for the elastase inhibition activity of Marula fractions and Marula stem extracts. Although the most intense peak in fraction S1 (quinic acid) was not active, the fraction showed activity against elastase, this could be attributed to synergistic effects between quinic acid and the minor peaks at *m/z* 169.0134 retention time 1.38 minutes, *m/z* 441.0840 retention time 3.59 minutes which corresponds to epicatechin gallate as identified in section 2.7.6 and the other compounds of minor intensity in the fraction. Synergistic effects were lost upon screening the pure compound.

Previous studies confirmed our findings of the inactivity of quinic acid [62]. Kim et al. [63] found catechin to show elastase inhibition activity of (>50%) at concentrations above 25 µg/ml. In our study screening was done at concentrations of (20 µg/ml and below) hence catechin showed no activity. It is surprising that Sartor et al. [56], showed epigallocatechin gallate to be a potent inhibitor of leukocyte elastase with an IC₅₀ of 0.4 µM. Another study showed epigallocatechin gallate to have moderate to weak inhibition of elastase with an IC₅₀ of 25.3 µM [64]. The variation in anti-elastase activity observed in our study from that reported in literature is difficult to explain as in our case elafin the positive control gave the inhibitory activity as expected indicating the validity of the assay. In the elastase and collagenase inhibition assays at all test concentrations with respect to the positive controls elafin and EDTA.

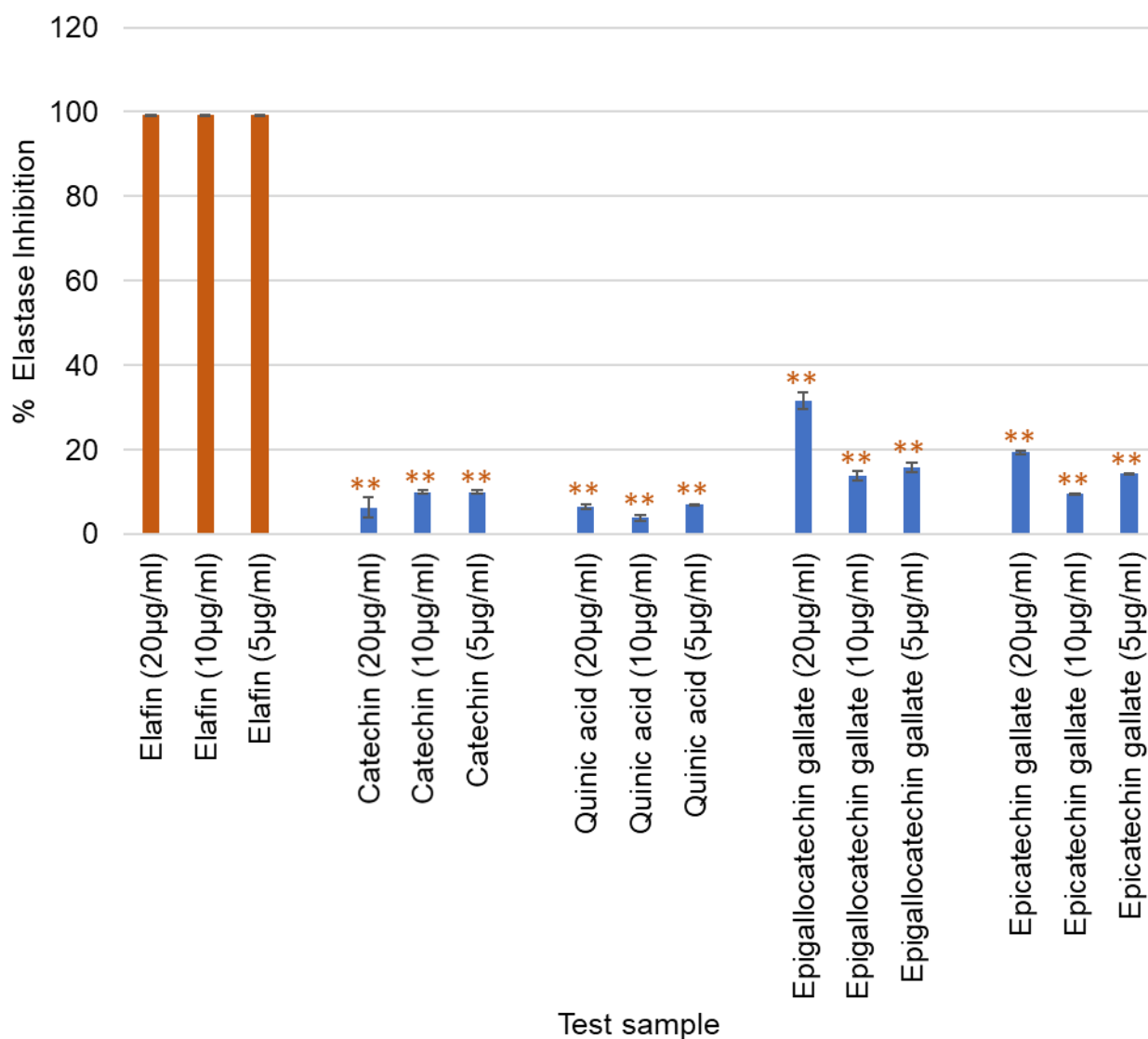


Figure 2.29. Elastase inhibition activities of major compounds identified in Marula stem ethanol extract at 20, 10 and 5 µg/ml. (Error bars represent SEM, with n=3). * = P<0.05, ** = P<0.01 represents a significant difference with elafin.

2.8 CONCLUSIONS

Extracts of *S. birrea* plant have the first time been scientifically shown to exhibit elastase and collagenase inhibition activities thus validating the traditional use of the plant for anti-aging purposes and exhibiting potential for the plant to be further developed into anti-aging ingredients. Marula stems exhibited the highest *in vitro* anti-aging activity in comparison to the extracts of the other parts of Marula. The active constituents were concentrated in the more

polar ethyl acetate, ethanol and methanol extracts for both the elastase and collagenase inhibition. Based on these activities and acceptability to the cosmetic industry, the ethanol extract of Marula stems was selected as the most appropriate extract for further research and development thus achieving the first objective of this study. The use of water as an extraction solvent could also be further investigated in the future. The harvesting of stems is often seen as being destructive and non-sustainable. To circumvent this, our study utilized the soft wood side stems or twigs which will not result in destructive harvesting. Sequential extraction successfully extracted compounds based on polarity and produced an extract with good antiaging activity. The concentration and defatting-concentration steps lowered the colour intensity and improved the anti-aging activity of the Marula stem ethanol extract thus achieving the third objective of this chapter. Marula oil, although traded as a cosmetic ingredient did not have any anti-collagenase or anti-elastase activity contributing to anti-aging claims on products containing the oil. Its application in cosmetic formulations is due to a different mode of action.

The chemical profile for Marula stems extracted with ethanol was developed for quality control purposes, thus achieving the second objective of this chapter. Eleven compounds were tentatively identified from Marula stems extracted with ethanol of which four have been confirmed with pure standards. The presence of quinic acid, catechin, epicatechin, epigallocatechin gallate and epicatechin gallate was confirmed using pure standards on UPLC-QTOF-MS. Upon *in vitro* screening in the collagenase assay, epigallocatechin gallate and epicatechin gallate were as potent as EDTA at 5 µg/ml and were found to contribute to the anti-aging activity of the Marula stem ethanol extract thus achieving the fourth objective of this chapter. Consequently, Marula stems have for the first time been shown to exhibit elastase and collagenase inhibition activities, further, epigallocatechin gallate and epicatechin gallate have been shown to be some of the compounds contributing to the collagenase inhibition activity of Marula stems and displaying potential to be developed into anti-aging ingredients. The compound 9,8,13 TriHOME has been tentatively identified for the first time in Marula

stems. In the elastase assay, the ethanol extract of Marula stems of the and its fractions showed activity. Undecanedioic acid a compound of low intensity in the Marula stem ethanol extract was tentatively identified as one of the compounds contributing to the elastase inhibition activity of the stems. Upon screening of pure compounds, none of the compounds showed activity showing that activity in the extract and the fractions was due to synergistic effects. As such, synergism was lost upon isolation of compounds, hence, the lack of activity upon screening pure compounds.

2.9 REFERENCES

1. Mariod A, Matthaus B, Eichner K: **Fatty acid, tocopherol and sterol composition as well as oxidative stability of three unusual Sudanese oils.** *Journal of Food Lipids* 2004, **11**(3):179-189.
2. Shackleton SE, Shackleton CM, Cunningham T, Lombard C, Sullivan CA, Netshiluvhi TR: **Knowledge on Sclerocarya birrea subsp. caffra with emphasis on its importance as a non-timber forest product in South and southern Mrica: A Summary: Part 1: Taxonomy, ecology and role in rural livelihoods.** *Southern African Forestry Journal* 2002, **194**(1):27-41.
3. Vermaak I, Kamatou GPP, Komane-Mofokeng B, Viljoen A, Beckett K: **African seed oils of commercial importance—Cosmetic applications.** *South African Journal of Botany* 2011, **77**(4):920-933.
4. Nghitoolwa E, Hall JB, Sinclair FL: **Population status and gender imbalance of the marula tree, Sclerocarya birrea subsp. caffra in northern Namibia.** *Agroforestry systems* 2003, **59**(3):289-294.
5. Emanuel P, Shackleton C, Baxter J: **Modelling the sustainable harvest of Sclerocarya birrea subsp. caffra fruits in the South African lowveld.** *Forest Ecology and Management* 2005, **214**(1):91-103.
6. Ojewole JA: **Evaluation of the anti-inflammatory properties of Sclerocarya birrea (A. Rich.) Hochst.(family: Anacardiaceae) stem-bark extracts in rats.** *Journal of Ethnopharmacology* 2003, **85**(2):217-220.
7. Ojewole JA: **Evaluation of the analgesic, anti-inflammatory and anti-diabetic properties of Sclerocarya birrea (A. Rich.) Hochst. stem-bark aqueous extract in mice and rats.** *Phytotherapy Research* 2004, **18**(8):601-608.
8. Ojewole JA: **Vasorelaxant and hypotensive effects of Sclerocarya birrea (A Rich) Hochst (Anacardiaceae) stem bark aqueous extract in rats: cardiovascular topic.** *Cardiovascular Journal of South Africa* 2006, **17**(3):117-123.
9. Ojewole J: **Hypoglycemic effect of Sclerocarya birrea {(A. Rich.) Hochst.}[Anacardiaceae] stem-bark aqueous extract in rats.** *Phytomedicine* 2003, **10**(8):675-681.
10. Shackleton S, Shackleton C: **The contribution of marula (Sclerocarya birrea) fruit and fruit products to rural livelihoods in the Bushbuckridge district, South Africa: Balancing domestic needs and commercialisation.** *Forests, Trees and Livelihoods* 2005, **15**(1):3-24.
11. Gouwakinnou GN, Lykke AM, Assogbadjo AE, Sinsin B: **Local knowledge, pattern and diversity of use of Sclerocarya birrea.** *Journal of Ethnobiology and Ethnomedicine* 2011, **7**(1):8.

12. Janick J, Paull RE: **The encyclopedia of fruit and nuts**: Center for Agriculture and Bioscience International; 2008.
13. Aganga A, Mosase K: **Tannin content, nutritive value and dry matter digestibility of Lonchocarpus capassa, Zizyphus mucronata, Sclerocarya birrea, Kirkia acuminata and Rhus lancea seeds**. *Animal Feed Science and Technology* 2001, **91**(1):107-113.
14. Ndhkala A, Kasiyamhuru A, Mupure C, Chitindingu K, Benhura M, Muchuweti M: **Phenolic composition of Flacourtia indica, Opuntia megacantha and Sclerocarya birrea**. *Food Chemistry* 2007, **103**(1):82-87.
15. Wynberg R, Laird S: **Less is often more: governance of a non-timber forest product, marula (Sclerocarya birrea subsp. caffra) in southern Africa**. *International Forestry Review* 2007, **9**(1):475-490.
16. Hiwilepo-van Hal P, Bille PG, Verkerk R, van Boekel MA, Dekker M: **A review of the proximate composition and nutritional value of Marula (Sclerocarya birrea subsp. caffra)**. *Phytochemistry Reviews* 2014, **13**(4):881-892.
17. Masoko P, Mmushi T, Mogashoa M, Mokgotho M, Mampuru L, Howard R: **In vitro evaluation of the antifungal activity of Sclerocarya birrea extracts against pathogenic yeasts**. *African Journal of Biotechnology* 2008, **7**(20).
18. Eloff JN: **Antibacterial activity of Marula (Sclerocarya birrea (A. rich.) Hochst. subsp. caffra (Sond.) Kokwaro) (Anacardiaceae) bark and leaves**. *Journal of Ethnopharmacology* 2001, **76**(3):305-308.
19. Ojewole JA: **Anticonvulsant effect of Sclerocarya birrea (A. Rich.) Hochst. subsp. caffra (Sond.) Kokwaro (Anacardiaceae) stem-bark aqueous extract in mice**. *Journal of Natural Medicines* 2007, **61**(1):67-72.
20. Sarkar R, Chaudhary SK, Sharma A, Yadav KK, Nema NK, Sekhoacha M, Karmakar S, Braga FC, Matsabisa MG, Mukherjee PK: **Anti-biofilm activity of Marula—A study with the standardized bark extract**. *Journal of Ethnopharmacology* 2014, **154**(1):170-175.
21. Gathirwa J, Rukunga G, Njagi E, Omar S, Mwitari P, Guantai A, Tolo F, Kimani C, Muthaura C, Kirira P: **The in vitro anti-plasmodial and in vivo anti-malarial efficacy of combinations of some medicinal plants used traditionally for treatment of malaria by the Meru community in Kenya**. *Journal of ethnopharmacology* 2008, **115**(2):223-231.
22. Hamza OJ, van den Bout-van CJ, Matee MI, Moshi MJ, Mikx FH, Selemani HO, Mbwambo ZH, Van der Ven AJ, Verweij PE: **Antifungal activity of some Tanzanian plants used traditionally for the treatment of fungal infections**. *Journal of Ethnopharmacology* 2006, **108**(1):124-132.
23. Komane B, Vermaak I, Summers B, Viljoen A: **Safety and efficacy of Sclerocarya birrea (A. Rich.) Hochst (Marula) oil: A clinical perspective**. *Journal of Ethnopharmacology* 2015, **176**:327-335.
24. Mckenzie LP: **Topical composition for the treatment of scar tissue**. In.: Patent WO 03/092634 A2; 2003.
25. Charlier DCP, Raynard M, Lombard CN: **Antioxidants based on Anacardiaceae species, methods for obtaining same and uses thereof**. In.: Patent WO2006097806A1; 2006.
26. Lall N, Kishore N: **Are plants used for skin care in South Africa fully explored?** *Journal of Ethnopharmacology* 2014, **153**(1):61-84.
27. Hillman Z, Mizrahi Y, Beit-Yannai E: **Evaluation of valuable nutrients in selected genotypes of marula (Sclerocarya birrea ssp. caffra)**. *Scientia Horticulturae* 2008, **117**(4):321-328.
28. Galvez J, Zarzuelo A, Crespo M, Utrilla M, Jimenez J, Spiessens C, de Witte P: **Antidiarrhoeic activity of Sclerocarya birrea bark extract and its active tannin constituent in rats**. *Phytotherapy Research* 1991, **5**(6):276-278.
29. Moyo M, Ndhkala AR, Finnie JF, Van Staden J: **Phenolic composition, antioxidant and acetylcholinesterase inhibitory activities of Sclerocarya birrea and**

- Harpephyllum caffrum (Anacardiaceae) extracts.** *Food Chemistry* 2010, **123**(1):69-76.
30. Gondwe M, Kamadyaapa D, Tufts M, Chuturgoon A, Musabayane C: **Sclerocarya birrea [(A. Rich.) Hochst.][Anacardiaceae] stem-bark ethanolic extract (SBE) modulates blood glucose, glomerular filtration rate (GFR) and mean arterial blood pressure (MAP) of STZ-induced diabetic rats.** *Phytomedicine* 2008, **15**(9):699-709.
 31. Tabit FT, Komolafe NT, Tshikalange TE, Nyila MA: **Phytochemical constituents and antioxidant and antimicrobial activity of selected plants used traditionally as a source of food.** *Journal of Medicinal Food* 2016, **19**(3):324-329.
 32. Peralta JG, Zarzuelo A, Busson R, Cobbaert C, de Witte P: **(-)-epicatechin-3-galloyl ester: a secretagogue compound from the bark of Sclerocarya birrea.** *Planta Medica* 1992, **58**(02):174-175.
 33. Kim Y, Choi Y, Ham H, Jeong H-S, Lee J: **Protective effects of oligomeric and polymeric procyanidin fractions from defatted grape seeds on tert-butyl hydroperoxide-induced oxidative damage in HepG2 cells.** *Food Chemistry* 2013, **137**(1):136-141.
 34. Russo D, Kenny O, Smyth TJ, Milella L, Hossain MB, Diop MS, Rai DK, Brunton NP: **Profiling of phytochemicals in tissues from Sclerocarya birrea by HPLC-MS and their link with antioxidant activity.** *ISRN Chromatography* 2013, **2013**(2013):1-11.
 35. Jiménez-Sánchez C, Lozano-Sánchez J, Gabaldón-Hernández JA, Segura-Carretero A, Fernández-Gutiérrez A: **RP-HPLC-ESI-QTOF/MS2 based strategy for the comprehensive metabolite profiling of Sclerocarya birrea (Marula) bark.** *Industrial Crops and Products* 2015, **71**:214-234.
 36. Borochoy-Neori H, Judeinstein S, Greenberg A, Fuhrman B, Attias J, Volkova N, Hayek T, Aviram M: **Phenolic antioxidants and antiatherogenic effects of Marula (Sclerocarya birrea Subsp. caffra) fruit juice in healthy humans.** *Journal of Agricultural and Food Chemistry* 2008, **56**(21):9884-9891.
 37. Song HS, Park TW, Sohn UD, Shin YK, Choi BC, Kim CJ, Sim SS: **The effect of caffeic acid on wound healing in skin-incised mice.** *The Korean Journal of Physiology & Pharmacology* 2008, **12**(6):343-347.
 38. Saija A, Tomaino A, Trombetta D, De Pasquale A, Uccella N, Barbuzzi T, Paolino D, Bonina F: **In vitro and in vivo evaluation of caffeic and ferulic acids as topical photoprotective agents.** *International Journal of Pharmaceutics* 2000, **199**(1):39-47.
 39. Ogbobe O: **Physico-chemical composition and characterisation of the seed and seed oil of Sclerocarya birrea.** *Plant Foods for Human Nutrition (Formerly Qualitas Plantarum)* 1992, **42**(3):201-206.
 40. Hilou A, Bougma A, Dicko MH: **Phytochemistry and Agro-Industrial Potential of Native Oilseeds from West Africa: African Grape (Lannea microcarpa), Marula (Sclerocarya birrea), and Butter Tree (Pentadesma butyracea).** *Agriculture* 2017, **7**(3):1-11.
 41. Braca A, Politi M, Sanogo R, Sanou H, Morelli I, Pizza C, De Tommasi N: **Chemical composition and antioxidant activity of phenolic compounds from wild and cultivated Sclerocarya birrea (Anacardiaceae) leaves.** *Journal of Agricultural and Food Chemistry* 2003, **51**(23):6689-6695.
 42. Kraunsoe JA, Claridge TD, Lowe G: **Inhibition of human leukocyte and porcine pancreatic elastase by homologues of bovine pancreatic trypsin inhibitor.** *Biochemistry* 1996, **35**(28):9090-9096.
 43. Moore S, Stein WH: **Photometric nin-hydrin method for use in the chromatography of amino acids.** *Journal of Biological Chemistry* 1948, **176**:367-388.
 44. Mandl I, MacLennan JD, Howes EL, DeBellis RH, Sohler A: **Isolation and characterization of proteinase and collagenase from Cl. histolyticum.** *The Journal of Clinical Investigation* 1953, **32**(12):1323.

45. Louvel S, Moodley N, Seibert I, Steenkamp P, Nthambeleni R, Vidal V, Maharaj V, Klimkait T: **Identification of compounds from the plant species *Alepidea amatymbica* active against HIV.** *South African Journal of Botany* 2013, **86**:9-14.
46. Row KH, Jin Y: **Recovery of catechin compounds from Korean tea by solvent extraction.** *Bioresource Technology* 2006, **97**(5):790-793.
47. Kroes R, Renwick AG, Feron V, Galli CL, Gibney M, Greim H, Guy RH, Lhuguenot JC, van de Sandt JJM: **Application of the threshold of toxicological concern (TTC) to the safety evaluation of cosmetic ingredients.** *Food and Chemical Toxicology* 2007, **45**(12):2533-2562.
48. De Azevedo A, Mazzafera P, Mohamed R, Melo S, Kieckbusch TG: **Extraction of caffeine, chlorogenic acids and lipids from green coffee beans using supercritical carbon dioxide and co-solvents.** *Brazilian Journal of Chemical Engineering* 2008, **25**(3):543-552.
49. Saldanha LL, Vilegas W, Dokkedal AL: **Characterization of flavonoids and phenolic acids in *Myrcia bella* cambess. Using FIA-ESI-IT-MSn and HPLC-PAD-ESI-IT-MS combined with NMR.** *Molecules* 2013, **18**(7):8402-8416.
50. Zywicki B, Reemtsma T, Jekel M: **Analysis of commercial vegetable tanning agents by reversed-phase liquid chromatography-electrospray ionization-tandem mass spectrometry and its application to wastewater.** *Journal of Chromatography A* 2002, **970**(1):191-200.
51. Chua LS, Latiff NA, Lee SY, Lee CT, Sarmidi MR, Aziz RA: **Flavonoids and phenolic acids from *Labisia pumila* (Kacip Fatimah).** *Food Chemistry* 2011, **127**(3):1186-1192.
52. Fecka I, Kucharska AZ, Kowalczyk A: **Quantification of tannins and related polyphenols in commercial products of tormentil (*Potentilla tormentilla*).** *Phytochemical analysis* 2015, **26**(5):353-366.
53. Nording ML, Yang J, Hegedus CM, Bhushan A, Kenyon NJ, Davis CE, Hammock BD: **Endogenous levels of five fatty acid metabolites in exhaled breath condensate to monitor asthma by high-performance liquid chromatography: electrospray tandem mass spectrometry.** *IEEE sensors journal* 2010, **10**(1):123-130.
54. Rohr GE, Riggio G, Meier B, Sticher O: **Evaluation of different detection modes for the analysis of procyanidins in leaves and flowers of *Crataegus* spp. Part II. Liquid chromatography–mass spectrometry.** *Phytochemical Analysis* 2000, **11**(2):113-120.
55. Mariod AA, Matthäus B, Hussein IH: **Antioxidant properties of methanolic extracts from different parts of *Sclerocarya birrea*.** *International Journal of Food Science and Technology* 2008, **43**(5):921-926.
56. Sartor L, Pezzato E, Garbisa S: **(–) Epigallocatechin-3-gallate inhibits leukocyte elastase: potential of the phyto-factor in hindering inflammation, emphysema, and invasion.** *Journal of Leukocyte Biology* 2002, **71**(1):73-79.
57. Makimura M, Hirasawa M, Kobayashi K, Indo J, Sakanaka S, Taguchi T, Otake S: **Inhibitory effect of tea catechins on collagenase activity.** *Journal of Periodontology* 1993, **64**(7):630-636.
58. Demeule M, Brossard M, Pagé M, Gingras D, Béliveau R: **Matrix metalloproteinase inhibition by green tea catechins.** *Biochimica et Biophysica Acta - Protein Structure and Molecular Enzymology* 2000, **1478**(1):51-60.
59. Teramachi F, Koyano T, Kowithayakorn T, Hayashi M, Komiyama K, Ishibashi M: **Collagenase Inhibitory Quinic Acid Esters from *Ipomoea pes-caprae*.** *Journal of Natural Products* 2005, **68**(5):794-796.
60. Madhan B, Krishnamoorthy G, Rao JR, Nair BU: **Role of green tea polyphenols in the inhibition of collagenolytic activity by collagenase.** *International Journal of Biological Macromolecules* 2007, **41**(1):16-22.
61. Xu G-H, Kim Y-H, Choo S-J, Ryoo I-J, Yoo J-K, Ahn J-S, Yoo I-D: **Chemical constituents from the leaves of *Ilex paraguariensis* inhibit human neutrophil elastase.** *Archives of Pharmacal Research* 2009, **32**(9):1215-1220.

62. Melzig M, Löser B, Ciesielski S: **Inhibition of neutrophil elastase activity by phenolic compounds from plants.** *Die Pharmazie* 2001, **56**(12):967-970.
63. Kim JH, Byun JC, Hyun C-G, Lee NH: **Compounds with elastase inhibition and free radical scavenging activities from *Callistemon lanceolatus*.** *Journal of Medicinal Plants Research* 2009, **3**(11):914-920.
64. Hrenn A, Steinbrecher T, Labahn A, Schwager J, Schempp CM, Merfort I: **Plant phenolics inhibit neutrophil elastase.** *Planta Medica* 2006, **72**(12):1127-1131.

Chapter 3: *Ficus sycomorus* (SYCAMORE)

3.1 BOTANY AND GEOGRAPHICAL DISTRIBUTION

Ficus sycomorus L. (Sycamore) is a large tree which belongs to the mulberry family, Moraceae and produces a fig-like fruit which is edible (Figure 3.1) [1-3]. The tree has a spreading crown, its trunk can grow up to 20 ft in diameter, 10 to 30 m high and its bark can be smooth or rough [4-6]. The tree is known as *ibbe* in Fulfulde, *tarmu* in Kanuri, *kamda* in Babur, *baure* in Hausa and *kwadachikwa* in Adamawa state Nigeria, *kankanga* in Moore [2, 5, 7]. In Afrikaans it is known as *sycomorusvy*, in Bemba and Nyanja (*mkuyu*), Shona and Swahili (*mukuyu*), Zulu (*umKhiwane*) and in French (Sycamore). The tree is monoecious with male and female flowers growing on the same syconium [8, 9]. In its natural habitat, *F. sycomorus* mainly grows in riverside forests or in woodlands found near streams of water [8, 10].

Moraceae family is made up of mostly shrubs and trees producing milky latex and juices [2, 5]. The genus *Ficus* made up of over 1500 species and is the largest in the family Moraceae [5]. The section *sycomorus* is mainly found in Africa and the Sycamore is a tropical tree found in several parts of Africa [8]. Its distribution extends from the southern parts of Africa where it is found in countries including but not limited to South Africa, Zimbabwe; to the north in countries like Sudan, and Ethiopia; to the south-western corner of the Arabic peninsula in countries like Yemen [6, 8, 10, 11]. The tree was spread north to countries like Egypt more than 5000 years ago during the dawn of civilisation in the Nile due to human activity and then to other Mediterranean countries [6, 8]. It is cultivated in various countries along the eastern and southern shores of the Mediterranean [8]. The Sycamore does not produce viable seeds in countries including Egypt, Israel and its neighbouring Mediterranean countries so its propagation is done through cuttings in such countries [6].

A. *F. sycomorus* tree



B. Leaves of *F. sycomorus* tree



Figure 3.1. Picture A showing the *F. sycamorus* tree and picture B shows a stem and leaves from the *F. sycamorus* plant.

3.2 TRADITIONAL USES OF THE PLANT

In ancient times, the *F. sycamorus* tree was cultivated in Israel for its shade, fruits and timber, Arabs also ate fruits and used wood from the tree [9]. The fruits were used to make wine which was also used for medicinal purposes [12]. In ancient Egypt, it was considered to be the tree of life and regarded as a holy tree [2, 11]. In the ancient times in different parts of the World, studies reveal that fresh or dried fruits from the tree were applied to the body or eaten for the treatment of cancer, hot swellings, hard tumours, swelling throat and an ointment made from fresh or dried fruits mixed with wax was also used in ancient medicine for treatment of tumours, swellings and furuncles [12]. Latex from the bark was applied to the body and taken orally for the treatment of hard tumours, spleen hardness and ulcers in the head [12]. Ashes from wood were used to treat gastric ulcers, deep putrid ulcers and spreading ulcers, further ashes are ground with vinegar and salt and applied topically to treat ulcers of the head [12]. An aqueous

decoction of fresh or dried fruit was gargled in or taken as a drink for the treatment of swollen tonsils, trachea and chronic cough [12]. Further, the tree was used for cosmetic purposes, milky sap from the plant was used by Egyptian peasants as a treatment for vitiliginous patches [1]. Fresh or dried fruits were applied to the skin or eaten for the treatment of skin ulcers and dermatitis[12].

The tree has found many uses in the traditional African communities in modern times. Communities in Adamawa State in Nigeria use the leaves as a cheap source of green vegetables [7]. In Northern Nigeria, Hausas use the leaves of *F. sycomorus* plant for ethnomedicinal purposes to treat diarrhoea [13]. Stem bark of Sycamore plant is used in Northern Nigeria to treat fungal diseases such as jaundice and dysentery [4, 11]. Traditional healers claim that the plant has psychotropic activities and is thus used in the treatment of psychiatric diseases [14]. In Burkina Faso, leaves of *F. sycomorus* plant are used for treatment of sickle cell disease [5]. Leaves and stem bark from the plant are traditionally used for dressing wounds [15]. Different parts of the *F. sycomorus* tree including fruits in different stages of ripening, fresh or dry tree barks, twigs and young shoots, latex from the bark, fruits and young branches, ashes from the tree have been used in the treatment of illnesses characterised by inflammation [12]. Chopped and dried fruits are eaten for the treatment of chronic diarrhoea. The plant has also been used traditionally in Egypt for the treatment of certain skin diseases [16].

3.3 PREVIOUS RESEARCH ON *F. SYCOMORUS*

3.3.1 Leaves

An organic (n- butanol) extract of air dried and ground leaves of the Sycamore tree was found to inhibit castor oil induced diarrhea and further exhibited 100% protection of against castor oil induced diarrhea in mice at doses of 120 mg/kg and 60 mg/kg [13]. The extract was as

potent as the commonly used anti-diarrheal drug loperamide. Their study validated the ethnomedicinal use of *F. sycomorus* leaves for treatment of diarrhea. The antioxidant activities of defatted 70% methanol extract of leaves of the Sycamore tree fractionated using chloroform, ethyl acetate and butanol were investigated using the DPPH radical scavenging assay [17].

Ethyl acetate and *n*-butanol extract were shown to possess high DPPH radical scavenging activities of ($SC_{50} = 13.48$ and $8.47 \mu\text{g/ml}$). Dried, ground leaves of the Sycamore tree were investigated for its antiradical activity using the DPPH method and antibacterial activity using the minimum inhibitory concentration (MIC) method [5]. Results showed that the leaf extract had an IC_{50} of $9.60 \pm 0.02 \mu\text{g/ml}$ antiradical activity while the reference antioxidant quercetin had an IC_{50} of $4.6 \pm 0.08 \mu\text{g/ml}$ showing that the extract had good antioxidant activity. Additionally, antibacterial activity of the extract against clinical isolates and American type culture collections (ATCC) reference strains of *Staphylococcus aureus*, *Escherichia coli* and *Salmonella typhimurium* was performed. The leaf extract had an MIC of 0.31 mg/ml against *S. aureus* and *S. aureus* ATCC and 0.63 mg/ml against *E. coli* and *E. coli* ATCC and showed no inhibition against *S. typhimurium* and *S. typhimurium* ATCC. The latex of the Sycamore plant had the lowest MIC of 0.13 mg/ml for *S. aureus* and 0.25 for *E. coli* respectively both of which were not as good as the positive controls ampicillin and gentamicin. Sickle cell disease is characterized by a release of high levels of free radicals which cause oxidative stress and a wide range of bacterial infections including *E. coli*, *S. aureus* and *S. typhi* are associated with this disease [5]. Consequently, the antiradical and antibacterial activity of the Sycamore extract validates the traditional applications of the *F. sycomorus* plant in treatment of disorders associated with sickle cell disease.

Leaves of the Sycamore tree were extracted using 70% aqueous ethanol, the antibacterial susceptibility test, minimum inhibitory concentration and minimum bacteriocidal concentrations were determined [15]. The zone of inhibition of the leaf extract of *F. sycomorus* was between 17.5 mm for sensitive *S. aureus*, 13.0 for resistant *S. aureus* and 21.5 for sensitive *S. typhi*. The minimum inhibitory concentration was 7.81 mg/ml for sensitive *S. aureus*, 15.6 for resistant *S. aureus*, 1.95 µg/ml for sensitive *S. typhi* and 15.6 µg/ml for resistant *S. typhi*. The minimum bacteriocidal concentrations were 15.6 mg/ml for sensitive *S. aureus*, 62.5 mg/ml for resistant *S. aureus*, 3.91 mg/ml for sensitive *S. typhi* and 31.3 mg/ml for resistant *S. typhi*. The antibacterial activity observed validate the traditional use of the plant in wound dressing. The free radical scavenging activity of the methanolic extract of leaves of the different *Ficus* species across Egypt was evaluated using the DPPH method. The crude extract of leaves of the *F. sycomorus* plant showed a very high activity of 79.50 µg/ml [18].

3.3.2 Stem bark

An aqueous extract of the stem bark of the Sycamore tree was shown to possess inhibitory effects on muscle contraction through its ability to lower the acetylcholine contractile responses of guinea pigs duodena and abdominal muscles of frogs [19]. Column chromatography fractions of the hexane, petroleum ether and chloroform extracts of stems bark of *F. sycomorus* stem bark were evaluated for *in vitro* antifungal activity against *Candida albicans*, *Trichophyton rubrum*, *Trichophyton mentagrophytes*, *Microsporium gypseum*, *Aspergillus niger* and *Aspergillus flavus* [4]. Their results revealed that the hexane fractions exhibited antifungal activity against *Microsporium gypseum*, *Aspergillus niger*, *Aspergillus flavus* and *Candida albicans*. On the other hand, the chloroform fractions only showed inhibition activity on *Trichophyton mentagrophytes* and *Trichophyton rubrum* and the petroleum ether fractions showed no inhibition activity against all the tested organisms. This study validated the ethnopharmacological medicinal use of the Sycamore tree as a treatment for fungal infections and further exhibited the potential of the stem bark to be developed into

plant-based antifungal drugs. The aqueous extract of stem-bark of the Sycamore tree was shown to exhibit sedative effects due to its capacity to increase amylobarbitone induced sleeping time and anticonvulsant effects were demonstrated by the ability of the extract to protect rats treated with a convulsive dose of pentylenetetrazol [20].

The stem bark of the Sycamore tree was extracted using 70 % aqueous ethanol, the antibacterial susceptibility, minimum inhibitory concentration and minimum bacteriocidal concentrations of the extract were determined [15]. The zone of inhibition of the stem bark extract was 17 mm for sensitive *S. aureus* 11.5 mm for resistant *S. aureus*, 21.5 mm for sensitive *S. typhi* and 16.0 mm for resistant *S. typhi*. The minimum inhibitory concentration of the stem bark extract was 15.6 mg/ml for sensitive *S. aureus*, 31.3 mg/ml for resistant *S. aureus*, 3.91 mg/ml for sensitive *S. aureus* and 15.6 mg/ml for resistant *S. typhi*. The minimum bacteriocidal concentration (MBC) of the stem extract was 31.3 mg/ml for resistant *S. aureus*, 250.0 mg/ml for resistant *S. aureus*, 15.6 mg/ml for sensitive *S. typhi* and 62.5 mg/ml for resistant *S. typhi*. The results indicate that the stem extract has potential to be developed into antimicrobial agents against ciprofloxacin resistant *S. typhi* and further validates the traditional application of the stem bark of the Sycamore as an antibacterium [15].

Other studies have been carried out to investigate the antifungal activity of extracts of the whole plant samples of *F. sycamorus* plant on the blood, kidney and liver of male toads infected with *Aspergillus niger* [11]. The fungus caused a reduction in blood cells and haemoglobin levels, degeneration of the liver and kidney. Pretreatment with the plant extract contributed to a reduction in growth of *A. niger* and an increase in the levels of blood cells and haemoglobin contents, kidney and liver protective effects against *A. niger*.

3.3.3 Roots

A root bark extract of the Sycamore tree was injected into rats to test for its toxicity on the kidney and liver [2]. The extract was shown to exhibit no toxicity to the kidney, but had potential hepatotoxicity and should be administered with caution [2]. Zaku et al.[14] investigated the effects of an aqueous root-bark extract of *F. sycomorus* on muscular relaxation, and sleeping time on rats and local its anesthetic effects on a rabbit [14]. The study revealed that the root bark extract has potential to produce relaxation effects in rats, increased aminobarbitone induced sleeping time in a dose dependent manner showing that it may have pharmacological action and further showed depressant effects on the peripheral and central nervous system in the rabbit [14]. As such, the plant demonstrated strong potential to be a valuable source of drugs for anesthesia.

3.3.4 Fruits

An extract of dried *F. sycomorus* fruits was screened in the brine shrimp bioassay, potato disc bioassay, calcium antagonism test, screened for antifungal activity and the antimicrobial test was done using the filter paper disk diffusion method [16]. Extracts of the *F. sycomorus* fruits were not active in the brine shrimp test indicating a lack of toxicity although the effect of efficacy against mammalian cells may reveal a different effect. The extract exhibited no activity in the calcium antagonistic activity test revealing that the traditional uses of the extracts in treatment of circulatory disorders could not be verified in this study. The fruit extract showed activity in the potato disc bioassay test with a 51% tumor inhibition thus demonstrating antitumor activity [16]. In the antifungal test, the extract showed no activity but was active against several bacteria at a concentration of 5 mg/disk giving a possible explanation to the traditional use of the plant in treating certain respiratory disorders and skin diseases [16].

3.5 PHYTOCHEMISTRY

3.5.1 Stems

Chemical constituents of the aqueous extract of sun-dried stem bark of *F. sycomorus* were studied using standard methods. The reddish-brown stems were found to contain polyuronides, reducing sugars, gallic tannins, catechol tannins, saponins, alkaloids, sterols and triterpenes and flavone aglycones [19]. Hassan et al.[4] investigated the phytochemical constituents of column chromatography fractions of the hexane, chloroform and petroleum ether fractions of stem bark extracts of the Sycamore tree. Phytochemical screening of the aqueous root bark extract of the Sycamore tree for the presence of carbohydrates, tannins, saponins, flavonoids and alkaloids was done using standard methods [2]. Screening results revealed the presence of saponins, flavonoids, alkaloids, tannins and reducing sugars. An aqueous extract of stem-bark of the Sycamore was screened for chemical constituents using standard methods, the results showed the presence of steroids, terpenoids, tannins, anthracenosides and alkaloids, however, flavonoids, saponins and reducing compounds were not present [14].

3.5.2 Leaves

Phytochemical analysis of n-butanol extracts of *F. sycomorus* leaves using standard methods revealed the presence of terpenes, sugars and tannins, however alkaloids, flavonoids and anthraquinones were not detected [13]. Leaves of the Sycamore tree were investigated to determine their proximate nutrient content, mineral and amino acid composition and anti-nutritional factors [7]. Results of the study revealed that the leaves had crude protein content (17.24 ± 0.71 g/100g dry weight), lipid content (3.00 ± 0.52 g/100g dry weight), carbohydrate (39.32 ± 0.38 g/100g dry weight), moisture (14.12 ± 0.22 g/100 g dry weight), crude fibre (31.54 ± 0.11 g/100 g dry weight), ash content (10.24 ± 0.68 g/100g dry weight) and moisture content (14.12 ± 0.22 g/100 g dry weight). The most abundant amino acids were lysine (12.75

g/100g protein), glutamic acid (10.95 g/100 g protein) and aspartic acid (8.71 g/100g protein). Phosphorus (380.25 ± 0.55 mg/100 g dry weight), magnesium (300.65 ± 0.67 mg/100g dry weight) and calcium (390.78 ± 0.65 mg/100 g dry weight) were the most abundant minerals. The anti-nutritional factors oxalate ($2.88\% \pm 0.37$), tannins ($4.01\% \pm 0.22$), saponins ($1.78\% \pm 0.11$), phytates ($1.98\% \pm 0.78$), alkaloids ($5.64\% \pm 0.41$) and HCN ($3.05\% \pm 0.51$) were below established toxic levels. Their results validated the traditional consumption of leaves of Sycamore tree as vegetables and provided scientific evidence to show that the leaves have substantial amounts of nutrients and are not inferior vegetables [7].

Column chromatography of an unsaponifiable fraction of fat extracted from *F. sycamoros* leaves on alumina led to the isolation of α amyirin, lupeol and β -sitosterol. In the same study, psoralene was isolated from *F. sycamoros* leaves by column chromatography of another fraction on silica gel [1]. Bioassay guided fractionation was used to isolate compounds from a 70% methanol extract of leaves of the Sycamore tree [17]. The defatted 70% methanol extract was dissolved in water and extracted using chloroform, ethyl acetate and *n*-butanol respectively. The compounds quercetin, gallic acid, rutin and isoquercetin were isolated from the ethyl acetate fraction using column chromatography. The *n*-butanol fraction produced quercetin 3,7,0, α -L-dirhamnoside, quercetin 3-O- β -D-galactopyranosyl (1-6) glucopyranoside and β -sitosterol-3- β -D-glucopyranoside following column chromatography. An aqueous extract of leaves of the Sycamore tree was screened for chemical constituents using standard methods, the extract was shown to have steroids, terpenoids, flavonoids, tannins, saponins, reducing compounds, anthracenosides and alkaloids [14]. The dried, ground leaves of the Sycamore tree were screened for its phytochemical constituents using standard methods, the presence of saponins, anthocyanins, cardenolides, coumarin derivatives, anthracenosides, flavonosides, reducing compounds, alkaloid salts, tannins, carotenoids and sterols was confirmed in the leaves while coumarins, anthracenosides aglycones, flavone aglycones and alkaloid bases were not detected [5].

3.5.3 Roots

A water extract of root-bark of *F. sycomorus* was screened for its chemical constituents using standard methods. The study revealed that the extract had steroids, terpenoids, flavonoids, tannins, saponins, reducing compounds, anthracenosides and alkaloids [14]. Research has been done to authenticate the traditional medicinal uses of the Sycamore tree and some have identified its active ingredients. Despite reports of traditional uses of the *F. sycomorus* plant for anti-aging purposes, very few studies have been conducted to scientifically validate anti-aging claims on the Sycamore plant, to identify the active ingredients and a chemical analysis of any anti-aging *F. sycomorus* extract for quality control purposes. Further, no reports have been made on the inhibition of collagenase and elastase activity of this plant, these enzymes are important in determining the anti-aging potential of ingredients

3.6 METHODOLOGY

3.6.1 Collection and extraction of plant material from KwaZulu Natal

Leaves from *F. sycomorus* plant were collected from Sodwana Nature Reserve in South Africa as part of a Council for Scientific and Industrial Research (CSIR) programme to collect and evaluate plants for their anti-aging potential. The plants were identified at the South African National Biodiversity Institute (SANBI, Tshwane) where voucher specimens are deposited (PRE 0893676). The collected plant materials were oven-dried at 30-60 °C. Dried plant material was ground to a coarse powder using a hammer mill and stored at ambient temperature prior to extraction. Dried and ground *F. sycomorus* leaves (100 g) was extracted with 1 L of methanol:DCM (1:1) for 24 hours at room temperature. The solvent was evaporated using a rotary evaporator at 50-60 °C and then further dried in a desiccator for 24 hours (Figure 3.2) and the extracts were stored in a cold room.

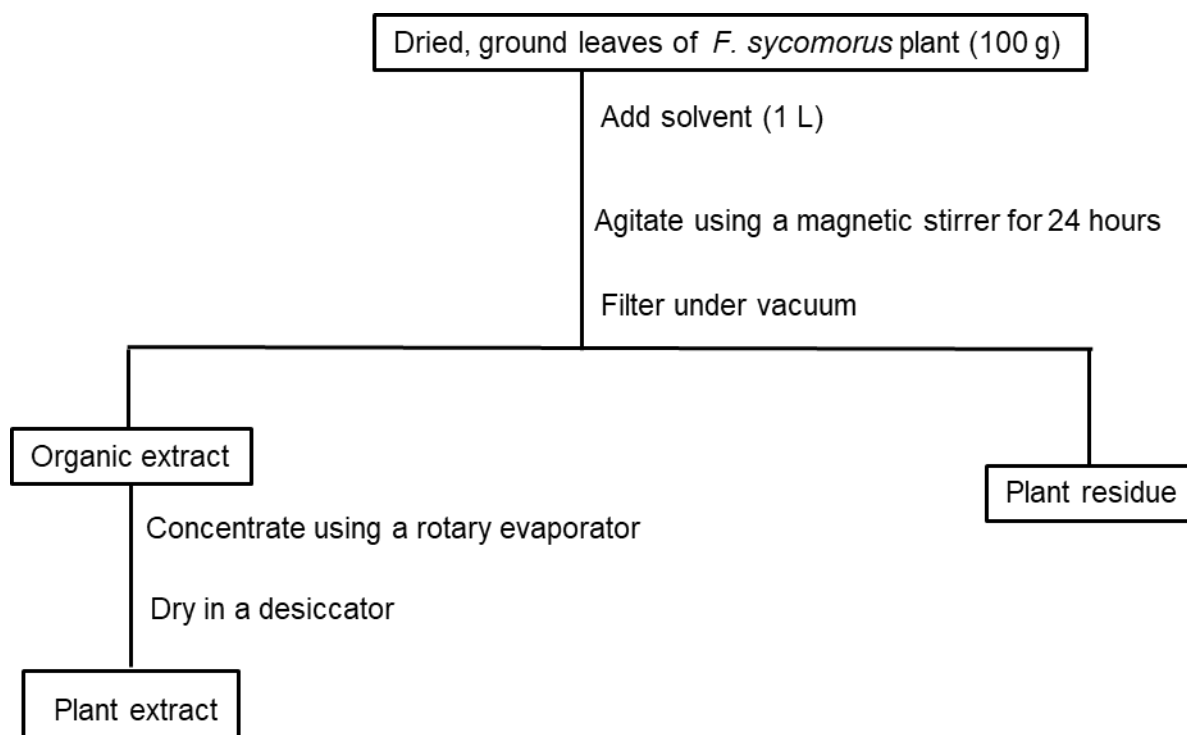


Figure 3.2. Flow diagram for the separate extraction of leaves of *F. sycomorus* plant using methanol : DCM (1:1)

3.6.2 Collection of plant material from the University of Pretoria garden and experimental farm

Leaves of *F. sycomorus* were harvested from the University of Pretoria garden and experimental farm and with the help of the curator Jason Samuels. The identity of the plants was confirmed at the herbarium of the University of Pretoria (voucher number PRU 123534). The plant material was diced into small pieces and air dried in the lab. Dried plant material was ground to a coarse powder using a hammer mill and stored in the dark.

3.6.3 Separate extraction of leaf material using polar solvents

The dried and ground leaves from *F. sycomorus* plant were extracted separately using ethanol, acetone and methanol:DCM (1:1). The plant material (100 g) was extracted by adding each solvent (1 L) and agitating for 3 hours using a magnetic stirrer. The mixture was filtered

under vacuum using a buchner funnel. The plant residue was discarded, and the organic extract was concentrated and dried using a rotary evaporator (Figure 3.3).

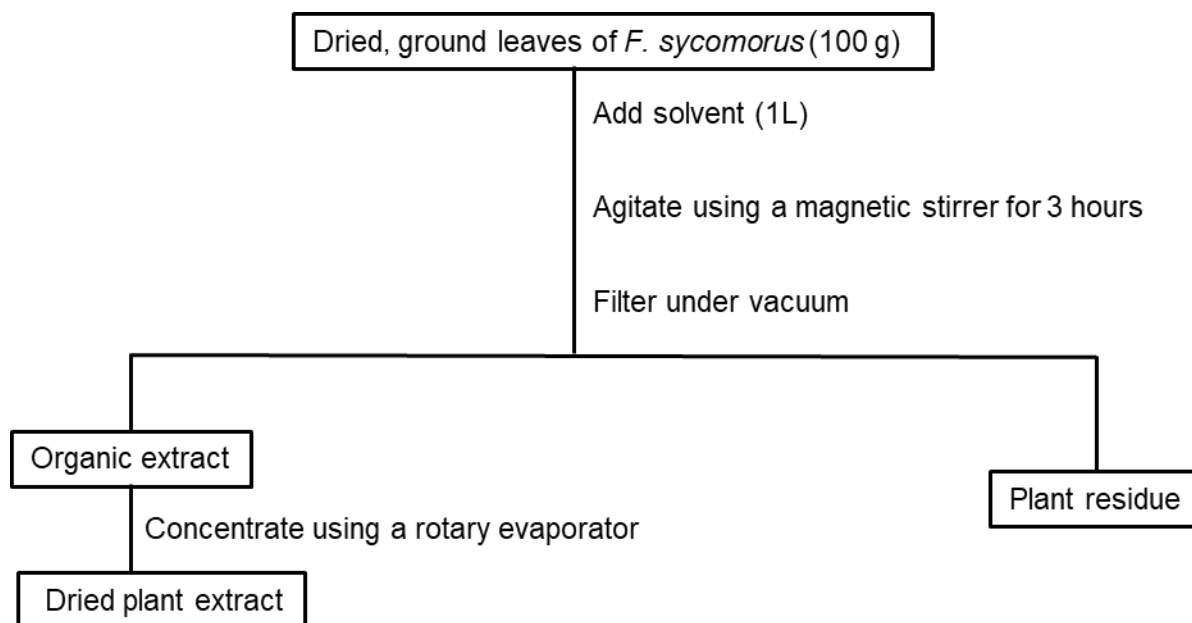


Figure 3.3. Flow diagram for the extraction of dried ground leaves of *F. sycomorus* separately using ethanol, acetone, and methanol:DCM (1:1)

3.6.4 Sequential extraction of leaf material

The dried ground leaf material of *F. sycomorus* (100 g) was sequentially extracted using hexane, DCM, ethyl acetate and methanol. Extraction was done using agitation with each solvent (1 L) with a magnetic stirrer for 2 hours followed by filtration under vacuum. The plant residue after the hexane extraction was extracted using DCM, the residue from the DCM extraction was extracted using ethyl acetate (EtOAc) and the residue from the EtOAc extraction was extracted using methanol. The organic extracts were evaporated to dryness using a rotor vapour and were stored at ambient temperatures (Figure 3.4).

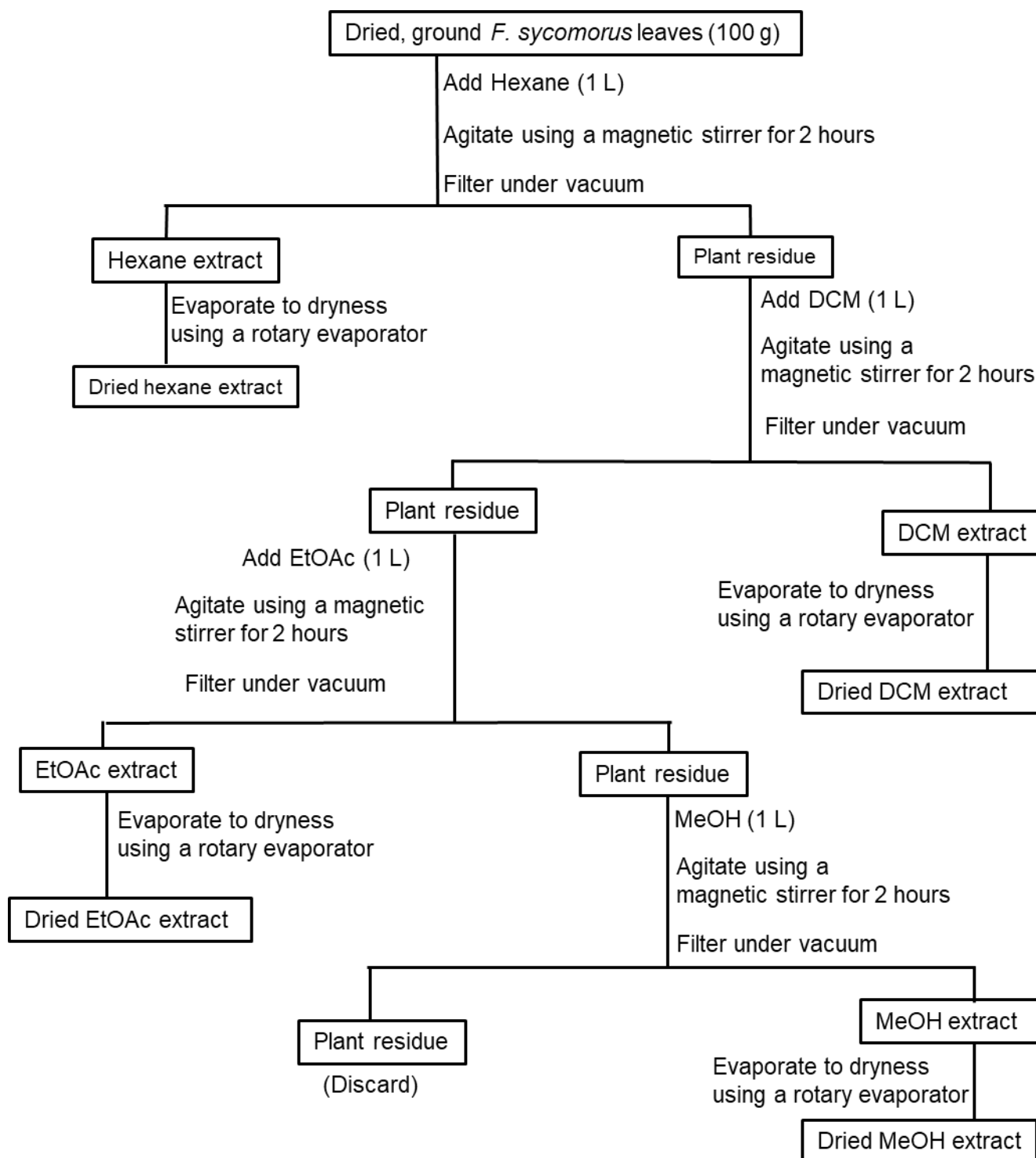


Figure 3.4. Flow diagram for the sequential extraction of dried ground leaf material of *F. sycomorus*

3.6.5 Bioassaying of crude extracts and fractions

The method according to Kraunsoe et al. [21] with a few modifications was used to determine anti-elastase inhibition activity. The elastase substrate N-Methoxysuccinyl-Ala-Ala-Pro-Val-*p*-nitroaniline is catalysed by the human leucocyte elastase (HLE) to give a yellow coloured product, *p*-nitroaniline which is detected by absorbance at 405 nm on a Tecan infinite 500 spectrophotometer. In this assay, in the presence of an inhibitor, the enzyme HLE is inhibited and the breakdown of the substrate proceeds at its natural rate of reaction, as such the yellow coloured product *p*-nitroaniline is not formed giving no colour change.

Anti-collagenase inhibition was determined according to Moore and Stein's method [22] incorporating modifications by Mandl et al. [23]. Collagen is degraded by the enzyme collagenase to produce peptides which react with ninhydrin to give a blue coloured product detected by absorbance at 540 nm on a Tecan Infinite 500 spectrophotometer. In the presence of an inhibitor the enzyme collagenase will not catalyse the reaction, hence the breakdown of collagenase will proceed at its natural rate of reaction and there will be no colour change.

3.6.6 Chemical profiling using UPLC MS and NMR

The samples were run on the UPLC and the separated compounds analysed by mass spectrometry (MS). The compounds were tentatively identified by generating molecular formula from MassLynx V 4.1 based on their isotopic fit value (iFit value), and by comparison of MS/MS fragmentation pattern with that of matching compounds from Metlin, Metfusion, Chempider, Massbank libraries and Dictionary of Natural products. The iFit value is an indication of how well the measured isotopic ion ratio compares to the theoretical ion ratio [24]. Additionally, acquired accurate masses were compared with those of known compounds in compound databases. Pure standards were used to confirm the presence of selected compounds.

For the purification and isolation of selected compounds, the crude ethanol extract of leaves of *F. sycomorus* was fractionated targeting those compounds which could not be identified using UPLC-QTOF-MS. The extract (20 g) was initially fractionated on column chromatography using silica gel (1500 g). The solvent system EtOAc:MeOH:H₂O:formic acid (FA) in the ratio 10:0.3:0.3:0.3 was used initially while the polarity was later increased to EtOAc:MeOH:H₂O:FA in the ratio 8:1:1:1 for the elution of the more polar compounds. A total of 72 fractions were collected, three of these fractions were selected following thin layer chromatography (TLC) and UPLC-MS-QTOF analysis. Selected fractions were purified using mass-directed purification by preparatory HPLC-MS to give three compounds. Figure 3.5 shows the flow diagram for fractionation.

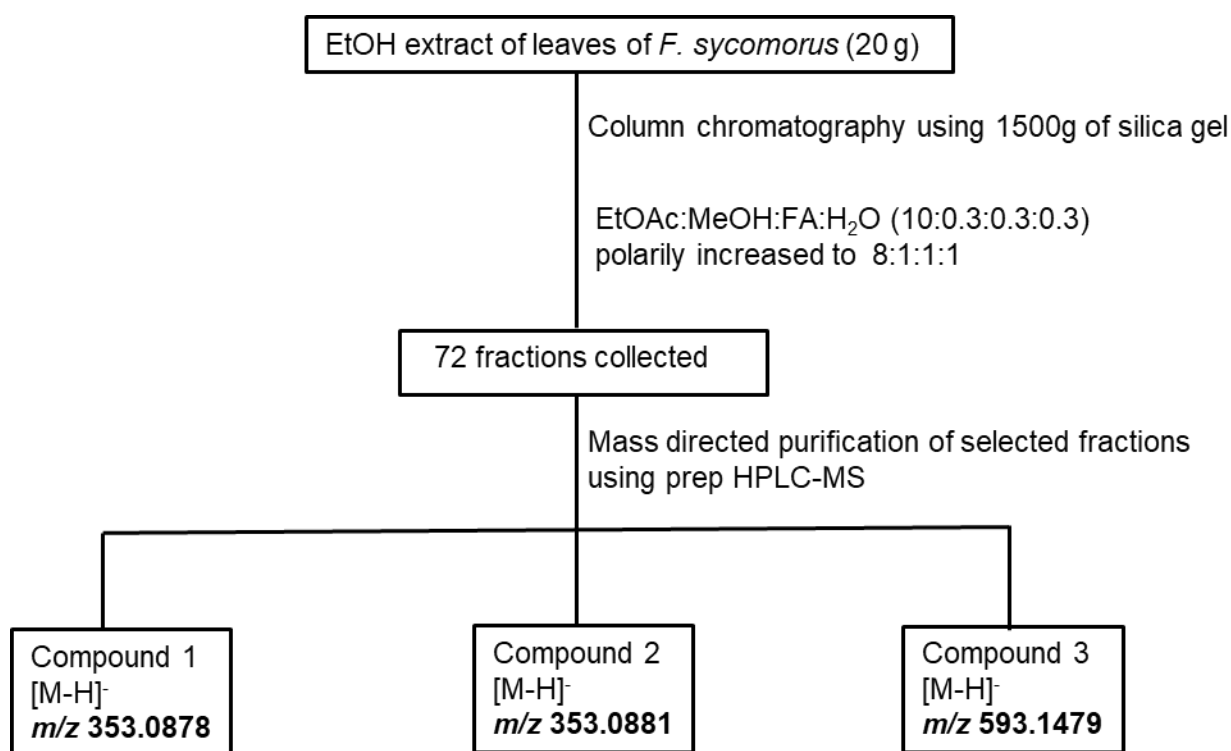


Figure 3.5. Flow diagram for the fractionation of crude ethanol extract of leaves of *F. sycomorus* using column chromatography followed by mass directed fractionation using preparatory HPLC-MS

3.6.7 Bioassay guided fractionation

The crude ethanol extract of leaves of *F. sycomorus* was fractionated using a prep HPLC-UV. Fractionation was undertaken with the aim of identifying active compounds in the fractions. The extract (100 mg) dissolved in DMSO (4 ml) was fractionated on prep HPLC-UV using a gradient elution method a reverse phase column and the solvents water with 1% FA and acetonitrile to produce 17-time base collected fractions. Each fraction was evaporated to dryness using a Speed vac and accurately weighed for bioassay guided fractionation. The fractions were screened for collagenase and elastase inhibition activities. Fractions displaying activity were chemically evaluated using a UPLC-QTOF-MS to identify the compounds responsible for activity (Figure 3.6).

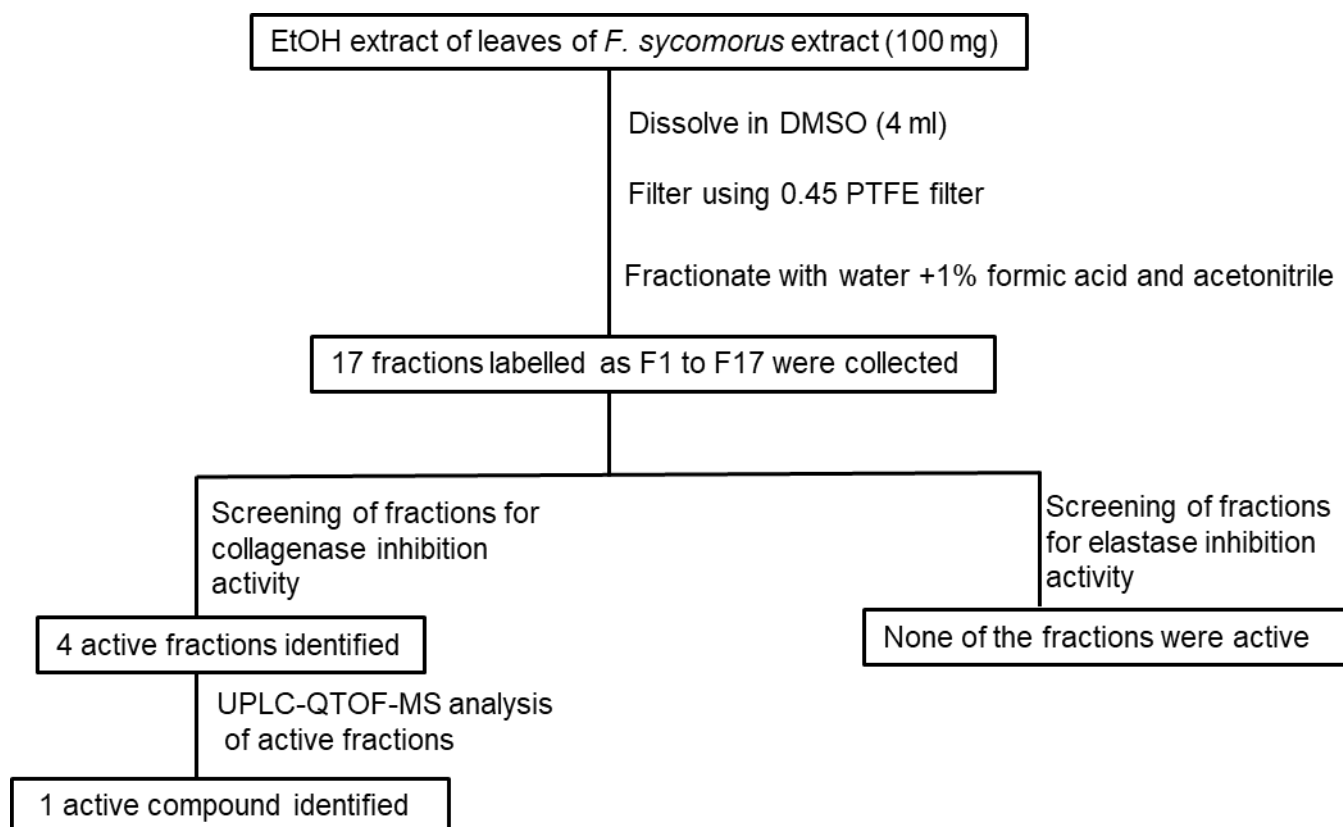


Figure 3.6. Flow diagram for bioassay guided fractionation of crude ethanol extract of leaves of *F. sycomorus*.

3.6.8 Defatting the crude ethanol extract of leaves of *F. sycomorus*

In order to remove the intense green colour, the crude ethanol extract of leaves of *F. sycomorus* (500 mg) was defatted by partitioning between 50 ml of water:ethanol (20 : 80) and hexane (50 ml). After separation of the two layers, the water/ethanol fraction was evaporated to dryness using a rotary evaporator and screened for its anti-aging properties (Figure 3.7).

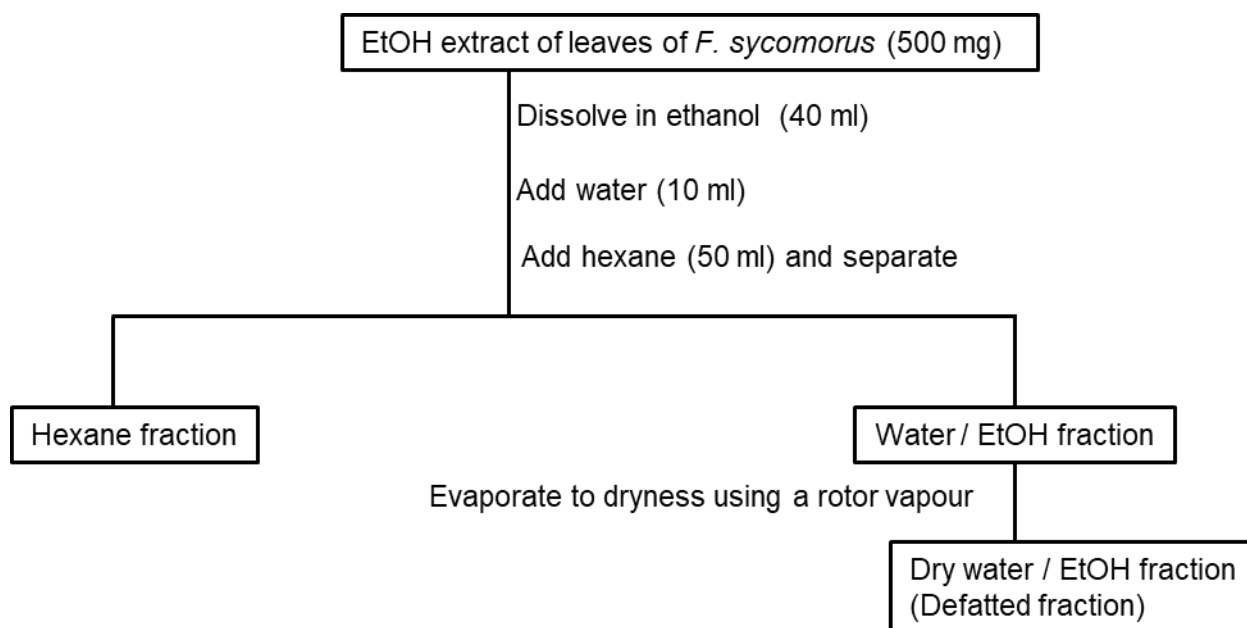


Figure 3.7. Flow diagram for the defatting of crude ethanol extract of leaves of *F. sycomorus*

3.7 RESULTS AND DISCUSSION

Screening results for the elastase and collagenase activities of the methanol:DCM (1:1) extract of leaves of the *F. sycomorus* plant collected from Sodwana Nature Reserve and the positive controls at 200 µg/ml are shown in Table 1. The extract exhibited very good anti-collagenase activity of 81.05% ± 3.65 and compared favourably to that of EDTA the positive control which had an inhibition activity of 79.88% ± 9.10. Similarly, the extract had very good elastase inhibition activity of 92.59% which was equivalent to that of the positive control (elafin) which exhibited 93.09% ± 4.10 inhibition. This extract collected from a wild environment exhibited good anti-aging activity and thus showed good potential to be developed into an anti-aging

ingredient. As such, further investigation is required to check if a Sycamore plant grown in a different geographical location would exhibit similar anti-aging activity.

Table 3.1. Inhibition of the elastase and collagenase activities for leaves of *F. sycamoros* tested at 200 µg/ml and the positive controls at EDTA at 143 µg/ml and elafin 1.43 µg/ml

Plant part	Elastase assay (% Inhibition ±SD)	Collagenase assay (% Inhibition ±SD)
Leaves	92.59 ± 3.72	81.05 ± 3.65
Controls		
10% MeOH	1.45 ± 1.50	1.32 ± 0.73
EDTA		79.88 ± 9.10
Elafin	93.09 ± 4.10	

3.7.1 Sequential extraction using polar and non-polar solvents and bio-assaying

Sequential extraction was done using different solvents to ensure that polar and non-polar compounds were extracted into the different solvents thereby offering partial separation of compounds from the plant. The extraction yields are shown in Table 2. Hexane, dichloromethane and ethyl acetate had lower yields of 2.17%, 1.17% and 0.43% respectively while methanol had the highest extraction yield of 9.78%. These results suggest that the leaves have more of the polar constituents than the non-polar constituents. The extracts were screened in the elastase and collagenase assay which revealed that the hexane and DCM sequential extracts showed no elastase inhibition activities. The methanol sequential extract showed high biological activity, however, upon comparison to elafin (99.21% ± 0.05), the elastase inhibition activities of both the methanol (89.55% ± 0.33) and ethyl acetate (1.77% ± 0.88) sequential extracts exhibited significantly lower activities ($p < 0.01$). In the collagenase assay, the hexane and ethyl acetate sequential extracts showed no collagenase inhibition activities. The DCM sequential extract had a significantly lower collagenase inhibition activity (11.02% ± 0.37, $p < 0.01$) than EDTA (94.13% ± 6.76). In contrast, the methanol sequential extract showed a 94.13% ± 6.76 inhibition which was similar ($p > 0.05$) potency to EDTA. These results reveal that the compounds responsible for anti-aging activity in leaves of *F. sycamoros* are concentrated in the polar extracts.

Table 3.2. Extraction yields, elastase and collagenase inhibition activities of leaves of *F. sycomorus* extracted using different solvents and tested at 200 µg/ml and the positive controls EDTA at 143 µg/ml and elafin at 1.43 µg/ml

Extraction solvent used for the stems	Extraction yield (calculated from dry plant material)	Elastase assay (% Inhibition ± SD)	Collagenase assay (% Inhibition ± SD)
Sequential extraction with hexane	2.17%	**0	**0
Sequential extraction with DCM	1.17%	**0	**11.02 ± 0.37
Sequential extraction with ethyl acetate	0.43%	**1.77±0.88	**0
Sequential extraction with methanol	9.78%	**89.55±0.33	94.13 ± 6.76
Controls			
10% MeOH		3.28 ± 0.34	0
10% DMSO		4.70 ± 0.53	1.58 ± 0.60
Elafin		99.21 ± 0.05	
EDTA			95.66 ± 2.11

**showing a significant difference of $p < 0.01$ compared to EDTA

*showing a significant difference of $p < 0.01$ compared to Elafin

3.7.2 UPLC-QTOF-MS analysis of *F. sycomorus* leaves extracted sequentially with polar and non-polar solvents

The chemical profile of the hexane extract was not analysed on the UPLC-QTOF-MS as the extract showed no activity in both the elastase and collagenase assay. Peaks in the DCM extract were mainly distributed within the 8 to 18-minute range of the 20-minute chromatogram. This is the general elution region for non-polar compounds. Compounds in the ethyl acetate extract eluted from 0.7 minutes to 15 minutes showing that the extract was constituted of both polar and non-polar compounds while compounds in the methanol sequential extract eluted in the 0 to 6 minutes region, revealing the extract was mainly constituted of polar compounds. These results confirm that sequential extraction was successful in extracting compounds based on polarity.

Common peaks identified between the ethyl acetate sequential extract and the active methanol sequential extract are likely to contribute to the elastase and collagenase inhibition activities of the extracts. These include a peak observed in the polar region of the EtOAc

extract at m/z 341.1088 retention time 0.73 minutes (Figure 3.8). The identity of the compound corresponding to this peak was identified as palatinose as described in section 3.7.5. The chloride adduct $[M+Cl]^-$ of this peak was observed as the most intense peak in the methanol extract at m/z 377.0861 retention time 0.74 minutes. Additional common peaks were observed in the ethyl acetate sequential extract at m/z 463.0887 retention time 4.98 minutes and in the methanol sequential extract at m/z 463.0881 retention time 4.95 minutes. The structure of the compound corresponding to this peak was identified as isoquercetin, confirmation of its identity is described in section 3.7.5. Another peak observed in the ethyl acetate extract at m/z 353.0880 retention time 3.18 minutes was also present in the methanol sequential extract at m/z 353.0876 retention time 3.18 minutes. The structure of the compound corresponding to this peak was elucidated in section 3.7.7 to be biflorin. The compounds biflorin, palatinose and isoquercetin are likely to be contributing to the activity of the methanol sequential extract and the ethyl acetate sequential extract. Consequently, screening of these pure compounds in both the collagenase and elastase inhibition assays was done in sections 3.7.13 and 3.7.16 respectively and isoquercetin was shown to be active in the collagenase assay thus confirming its contribution to anti-aging activities of these extracts. None of the compounds screened were active in the elastase inhibition assay.

The lack of elastase and collagenase inhibition activity in the ethyl acetate extract could be attributed to the dilution of the active compounds by the additional non-active constituents which were present in the ethyl acetate extract but absent from the methanol extract. The additional non-active compounds in the ethyl acetate extract were identified at m/z 269.0450 retention time 8.33 minutes, m/z 383.1148 retention time 9.00 minutes, m/z 337.1082 retention time 11.08 minutes, m/z 967.5641 retention time 13.27 minutes, m/z 997.5701 retention time 15.11 minutes, and m/z 959.5945 retention time 16.06 minutes. Further, the non-polar region of the ethyl acetate extract had common peaks with the inactive DCM sequential extract. The peak at m/z 337.1082 retention time 11.24 minutes in the DCM extract was present in the ethyl

acetate extract at m/z 337.1082 retention time 11.08 minutes. In addition, the peak observed in the DCM extract at m/z 293.2122 retention time 11.98 minutes was present in ethyl acetate extract at m/z 293.2118 retention time 11.98 minutes. Another intense peak identified in the ethyl acetate sequential extract at m/z 805.5082 retention time 14.07 minutes was observed in the DCM sequential extract at m/z 805.5101 retention time 14.07 minutes. These peaks are likely to correspond to inactive compounds which significantly contributed to the dilution of active compounds resulting in loss of elastase and collagenase inhibition activity in the ethyl acetate extract. The identities of the inactive compounds have not been established.

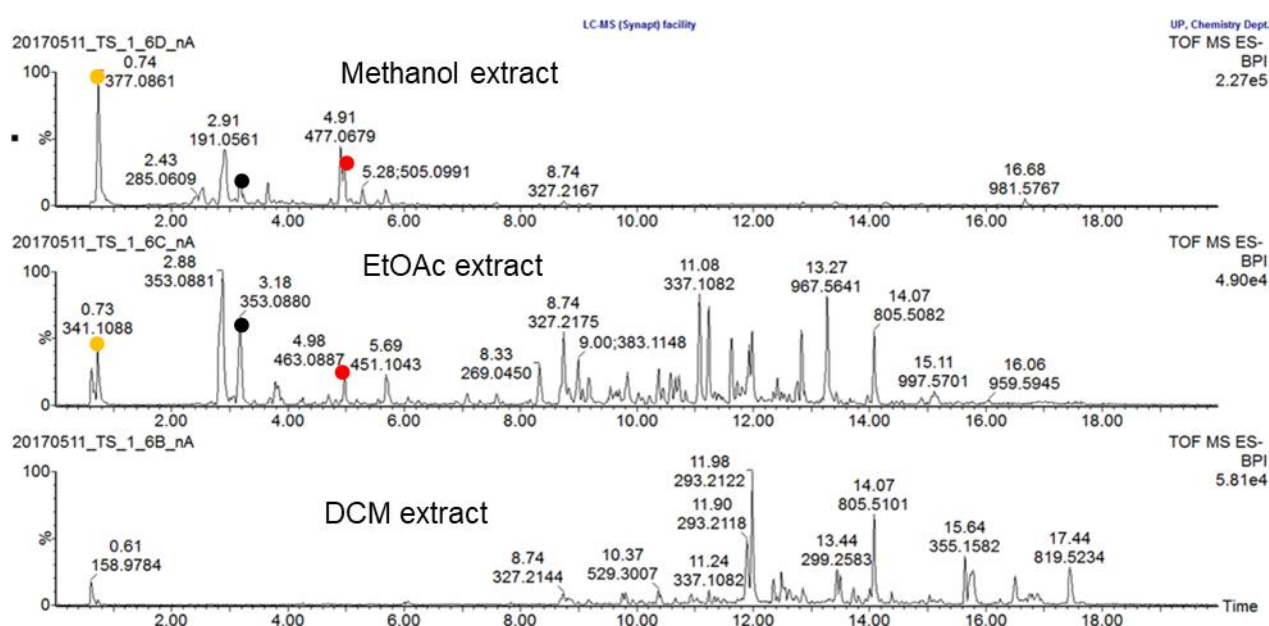


Figure 3.8. ESI negative mode BPI chromatograms of leaves of *F. sycomorus* extracted sequentially. ● Palatinose (m/z 377.0861 retention time 0.74 minutes in MeOH extract and m/z 341.1088 retention time 0.73 minutes in EtOAc extract), ● Isoquercetin (m/z 463.0887 retention time 4.98 minutes) and ● biflorin (m/z 353.0880 retention time 2.88 minutes) are likely to be responsible for elastase and collagenase inhibition activities of the extracts.

3.7.3 Separate extraction using different polar solvents and their bioassaying

Sequential extraction revealed that the more polar solvents extracted the active anti-aging constituents. As a result, the polar ethanol and acetone solvents were selected from the list of solvents acceptable to the cosmetic industry for extraction of cosmetic ingredients.

Methanol:DCM (1:1) was also selected in order to facilitate comparison of anti-aging activities of plants collected from the University of Pretoria garden and experimental farm with the activities of extracts previously collected by the CSIR. The dried and ground leaves were extracted separately using acetone, ethanol and methanol:DCM (1:1) in order to identify the most suitable polar solvent for extraction of the most active ingredients from the leaves.

The extraction yields for acetone and ethanol were 5.21% and 4.19%, respectively while methanol:DCM (1:1) yield was 6.95% from the same plant material (Table 3). These polar solvents had good extraction yields of > 4.00% with the methanol:DCM (1:1) extract showing the highest yield. The higher extraction yield obtained using methanol:DCM (1:1) can be attributed to a combination of a polar and a non-polar solvent having a greater extraction capacity in a matrix composed of both polar and non-polar constituents. The extracts were screened in the elastase and collagenase assay and the results revealed that although the methanol:DCM (1:1) and ethanol extracts exhibited high anti-elastase activities of $79.97\% \pm 0.46$ and $83.85\% \pm 0.91$, respectively, they exhibited significantly lower ($p < 0.01$) elastase inhibition activities than elafin ($99.21\% \pm 0.05$). In the collagenase assay, the methanol:DCM (1:1) ($88.91\% \pm 6.62$) extract showed good collagenase inhibition activities similar ($p > 0.05$) to that of EDTA ($95.66\% \pm 2.11$). However, the ethanol extract showed collagenase inhibition activity ($102.06\% \pm 0.84$) significantly higher ($0.01 < p < 0.05$) than that of EDTA. Surprisingly, the acetone extract showed no inhibition activity in both the elastase and collagenase assays. Consequently, chemical analysis was necessary to identify the compounds which are responsible for elastase and collagenase inhibition activities of the extracts and to provide a possible explanation on the observed activities.

The elastase inhibition activity of the methanol:DCM (1:1) extract ($79.97\% \pm 0.46$) of the recollected *F. sycomorus* leaves from the University of Pretoria gardens was similar to the earlier collections from Kwazulu Natal which had an elastase inhibition of $92.59\% \pm 3.72$.

Similarly, the collagenase inhibition activity of $88.91\% \pm 6.62$ for the recollected *F. sycomorus* leaves extracted with methanol:DCM (1:1) showed potency in the same range as the collections from KwaZulu Natal which had $81.05\% \pm 3.65$ elastase activity. This result indicated that the geographical location does not appear to have an effect on the active ingredients.

Table 3.3. Extraction yields, elastase and collagenase inhibition activities of leaves of *F. sycomorus* extracted using different solvents.

Extraction solvent used for the stems	Extraction yield (calculated from dry plant material)	Elastase assay (% Inhibition \pm SD)	Collagenase assay (% Inhibition \pm SD)
Acetone	5.21%	**0	**0
Methanol: DCM (1:1)	6.95%	**79.97 \pm 0.46	88.91 \pm 6.62
Ethanol	4.19%	**83.85 \pm 0.91	*102.06 \pm 0.84
		Controls	
10% MeOH		3.28 \pm 0.34	
10% DMSO		4.70 \pm 0.53	
Elafin		99.21 \pm 0.05	
10% MeOH			0
10% DMSO			1.58 \pm 0.60
EDTA			95.66 \pm 2.11

**showing a significant difference of $p < 0.01$ compared to EDTA

*showing a significant difference of $0.01 < p < 0.05$ compared to EDTA

**showing a significant difference of $p < 0.05$ compared to Elafin

3.7.4 UPLC-QTOF-MS analysis of *F. sycomorus* leaves extracted separately with polar solvents

Chemical analysis was done on the active ethanol and methanol:DCM (1:1) extracts and the inactive acetone extract. A comparison of the chemical profiles revealed that there were common peaks observed in the active methanol:DCM (1:1) and the ethanol extracts. The chloride adduct $[M+Cl]^-$ of palatinose was observed in the ethanol extract at m/z 377.0872 retention time 0.74 minutes and in the methanol:DCM (1:1) extract at m/z 377.0855 retention time 0.74 minutes. Confirmation of identity of the chloride adduct of palatinose is described in section 3.7.5. The peak observed in the ethanol extract at m/z 353.0879 retention time 2.92 minutes was also present in the methanol:DCM (1:1) extract as a peak of lower intensity at m/z 353.0871 retention time 2.87 minutes (Supplementary data 28). The structure of the

compound was elucidated to be isobiflorin in section 3.7.7. Another peak at m/z 353.0881 retention time 3.23 minutes was observed in the ethanol extract, this peak was also present in the methanol:DCM (1:1) extract at m/z 353.0881 retention time 3.17 minutes (supplementary data 28). The structure of the compound was elucidated as described in section 3.7.7 to be biflorin. The intense peak observed at m/z 191.0547 retention time 2.92 minutes in the methanol:DCM (1:1) extract was also present in the ethanol extract at m/z 191.0555 at retention time 2.96 minutes (supplementary data 28). The compound corresponding to this peak was established to be chlorogenic acid as described in section 3.7.5. The peak observed in the ethanol extract at m/z 593.1500 retention time 3.69 minutes was also present in the methanol:DCM (1:1) extract at m/z 593.1500 retention time 3.65 minutes (supplementary data 28). The compound was isolated, purified its structure elucidated as vicenin-2. Structure elucidation of this compound is described in section 3.7.7. A prominent peak observed in the ethanol extract at m/z 463.0880 retention time 5.00 minutes was also observed in the methanol:DCM (1:1) extract at m/z 463.0871 retention time 4.95 minutes. The compound corresponding to this peak was identified in section 3.7.5. as isoquercetin. A less intense peak in the ethanol extract observed at m/z 609.1465 retention time 4.78 minutes was also observed in the methanol:DCM (1:1) extract at m/z 609.1456 retention time 4.74 minutes (supplementary data 28). The compound was identified in section 3.7.5 to be rutin.

The analysis of chemical profiles of the active ethanol and acetone extracts of the Sycamore tree clearly revealed the presence of common compounds which were identified to be palatinose, isoquercetin, biflorin, isobiflorin, rutin, vicenin-2 and chlorogenic acid. These pure compounds were screened in the collagenase and elastase assays in sections 3.7.13 and 3.7.15 respectively. The results revealed that isoquercetin was active in the collagenase inhibition assay, clearly showing that this glycoside of quercetin is one of the compounds contributing to the collagenase inhibition activity of the ethanol extract. On the other hand, none of these compounds exhibited elastase inhibition activity.

The active compound isoquercetin (m/z 463.0879 retention time 4.95 minutes) was also observed in the inactive acetone extract. Further, several additional peaks which were absent from the active methanol:DCM (1:1) and ethanol extracts were observed in the acetone extract at m/z 805.5101 retention time 14.07 minutes, m/z 967.5631 retention time 13.27 minutes, m/z 981.5787 retention time 16.68 minutes, m/z 819.5288 retention time 17.44 minutes, and at m/z 293.2105 retention time 11.98 minutes (Figure 3.9). The compounds corresponding to the additional peaks observed in the acetone extract are inactive as they were absent in the active extracts. Consequently, although acetone extracted some compounds which are likely to contribute to elastase and collagenase inhibition activity, the presence of intense peaks corresponding to inactive compounds in the extract may have diluted the active constituents leading to loss of activity of the acetone extract.

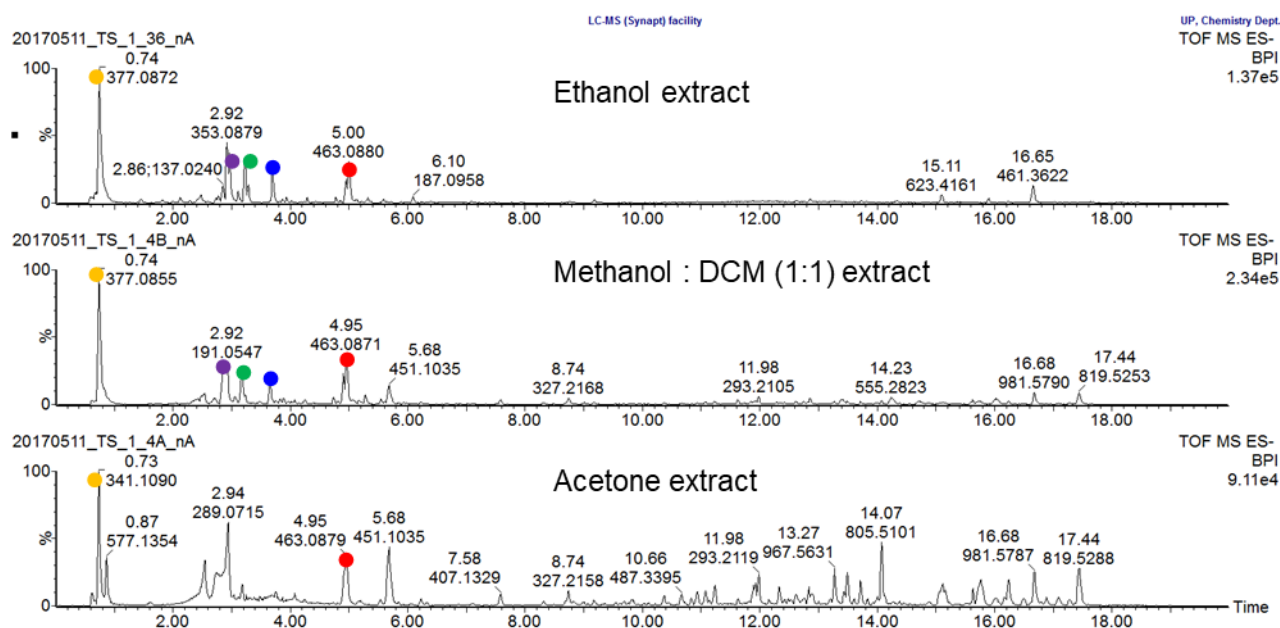


Figure 3.9. ESI negative mode BPI chromatograms of leaves of *F. sycomorus* extracted sequentially. The compounds ● palatinose (m/z 377.0855 retention time 0.74 minutes), ● chlorogenic acid (191.0547 retention time 2.92 minutes), ● biflorin m/z 353.0881 retention time 3.17 minutes, ● vicenin-2 (m/z 593.1500 retention time 3.65 minutes), and isobiflorin at m/z 353.0871 retention time 2.87 minutes (supplementary data 28), ● isoquercetin (m/z 463.0887 retention time 4.98 minutes) were identified as some of the compounds likely to contribute to the collagenase inhibition activities of the extracts.

The methanol sequential, ethanol and the methanol:DCM (1:1) extracts were active in both elastase and collagenase inhibition assays. These extracts have potential to be developed into anti-aging ingredients. Nevertheless, in the cosmetic industry, the solvent ethanol is acceptable for extraction of ingredients which will be used to formulate cosmetics [25]. Consequently, based on the high elastase and collagenase inhibition activities, and its acceptability to the cosmetic industry, the ethanol extract was selected for further research and development.

3.7.5 Chemical marker identification and phytochemical analysis

In order to guarantee safe use, quality control of herbal medicines is needed. Chemical profiling has been demonstrated to be a useful technique in quality control of herbal medicines [26]. A chemical profile or fingerprint is a unique pattern indicating the presence of various chemical markers in a sample [26]. Chemical profiling can be used for the purpose of authenticating a plant sample to identify if it is the genuine species [26]. The guarantee of quality is the basis for reliable efficacy and safety of herbal products. The use of hyphenated chromatographic techniques such as UPLC-QTOF-MS is strongly recommended for the purpose of quality control of herbal medicines as they appropriately represent the chemical constituents of herbal medicines. Chemical profiling of the crude ethanol extract of leaves of *F. sycomorus* extract was done for quality control purposes.

The chemical fingerprint generated from the evaluation of the extract using UPLC-QTOF-MS operating in the ESI negative mode is shown in Figure 3.10. Eight peaks which did not appear to have significant overlap or co-eluting compounds were selected for identification. However, peak 1 was later confirmed to be composed of two co-eluting compounds. Table 4 shows the compounds which were identified and those which could not be identified using mass

spectrometry. A total of nine compounds were tentatively identified in both the electrospray positive and negative modes. The compounds were made up of two chromone C-glycosides, three flavonol glycosides, one caffeoyl quinic acid, one organic acid and one disaccharide and one apigenin-C-glycoside. The structures of five of these compounds was confirmed using pure standards purchased from commercial suppliers and four were isolated and identified using NMR while one compound remained tentatively identified. Supplementary data 29 shows the positive mode ESI chromatogram of *F. sycomorus* leaf ethanol extract.

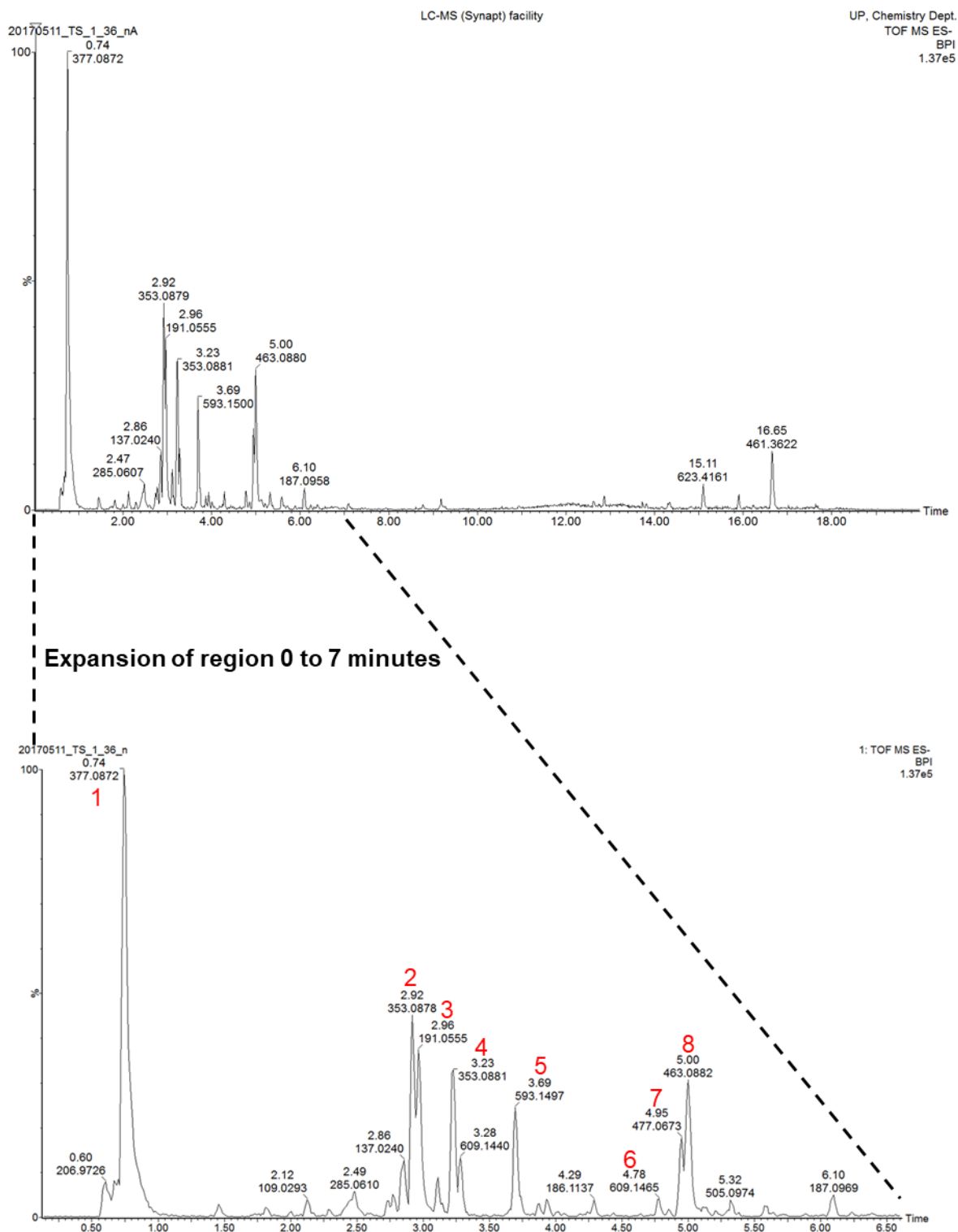


Figure 3.10. ESI negative mode BPI chromatogram of crude ethanol extract of leaves of *F. sycomorus*. A total of ten compounds were identified, the presence of five of these; palatinose and quinic acid (peak 1), chlorogenic acid (peak 3), rutin (peak 6), isoquercetin (peak 8) were confirmed using pure standards on a UPLC-QTOF-MS. The presence of four compounds isobiflorin (peak 2), biflorin (peak 4) and vicenin-2 (peak 5) was confirmed using NMR. Quercetin-3-glucuronide (peak 7) was tentatively identified.

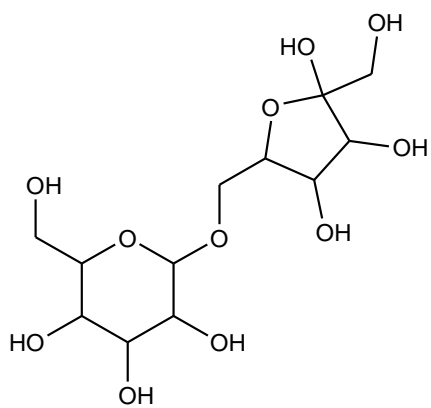
Table 3.4. Chemical profile of ethanol extract of leaves of *F. sycomorus* extracted with ethanol

Peak #	*RT	Acquired [M-H] ⁻ m/z	Formula of possible structure	Theoretical [M-H] ⁻ m/z	Calculated accurate mass (Da)	Possible structure	Mass error (ppm)	MS/MS Data (fragments)		Confirmation with a standard		Ref
										RT	[M-H] ⁻ m/z	
1	0.74	341.1093	C ₁₂ H ₂₂ O ₁₁	341.1089	342.1162	Palatinose (Disaccharide)	-1.2	250.9994	[M-H] ⁻ - C ₃ H ₆ O ₃ ⁻	0.74	341.1047	[27]
								179.0438	[M-H] ⁻ - C ₆ H ₁₀ O ₅ ⁻			
								221.0618	[M-H] ⁻ - C ₄ H ₈ O ₄ ⁻			
								161.0380	[M-H] ⁻ - C ₆ H ₁₁ O ₆ ⁻			
	0.74	191.0562	C ₇ H ₁₂ O ₆	191.0561	192.0634	Quinic acid (Organic acid)	-0.5	172.9910	[M-H] ⁻ - H ₂ O	0.74	191.0567	[28]
								127.9101	[M-H] ⁻ - CO-2H ₂ O			
								85.0265	[M-H] ⁻ - CO ₂ -H ₂ O- C ₂ H ₆ O ₂			
								59.0195	[M-H] ⁻ - C ₅ H ₈ O ₄ ⁻			
2	2.92	353.0878	C ₁₆ H ₁₈ O ₉	353.0878	354.0951	Isobiflorin (Chromone C-glucoside)	0	233.0458	[M-H] ⁻ - C ₄ H ₈ O ₄ ⁻			[29]
								205.0504	[M-H] ⁻ - C ₄ H ₈ O ₄ ⁻ - H ₂ O- CH ₃			
								191.0327	[M-H] ⁻ -C ₆ H ₁₀ O ₅ ⁻			
								161.0502	[M-H] ⁻ -C ₁₀ H ₆ O ₄ ⁻			

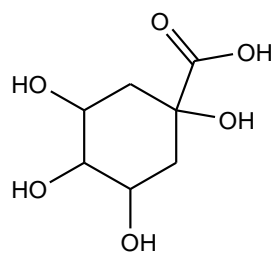
3	2.96	353.0869	C ₁₆ H ₁₈ O ₉	353.0878	354.0951	Chlorogenic acid (Caffeoylquinic acid)	2.5	191.0547	[M-H] ⁻ - C ₉ H ₆ O ₃ ⁻	2.95	353.0858	[30]
								179.0322	[M-H] ⁻ - C ₇ H ₁₁ O ₅ ⁻			
								173.0464	[M-H] ⁻ - C ₉ H ₆ O ₃ ⁻ - H ₂ O			
								161.0225	[M-H] ⁻ - C ₇ H ₁₀ O ₅ ⁻ - H ₂ O			
								135.0434	[M-H] ⁻ - C ₇ H ₁₁ O ₅ ⁻ - CO ₂			
								85.0290	[M-H] ⁻ - C ₉ H ₆ O ₃ ⁻ - CO ₂ - H ₂ O - C ₂ H ₆ O ₂			
4	3.23	353.0881	C ₁₆ H ₁₈ O ₉	353.0878	354.0951	Biflorin (Chromone C-glucoside)	-0.9	233.0457	[M-H] ⁻ - C ₄ H ₈ O ₄ ⁻			[29]
								205.0509	[M-H] ⁻ - C ₄ H ₈ O ₄ ⁻ - H ₂ O - CH ₃			
								191.0305	[M-H] ⁻ - C ₆ H ₁₀ O ₅ ⁻			
								161.0516	[M-H] ⁻ - C ₁₀ H ₆ O ₄ ⁻			
5	3.69	593.1497	C ₂₇ H ₃₀ O ₁₅	593.1512	594.1585	Vicenin-2 (apigenin C-glycoside) Unidentified through mass spectrometry data analysis	2.5	503.1246	[M-H] ⁻ - C ₃ H ₆ O ₃ ⁻			[31-33]
								473.1085	[M-H] ⁻ - C ₄ H ₈ O ₄ ⁻			
								383.0770	[M-H] ⁻ - C ₄ H ₈ O ₄ ⁻ - C ₃ H ₆ O ₃ ⁻			
								353.0650	[M-H] ⁻ - C ₄ H ₈ O ₄ ⁻ - C ₄ H ₈ O ₄ ⁻			
6	4.78	609.1465	C ₂₇ H ₃₀ O ₁₆	609.1461	610.1534	Quercetin-3-O-glucosylrhamnose (Rutin) (Flavonol glycoside)	-0.7	300.0258	[M-H] ⁻ - C ₆ H ₁₁ O ₄ ⁻ - C ₆ H ₁₀ O ₅ ⁻	4.74	609.1460	[34]
								271.0356	[M-H] ⁻ - C ₆ H ₁₁ O ₄ ⁻ - C ₆ H ₁₀ O ₅ ⁻ - CO			
								191.0224	[M-H] ⁻ - C ₆ H ₁₁ O ₄ ⁻ - C ₆ H ₁₀ O ₅ ⁻ - C ₆ H ₅ O ₂ ⁻			
								160.9951	[M-H] ⁻ - C ₁₅ H ₈ O ₇ ⁻ - C ₆ H ₁₁ O ₄ ⁻			
								151.0414	[M-H] ⁻ - C ₆ H ₁₁ O ₄ ⁻ - C ₆ H ₁₀ O ₅ ⁻ - C ₈ H ₅ O ₃ ⁻			

								146.9656	[M-H] ⁻ - C ₁₅ H ₈ O ₇ ⁻ - C ₆ H ₁₀ O ₅ ⁻			
7	4.95	477.0673	C ₂₁ H ₁₈ O ₁₃	477.0674	478.0747	Quercetin-3-glucuronide (Flavonol glycoside)	0.2	301.0364	[M-H] ⁻ - C ₆ H ₈ O ₆ ⁻			[35]
								273.0436	[M-H] ⁻ - C ₆ H ₈ O ₆ ⁻ - CO			
								255.0295	[M-H] ⁻ - CO ₂			
								178.9979	[M-H] ⁻ - C ₆ H ₈ O ₆ ⁻ - C ₇ H ₅ O ₂ ⁻			
								151.0040	[M-H] ⁻ - C ₁₄ H ₁₄ O ₉ ⁻			
8	5.00	463.0882	C ₂₁ H ₂₀ O ₁₂	463.0882	464.0955	Quercetin-3-O-glucoside (Isoquercetin) (Flavonol glycoside)	0	300.0269	[M-H] ⁻ - C ₆ H ₁₁ O ₅ ⁻	5.04	463.0875	[36]
								271.0257	[M-H] ⁻ - C ₆ H ₁₁ O ₅ ⁻ - CO			
								255.0291	[M-H] ⁻ - C ₆ H ₁₁ O ₅ ⁻ - CO ₂			
								179.0050	[M-H] ⁻ - C ₆ H ₁₁ O ₅ ⁻ - C ₇ H ₅ O ₂ ⁻			
								151.0069	[M-H] ⁻ - C ₆ H ₁₁ O ₅ ⁻ - C ₈ H ₅ O ₃ ⁻			

*Retention time (RT) is given in minutes

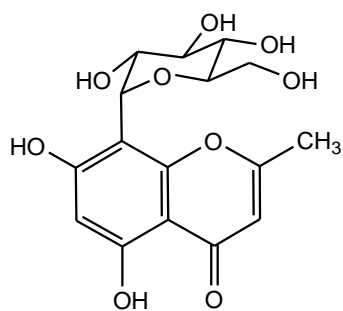


palatinose

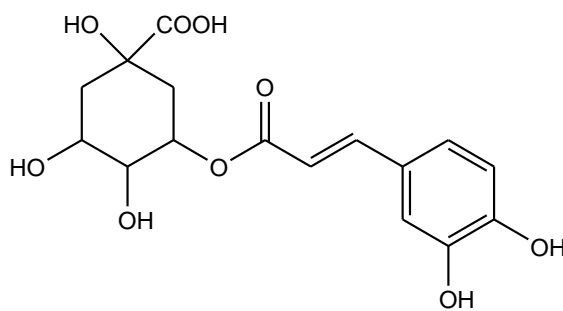


quinic acid

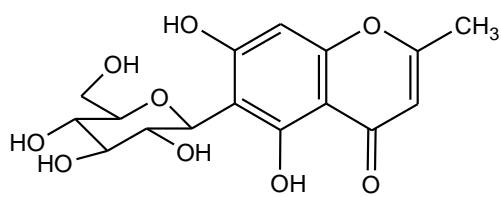
Peak 1: palatinose and quinic acid



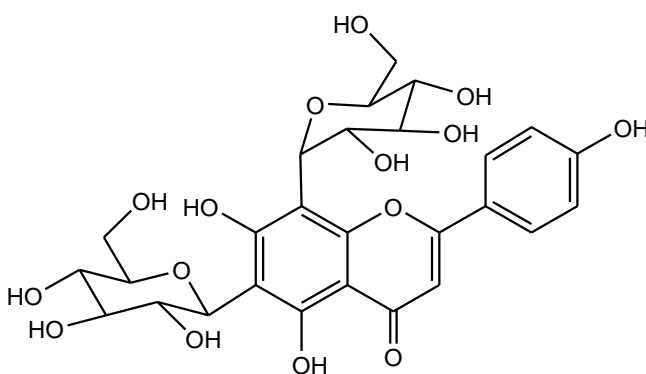
Peak 2: isobiflorin



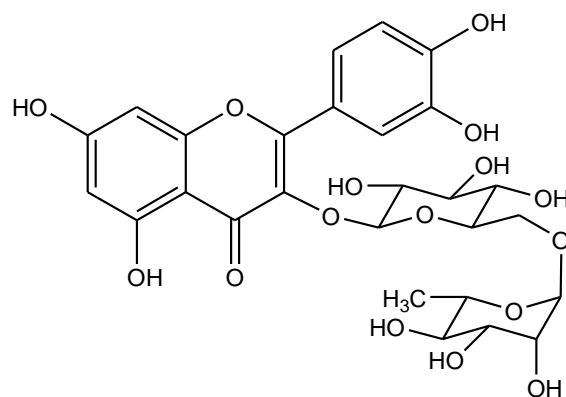
Peak 3: chlorogenic acid



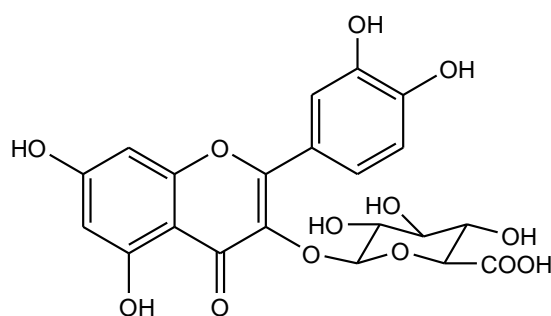
Peak 4: biflorin



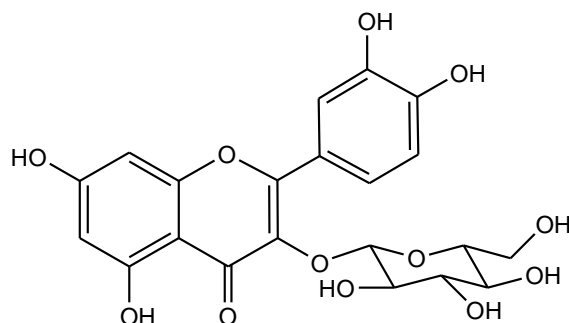
Peak 5: vicenin-2



Peak 6: quercetin 3-O-glucosylrhamnoside (rutin)



Peak 7: quercetin 3-glucuronide



Peak 8: quercetin 3-O-glucoside

Figure 3.11. Chemical structures of compounds identified from *F. sycomorus* leaves

Peak 1 was identified as a mixture of two highly polar compounds which could not be separated by UPLC. One of the compounds was identified as palatinose and its structure is shown in Figure 3.11. The negative mode ESI mass spectrum for the first compound displayed a chloride adduct ion $[M+Cl]^-$ at m/z 377.0868 (Figure 3.12). The MassLynx software algorithm

for elemental composition determination was used to establish a molecular formula of ($C_{12}H_{22}O_{11}Cl$) with a normalised iFit value of 0.023 (supplementary data 30). Its deprotonated ion $[M-H]^-$ was observed at m/z 341.1093 ($C_{12}H_{21}O_{11}$) with a normalised iFit value of 0.022 (supplementary data 31). In the second order mass spectrum (supplementary data 32), the chloride adduct was fragmented to produce $[M+Cl-36]^-$ due to loss of an HCl to form the $[M-H]^-$ ion at m/z 341.1093. Other fragments of palatinose similar to those observed by Guan and Cole [27] were observed at m/z 179.0438 $[M-H-162]^-$ from the loss the fructose unit, at m/z 161.0380 $[M-H-179]^-$ from the loss of a glucose unit, at m/z 221.0618 $[M-H-120]^-$ from an RDA fragmentation of the glucose ring of palatinose and at m/z 250.9994 $[M-H-90]^-$ resulting from cleavage of the glucose ring.

In addition, another co-eluting compound had a deprotonated $[M-H]^-$ ion at m/z 191.0562, using MassLynx software its molecular formula was determined to be ($C_7H_{11}O_6$) with a near perfect normalised iFit value of 0.190 (supplementary data 33). A comparison of the theoretical and the experimental accurate masses confirmed the formulas. The compound was tentatively identified as quinic acid, its structure is shown in Figure 3.11. Fragments from quinic acid were observed at m/z 172.9863 $[M-H-18]^-$ from the loss of a water molecule, at m/z 127.0451 $[M-H-28-36]^-$ from the subsequent loss of a carbon monoxide molecule and two water molecules, at m/z 85.0259 $[M-H-44-18-62]^-$ from the consecutive loss of a carbon dioxide molecule, a water molecule and RDA fragmentation of the ring, and at m/z 59.0177 $[M-H-132]^-$ from the RDA fragmentation of the ring. Using a quinic acid pure standard with an m/z of 191.0567 and retention time of 0.74 minutes and a palatinose pure standard at m/z 377.0847 retention time 0.74 minutes corresponding retention time 0.74 minutes of peak 1 at m/z 377.0851 (Figure 3.13) the peak was identified as a result of co-elution of palatinose and quinic acid. Further, based on accurate mass comparison, the peak was confirmed to be a mixture of quinic acid and palatinose.

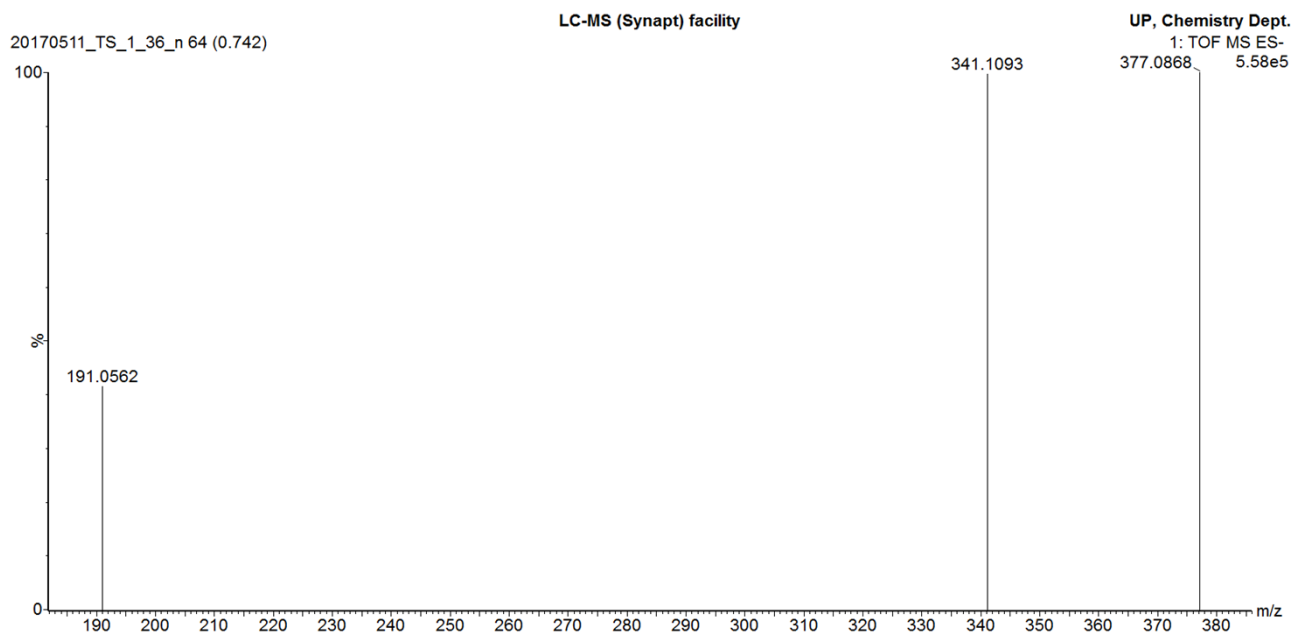


Figure 3.12. Negative mode ESI mass spectrum of peak 1 showing a mixture of palatinose and quinic acid. The chloride adduct of palatinose is shown at m/z 377.0868 and its $[M-H]^-$ ion at m/z 341.1093 and the $[M-H]^-$ ion of quinic acid at m/z 191.0562.

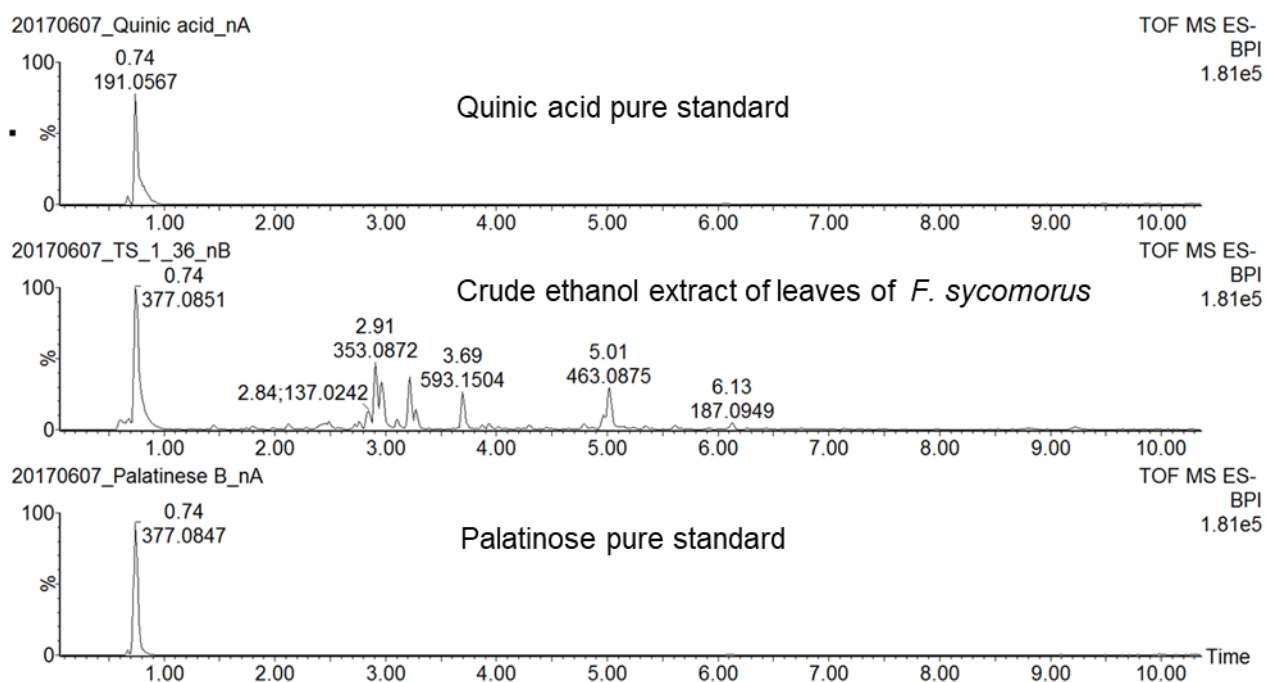


Figure 3.13. ESI negative mode BPI chromatogram of the ethanolic extract of leaves of *F. sycomorus* overlaid with quinic acid and palatinose pure standards. The pure standards and the extract showed peaks at retention time 0.74 minutes, quinic acid peak was at m/z 191.0567 and the chloride adduct ion of palatinose at m/z 377.0847.

Peaks 2 and 4 were identified as isobiflorin and biflorin based on mass spectral analysis and NMR after their subsequent purification, their structures are shown in Figure 3.11. The compounds are regio-isomers as they displayed similar $[M-H]^-$ ions in the negative mode ESI-MS spectrum at m/z 353.0876 (supplementary data 34) for isobiflorin and m/z 353.0881 (supplementary data 35) for biflorin. Using MassLynx software, the two peaks gave the same molecular formula ($C_{16}H_{17}O_9$) with a normalised iFit value of 0.072 for isobiflorin (supplementary data 36) and 0.002 for biflorin (supplementary data 37). Moreover, they exhibited similar MS/MS fragmentation patterns (supplementary data 38).

In the MS/MS spectrum, the base peak ion for peak 2 was at m/z 205.0504 and secondary fragments at m/z 233.0458, m/z 191.0327 and m/z 161.0502 (supplementary data 34). In comparison, the MS/MS spectrum of peak 4 had the base peak ion at m/z 205.0509 and secondary fragments at m/z 233.0457, m/z 191.0305 and m/z 161.0516 (supplementary data 35). The base peak ion at m/z 205.0509 $[M-H-120-15-18]^-$ is due to loss of an RDA fragment from the glycosyl unit followed by loss of a methyl and a water molecule. The secondary fragment observed at m/z 233.0458 $[M-H-120]$ was due to loss of an RDA fragment from the glycosyl unit. Minor fragments were observed at m/z 191 $[M-H-162]$ due to loss of the glucosyl unit and at m/z 161 $[M-H-190]^-$ due to loss of the chromone moiety from the parent ion. The MS/MS pattern of peak 2 and peak 4 compared favourably with that provided by Yang et al. [29] for biflorin in which they observed two major fragments at m/z 232.8 and 205.0 and some minor fragments.

In order to unambiguously identify peak 2 and peak 4, the compounds were isolated and their structures elucidated using data from NMR analysis. Further, the purified biflorin and isobiflorin as well as the crude ethanol extract of leaves of *F. sycomorus* were reinjected onto the UPLC-Q-TOF-MS. Based on comparison of MS/MS fragmentation patterns

(supplementary data 39) and retention times of peak 2 in the extract (2.92 minutes at m/z 353.0878) with that of purified isobiflorin (2.94 minutes at m/z 353.0880), peak 2 was confirmed to be isobiflorin (Figure 3.14). Similarly, comparison of MS/MS fragmentation patterns (supplementary data 40) and retention times of peak 4 in the extract (3.23 minutes at m/z 353.0881) with that of purified biflorin (3.21 minutes at m/z 353.0864), peak 4 was confirmed to be biflorin (Figure 3.15). The isolation and structure elucidation of compounds is described in section 3.7.7 and the NMR spectra are given in the supplementary information. To the best of our knowledge this is the first identification of isobiflorin and biflorin in *F. sycomorus*.

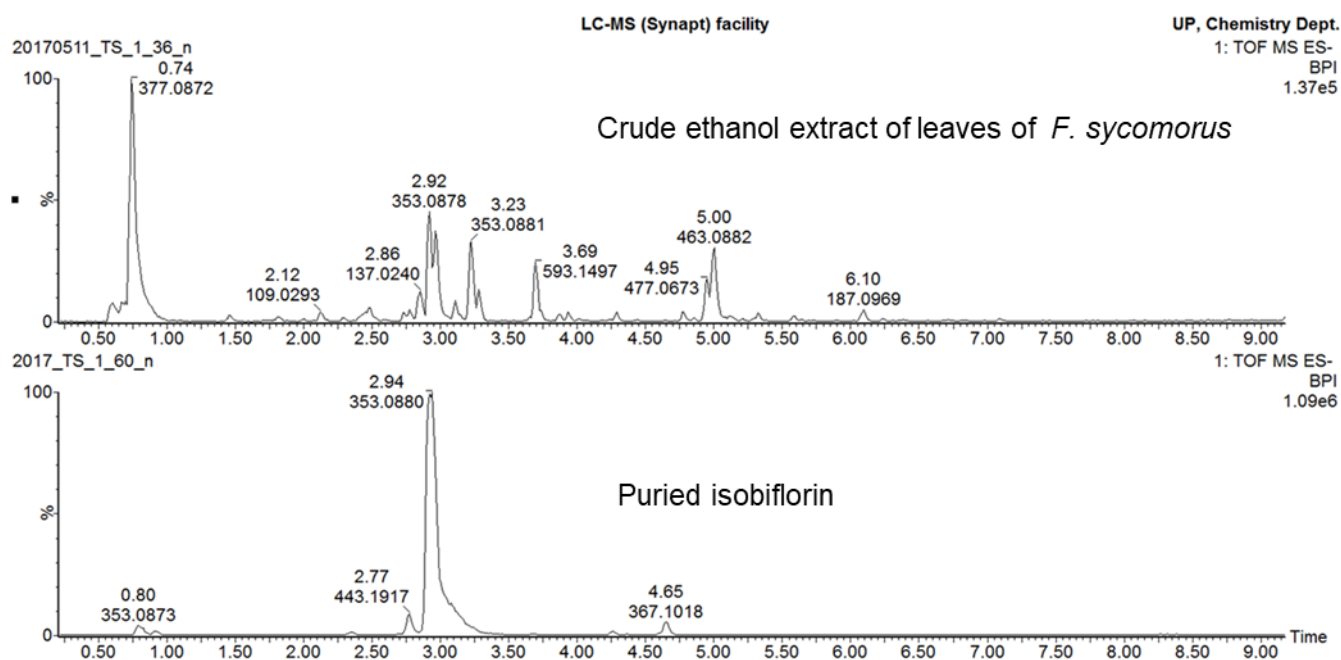


Figure 3.14. ESI negative mode BPI chromatogram of leaves of *F. sycomorus* extracted with ethanol overlaid with purified isobiflorin. The purified isobiflorin had a retention time of 2.94 minutes and an m/z of 353.0880 which corresponded to peak 2 at retention time 2.92 minutes and m/z 353.0878 in the extract.

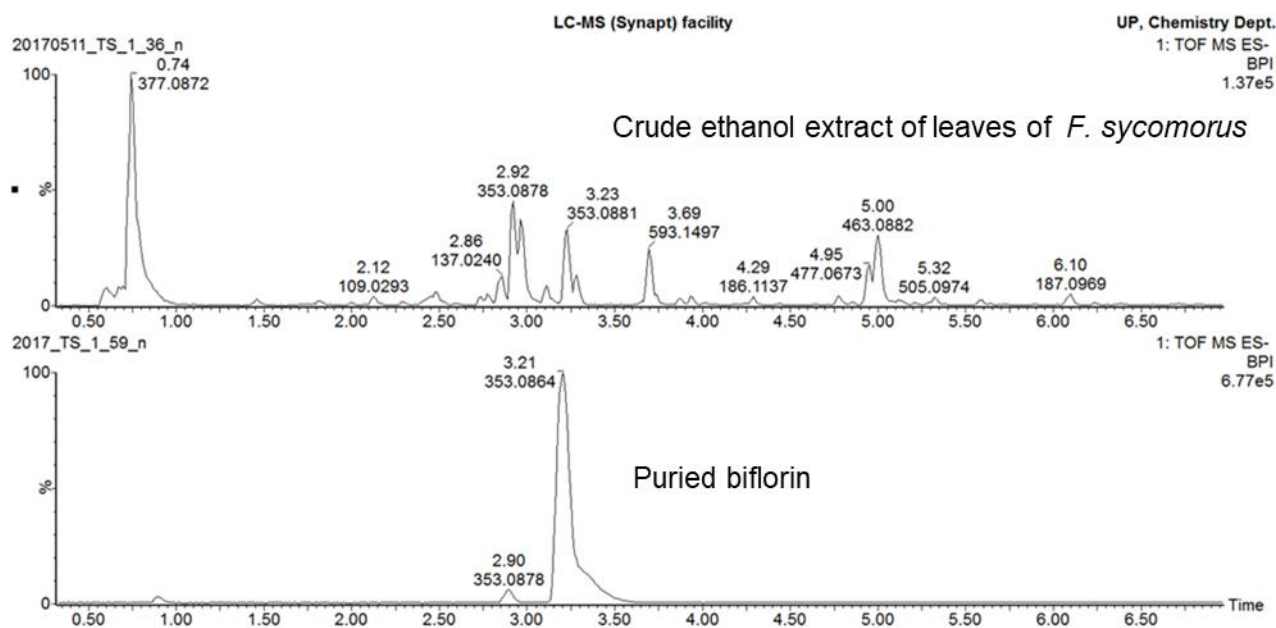


Figure 3.15. ESI negative mode BPI chromatogram of leaves of *F. sycomorus* extracted with ethanol overlaid with purified biflorin. The purified biflorin had a retention time of 3.21 minutes and an m/z of 353.0864 which corresponded to peak 5 at retention time 3.23 minutes and m/z 353.0881 in the extract.

Peak 3 was identified as chlorogenic acid based on the analysis of the mass spectra and a pure standard, its structure is shown in Figure 3.11. The first-order mass spectrum of peak 3 displayed the parent ion $[M-H]^-$ at m/z 353.0869 (supplementary data 41). Elemental composition analysis using MassLynx provided the molecular formula ($C_{16}H_{17}O_9$) with a normalised iFit value of 0.246 (supplementary data 42). In the MS/MS spectrum (supplementary data 41), the compound was fragmented to produce the base peak ion at m/z 191.0547 $[M-H-162]^-$ through the loss of a caffeic acid fragment. Secondary fragments were observed at m/z 179.0322 $[M-H-174]^-$ through the loss of a quinic acid residue, at m/z 135.0434 $[M-H-174-44]^-$ from the subsequent loss of a quinic acid residue and carbon dioxide and at m/z 173.0464 $[M-H-162-18]^-$ from the consecutive loss of a caffeic acid residue and a water molecule. According to He et al. [34], the fragmentation pattern is diagnostic of caffeoyl quinic acids. In addition to these fragments, this study observed fragments at m/z 161.0225 $[M-H-174-18]^-$ due to consecutive loss of a quinic acid fragment and a water molecule and at m/z 85.0290 $[M-H-162-44-18-62]^-$ due to successive losses of a caffeic acid fragment, carbon

dioxide, water and a RDA fragment. In another study, Fu et al. [30] also observed the fragments at m/z 85.0302 and at m/z 161.0239 upon analysis of the MS/MS spectra of a chlorogenic acid. The presence of chlorogenic acid was confirmed using a pure standard (Figure 3.16). The pure standard had a retention time of 2.95 minutes and an m/z of 191.0559 which corresponded to the peak at retention time 2.96 minutes and m/z 191.0555 in the extract. Based on the fragmentation patterns of the standard and that of peak 3 which were identical and accurate mass measurement, peak 3 was confirmed to be chlorogenic acid. The fragmentation pattern of chlorogenic acid pure standard and that of peak 3 in *F. sycomorus* ethanol extract is given in the supplementary data 43. To the best of our knowledge this is the first identification of chlorogenic acid in *F. sycomorus*.

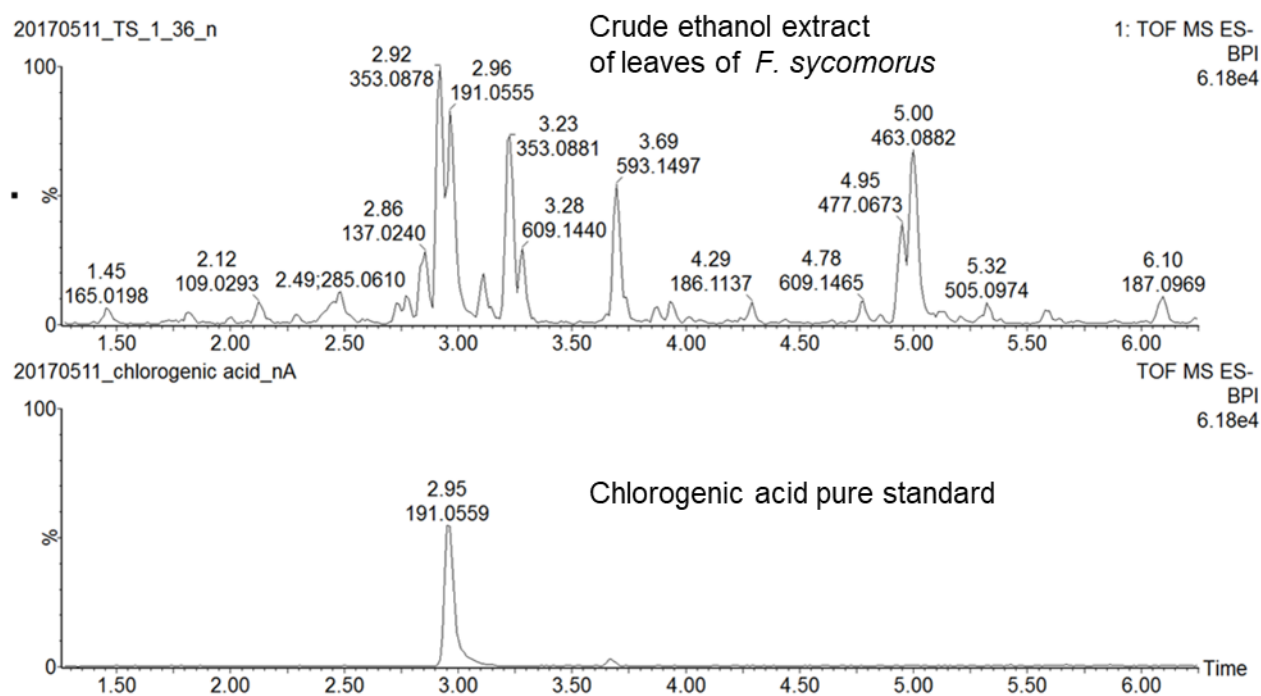


Figure 3.16. ESI negative mode BPI chromatogram of leaves of *F. sycomorus* extracted with ethanol overlaid with chlorogenic acid pure standard. The pure standard had a retention time of 2.95 minutes and an m/z of 191.0559 which corresponded to the peak at retention time 2.96 minutes and m/z 191.0555 in the extract.

Peak 5 could not be identified tentatively through comparison of MS/MS fragmentation pattern of the peak with that of known compounds in mass bank libraries as the MS/MS data of this compound was not present in the mass bank libraries searched. As a result, identification of the compound corresponding to this peak was carried out through isolation, purification and structure elucidation through analysis of NMR data.

The structure shown Figure 3.11 was identified to be vicenin-2 and elucidation of its structure is described in section 3.7.5. The first-order mass spectrum of peak 5 showed an [M-H]⁻ ion at *m/z* 593.1498 (supplementary data 44). MassLynx was used to determine its elemental composition to be C₂₇H₂₉O₁₅ with a normalised iFit of 0.101 (supplementary data 45). The MS/MS fragmentation pattern of vicenin-2 (supplementary data 44) showed fragments which were mainly a result of fragmentation of the C-glycosidic units. A base peak ion was observed at *m/z* 353.0650 [M-H-120-120]⁻ due to cross-ring cleavages of the sugar units resulting in losses of two sugar fragments thus confirming the presence of two hexose units. Secondary fragments were observed at *m/z* 503.1246 [M-H-90]⁻ due to cross-ring cleavage of one of the hexose units leading to loss of a sugar fragment, at *m/z* 473.1085 [M-H-120]⁻ due to a cross ring cleavage of one sugar unit leading to loss of a sugar fragment, *m/z* 383.0770 [M-H-120-90]⁻ due to subsequent cross ring cleavage of the sugar units leading to loss of two fragments. This fragmentation pattern of vicenin-2 was also observed in the studies done by Parejo et al.[31], Silva et al [32], Goureva et al. [33].

To the best of our knowledge this is the first report of vicenin-2 in *F. sycomorus* plant. Purified compound vicenin-2 was reinjected onto the UPLC-Q-TOF-MS with the crude ethanol extract of leaves of *F. sycomorus*. A comparison of the MS/MS fragmentation pattern of the purified vicenin-2 and the MS/MS fragmentation pattern of peak 5 in the crude extract showed that the two peaks were similar (supplementary data 46). Further, the purified peak 5 had a retention

time of 3.59 minutes and an m/z of 593.1498 which corresponded to peak 5 at m/z 593.1508 and retention time 3.60 minutes in the crude extract (Figure 3.17).

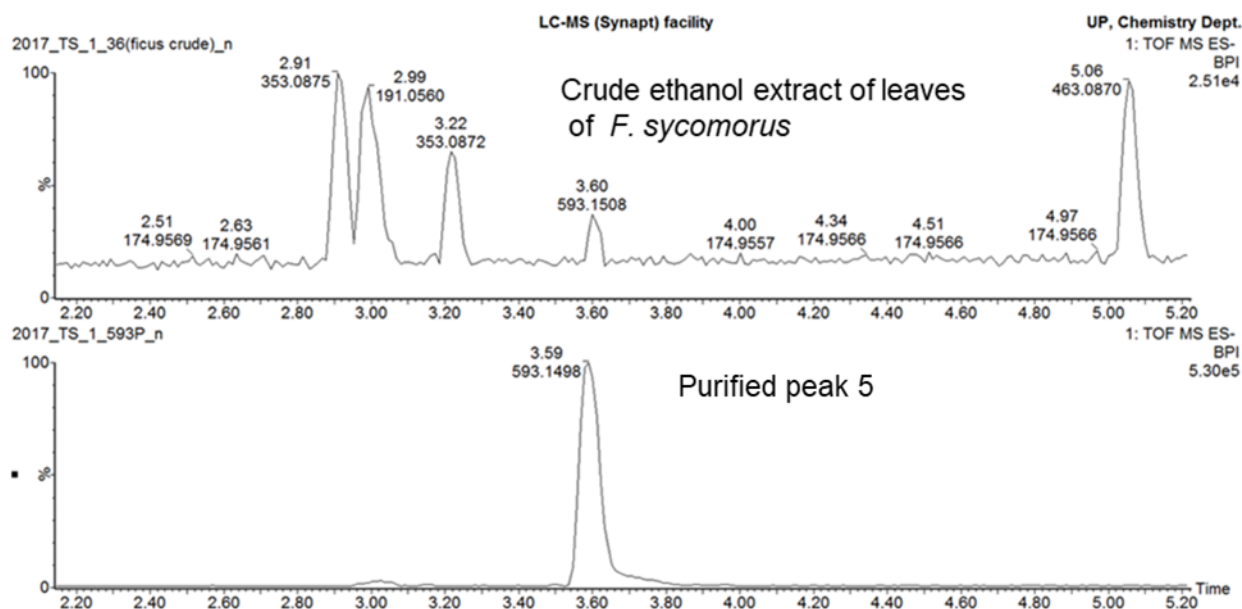


Figure 3.17. ESI negative mode BPI chromatogram of leaves of *F. sycomorus* extracted with ethanol overlaid with purified peak 6. The purified peak had a retention time of 3.59 minutes and an m/z of 593.1498 which corresponded to peak 4 at m/z 593.1508 and retention time 3.60 minutes in the extract.

Peak 6 was tentatively identified as rutin based on analysis of the mass spectra and its structure is shown in Figure 3.11. The first-order mass spectrum of peak 6 (supplementary data 47), showed an $[M-H]^-$ ion at 609.1436 ($C_{27}H_{29}O_{16}$) with a normalised iFit value of 0.022 (supplementary data 48). In the MS/MS spectrum (supplementary data 47), a base peak ion was observed at m/z 300.0258 $[M-H-147-162]^-$ through the subsequent loss of the rhamnose and the glucosyl units from the parent ion. According to Madala et al. [36], He et al. [34] and Duenaz et al. [35] the base peak ion at m/z 300/301 is characteristic of quercetin derivatives. In this study, secondary fragments of rutin were observed at m/z 191.0224 $[M-H-147-162-109]^-$ from the subsequent loss of the rhamnose moiety, glucosyl residue and a quercetin fragment. The fragment m/z 160.9951 $[M-H-147-300]^-$ is the glucosyl residue produced from the loss of the rhamnose moiety and the quercetin unit from the parent ion. The rhamnose

fragment was observed at m/z 146.9656 [M-H-300-162]⁻ from the consecutive loss of the quercetin unit and the glucosyl residue. Another fragment was observed at m/z 151.0414 [M-H-147-162-149]⁻ from the subsequent loss of the rhamnose moiety, glucosyl residue and an RDA fragment from quercetin. The fragment at m/z 271.0356 is result of loss of carbon monoxide from the quercetin moiety. Based on the fragmentation pattern and accurate mass measurement, peak 6 was tentatively identified as rutin.

He et al. [34] tentatively identified rutin from Gardenia fruit extracts based on its fragmentation pattern. In the ESI MS spectrum they observed the parent ion at m/z 609 and a fragment at m/z 463 [M-H-147]⁻ which was due to the loss of the rhamnose moiety from the parent ion, and an MS/MS fragment at m/z 301 which matched with quercetin derivatives. Figure 3.18 shows the unambiguous identification of Peak 6 in the ethanol extract of leaves of *F. sycomorus* using a pure standard of rutin. A comparison of the MS/MS fragmentation pattern of peak 6 (rutin) in the crude extract with that of the pure standard of rutin confirmed the identity of peak 6 as rutin (supplementary data 49). Further, the retention time of the pure standard of rutin of 4.74 minutes (m/z 609.1460) with that of peak 6 in the crude extract retention time 4.78 minutes at m/z 609.1465 confirmed the identity of peak 6 as rutin. El-Sayed et al. [17] previously isolated rutin from the leaves of *F. sycomorus* and identified the compound using NMR.

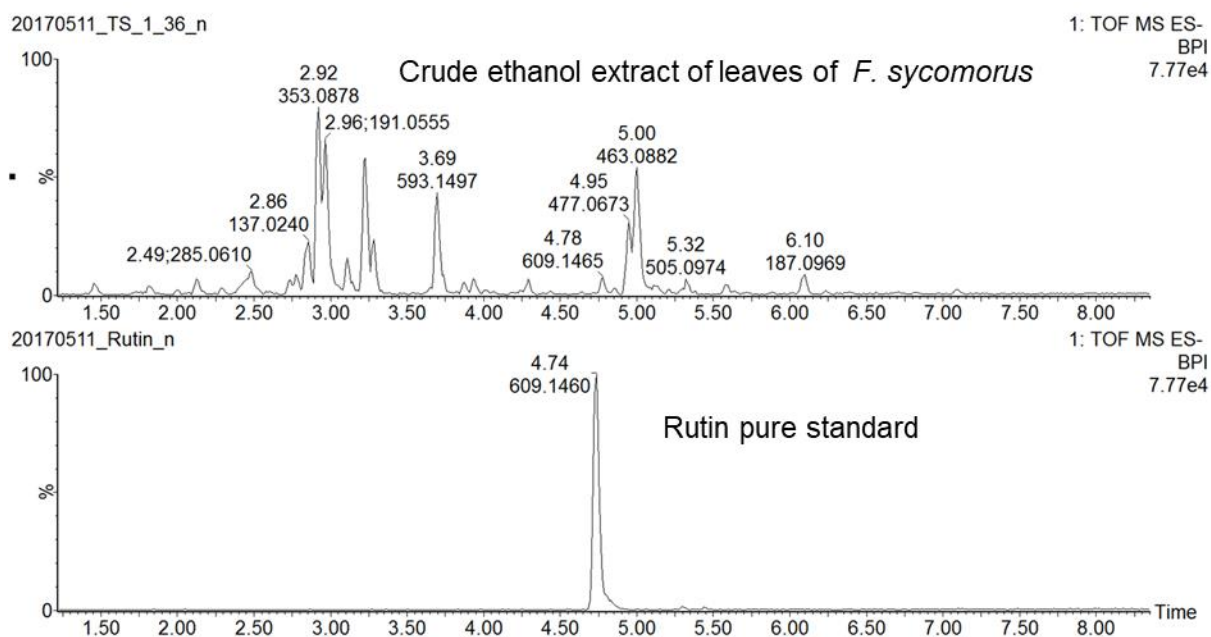


Figure 3.18. ESI negative mode BPI chromatogram of *F. sycamoros* leaf ethanol extract overlaid with rutin pure standard. The pure standard peak was at retention time 4.74 minutes and m/z 609.1460 which corresponded to the peak at retention time 4.78 minutes and m/z 609.1465 in the extract.

Peak 7 was tentatively identified as quercetin 3-glucuronide based on the analysis of the mass spectra and its structure is shown in Figure 3.11. The ESI-MS spectrum of peak 7 (supplementary data 50) had an $[M-H]^-$ ion at m/z 477.0673 ($C_{21}H_{17}O_{13}$) with a normalised iFit value of 0.009 (supplementary data 51). The MS/MS chromatogram (supplementary data 50) had the base peak ion at m/z 301.0364 $[M-H-176]^-$ due to loss of a glucuronyl moiety. As reported by Madala et al. [36], He et al. [34] and Duenaz et al. [35] the fragment at m/z 300/301 is characteristic of the presence of quercetin. In this study, secondary fragments observed were mainly due to fragmentation of the quercetin moiety. The fragment at m/z 151.0040 $[M-H-176-150]^-$ was a result of consecutive loss of the glucuronyl moiety and a RDA fragmentation of the quercetin C ring leading to loss of the aromatic B ring and a fragment of the C ring. The fragment observed at m/z 255.0295 $[M-H-176-44]^-$ was due to subsequent loss of the glucuronyl moiety and a carbon dioxide molecule and another fragment at m/z 273.0436 $[M-H-176-28]^-$ was due to consecutive loss of the glucuronyl moiety and a carbon monoxide

molecule. In addition, a fragment was observed at m/z 178.9979. Duenas et al. [35], also observed this fragment at m/z 179 and explained that it was due to retrocyclisation after fission on bonds 1 and 2 of the C ring of quercetin (Figure 3.19). The MS/MS fragmentation pattern observed in this study (supplementary data 50) was similar to the pattern observed by Duenas et al. [35] for quercetin 3-glucuronide isolated from green beans. To the best of our knowledge this is the first identification of quercetin 3-glucuronide in *F. sycomorus*.

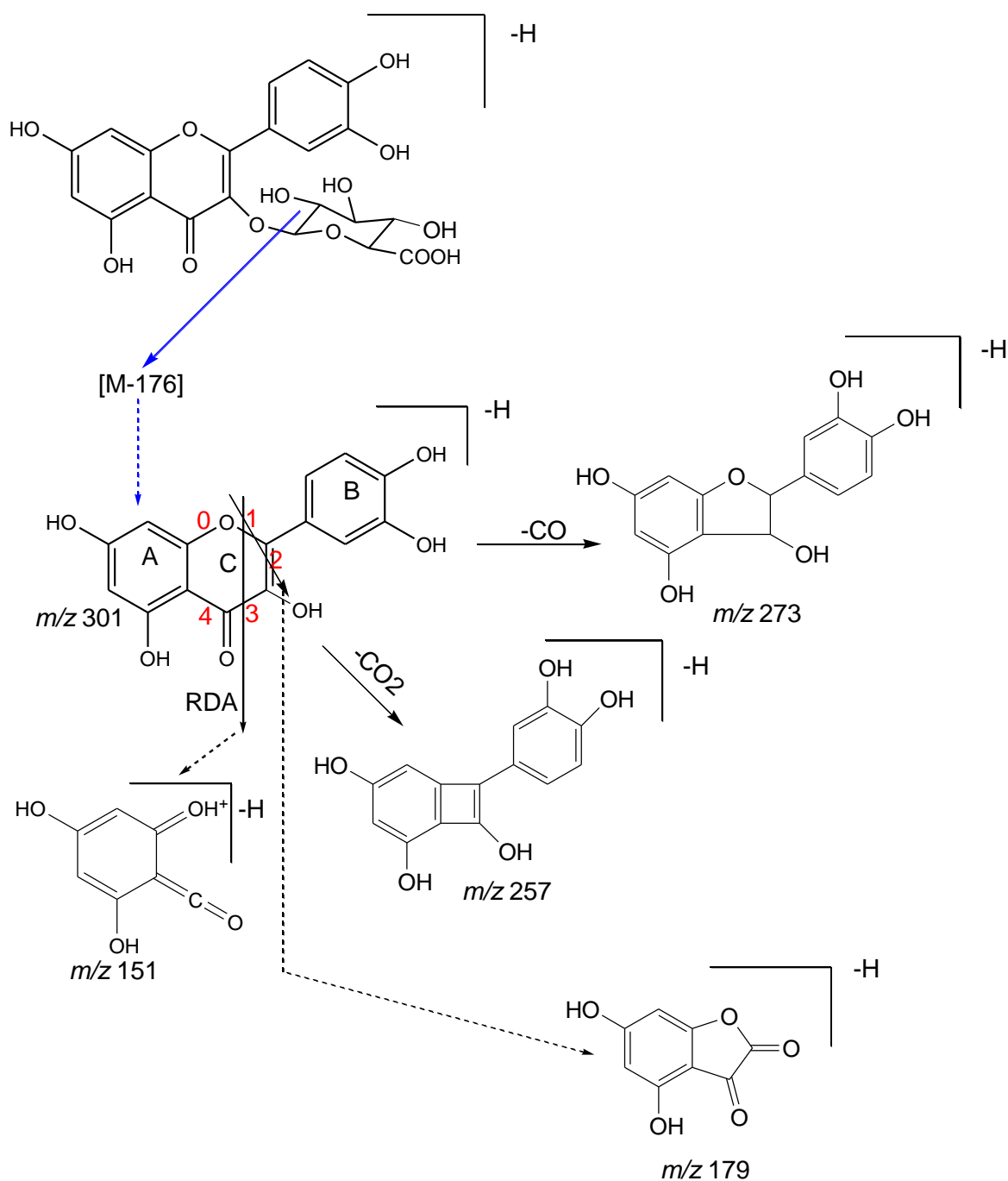


Figure 3.19. Fragmentation of quercetin-3-glucuronide showing formation of fragments with m/z 301 from loss of the glycoronyl moiety, m/z 151 from RDA fragmentation, m/z 179 due to retrocyclisation after fission on bonds 1 and 2 of the C ring of quercetin m/z 179, m/z 273 from loss of CO from the quercetin moiety, m/z 255 from loss of CO_2 from the quercetin moiety. Adapted from Duenas et al.[35].

Peak 8 was identified as isoquercetin based on comparison of MS/MS data of the peak and that in massbank libraries and its structure is given in Figure 3.11. The ESI-MS spectrum of

peak 8 (supplementary data 52) showed an $[M-H]^-$ ion at m/z 463.0876 ($C_{21}H_{19}O_{12}$) with a normalised iFit value of 0.008 (supplementary data 53). Product ions in the second-order mass spectrum (supplementary data 52) exhibited the base peak ion at m/z 300.0269 $[M-H-163]^-$ through the loss of a glucosyl unit. The fragment ion as reported by He et al [34], Madala et al [36] and Duenaz et al.[35] at m/z 300/301 suggests the presence of quercetin [34, 36] indicating that peak 8 is a quercetin aglycone. A fragment was observed at m/z 151.0069 $[M-H-163-149]^-$ from the successive loss of a glycosyl unit and an RDA fragment. The fragment at m/z 179.0050 was due to retrocyclisation after fission on bonds 1 and 2 of the C ring of quercetin (Figure 3.19) as explained by Duenas et al. [35]. Other fragments were observed at m/z 271.0257 and m/z 255.0291 were due to loss of carbon monoxide and carbon dioxide respectively from quercetin. This fragmentation pattern of was similar to the pattern reported by Madhala et al.[36] for quercetin 3-glucoside. In their study, using three positional isomers of quercetin glycoside they could positively determine the position of the sugar moiety based on the fragmentation pattern. The presence of isoquercetin was confirmed using a pure standard of isoquercetin (retention time 5.04 minutes and m/z 463.0875) based on comparison of the retention time of peak 9 (5.00 minutes at m/z 463.0882) and the MS/MS fragmentation pattern of the pure standard and that of peak 9 (supplementary data 54). El-Sayed et al. [17] previously isolated isoquercetin from *F. sycomorus* leaves and identified the compound using NMR.

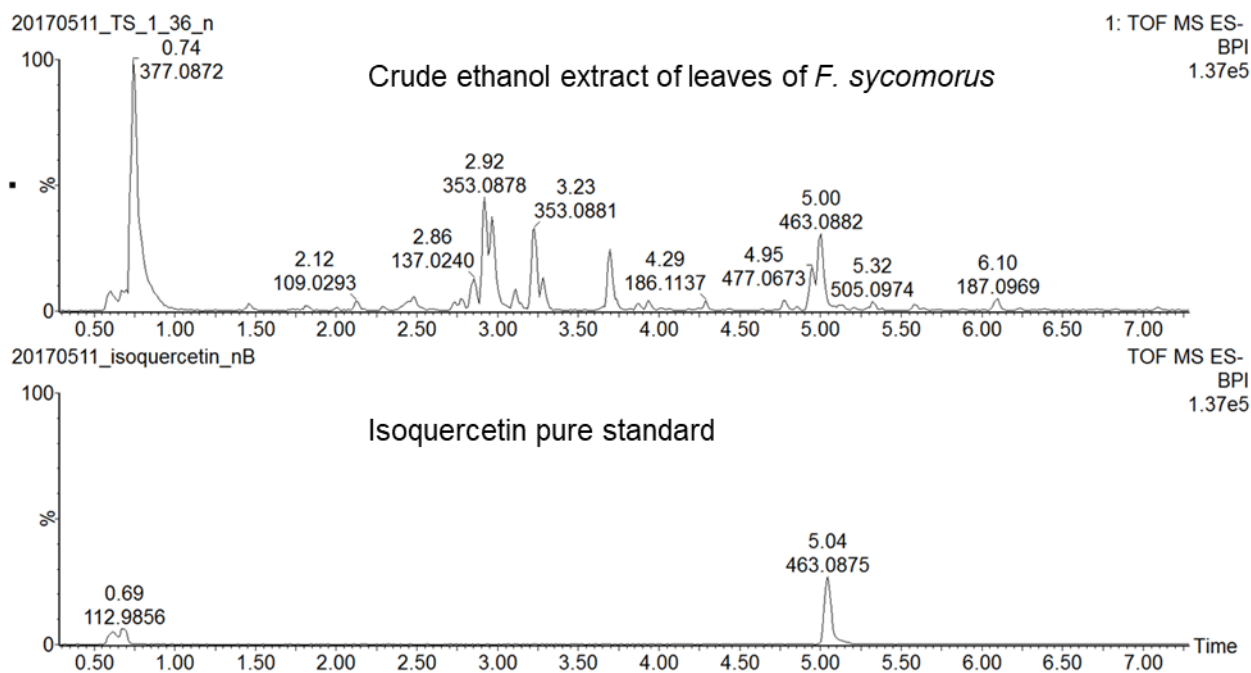


Figure 3.20. ESI negative mode BPI chromatogram of leaves of *F. sycomorus* extracted with ethanol overlaid with isoquercetin pure standard. The pure standard peak was at retention time 5.04 minutes and m/z 463.0875 which corresponded to the peak at retention time m/z 5.00 and m/z 463.0882 in the extract.

3.7.6 Fractionation of ethanol extract of leaves of *F. sycomorus*

In order to identify major peaks which could not be identified through mass spectral analysis and comparison of fragmentation patterns in Massbank libraries, the ethanol extract of leaves of *F. sycomorus* was subsequently fractionated using column chromatography and mass directed fractionation by semi preparatory HPLC-MS as shown in Figure 3.5. Three compounds; compound 1 with the $[M-H]^-$ ion at m/z 353.0878, compound 2 having the $[M-H]^-$ ion at m/z 353.0881, compound 3 with the $[M-H]^-$ ion at m/z 593.1497.

3.7.7 Structure elucidation using NMR

Compound 1 was obtained as a yellowish solid weighing 15 mg. The ESI negative mode mass spectrum gave an $[M-H]^-$ ion at m/z 353.0881 (supplementary data 35) and through MassLynx the molecular formula was determined to be $C_{16}H_{18}O_9$ with an iFit value of 0.002 (supplementary data 37). The number of protons and carbon atoms were confirmed using 1H

and ^{13}C NMR respectively (supplementary data 56 and 57). The compound was determined to be a chromone biflorin (5,7-dihydroxy-2-methylchromone-6-C- β -D-glucopyranoside), its structure is shown in Figure 3.21). The ^1H NMR spectrum (MeOD- d_4 , 600 MHz) of this compound showed an aromatic proton at δ 6.37 (1H, s, H-8) and a double bond proton at δ 6.07 (1H, s, H-3). The spectrum also showed signals at δ 4.88 (1H, *d*, H-1'), δ 4.15 (1H, *ddd*, H-2'), δ 3.86 (1H, *dd*, H-6'), δ 3.73 (1H, *dd*, H-6'), δ 3.47 (1H, *m*, H-5'), δ 3.46 (1H, *m*, H-4'), δ 3.40 (1H, *m*, H-3'), and which are indicative of oxygen bearing protons. In addition, a methyl proton signal was observed at δ 2.36 (3H, s, Me-2). The anomeric proton doublet at δ 4.88 was partially obscured by a signal for water present in the MeOD- d_4 as a result the configuration for the anomeric proton could not be determined. In order to remove this overlap, the ^1H NMR of compound 1 was rerun in ($\text{CD}_3\text{CN}-d_3$, 500 MHz) after removal of the MeOD- d_4 . Subsequently, the anomeric proton was clearly visible at δ 5.01 (1H, *d*, 9.8Hz). The large coupling constant of 9.8Hz confirmed the beta coupling of the chromone to the aglycone [37, 38].

The ^{13}C had a total of sixteen carbon atoms with one conjugated carbonyl signal at δ 184.27 (C-4), one oxygen bearing olefinic carbon signal at δ 169.40 (C-2) and signals of three oxygen bearing aromatic carbons at δ 162.19 (C-5), δ 165.06 (C-7) and δ 159.33 (C-8a). ^{13}C and DEPT-135 (supplementary data 58) revealed a total of seven quaternary resonances at δ 184.27 (C-4), δ 169.40 (C-2), δ 165.06 (C-7), δ 162.19 (C-5), δ 159.33 (C-8a), δ 109.23 (C-6) and δ 105.03 (C-4a); seven CH signals at δ 109.11 (C-3), δ 95.25 (C-8), δ 82.71 (C-3'), δ 80.25 (C-5'), δ 75.35 (C-1') δ 72.65 (C-2'), δ 71.88 (C-4'); a CH_2 signal at δ 62.96 (C-6') and a methyl signal at δ 19.66. The HSQC and COSY correlations (supplementary data 59 and 60) led to the assignments of the proton and carbon signals as shown in Table 3.5 while the ^1H and ^{13}C NMR data compares favourably with that published by Zhang and Chen [37] as well as the ^1H NMR published by Oya et al. [38] for biflorin. There were small differences in the chemical shifts (approximately 0.2 ppm) observed between our ^1H NMR and the ^1H NMR

obtained in the study of Oya et al. [38] who also analysed biflorin in MeOD-*d*4, (400 MHz). Larger differences in chemical shifts were observed between biflorin analysed in our study and biflorin analysed by Zhang and Chen [37] who used DMSO-*d*6 for NMR analysis.

Table 3.5. Comparison of ¹H and ¹³C NMR data of biflorin in MeOD-*d*4 and the published ¹H and ¹³C data of biflorin in DMSO-*d*6 and ¹H data of biflorin in MeOD-*d*4.

Isolated biflorin			¹³ C and ¹ H Literature data in DMSO- <i>d</i> 6 Zhang and Chen. [37]		¹ H Literature data in CD ₃ OD (Oya et al.[38])
Position	δC (ppm)	δH(ppm), J in Hz	δC (ppm)	δH(ppm), J in Hz	δH(ppm), J in Hz
2	169.40	-	167.01	-	-
3	109.11	6.07 (1H, s)	107.76	6.13 (s)	6.05 (1H, s)
4	184.27	-	181.76	-	-
4a	105.03	-	103.06	-	-
5	162.19	-	160.48	-	-
6	109.23	-	108.56	-	-
7	165.06	-	162.96	-	-
8	95.25	6.37 (1H, s)	93.36	6.35 (s)	6.39 (1H, s)
8a	159.33	-	156.57	-	-
1'	75.35	4.88 (1H, <i>d</i> , 9.8 Hz)	72.95	4.56 (<i>d</i> , 9.8 Hz)	4.81 (1H, <i>d</i> , 9.9 Hz)
2'	72.65	4.15 (1H, <i>ddd</i> , 9.8 Hz)	70.41	3.99 (<i>t</i> , 9.8 Hz)	4.15 (1H, <i>m</i>)
3'	82.71	3.41 (1H, <i>m</i>)	78.75	3.17 (<i>t</i> , 8.7Hz)	3.48 (1H, <i>m</i>)
4'	71.88	3.46 (1H, <i>m</i>)	70.25	3.12 (<i>br s</i>)	3.45 (1H, <i>m</i>)
5'	80.25	3.47(1H, <i>m</i>)	81.18	3.12 (<i>br s</i>)	3.43 (1H, <i>m</i>)
6'	62.96	3.73 (1H, <i>dd</i> , 12.1 Hz, 5.3 Hz) 3.86 (1H, <i>dd</i> , 12.1 Hz, 2.3 Hz)	61.28	3.67(<i>dd</i> ,11.5Hz,5.0 Hz) 3.41(<i>br d</i> ,11.5 Hz)	3.71 (1H, <i>dd</i> , 12.3Hz, 5.0 Hz) 3.80 (1H, <i>dd</i> ,12.3Hz)
Me-2	20.36	2.36 (3H, <i>s</i> , Me-2)	19.66	2.34 (<i>s</i> , Me-2)	2.31 (3H, <i>s</i> , Me-2)
OH				13.37(<i>s</i> , 5-OH)	

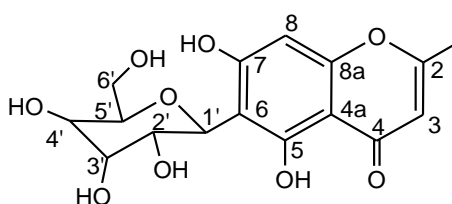


Figure 3.21. Structure of compound 1 (biflorin)

HMBC (supplementary data 61) was used to confirm correlations between carbon and protons which are separated by two and three bonds as shown in Figure 3.22 for biflorin (compound 1). The proton at δ 6.37 (C-8) showed strong HMBC correlations with C-7 (δ 165.06), C-8a (δ 159.33), C-6 (δ109.23) and C-4a (δ 105.03) confirming the position of the proton to be at C-8. The proton at δ 6.07 was confirmed to be at position C-3 due to its HMBC correlations with C-

2 (δ 169.40), C-4 (δ 184.27), C-4a (δ 105.03) and Me-2 (δ 20.36). Methyl protons at δ 2.36 (Me-2) showed strong HMBC correlations with C-3 (δ 109.1) and C-2 (δ 20.36) thus confirming its position to be C-2 (δ 20.36). The anomeric proton H-1' (δ 4.88) showed HMBC correlations with C-6 (δ 109.23), C-5 (δ 162.19) and C-7 (δ 165.06). These correlations confirm the attachment of the glucosyl residue at position C-6 position.

COSY correlations and ^1H - ^1H coupling were used to determine correlations between neighbouring protons which couple to each other. The anomeric proton H-1' (δ 4.88, 9.8 Hz) had a large coupling constant indicating beta coupling to the aromatic ring thus verifying the β orientation of glycoside which was reported by Zhang and Chen [37] and Ghosal et al. [39]. The large coupling between the anomeric proton H-1' (δ 4.88, 9.8 Hz) and proton H-2' (δ 4.15, 9.8 Hz), confirmed the protons are transdiaxial. A correlation was observed between proton H-2' (δ 4.15, 9.8 Hz) and proton H-3' (δ 3.4) (a multiplet). COSY correlations were also observed between proton H-5' (δ 3.47) with the two methylene protons H-6' (δ 3.73 and δ 3.86). These methylene protons also coupled which each other, hence the two sets of doublets of doublets at (δ 3.7, 12.0 Hz, 5.3Hz) and 3.9 (1H, 12.1 Hz, 2.3 Hz, H-6').

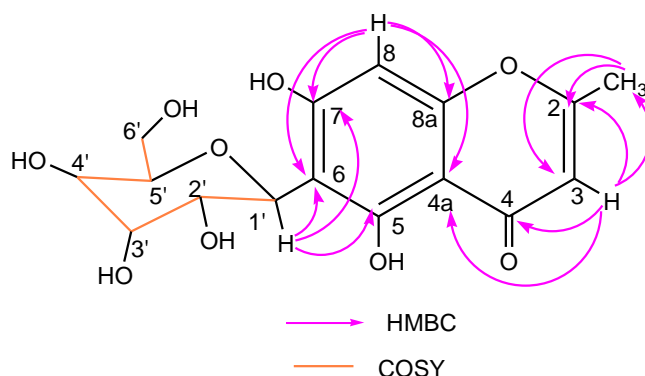


Figure 3.22. Key HMBC and COSY correlations of compound 1 (biflorin)

Biflorin was originally isolated from the roots of *Pancratium biflorum*, its structure was confirmed as a new polyoxygenated chromone C-glucoside [39]. As in our study, biflorin has also been isolated in several other studies from plants where it was found to occur together

with its regio-isomer isobiflorin [37, 38, 40]. To the best of our knowledge, this is the first report of the isolation of biflorin from *F. sycomorus*.

Compound 2 was obtained as a yellow amorphous powder (10 mg) which showed a similar ^1H and ^{13}C NMR pattern to compound 1 (supplementary data 62 and 64). The ESI negative mode MS data gave an $[\text{M-H}]^-$ ion at m/z 353.0880 and through MassLynx the molecular formula was determined to be $\text{C}_{16}\text{H}_{18}\text{O}_9$. The number of protons and carbon atoms were confirmed using ^1H and ^{13}C NMR respectively. The compound was determined to be the chromone, isobiflorin (5,7-dihydroxy-2-methylchromone-8-C- β -D-glucopyranoside), its structure is shown in Figure 3.23. The ^1H NMR spectrum (MeOD- d_4 , 400 MHz) of compound 2 consisted of; one aromatic proton at δ 6.04 (1H, s, H-3), a double bond proton at δ 6.21 (1H, s, H-6); a methyl group at δ 2.36 (3H, s, Me-2). The spectrum also showed protons at δ 4.06 (1H, *m*, H-2), δ 3.84 (1H, *br d*, H-6'), δ 3.68 (1H, *dd*, H-6'), δ 3.45 (1H, *m*, H-4'), δ 3.44 (1H, *m*, H-5') and δ 3.38 (1H, *m*, H-3') which are indicative of oxygen bearing protons. The anomeric proton doublet at δ 4.87 was partially obscured by the overlapping signal of water present in the MeOD- d_4 . In order to determine the multiplicity of the anomeric proton, the ^1H NMR of isobiflorin (compound 2) was rerun in ($\text{CD}_3\text{CN-}d_3$, 500 MHz) after removal of the MeOD- d_4 . Under these conditions, a doublet for the anomeric proton was clearly visible at δ 4.94 (1H, *d*, 9.8Hz) (supplementary data 63). In addition, the aromatic proton at δ 6.25 (1H, s, H-6) and the double bond proton at δ 6.06 (1H, s, H-3) were observed. As in the study of Zhang and Chen [37], a signal was observed for the hydroxyl group at C-5 (δ 13.00) which indicated chelation through a strong hydrogen bond with the *ortho* carbonyl group at C-4. However, the singlet for methyl protons was obscured with the water peak due to water present in the deuterated acetonitrile.

The ^{13}C NMR spectrum consisted of 16 carbon atoms which reflected the presence of one conjugated carbonyl signal at δ 184.43 (C-4); one oxygen linked olefinic carbon signal at δ

169.4 (C-2) and 3 oxygen bearing aromatic carbon atoms at δ 164.74 (C-7), δ 162.88 (C-5), and δ 158.43 (C-8a). ^{13}C and DEPT-135 showed seven quaternary resonances at δ 184.42 (C-4), δ 169.49 (C-2), δ 164.74 (C-7), δ 162.88 (C-5), δ 158.43 (C-8a), δ 105.38 (C-4a) and δ 104.87 (C-8); seven CH signals at δ 108.84 (C-3), δ 100.23 (C-6), δ 82.52 (C-3'), δ 80.10 (C-5'), δ 75.42 (C-1'), δ 72.91 (C-2'), δ 71.92 (C-4'); a CH_2 signal at δ 63.00 (C-6') and a methyl signal at δ 20.40 (Me-2). The one bond carbon hydrogen HSQC (supplementary data 66) and COSY correlations (supplementary data 67) led to the assignments of the proton and carbon signals as shown in Table 3.6 and the ^1H and ^{13}C NMR data compares favourably with that published by Zhang and Chen [37] and Oya et al. [38] for isobiflorin. However, small differences in chemical shifts (approximately 0.2 ppm) were observed between our ^1H NMR and the ^1H NMR obtained in the study of Oya et al. [38] who also analysed isobiflorin (MeOD-*d*4, 400 MHz). Larger differences in chemical shifts were observed between isobiflorin analysed in our study and isobiflorin analysed by Zhang and Chen [37] who used DMSO-*d*6 for NMR analysis.

Table 3.6. ^1H and ^{13}C -NMR data of isobiflorin in MeOD-*d*4 as compared with ^1H and ^{13}C data of isobiflorin in DMSO-*d*6 and ^1H data of isobiflorin in MeOD-*d*4 from literature.

Isolated isobiflorin			^{13}C and ^1H Literature data in DMSO- <i>d</i> 6 (Zhang and Chen [37])		^1H Literature data in CD_3OD (Oya et al.[38])
Position	δC (ppm)	δH (ppm), <i>J</i> in Hz	δC (ppm)	δH (ppm), <i>J</i> in Hz	δH (ppm), <i>J</i> in Hz
2	169.49	-	167.02	-	-
3	108.84	6.04 (1H, s)	107.43	6.17 (s)	6.08 (2H, s)
4	184.43	-	181.94	-	-
5	105.38	-	160.35	-	-
6	100.23	6.21 (1H, s)	98.44	6.23 (s)	6.25 (1H, s)
7	164.74	-	162.51	-	-
8	104.87	-	104.27	-	-
8a	158.43	-	156.14	-	-
1'	75.42	4.87 (1H, <i>d</i> , 9.8 Hz)	73.12	4.63 (<i>d</i> , 9.8 Hz)	4.90 (1H, <i>d</i> , 9.9 Hz)
2'	72.91	4.06 (<i>m</i>)	70.95	3.86 (<i>t</i> , 9.8 Hz)	4.08 (1H, <i>m</i>)
3'	82.52	3.38 (<i>m</i>)	78.46	3.20 (<i>t</i> , 8.7 Hz)	3.48 (1H, <i>m</i>)
4'	71.92	3.45 (<i>m</i>)	70.34	3.16 (<i>br s</i>)	3.46 (1H, <i>m</i>)
5'	80.10	3.44 (<i>m</i>)	81.08	3.16 (<i>br s</i>)	3.42 (1H, <i>m</i>)
6'	63.00	3.68 (1H, <i>dd</i> , 12.1 Hz, 5.3 Hz) 3.84 (<i>br d</i> , 12.1 Hz)	61.25	3.67 (<i>dd</i> , 11.5 Hz, 5.0 Hz) 3.41 (<i>br d</i> , 11.5 Hz)	3.70 (1H, <i>m</i>) 3.84 (1H, <i>m</i>)
Me-2	20.40	2.36 (3H, s, Me-2)	19.63	2.34 (s, Me-2)	2.38 (s, Me-2)
OH	-	-	-	13.00 (s, 5-OH)	-
OH	-	-	-	10.70 (<i>br, s</i> , 7-OH)	-

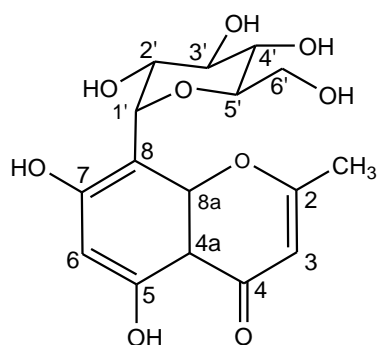


Figure 3.23. Structure of compound 2 (isobiflorin)

HMBC (supplementary data 68) was used to confirm correlations between carbon and protons which are separated by two and three bonds as shown in Figure 3.24 for isobiflorin. The proton at H-6 (δ 6.21) showed HMBC correlations with C-8 (δ 104.87), C-7 (δ 164.74), C-5 (δ 162.88) and C-4a (δ 105.38) thereby confirming its position at C-6. The position of the singlet at H-3 (δ 6.04) was confirmed to be C-3 through its HMBC correlations with C-4a (δ 105.38), C-2 (δ 169.49), C-4 (δ 184.42), Me-2 (δ 20.40). The methyl protons at C-2 showed correlations with C-3 (δ 108.84) and C-2 (δ 169.49) thereby confirming its position. The anomeric proton showed HMBC correlations with C-7 (δ 164.7), C-8a (δ 158.4) and C-8 (δ 104.9), thus revealing the position of the glycoside to be attached to C-8.

COSY correlations (supplementary data 67) and ^1H - ^1H coupling were used to determine correlations between neighbouring protons which couple to each other. The large coupling constant of the anomeric proton at (δ 4.87, 9.8 Hz) indicates beta coupling to the aromatic ring which corroborates the β orientation of the glycoside identified by Zhang and Chen [37]. There was a COSY correlation between the anomeric proton at C-1' (δ 4.88, 9.8 Hz) and the proton at C-2' (δ 4.15). Another correlation was observed between the proton at C2' (δ 4.06) and the proton at C3' (δ 3.38) (a multiplet). The proton at C5' (δ 3.44) coupled with the two methylene protons at C6' (δ 3.68 and 3.84) to give a multiplet. These methylene protons also coupled

which each other, hence the two sets of doublets of doublets at δ 3.68 (*dd*, 12.1 Hz, 5.3 Hz, H-6') and δ 3.84 (*br d*, 12.1Hz, H-6').

Isobiflorin was originally isolated from *Eugenia caryophyllata* buds [37] and has also been isolated from *Syzygium aromaticum* [38] and *Dryopteris crassirhizoma* [40]. To the best of our knowledge, this is the first report of the isolation of isobiflorin from *F. sycomorus*.

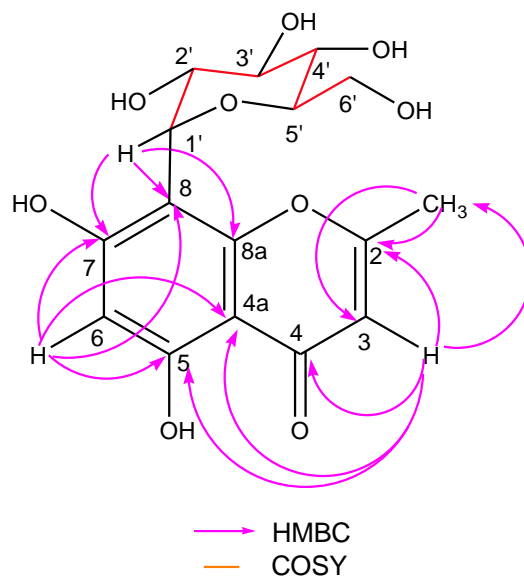


Figure 3.24. Key HMBC and COSY correlations of compound 2 (isobiflorin)

Compound 3 (7 mg) was obtained a yellow amorphous solid. The ESI negative mode spectrum gave an $[M-H]^-$ ion at m/z 593.1498 (supplementary data 44) and using Mass Lynx the molecular formula was determined to be $C_{27}H_{30}O_{16}$. The number of protons and carbon atoms were confirmed using 1H and ^{13}C NMR respectively (supplementary data 69 and 71). The compound was determined to be a 6,8-di-C- β -D-glucoside of apigenin (vicenin-2) its structure is shown in Figure 3.25. The 1H NMR spectrum (MeOD-*d*4, 600 MHz) of this compound showed aromatic protons at δ 7.98 (2H, *d*, 8.7 Hz, H-2' and H-6') and at δ 6.93 (2H, *d*, 8.7 Hz, H-3' and H-5'), and a double bond proton at δ 6.60 (1H, *s*, H-3). The spectrum also showed signals at δ 5.07 (1H, *d*, 9.8 Hz, H-1''), δ 5.00 (1H, *d*, 9.7 Hz, H-1'''), δ 4.10 (1H, *m*, 9.7 Hz), δ 3.93 (2H, *m*, H-6'' and H-6'''), δ 3.80 (2H, *m*, H-6'' and H-6'''), δ 3.64 (1H, *m*, H-2'''), δ 3.58 (1H,

m, H-4''), δ 3.54 (1H, *m*, H-3''), δ 3.52 (1H, *m*, H-3'''), δ 3.50 (1H, *m*, H-4'''), δ 3.48 (1H, *m*, H-5'') and δ 3.46 (1H, *m*, H-5''') which are indicative of oxygen bearing protons. The anomeric protons were observed at δ 5.07(1H, *d*, 9,8 Hz, H-1'') and δ 5.00 (1H, *d*, 9.8 Hz, H-1'''). The large coupling constants of 9.8 Hz in both cases for the anomeric protons confirmed the beta coupling of sugar moieties to the aglycone units. The ^1H NMR spectra of the compound was rerun in DMSO-*d*₆ (supplementary data 70), the spectrum which showed an additional signal at δ 13.71 (1H, *br s*, OH-5) for the hydroxyl group which indicated chelation through a strong hydrogen bond with the *ortho* carbonyl group at C-4. This signal was also observed by Veloso et al.[41] in his study of vicenin-2 (DMSO-*d*₆, 500 MHz) isolated from the aerial parts of *Peperomia blanda*.

The ^{13}C spectrum consisted of 27 carbon atoms which showed the presence of one conjugated carbonyl signal at δ 184.03 (C-4); one oxygen linked olefinic carbon signal at δ 166.44 (C-2) and four oxygen bearing aromatic carbon atoms at δ 162.92 (C-7), δ 160.80 (C-5), δ 161.83 (C-4') and δ 157.69 (C-9). ^{13}C and DEPT-135 (supplementary data 72) showed nine quaternary resonances at δ 184.03 (C-4), δ 166.44 (C-2), δ 162.92 (C-7), δ 160.80 (C-5), δ 157.69 (C-9), δ 123.49 (C-1'), δ 106.21 (C-8), δ 108.54 (C-6) and δ 104.64 (C-10); thirteen CH signals at δ 130.09 (C-2' and C-6'), δ 117.05 (C-3' and C-5'), δ 103.60 (C-3), δ 83.01 (C-5''), δ 82.57 (C-5'''), δ 80.44 (C-3'''), δ 79.42 (C-3''), δ 76.17(C-1'''), δ 75.26 (C-1''), δ 73.15 (C-2''), δ 72.42 (C-2'''), δ 71.65 (C-4''), δ 71.01 (C-4'''), two CH₂ signals at δ 63.09 (C-6'') and δ 61.88 (C-6'''). The one bond carbon hydrogen HSQC (supplementary data 73) and COSY correlations led to the assignments of the proton and carbon signals as shown in Table 3.7 and the ^1H and ^{13}C NMR data compares favourably with that published by Lu et al.[42], Veloso et al. [41], Islam et al. [43] and Xie et al.[44]. There were, however, small differences in chemical shifts (approximately 0.3 ppm) observed between our ^1H NMR and the ^1H NMR obtained in the study of Lu et al.[42] who analysed vicenin-2 using (DMSO-*d*₆, 600 MHz).

Table 3.7. ^1H and ^{13}C -NMR data of vicenin-2 in MeOD- d_4 as compared with ^1H and ^{13}C data of vicenin-2 in DMSO- d_6

Isolated vicenin-2 in methanol			^{13}C and ^1H Literature data in DMSO- d_6 Lu et al. [42]	
Position	δC (ppm)	δH (ppm), J in Hz	δC (ppm)	δH (ppm), J in Hz
2	166.44		164.13	
3	103.60	6.60 (1H, s)	102.86	6.59 (1H, s)
4	184.03		182.30	
5	160.80		159.58	
6	108.54		108.50	
7	162.92		162.78	
8	106.21		104.78	
9	157.69		155.23	
10	104.64		103.60	
1'	123.49		122.01	
2'	130.09	7.98 (1H, <i>d</i> , 8.7 Hz)	128.93	7.92 (<i>d</i> , 8.7Hz)
3'	117.05	6.93 (1H, <i>d</i> , 8.7 Hz)	116.27	6.91 (<i>d</i> , 8.5Hz)
4'	161.83		161.42	
5'	117.05	6.93 (1H, <i>d</i> , 8.7 Hz)	116.37	6.91 (<i>d</i> , 8.5Hz)
6'	130.09	7.98 (1H, <i>d</i> , 8.7 Hz)	128.93	7.92 (<i>d</i> , 8.7Hz)
1''	75.26	5.00 (1H, <i>d</i> , 9.8 Hz)	74.32	4.76 (<i>d</i> , 9.8 Hz)
2''	73.15	4.10 (1H, <i>m</i> , 9.8 Hz)	71.87	3.86 (<i>t</i> , 8.7Hz)
3''	79.42	3.54 (<i>m</i>)	78.76	3.32 (<i>m</i>)
4''	71.65	3.58 (<i>m</i>)	70.32	3.32 (<i>m</i>)
5''	83.01	3.48 (<i>m</i>)	81.41	3.30 (<i>m</i>)
6''	61.88	3.80 (<i>m</i>), 3.93 (<i>m</i>)	61.07	3.58, <i>dd</i> , 11.9 Hz, 7.8Hz 3.70, <i>d</i> , 11.0 Hz
1'''	76.17	5.07 (1H, <i>d</i> , 9.8 Hz)	74.51	4.88, <i>d</i> , 9.8Hz
2'''	72.42	3.64 (<i>m</i>)	71.87	3.86, <i>t</i> , 8.7Hz
3'''	80.44	3.52 (<i>m</i>)	79.10	3.38 (<i>m</i>)
4'''	71.01	3.50 (<i>m</i>)	70.85	3.42 (<i>m</i>)
5'''	82.57	3.46 (<i>m</i>)	81.88	3.35 (<i>m</i>)
6'''	63.09	3.80 (<i>m</i>), 3.93 (<i>m</i>)	61.53	3.58, <i>dd</i> , 11.9 Hz, 7.8Hz 3.76, <i>d</i> , 11.0 Hz

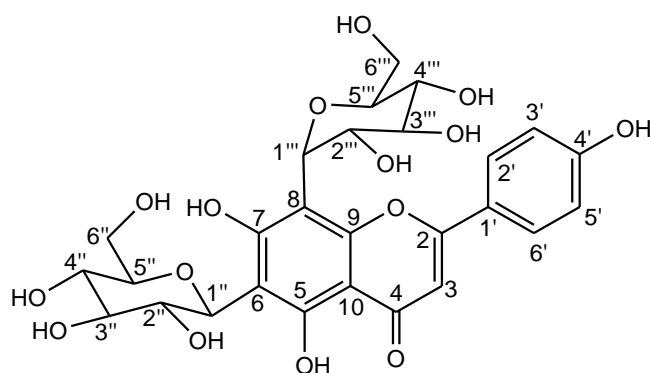


Figure 3.25. Structure of compound 3 (vicenin-2)

HMBC (supplementary data 75) was used to confirm correlations between carbon and protons which are separated by two and three bonds as shown in Figure 3.26. The singlet at δ 6.60

(H-3) showed HMBC correlations with C-1' (δ 123.49), C-2 (δ 166.44), C-4 (δ 184.03) and C10 (δ 104.64) thereby confirming its position at C-3. The proton at δ 7.98 (H-2') had HMBC correlations with C-6' (δ 130.09), C-4' (δ 161.83) and C-2 (δ 166.44) thus confirming its position at C-2'. The proton at 7.98 (H-6') showed correlations with C-2' (δ 130.09), C-4' (δ 161.83) and C-2 (δ 166.44) thus determining its position to be at C-6'. The position of the doublet at δ 6.93 (H-5') was confirmed to be C-5' through its HMBC correlations with C-3' (δ 117.05), C-1' (δ 123.49) and C-4' (δ 161.83). The position of the aromatic proton at C-3' (δ 117.05) was determined due to its HMBC correlations with C-5' (δ 117.05), C-1' (δ 123.49) and C4' (δ 161.83). The position one of the sugar moiety was confirmed to be at position C-8 (δ 106.21) due to the HMBC correlations of the anomeric proton at H-1''' (δ 5.07) with C-8 (δ 106.21) and C-9 (157.69). The HMBC correlations between the anomeric proton H-1'' and C-6 (δ 108.54) were not clearly visible, however, position C-6 was determined taking into consideration that position C-8 had a glycoside unit, and position C-5 had been previously determined to be occupied by a hydroxyl group leaving positions C-7 and C-6 as the possible locations for the second sugar moiety. Position C-6 was more likely to be occupied than position C-7.

COSY correlations (supplementary data 74) were used to determine correlations between neighbouring protons which couple to each other. The proton at C2'' (δ 4.10) had a cosy correlation with proton at C3' (δ 3.54) (a multiplet). The multiplet at C5'' (δ 3.48) also showed a cosy correlation with the two methylene protons at C6'' (δ 3.80 and δ 3.93). These methylene protons also showed cosy correlation which each other but the shapes of the peaks were only observed as multiplets. Similarly, in the second glycoside, the proton at C2''' (δ 3.64) showed a cosy correlation with proton at C3''' (δ 3.52) (a multiplet). The multiplet at C5''' (δ 3.46) was also correlating with the two methylene protons at C6''' (δ 3.80 and δ 3.93). These methylene protons had a cosy correlation which each other but the shapes of the peaks were only observed as multiplets.

Vicenin-2 has been reported to exhibit a wide range of activities including, anti-inflammatory activity Marrassini et al. [45], anticancer activity Nagaprashantha et al. [46] and antioxidant activity Velozo et al.[41]. In a study by Islam et al. [43] vicenin 2 was found to be a potent inhibitor of α -glucosidase, inhibited formation of advanced glycation end products, suppressed glycation -induced protein oxidation, it suppressed formation of amyloid cross β structures. To the best of our knowledge, this is the first report of the isolation of vicenin-2 from the *F. sycomorus* plant.

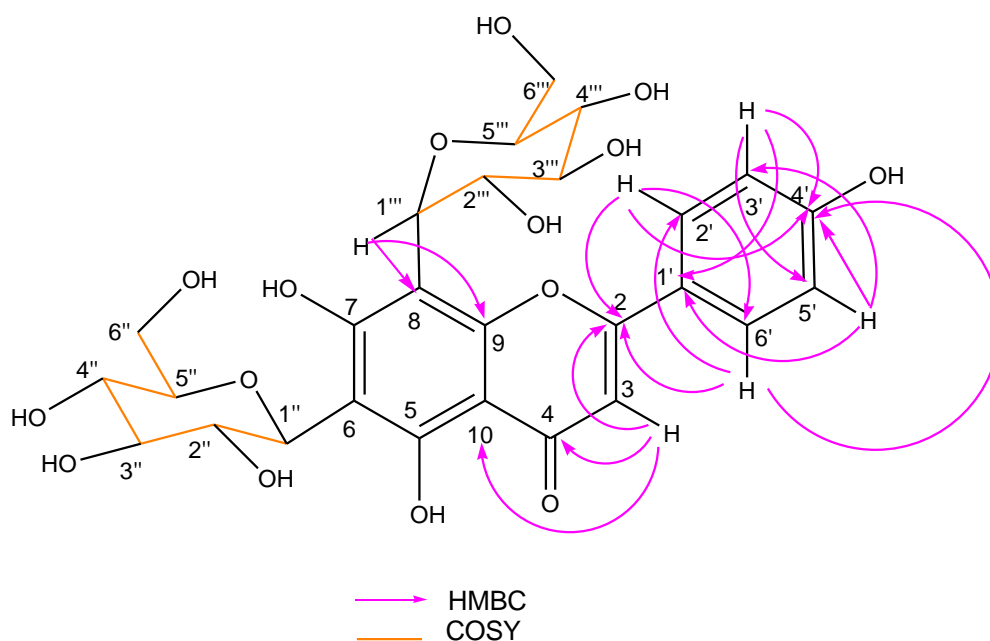


Figure 3.26. Key HMBC and COSY correlations of compound 3 (vicenin-2)

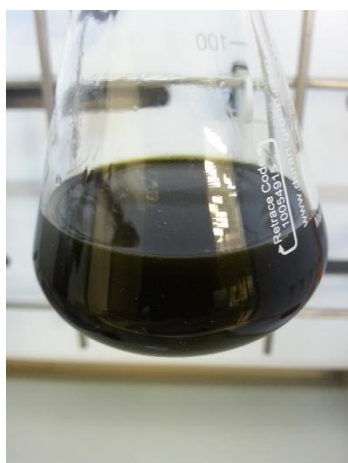
The isolation and purification of compounds and confirmation of their identity using NMR was valuable in confirming the identity of compound 1 (biflorin) and compound 2 (isobiflorin) which had been tentatively identified in section 3.7.5 based on accurate mass comparisons and matching of the fragmentation pattern of the compounds with data from stored in massbank libraries. Further, the identity of compound 3 (vicenin-2) which could not be tentatively identified through either comparison of accurate masses or matching of the fragmentation pattern of the compound to data with Massbank libraries was established through isolation,

purification and identification using NMR. Thus, different methods of chemical analysis can be used to complement each other in developing chemical fingerprints of plant extracts.

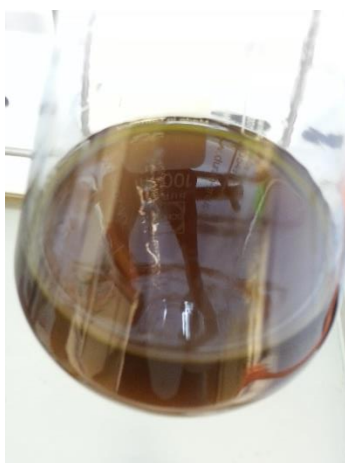
3.7.8 Improving the quality of the ethanol extract as a cosmetic ingredient

The crude ethanol extract was selected as the most suitable extract for further development, however, its intense green colour could hinder its use as a cosmetic ingredient. The ethanolic extract of the leaves was defatted (Figure 3.7) with the aim of reducing the intensity of the green colour while retaining or improving enzyme inhibition. Yields obtained after defatting were 55.07 % for the defatted fraction and 30.85% for hexane fraction. The defatted fraction had a significantly reduced intensity of the green colour in comparison to the crude ethanol extract. This is a result of removal of chlorophyll, the main pigment responsible for the dark green colour in the leaves. The defatted leaf extract had a brownish colour which could be due to a combination of more polar pigments like carotenoids and anthocyanins which could not be removed using the non-polar hexane solvent. The hexane layer had the green colour which was due to chlorophyll (Figure 3.27).

A. Crude extract



B. Defatted leaf extract



C. Hexane layer



Figure 3.27. Picture A shows the dark-green colour of the ethanol extract of leaves of *F. sycamorus*, picture B shows the defatted leaf extract with the dark-green colour removed. Picture C is the hexane layer showing the green colour of chlorophyll removed from the crude extract.

In order to investigate the effect of defatting on the elastase and collagenase inhibition activities, the crude extract, defatted extract, hexane layer and the positive controls were screened for anti-aging activity at 100 and 10 µg/ml (Figure 3.28). Screening results for collagenase activity at 10 µg/ml revealed that the crude extract had a 3.42% ± 0.85 inhibition and the defatted extract had a 24.49% ± 1.28 inhibition, significantly lower ($p < 0.01$) collagenase inhibition than EDTA of 76.26% ± 2.47. The hexane fraction showed no collagenase inhibition activity at 10 µg/ml. Results at 100 µg/ml revealed that the *F. sycamor* crude extract had a 59.24% ± 3.50 inhibition and the hexane fraction a 21.32% ± 1.82 inhibition significantly lower ($p < 0.01$) activities than the positive control EDTA (76.26% ± 2.47). In contrast, the defatted fraction had an 82.79% ± 0.89 inhibition and was as potent as ($p > 0.05$) EDTA. These results reveal that defatting successfully improved the collagenase inhibition activity of the *F. sycamor* leaf ethanol extract. This is due to a concentration effect resulting from removal of the inactive non-polar components which would have diluted the active ingredients. Further, the inactivity of the hexane fraction at 10 µg/ml and its limited activity at 100 µg/ml provides evidence that defatting did not remove active ingredients. Due to the improved colour and collagenase inhibition activity, the ethanol extract of leaves of *F. sycamor* (coded FD extract) was selected for combination and formulation studies in Chapter 4.

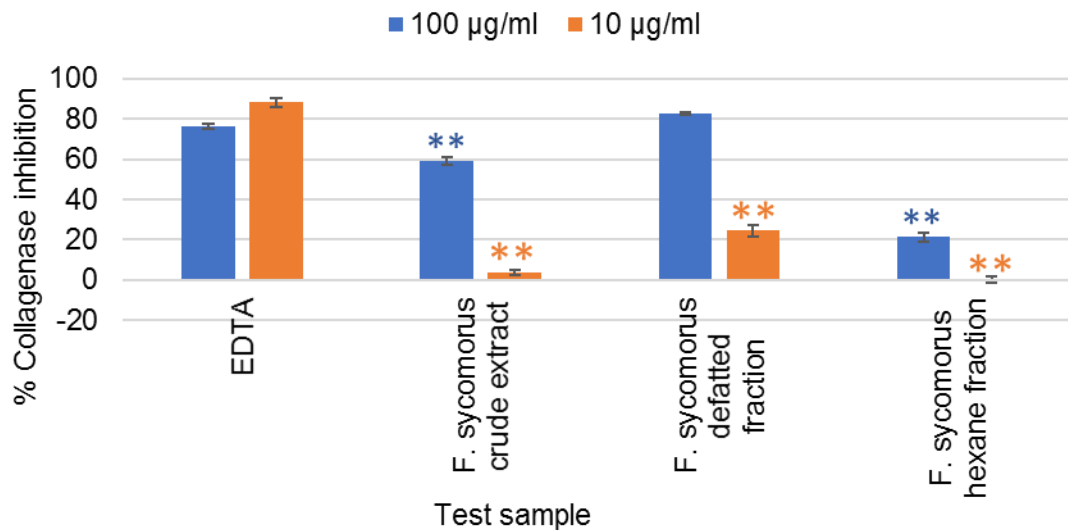


Figure 3.28. Collagenase inhibition activities of *F. sycomorus* crude extract and its fractions produced by defatting. The samples were screened at concentrations 100 and 10 µg/ml and the positive control EDTA at 143 µg/ml (Error bars represent SEM, with n=3). ** = p <0.01 represents a significant difference with EDTA at 10 µg/ml and ** = p <0.01 represent a significant difference with EDTA at 100 µg/ml

The bio-assaying of the extracts and fractions against elastase enzyme is shown in Figure 3.29. The results show that at 100 µg/ml, although good elastase inhibition of the defatted fraction (78.32% ± 0.70) and the crude extract (78.33% ± 1.02) was observed, these samples exhibited lower elastase inhibition activities (p<0.01) than the positive control elafin (99.81% ± 0.01). This suggests that the removal of the inactive non-polar components through defatting had no effect on the concentration of compounds responsible for elastase inhibition of the extract since the crude extract and the defatted fraction were equipotent. The hexane fraction showed very limited elastase inhibition activity (19.36% ± 0.60) revealing that no active compounds were extracted in the hexane during defatting. At the lower concentration of 10 µg/ml, all fractions exhibited no anti-elastase activity. The inactivity of the crude and defatted extracts at 10 µg/ml may be attributed to the samples being tested at too low a concentration.

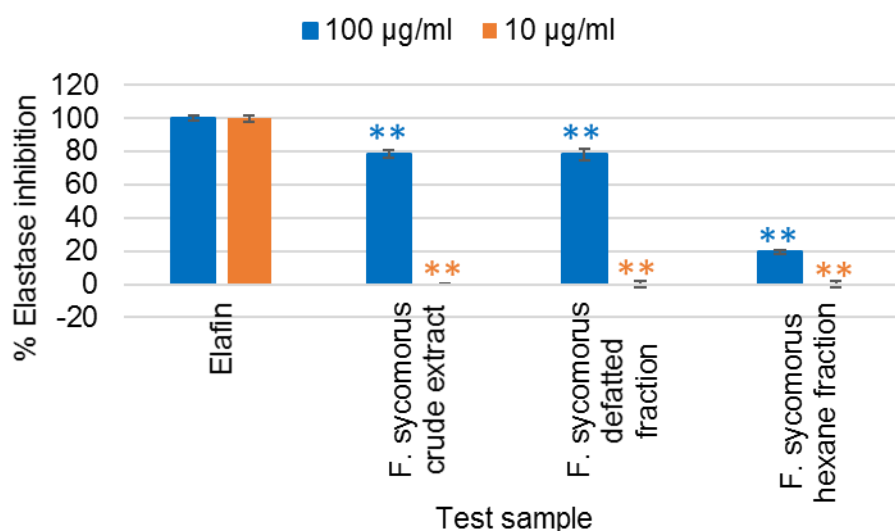


Figure 3.29. Elastase inhibition activities of *F. sycomotorus* crude extract and its fractions produced by defatting. The samples were screened at concentrations 100 and 10 µg/ml and the positive control elafin at 1.43 µg/ml (Error bars represent SEM, with n=3). ** = P<0.01 represents a significant difference with EDTA at 10 µg/ml and * = P<0.01 represent a significant difference with EDTA at 100 µg/ml.

3.7.9 Comparison of chemical profiles of the *F. sycomotorus* crude extract and its defatted fraction

The chemical profiles of *F. sycomotorus* crude ethanol extract and its defatted extract were analysed using UPLC-QTOF-MS (Figure 3.30). The major peak in the crude extract at m/z 377.0872 retention time 0.74 minutes previously identified as palatinose in section 3.7.5 was present in the defatted extract at m/z 377.0851 retention time 0.74 minutes. The peak observed in the crude extract at m/z 353.0879 retention time 2.92 minutes was also observed after defatting at m/z 353.0872 retention time 2.91 minutes. Its identity was elucidated to be isobiflorin in section 3.7.7. A peak observed at m/z 191.0555 retention time 2.96 minutes in the crude extract previously identified in section 3.7.5 as chlorogenic acid was also present in the defatted extract at m/z 191.0557 retention time 2.96 minutes (supplementary data 55). The regio-isomer of isobifin observed in the crude extract at m/z 353.0881 retention time 3.23 minutes identified in section 3.7.7 to be biflorin was present in the defatted fraction at m/z 353.0883 retention time 3.22 minutes. The peak at m/z 593.1500 retention time 3.69 minutes

in the crude extract previously elucidated in section 3.7.7 to be vicenin 2 was observed in the defatted extract at m/z 593.1504 retention time 3.69 minutes. Three other peaks previously identified in the crude ethanol extract in section 3.7.7 as glycosides of quercetin at m/z 609.1467 retention time 4.78 minutes identified as rutin; m/z 477.0673 retention time 4.95 minutes identified as quercetin-3-glucuronide and m/z 463.0880 retention time 5.00 minutes identified as isoquercetin were also observed in the defatted extract. The presence of these major and minor common peaks in the *F. sycomorus* ethanol extract before and after defatting reveals the similarity of the chemical profiles and accounts for the similarity in the elastase inhibition activities observed for the extract and the defatted fraction. Hexane therefore removed chlorophyll, fatty acids and other non-polar minor compounds which could not be identified on the chromatogram before and after the defatting process due to their suppression by the major polar compounds in the extract.

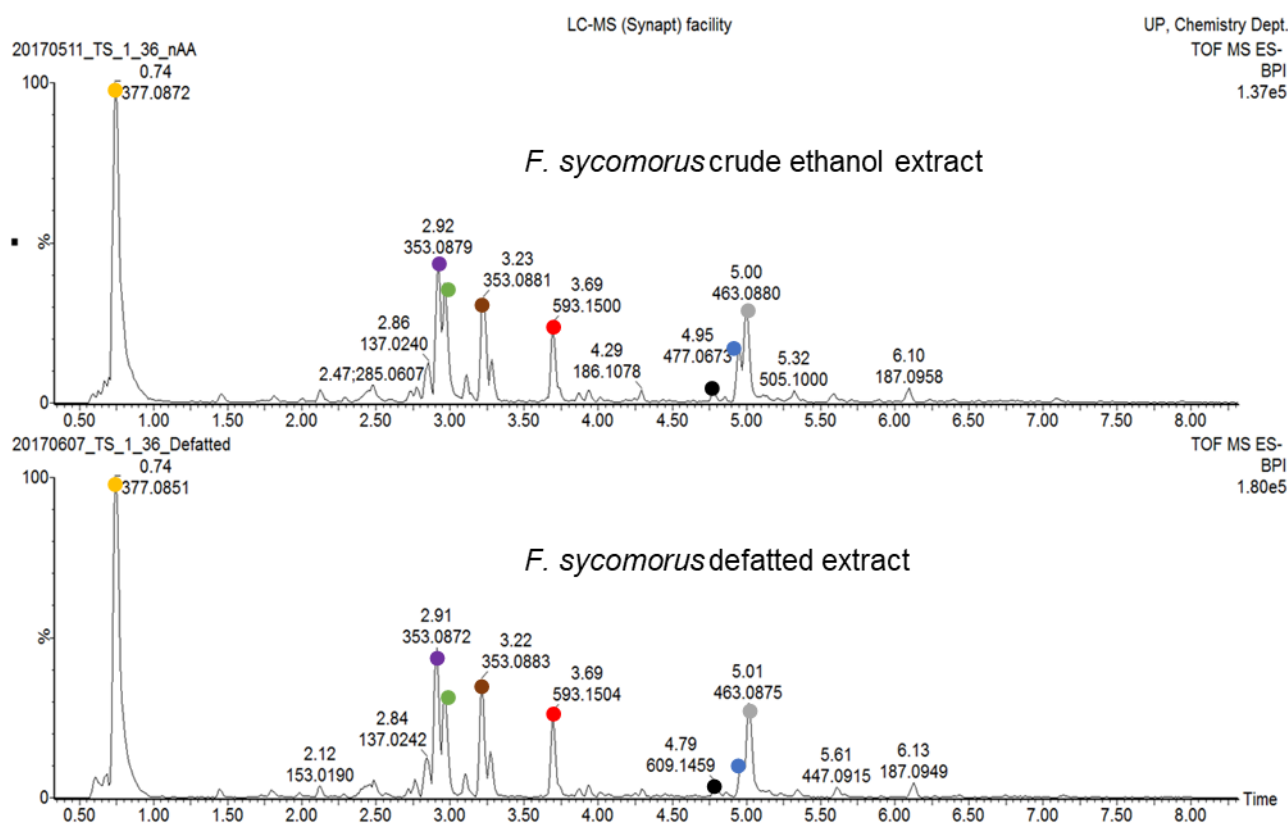


Figure 3.30. Negative mode BPI chromatograms of crude *F. sycomorus* ethanol extract and its defatted fraction. The peaks observed in the crude extract; ● palatinose (m/z 377.0872 retention time 0.74 minutes), ● isobiflorin (m/z 353.0879 retention time 2.92 minutes),

•chlorogenic acid (m/z 191.0555 retention time 2.96 minutes), •biflorin (m/z 353.0881 retention time 3.23 minutes), •vicenin-2 (m/z 593.1500 retention time 3.69 minutes), rutin (m/z 477.0673 retention time 4.95 minutes), •quercetin-3-glucuronide (m/z 477.0673 retention time 4.95 minutes) and •isoquercetin (m/z 463.0880 retention time 5.00 minutes) were also present in the defatted extract. Thus, chemical analysis revealed that there was no difference in the chemical profile of the crude Sycamore ethanol extract and its defatted fraction.

3.7.10 Bioassay guided fractionation

Fractionation of ethanol extracts of leaves of *F. sycomorus* was undertaken with the aim of identifying the possible active compound/s responsible for the in vitro anti-aging activity. Fractionation was done on prep-HPLC-UV, using time-based collections and seventeen fractions labelled F1 to F17 were produced. Each fraction was dried down using a speed vac and a sample (1mg quantities) of each fraction was accurately weighed for bioassay.

3.7.11 Collagenase inhibition activity of fractions of *F. sycomorus*

At a test concentration of 200 $\mu\text{g/ml}$, collagenase inhibition activity was >70% for most fractions showing limited selectivity. In order to address this lack of selectivity, fractions were screened at lower concentrations of 100 $\mu\text{g/ml}$ and 25 $\mu\text{g/ml}$. The results obtained at 25 $\mu\text{g/ml}$ showed greater selectivity between active and non-active fractions. At this concentration, the positive control EDTA exhibited a good collagenase inhibition activity of $74.90\% \pm 0.45$. Based on the activity of EDTA, fractions exhibiting (>70%) collagenase inhibition activity were considered to be active. Thus, fractions which exhibited good collagenase inhibition activities with respect to EDTA ($74.90\% \pm 0.45$) which are F5 ($75.54\% \pm 2.60$), F8 ($77.37\% \pm 2.40$) and F13 ($74.64\% \pm 2.20$) (Figure 3.31) were selected for chemical analysis.

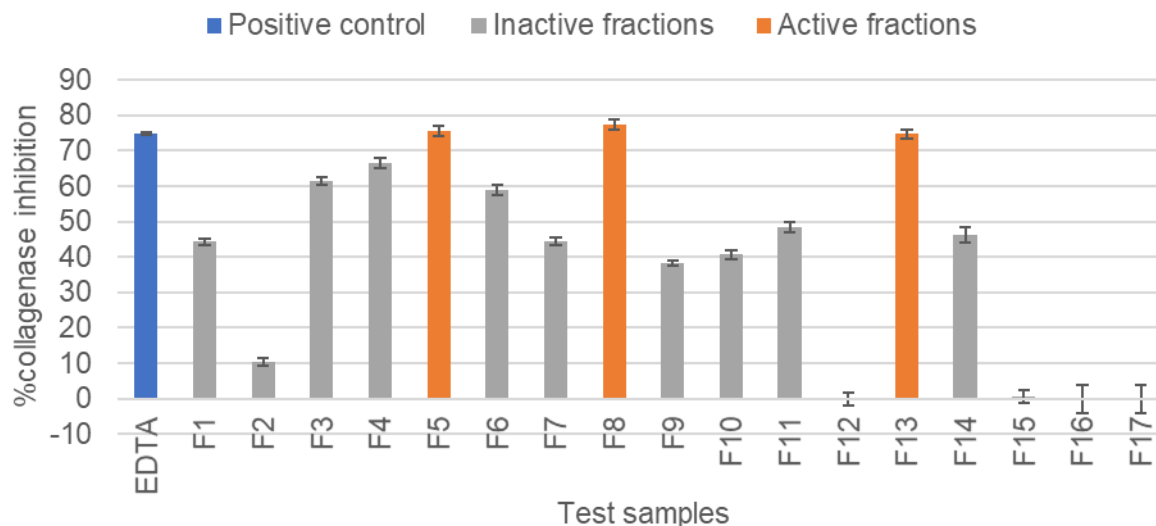


Figure 3.31. Collagenase inhibition activity of *F. sycomorus* fractions at 25µg/ml. Fractions F5, F8 and F13 showed inhibition activity (>70%) in the same range as EDTA the positive control.

3.7.12 UPLC-QTOF-MS analysis of active fractions

Chemical analysis was done in the negative ESI mode as most compounds were ionising well in this mode. An analysis of fraction F8 revealed the presence of the most intense peak at m/z 463.0892 retention time 3.50 minutes. Based on previous analysis of the chemical profile of the ethanol extract of leaves of the Sycamore tree in section 3.7.5 the compound corresponds to isoquercetin. Its presence in fraction F8 was confirmed by injecting a mixture of pure standards consisting of 4-O-caffeoylquinic acid (peak 1), epicatechin (peak 2) and isoquercetin (peak 3). The peak corresponded to peak 3 (isoquercetin) at m/z 463.0881 retention time 3.50 minutes (Figure 3.32), thus, confirming its identity to be isoquercetin. Based on the intensity of the peak it was highly likely that this major compound (isoquercetin) is the main compound that significantly contributes to the collagenase inhibition activity of this fraction. In addition to isoquercetin as the major compound, active fraction F8 had lower intensity peaks observed at m/z 451.1028 retention time 3.91 minutes, m/z 609.1423 retention time 3.35 minutes, m/z 447.0779 retention time 4.65 minutes and m/z 137.0251 retention time 2.38 minutes. These compounds could also have been contributing to the collagenase

inhibition activity of fraction F8 due to their potency against the enzyme or through synergistic effects. The identities of these peaks were not established in this study, as the pure compound isoquercetin was screened and confirmed as the main active ingredient, hence there was no reason for further purification (see section 3.7.13).

The most intense peak in fraction F5 was observed at m/z 431.1931 retention time 2.94 minutes. The identity of this peak has not been established in this study as the peak was absent from the ethanol extract of leaves of *F. sycomorus* analysed in section 3.7.7. As such, the compound corresponding to this peak is not likely to be one of the compounds contributing to the activities of this fraction or the *F. sycomorus* leaf extract. Similar to active fraction F8, an analysis of active fraction F5 revealed the presence of one of the peaks at m/z 463.0894 retention time 3.49 minutes which corresponds to isoquercetin identified earlier in section 3.7.5. The identity of this peak in fraction F5 was confirmed by injecting a mixture of pure standards consisting of 4-O-caffeoylquinic acid (peak 1), epicatechin (peak 2) and isoquercetin (peak 3). The peak corresponded to peak 3 (isoquercetin) at m/z 463.0881 retention time 3.50 minutes (Figure 3.32), thus, confirming its identity to be isoquercetin. This glycoside of quercetin was shown in section 3.7.13 to be one of the compounds from this fraction exhibiting collagenase inhibition activity. In addition to isoquercetin, active fraction F5 had an intense peak at m/z 593.1501 retention time 2.76 minutes which was elucidated to be vicenin 2 (in section 3.7.7). Biological screening in section 3.7.13 revealed that vicenin-2 is not one of the compounds exhibiting collagenase inhibition activity in fraction F5. Other low intensity peaks in fraction F5 were not identified as they had very small intensities in the active ethanol extract of leaves of *F. sycomorus*.

Active fraction F13 was obtained in very low quantities which could not give much detail upon analysis. Due to the low concentration of the fraction there was extensive background noise

and the peaks responsible for activity could not be clearly identified. Despite the complexity of fraction F13, close analysis clearly revealed that the compounds contributing to the activity of this fraction are different from those responsible for the collagenase inhibition activity of fractions F5 and F8.

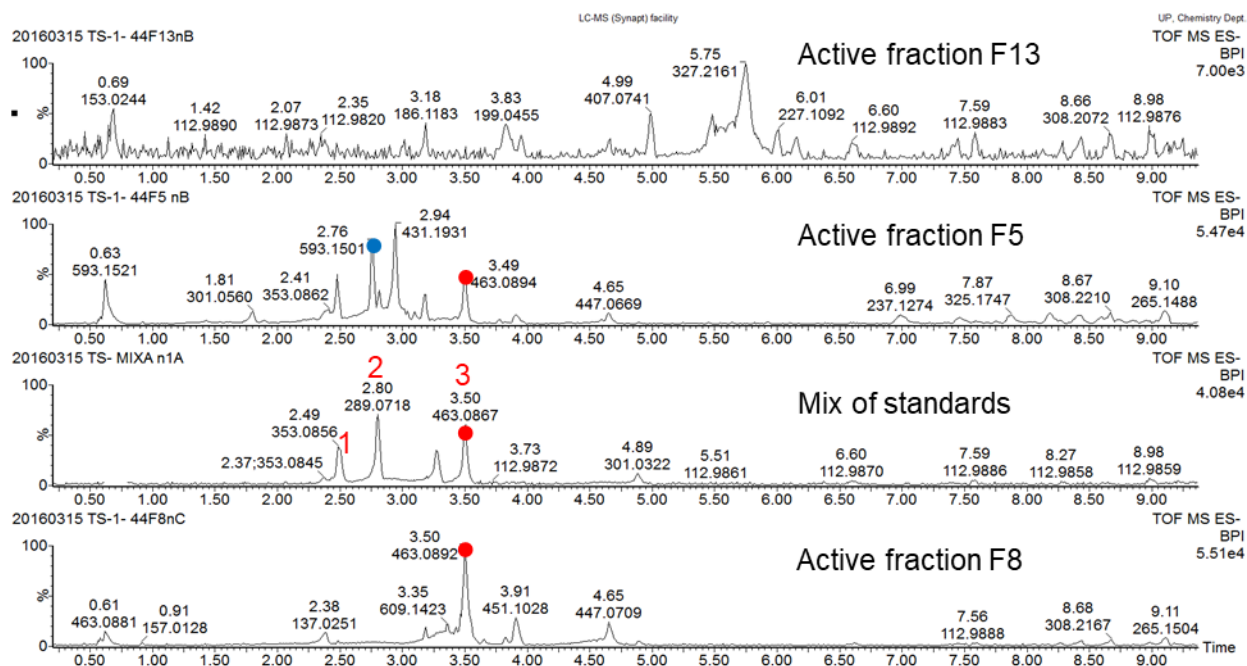


Figure 3.32. ESI negative mode BPI chromatograms of the four active fractions from *F. sycomorus* leaf ethanol extract overlaid with a mix of standards consisting of 4-O-caffeoylquinic acid (1), epicatechin (2) and • isoquercetin (3). The major peak in fraction F8 at retention time 3.50 minutes and m/z 463.0892 corresponded with isoquercetin (•) standard at m/z 463.0867 and retention time 3.50 minutes. Further, isoquercetin corresponded to the peak at m/z 463.0894 retention time 3.49 minutes in fraction F5. Isoquercetin is likely to contribute to the collagenase inhibition activities of fractions F8 and F5. • Vicenin-2 was also present in fraction F5.

3.7.13 Collagenase inhibition assay of pure compounds

The compounds confirmed to be present in *F. sycomorus* leaf ethanol extract through pure standards and those isolated from the extract were screened for collagenase inhibition activities at test concentrations of 5, 10 and 20 $\mu\text{g/ml}$ to confirm if they are responsible for collagenase inhibition activity. The compounds screened were palatinose, quinic acid, isobiflorin, biflorin, chlorogenic acid, rutin, isoquercetin and vicenin-2. Screening results

revealed that palatinose, quinic acid, chlorogenic acid, isobiflorin, biflorin, rutin and vicenin-2 showed limited activity of (<20%) in the collagenase inhibition tests at all concentrations (Figure 3.33). Previous studies confirmed the limited or lack of activity of quinic acid in the collagenase inhibition assay [47]. There have been no previous reports on the anti-elastase and anti-collagenase activity of biflorin, isobiflorin and palatinose.

The positive control EDTA exhibited good inhibition activity of (>72%) at the three test concentrations. Statistically, all the compounds screened showed significantly lower ($p > 0.01$) collagenase inhibition activity than EDTA at all concentrations. At 20 and 10 $\mu\text{g/ml}$ isoquercetin exhibited moderate collagenase inhibition activities of $49.66\% \pm 1.36$ and $56.18\% \pm 1.72$ respectively in comparison to EDTA. At a lower concentration of 5 $\mu\text{g/ml}$ isoquercetin was inactive against the collagenase enzyme. This is the first report on the collagenase inhibition activity of isoquercetin and based on the data, the compound warrants further development as a cosmetic ingredient.

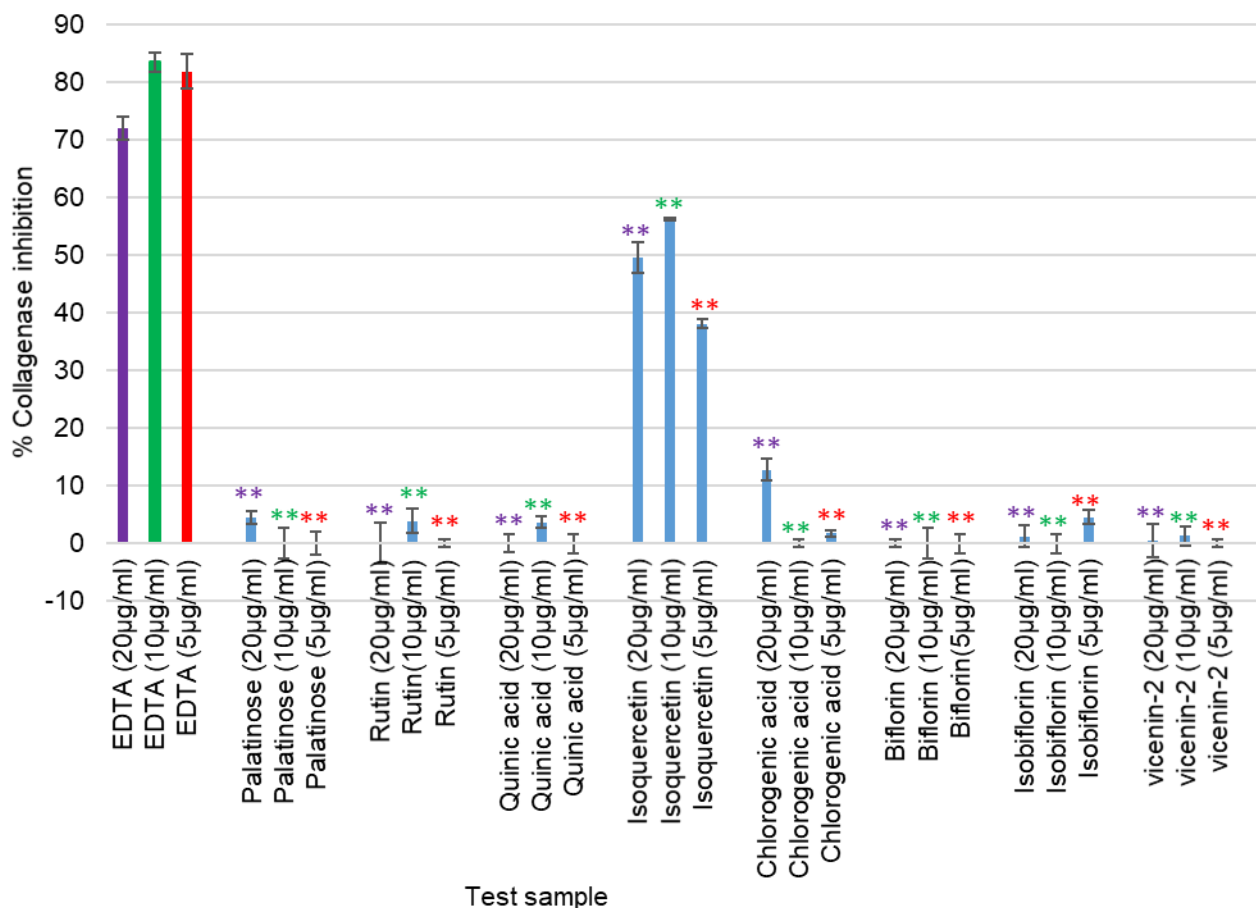


Figure 3.33. Collagenase inhibition activities of major compounds identified in leaves of *F. sycomorus* ethanol extract at 20, 10 and 5 µg/ml. (Error bars represent SEM, with n=3). ** = P<0.01 represent a significant difference with EDTA at 5 µg/ml, * = P<0.01 represent a significant difference with EDTA at 10 µg/ml, ** = P <0.01 represent a significant difference with EDTA at 20 µg/ml.

3.7.14 Elastase inhibition activity of fractions of *F. sycomorus*

Fractions from Sycamore leaf ethanol extract were screened for elastase inhibition activity. At a test concentration of 200 µg/ml, elastase inhibition activity was >70% for most fractions showing limited selectivity (Figure 3.34). To address this lack of selectivity, fractions were screened at lower concentrations of 100 µg/ml and 25 µg/ml. Nevertheless, the results obtained at 25 µg/ml did not show much improvement in selectivity between active and non-active fractions as nine (9) of the seventeen (17) fractions showed elastase inhibition activity

above 70%. The lack of selectivity can be attributed to different compounds scattered throughout the extract being responsible for the elastase inhibition activity of the extract.

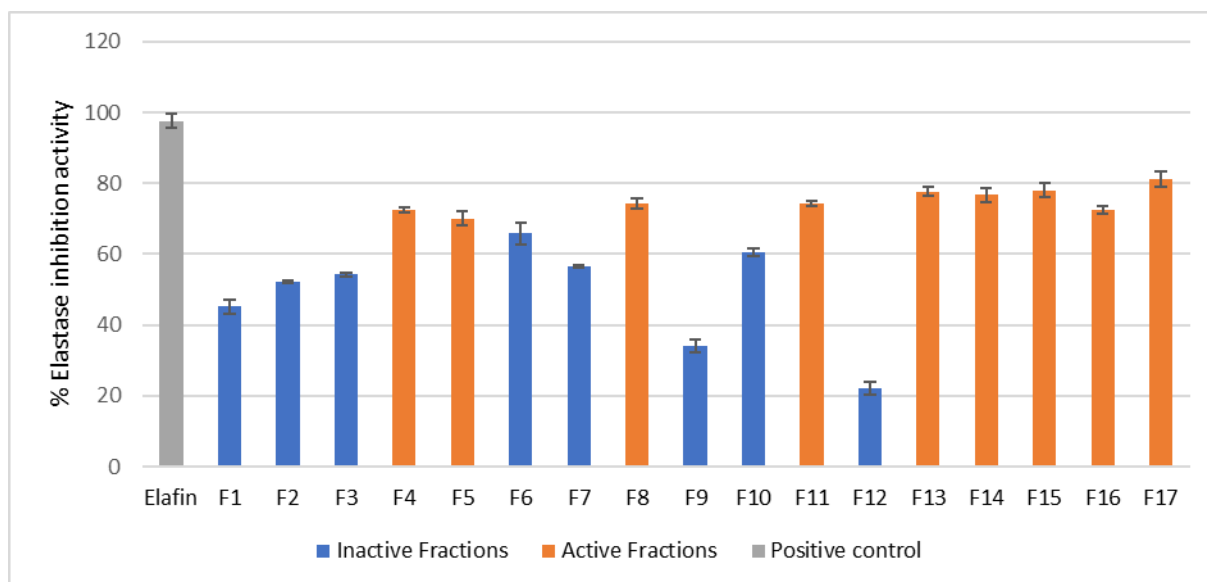


Figure 3.34. % Elastase inhibition activity of *F. sycomorus* fractions at 25 µg/ml. Nine fractions; F4, F5, F8, F11, F13, F14, F15, F16, F17 showed elastase inhibition activities above 70% showing lack of selectivity. (Error bars represent SEM, with n=3).

3.7.15 UPLC-QTOF-MS analysis of active fractions

The chemical profile of active fraction F4 is shown in Figure 3.35. The most intense peak at retention time 2.57 minutes and m/z 353.0889 was previously identified in section 3.7.5 as biflorin. In addition, a peak observed at retention time 2.41 minutes and m/z 353.0883 was also previously identified in section 3.7.5 to be chlorogenic acid, based on comparison of fragmentation patterns of this peak with that of chlorogenic acid. The peak at retention time 0.61 minutes and m/z 353.0891 was previously identified to be isobiflorin while the peak at retention time 2.76 minutes and m/z 593.1487 was previously identified as vicenin-2. The chemical profile of active fractions F5 and F8 are given in Figure 3.32 above. The compounds identified in fractions F4, F5 and F8 which include chlorogenic acid, biflorin, isobiflorin, isoquercetin and vicenin 2 were screened in the elastase inhibition assay in section 3.7.15.

The results showed that none of these compounds showed activity. The lack of activity in these pure compounds while the fractions exhibit activity suggests that activity was due to synergistic effects and this was lost upon fractionation. Fractions F11 to F17 were constituted of mainly non-polar compounds which were obtained in low quantities, the constituents of the fractions were thus difficult to identify.

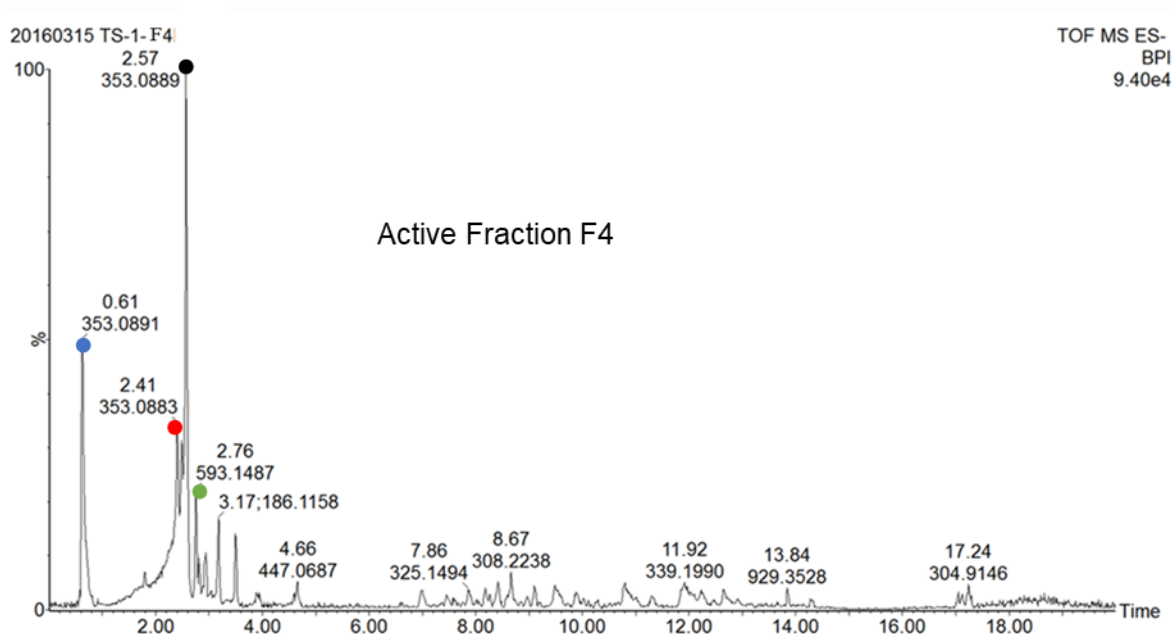


Figure 3.35. ESI negative mode BPI chromatograms of fraction F4. ● Biflorin (at retention time 2.57 minutes and m/z 353.0889), ● chlorogenic acid (retention time 2.41 minutes and m/z 353.0883), ● isobiflorin (peak at retention time 0.61 minutes at m/z 353.0891), ● vicenin-2, (retention time 2.76 minutes at m/z 593.1487) identified from fraction F4 were likely to contribute to the anti-aging activity of fraction F4.

3.7.16 Elastase inhibition activity of pure compounds

The compounds confirmed to be present in *F. sycomorus* leaf ethanol extract through pure standards and those isolated from the extract were screened for elastase inhibition activity at test concentrations of 5, 10 and 20 $\mu\text{g/ml}$. These compounds were palatinose, quinic acid, isobiflorin, biflorin, chlorogenic acid, rutin, isoquercetin, and vicenin-2. The positive control elafin had $99.24\% \pm 0.097$ elastase inhibition activity while all the compounds screened showed limited activity of ($< 20\%$) and showed significantly lower ($p > 0.01$) elastase inhibition

activities than elafin at all concentrations tested (Figure 3.35). Previous studies confirmed the limited or lack of activity of quinic acid, rutin and chlorogenic acid, isoquercetin [47-51] in the elastase assay. Thus, the elastase inhibition activities exhibited by the crude extract and the fractions may be a result of synergistic effects which were lost upon isolation of compounds.

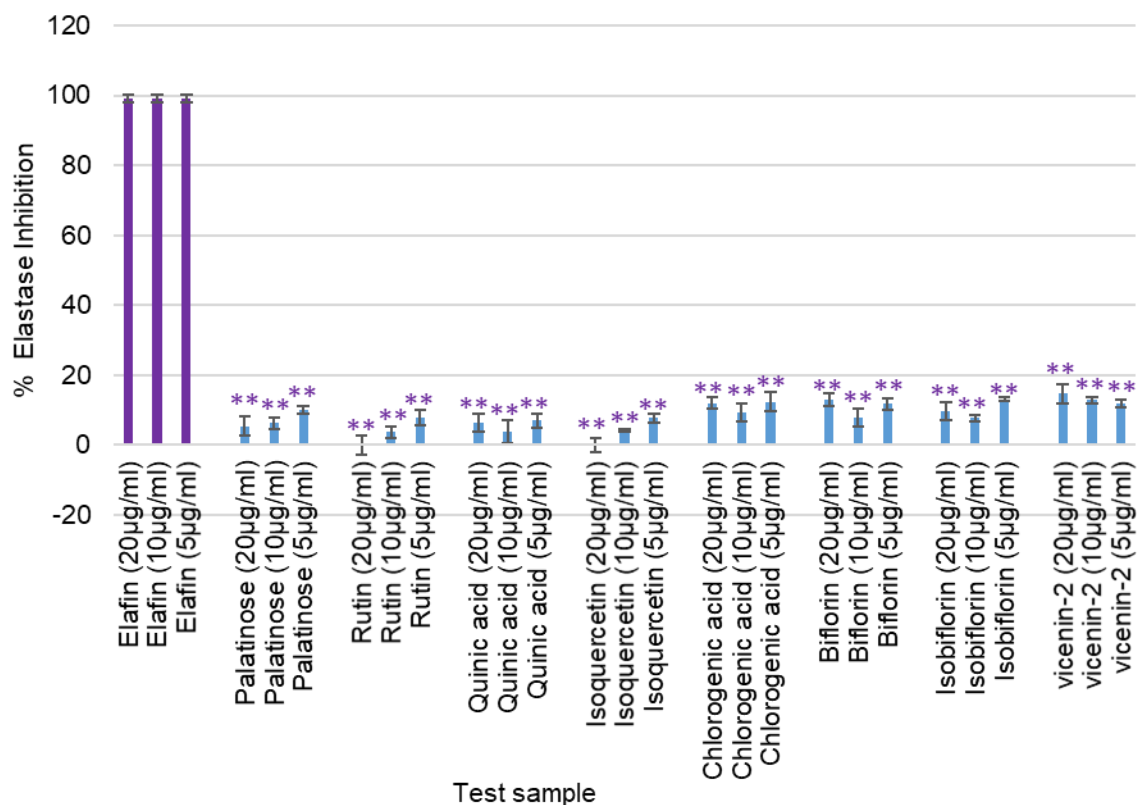


Figure 3.36. Elastase inhibition activities of major compounds identified in *F. sycomorus* ethanol extract at 20, 10 and 5 µg/ml. (Error bars represent SEM, with n=3). ** = P<0.01 represents a significant difference with elafin.

3.8 CONCLUSIONS

Leaves of the Sycamore tree have for the first time been shown to exhibit elastase and collagenase inhibition activities and thus validating its traditional use for anti-aging purposes and showing potential for further development into anti-aging ingredients. The active constituents of leaves of *F. sycomorus* were concentrated in the more polar ethanol and methanol sequential and methanol:DCM (1:1) extracts for both the elastase and collagenase

inhibition. Based on these activities and acceptability to the cosmetic industry, the ethanol extract of leaves of the Sycamore tree was selected as the most appropriate extract for further research and development, thus, achieving the first objective of this chapter. The use of water as an extraction solvent could also be further investigated in the future.

Sequential extraction successfully extracted compounds based on polarity and produced an extract with good anti-aging activity. The chemical profile for the ethanol extract of leaves of *F. sycomorus* was developed for quality control purposes achieving the second objective of this chapter. Nine compounds were identified from ethanol extracts of leaves of *F. sycomorus*. The presence of five of these palatinose, quinic acid, chlorogenic acid, rutin and isoquercetin was confirmed using pure standards on UPLC-QTOF-MS. The presence of vicenin-2, biflorin and isobiflorin was confirmed through isolation, purification and structure elucidation using NMR while quercetin-3-glucuronide was tentatively identified. This is the first report of the presence of palatinose, quinic acid, isobiflorin, chlorogenic acid, biflorin, vicenin 2, quercetin-3-glucuronide in the *F. sycomorus* plant.

The defatting step lowered the colour intensity and improved the collagenase inhibition activity of the *F. sycomorus* ethanol extract thus achieving the third objective of this chapter. Upon *in vitro* screening of pure compounds identified and those isolated from the ethanol extract of leaves of the Sycamore tree in the collagenase assay and elastase assays, isoquercetin showed collagenase inhibition activity at a low concentration of 10 µg/ml thus achieving the fourth objective of this chapter. This is the first time isoquercetin has been shown to exhibit potent collagenase inhibition activity. Thus, isoquercetin showed potential for further development into anti-aging ingredients. In the elastase assay, the ethanol extract of leaves of the Sycamore tree and its fractions showed activity but upon screening pure compounds, none of the compounds showed activity showing that activity in the extract and the fractions was due to synergistic effects that was lost upon fractionation or as single chemical entities.

Consequently, synergism was lost upon isolation of compounds, hence, the lack of activity upon screening pure compounds.

3.9 REFERENCES

1. Abu-Mustafa EA, H. El-Tawil BA, Fayez MBE: **Constituents of local plants—IV.: Ficus carica L., F. sycomorus L. and F. salicifolia L. leaves.** *Phytochemistry* 1963, **3(6):701-703.**
2. Garba S, Prasad J, Sandabe U: **Histomorphological effect of the aqueous root-bark extract of Ficus sycomorus (Linn) on the liver and kidney of albino rats.** *International Journal of Pharmacology* 2006, **2:628-632.**
3. **The Plant List (2013), <http://www.theplantlist.org/> (Version 1.1) (Accessed 1 July 2018)**
4. Hassan S, Lawal M, Muhammad B, Umar R, Bilbis L, Faruk U, Ebbo A: **Antifungal activity and phytochemical analysis of column chromatographic fractions of stem bark extracts of Ficus sycomorus L (Moraceae).** *J. Plant Science* 2007, **2(2):209-215.**
5. Ramde-Tiendrebeogo A, Tibiri A, Hilou A, Lompo M, Millogo-Kone H, Nacoulma OG, Guissou IP: **Antioxidative and antibacterial activities of phenolic compounds from Ficus sur Forssk. and Ficus sycomorus L.(Moraceae): potential for sickle cell disease treatment in Burkina Faso.** *International Journal of Biological and Chemical Sciences* 2012, **6(1):328-336.**
6. Galil J, Eisikowitch D: **Flowering cycles and fruit types of Ficus sycomorus in Israel.** *New Phytologist* 1968, **67(3):745-758.**
7. Nkafamiya I, Osemeahon S, Modibbo U, Aminu A: **Nutritional status of non-conventional leafy vegetables, Ficus asperifolia and Ficus sycomorus.** *African Journal of Food Science* 2010, **4(3):104-108.**
8. Galil J, Eisikowitch D: **On the pollination ecology of Ficus sycomorus in East Africa.** *Ecology* 1968, **49(2):259-269.**
9. Galvez J, Zarzuelo A, Crespo M, Utrilla M, Jimenez J, Spiessens C, de Witte P: **Antidiarrhoeic activity of Sclerocarya birrea bark extract and its active tannin constituent in rats.** *Phytotherapy Research* 1991, **5(6):276-278.**
10. Proffit M, Johnson S: **Specificity of the signal emitted by figs to attract their pollinating wasps: comparison of volatile organic compounds emitted by receptive syconia of Ficus sur and F. sycomorus in Southern Africa.** *South African Journal of Botany* 2009, **75(4):771-777.**
11. Bekheet SH, Abdel-Motaal FF, Mahalel UA: **Antifungal effects of Ficus sycomorus and Pergularia tomentosa aqueous extracts on some organs in Bufo regularis treated with Aspergillus niger.** *Tissue and Cell* 2011, **43(6):398-404.**
12. Lansky EP, Paavilainen HM, Pawlus AD, Newman RA: **Ficus spp.(fig): Ethnobotany and potential as anticancer and anti-inflammatory agents.** *Journal of Ethnopharmacology* 2008, **119(2):195-213.**
13. Ahmadua A, Zezi A, Yaro A: **Anti-diarrheal activity of the leaf extracts of Daniellia oliveri hutch and Dalz (Fabaceae) and ficus sycomorus Miq (Moraceae).** *African Journal of Traditional, Complementary and Alternative Medicines* 2007, **4(4):524-528.**
14. Zaku S, Abdulrahman F, Onyeyili P, Aguzue O, Thomas S: **Phytochemical constituents and effects of aqueous root-bark extract of Ficus sycomorus L.(Moraceae) on muscular relaxation, anaesthetic and sleeping time on laboratory animals.** *African Journal of Biotechnology* 2009, **8(21).**
15. Olusesan AG, Ebele OC-L, Onwuegbuchulam ON, Olorunmolaa EJ: **Preliminary in-vitro antibacterial activities of ethanolic extracts of Ficus sycomorus Linn. and**

- Ficus platyphylla Del.(Moraceae).** *African Journal of Microbiology Research* 2010, **4**(8):598-601.
16. Mousa O, Vuorela P, Kiviranta J, Wahab SA, Hiltunen R, Vuorela H: **Bioactivity of certain Egyptian Ficus species.** *Journal of Ethnopharmacology* 1994, **41**(1-2):71-76.
 17. El-Sayed MM, Mahmoud M, El-Nahas H, El-Toumy S, El-Wakil EA, Ghareeb M: **Bio-guided isolation and structure elucidation of antioxidant compounds from the leaves of Ficus sycomorus.** *Pharmacologyonline* 2010, **3**:317-332.
 18. Abdel-Hameed E-SS: **Total phenolic contents and free radical scavenging activity of certain Egyptian Ficus species leaf samples.** *Food chemistry* 2009, **114**(4):1271-1277.
 19. Sandabe U, Onyeyili P, Chibuzo G: **Phytochemical screening and effect of aqueous extract of Ficus sycomorus L.(Moraceae) stem bark on muscular activity in laboratory animals.** *Journal of Ethnopharmacology* 2006, **104**(1):283-285.
 20. Sandabe UK, Onyeyili PA, Chibuzo GA: **Sedative and anticonvulsant effects of aqueous extract of Ficus sycomorus L.(Moraceae) stem bark in rats.** *Veterinarski arhiv* 2003, **73**(2):103-110.
 21. Kraunsoe JA, Claridge TD, Lowe G: **Inhibition of human leukocyte and porcine pancreatic elastase by homologues of bovine pancreatic trypsin inhibitor.** *Biochemistry* 1996, **35**(28):9090-9096.
 22. Moore S, Stein WH: **Photometric nin-hydrin method for use in the chromatography of amino acids.** *Journal of Biological Chemistry* 1948, **176**:367-388.
 23. Mandl I, MacLennan JD, Howes EL, DeBellis RH, Sohler A: **Isolation and characterization of proteinase and collagenase from Cl. histolyticum.** *The Journal of Clinical Investigation* 1953, **32**(12):1323.
 24. Louvel S, Moodley N, Seibert I, Steenkamp P, Nthambeleni R, Vidal V, Maharaj V, Klimkait T: **Identification of compounds from the plant species Alepidea amatymbica active against HIV.** *South African Journal of Botany* 2013, **86**:9-14.
 25. De Azevedo A, Mazzafera P, Mohamed R, Melo S, Kieckbusch TG: **Extraction of caffeine, chlorogenic acids and lipids from green coffee beans using supercritical carbon dioxide and co-solvents.** *Brazilian Journal of Chemical Engineering* 2008, **25**(3):543-552.
 26. Li S, Han Q, Qiao C, Song J, Cheng CL, Xu H: **Chemical markers for the quality control of herbal medicines: an overview.** *Chinese Medicine* 2008, **3**(1):7.
 27. Guan B, Cole RB: **MALDI linear-field reflectron TOF post-source decay analysis of underivatized oligosaccharides: determination of glycosidic linkages and anomeric configurations using anion attachment.** *Journal of the American Society for Mass Spectrometry* 2008, **19**(8):1119-1131.
 28. Saldanha LL, Vilegas W, Dokkedal AL: **Characterization of flavonoids and phenolic acids in Myrcia bella cambess. Using FIA-ESI-IT-MSn and HPLC-PAD-ESI-IT-MS combined with NMR.** *Molecules* 2013, **18**(7):8402-8416.
 29. Yang SJ, Ryu JH, Jang DS, Yang L, Han H-K: **A sensitive LC-MS/MS method for the quantitative determination of biflorin in rat plasma and its application to pharmacokinetic studies.** *Journal of pharmaceutical and biomedical analysis* 2015, **115**:272-276.
 30. Fu Z, Ling Y, Li Z, Chen M, Sun Z, Huang C: **HPLC-Q-TOF-MS/MS for analysis of major chemical constituents of Yinchen-Zhizi herb pair extract.** *Biomedical Chromatography* 2014, **28**(4):475-485.
 31. Parejo I, Jauregui O, Sánchez-Rabaneda F, Viladomat F, Bastida J, Codina C: **Separation and characterization of phenolic compounds in fennel (Foeniculum vulgare) using liquid chromatography- negative electrospray ionization tandem mass spectrometry.** *Journal of Agricultural and Food Chemistry* 2004, **52**(12):3679-3687.

32. Silva DB, Turatti ICC, Gouveia DR, Ernst M, Teixeira SP, Lopes NP: **Mass spectrometry of flavonoid vicenin-2, based sunlight barriers in *Lychnophora* species.** *Scientific reports* 2014, **4**.
33. Gouveia DR, Buqui GA, Lopes JLC, Diniz A, Lopes NP: **An UPLC-MS/MS Method for Determination of Vicenin-2 and Lychnopholic Acid in Rat Plasma and its Application to a Pharmacokinetic Study.** *Journal of the Brazilian Chemical Society* 2017, **28**(3):427-434.
34. He W, Liu X, Xu H, Gong Y, Yuan F, Gao Y: **On-line HPLC-ABTS screening and HPLC-DAD-MS/MS identification of free radical scavengers in *Gardenia (Gardenia jasminoides Ellis)* fruit extracts.** *Food Chemistry* 2010, **123**(2):521-528.
35. Dueñas M, Mingo-Chornet H, Pérez-Alonso JJ, Di Paola-Naranjo R, González-Paramás AM, Santos-Buelga C: **Preparation of quercetin glucuronides and characterization by HPLC-DAD-ESI/MS.** *European Food Research and Technology* 2008, **227**(4):1069-1076.
36. Madala NE, Piater L, Dubery I, Steenkamp P: **Distribution patterns of flavonoids from three *Momordica* species by ultra-high performance liquid chromatography quadrupole time of flight mass spectrometry: a metabolomic profiling approach.** *Revista Brasileira de Farmacognosia* 2016, **26**(4):507-513.
37. Zhang Y, Chen Y: **Isobiflorin, a chromone C-glucoside from cloves (*Eugenia caryophyllata*).** *Phytochemistry* 1997, **45**(2):401-403.
38. Oya T, Osawa T, Kawakishi S: **Spice constituents scavenging free radicals and inhibiting pentosidine formation in a model system.** *Bioscience, biotechnology, and biochemistry* 1997, **61**(2):263-266.
39. Ghosal S, Kumar Y, Singh S, Ahad K: **Biflorin, a chromone-C-glucoside from *Pancreatium biflorum*.** *Phytochemistry* 1983, **22**(11):2591-2593.
40. Chang X, Li W, Koike K, Wu L, Nikaido T: **Phenolic constituents from the rhizomes of *Dryopteris crassirhizoma*.** *Chemical and Pharmaceutical Bulletin* 2006, **54**(5):748-750.
41. Velozo LS, Ferreira MJ, Santos MIS, Moreira DL, Guimarães EF, Emerenciano VP, Kaplan MAC: **C-glycosyl flavones from *Peperomia blanda*.** *Fitoterapia* 2009, **80**(2):119-122.
42. Lu Y, Foo LY: **Flavonoid and phenolic glycosides from *Salvia officinalis*.** *Phytochemistry* 2000, **55**(3):263-267.
43. Islam MN, Ishita IJ, Jung HA, Choi JS: **Vicenin 2 isolated from *Artemisia capillaris* exhibited potent anti-glycation properties.** *Food and chemical toxicology* 2014, **69**:55-62.
44. Xie C, Veitch NC, Houghton PJ, Simmonds MS: **Flavone C-glycosides from *Viola yedoensis* Makino.** *Chemical and pharmaceutical bulletin* 2003, **51**(10):1204-1207.
45. Marrassini C, Davicino R, Acevedo C, Anesini C, Gorzalczy S, Ferraro G: **Vicenin-2, a potential anti-inflammatory constituent of *Urtica circularis*.** *Journal of Natural Products* 2011, **74**(6):1503-1507.
46. Nagaprashantha LD, Vatsyayan R, Singhal J, Fast S, Roby R, Awasthi S, Singhal SS: **Anti-cancer effects of novel flavonoid vicenin-2 as a single agent and in synergistic combination with docetaxel in prostate cancer.** *Biochemical Pharmacology* 2011, **82**(9):1100-1109.
47. Teramachi F, Koyano T, Kowithayakorn T, Hayashi M, Komiyama K, Ishibashi M: **Collagenase Inhibitory Quinic Acid Esters from *Ipomoea pes-caprae*.** *Journal of Natural Products* 2005, **68**(5):794-796.
48. Melzig M, Löser B, Ciesielski S: **Inhibition of neutrophil elastase activity by phenolic compounds from plants.** *Die Pharmazie* 2001, **56**(12):967-970.
49. Park CH, Ahn MJ, Hwang GS, An SE, Whang WK: **Cosmeceutical bioactivities of isolated compounds from *Ligularia fischeri* Turcz leaves.** *Applied Biological Chemistry* 2016, **59**(3):485-494.

50. Xu G-H, Ryoo I-J, Kim Y-H, Choo S-J, Yoo I-D: **Free radical scavenging and antielastase activities of flavonoids from the fruits of Thuja orientalis.** *Archives of Pharmacal Research* 2009, **32**(2):275-282.
51. Kim SY, Kim JE, Bu HJ, Hyun C-G, Lee NH: **Chemical constituents of Tilia taquetii leaves and their inhibition of MMP-1 expression and elastase activities.** *Natural Product Communications* 2014, **9**(12):1683-1685.

CHAPTER 4: COMBINATION AND FORMULATION STUDIES

4.1 INTRODUCTION

This chapter discusses the anti-aging effect on the combination of the Marula and Sycamore extracts and targeted their formulation into herbal cosmetic products for facial skin care as part of proof of concept studies. Based on the anti-aging properties and the improvements on the extracts discussed in the Chapters 2 and 3, the defatted and concentrated ethanol extract of Marula stem extract (**coded MDC extract**) and the defatted ethanol extract of *F. sycamorus* (**coded FD extract**) were selected as ingredients for the combination studies and formulation.

4.2 COMBINATION STUDIES

The Marula extract (coded MDC) and the Sycamore extract (coded FD) extracts were screened in sections 2.7.7 and 3.7.8 respectively and results revealed that the extracts were not active at 10 µg/ml in both the elastase and the collagenase assays while the positive controls exhibited activity at this concentration. Consequently, lower potency would mean more extract should be added to the formulation to achieve the required level of activity. Therefore, to attempt to improve potency of the extracts of the two plants to the same efficacy range as the positive controls at 10 µg/ml, a combination of the relevant active extracts and compounds could be used as ingredients. To evaluate this, the Marula MDC and the Sycamore FD extracts were combined in equal portions (ratio 1:1). Further, a separate combination the FD extract with the pure compounds epigallocatechin gallate (EGCg) and epicatechin gallate (ECg) was done in a 10:0.1:0.1 ratio. The rationale being that EGCg and ECg have been identified in section 2.7.12 to be highly potent inhibitors of collagenase in Marula stems. Thus, a combination of these compounds with the FD extract and the

combination of the MDC:FD extracts in a 1:1 ratio were evaluated for their potential to improve the anti-aging activity.

4.3 FORMULATION STUDIES

Formulation studies were aimed at developing product prototypes of an anti-aging day cream and a nourishing night cream containing the *F. sycomorus* extract (FD extract) and the Marula extract (MDC extract) as the active anti-aging ingredients. The cosmetic development process was done by mixing the cosmetic ingredients with the FD extract and the MDC extract in appropriate ratios as determined by the screening results and the appropriate combination producing the most stable products for market sample evaluations. Consequently, constant formulation improvements were carried out during prototype development.

4.4 METHODOLOGY

4.4.1 Preparation of mixtures

The MDC extract and the FD extracts were combined in the ratios (1:1) and the FD extract: epicatechin gallate: epigallocatechin gallate were combined in the ratio (10:0.1:0.1). The details on the procedures and quantities are given in Chapter 5.

4.4.2 Bioassay of the combinations/mixtures

The method according to Kraunsoe et al. [1] with a few modifications was used to determine anti-elastase inhibition activity. The elastase substrate N-Methoxysuccinyl-Ala-Ala-Pro-Val-*p*-nitroaniline is catalysed by the human leucocyte elastase (HLE) to give a yellow coloured product, *p*-nitroaniline which is detected by absorbance at 405 nm on a Tecan infinite 500 spectrophotometer. In this assay, in the presence of an inhibitor, the enzyme HLE is inhibited and the breakdown of the substrate proceeds at its natural rate of reaction, as such the yellow coloured product *p*-nitroaniline is not formed, hence there will be no colour change. Anti-

collagenase inhibition was determined according to Moore and Stein's method [2] incorporating modifications by Mandl et al. [3]. Collagen is degraded by the enzyme collagenase to produce peptides which react with ninhydrin to give a blue coloured product detected by absorbance at 540 nm on a Tecan Infinite 500 spectrophotometer. In the presence of an inhibitor the enzyme collagenase will not catalyse the reaction, hence the breakdown of collagenase will proceed at its natural rate of reaction and there will be no colour change.

All enzyme assays were done in triplicate. MS Excel was used to analyse the enzyme assay results which were presented as percentage inhibition. The results given in Figures 4.1 and 4.2 are shown as mean \pm standard error of the mean (SEM). The Student's t-test function in Excel was used to compare the significance of the differences between the activity of the positive controls, the crude extracts and the combined extracts.

4.4.3 Formulation of the anti-aging day cream at lab scale

The formulation was done using a standard method and carried out by premixing individual ingredients as part A; deionised water (diluent), disodium EDTA (stabiliser) and xanthum gum (thickener), part B; emulsifying wax (emulsifier), liponate NEB (emollient), beeswax (emulsifier), Parsol MCX (UVB absorber) and cocoa butter (emollient); part C; titanium dioxide (UVA/B protector), dimethicone (conditioner/ emollient) and 99% TEA (chelating agent) and part D; vitamin E acetate (anti-oxidant), MDC extract (1.0%), FD extract (0.5%), spearmint fragrance (fragrance), Marula fragrance (fragrance) (which had been purchased) and euxyl K100 (preservative). Detailed mixing quantities and procedures are given in Chapter 5.

4.4.4 Formulation of the nourishing night cream at lab scale

Preparation using a standard method was done by premixing the individual ingredients as part A; deionised water, disodium EDTA and xanthum gum, part B; emulsifying wax, tegosoft TN (emollient), beeswax and cocoa butter and part C; coconut oil (conditioner), glycerine (humectant), vitamin E acetate (antioxidant), MDC extract (1.0%), FD extract (0.5%),

spearmint fragrance and Marula fragrance (procured) and part D; euxyl K100. Detailed preparation procedures are given in Chapter 5.

4.4.5 Formulation of the anti-aging day cream at kilogram scale

The formulation was carried out by pre-mixing the individual ingredients as part A; deionised water, disodium EDTA, xanthum gum and 99% TEA, part B emulsifying wax, liponate NEB, beeswax, Parsol MCX, Parsol 1789 (UVA absorber) and cocoa butter, part C; titanium dioxide and dimethicone, part D; Vitamin E acetate, Marula extract (MDC extract), *F. sycomorus* (FD extract), Marula fragrance (purchased) and Euxyl K100. Detailed preparation procedures are given in Chapter 5.

4.4.6 Formulation of nourishing night cream at kilogram scale

The formulation was carried out by premixing the individual ingredients in part a; deionised water, disodium EDTA and xanthum gum, part b; emulsifying wax, tegosoft TN, beeswax and cocoa butter, part C; coconut oil, glycerine, vitamin E acetate, Marula extract (MDC extract), *F. sycomorus* extract (FD extract), spearmint fragrance, Marula fragrance and part D; euxyl D. Detailed preparation procedures are given in Chapter 5.

4.5 RESULTS AND DISCUSSION

4.5.1 Bioassay of the combinations/mixtures

4.5.1.1 Collagenase inhibition activity

The efficacy of the FD:MDC mix (1:1), FD extract:EGCg:ECg (10:0.1:0.1) combination and the separate MDC and FD extracts was evaluated in the collagenase assay at 10 and 100 µg/ml. The results revealed that at 100 µg/ml the collagenase inhibition activities of the combinations FD extract:MDC extract (1:1) and the FD extract: EGCg:ECg (10:0.1:0.1) showed good collagenase inhibition activities of 84.56% ± 1.73 and 82.79% ± 1.23 which was as potent as EDTA (88.23% ± 0.68) ($p > 0.05$) (Figure 4.1). In comparison, the MDC extract was significantly

more potent ($0.01 < p < 0.05$) than the positive control EDTA clearly showing that this separate extract exhibited more potency than both the FD:MDC (1:1) mixture and the FD:EGCg:ECg (10:0.1:0.1) mixture at 100 $\mu\text{g/ml}$. On the other hand, the FD extract had the same level of potency ($p > 0.05$) as the positive control showing that the FD extract, the FD:MDC (1:1) mixture and the FD:EGCg:ECg (10:0.1:0.1) mixture exhibited the same levels of potency when tested at 100 $\mu\text{g/ml}$. At the lower concentration of 10 $\mu\text{g/ml}$ all combinations showed collagenase inhibitions of $< 3\%$ which was significantly ($p < 0.01$) lower than that of EDTA ($88.23\% \pm 0.68$). The results revealed that mixing the FD and the MDC extracts and the FD extract and the active compounds from Marula stems (EGCg and ECg) did not improve the collagenase inhibition activities of the extracts at 10 $\mu\text{g/ml}$ but maintained equivalent levels of potency as EDTA at 100 $\mu\text{g/ml}$.

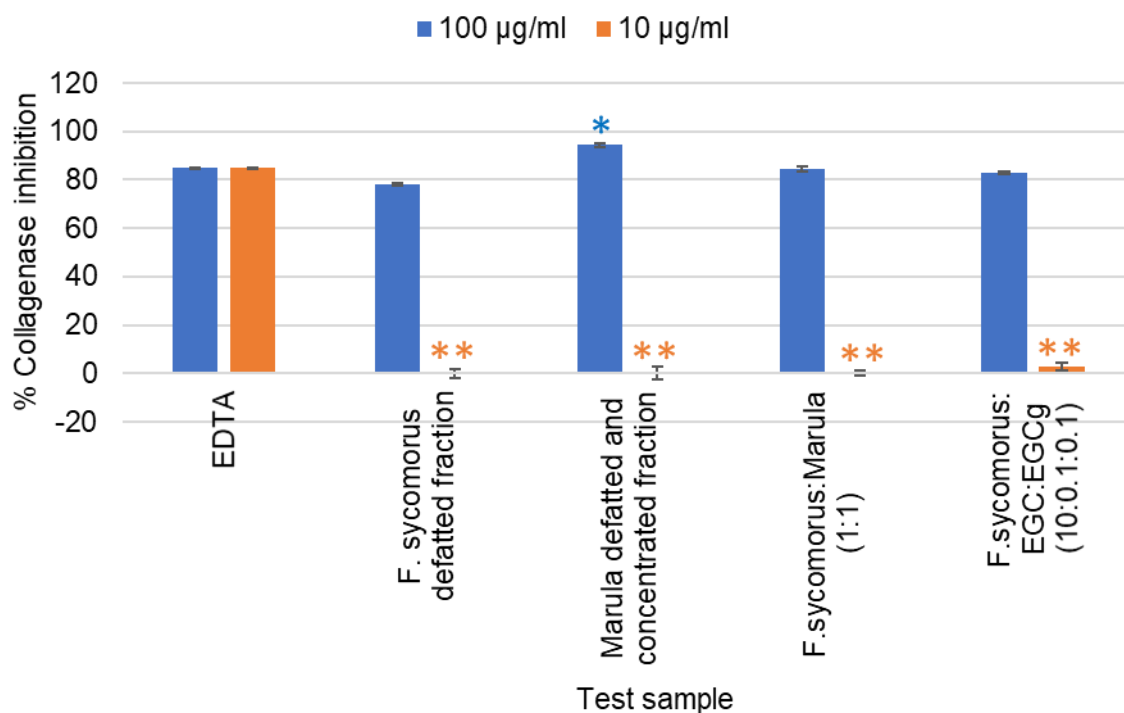


Figure 4.1. Collagenase inhibition of combinations of defatted *F. sycomorus* and Marula defatted and concentrated fractions screened at 100 and 10 $\mu\text{g/ml}$ (Error bars represent SEM, with $n=3$). ** = $P < 0.01$ represent a significant difference with EDTA at 10 $\mu\text{g/ml}$ * = $P < 0.01$ represent a significant difference with EDTA at 100 $\mu\text{g/ml}$.

4.5.1.2 Elastase inhibition activity

The potency of the FD:MDC mix (1:1), FD extract:EGCg:ECg (10:0.1:0.1) combination and the separate MDC and FD extracts was evaluated in the elastase assay at 10 and 100 $\mu\text{g/ml}$. Results of the elastase inhibition activity showed that at 100 $\mu\text{g/ml}$ the FD:MDC (1:1) combination had an elastase inhibition activity of $84.10\% \pm 0.58$ which was significantly lower than ($p < 0.01$) than elafin ($99.15\% \pm 0.079$) (Figure 4.2). The separate FD extract and the MDC extracts also had elastase inhibition activities which significantly were lower than that of ($p < 0.01$) elafin revealing that the FD extract, the MDC extract and the FD:MDC (1:1) extract were in the same potency range. At 10 $\mu\text{g/ml}$ all the extracts exhibited elastase inhibition activities of ($< 31\%$) which was significantly lower ($p < 0.01$) than that of elafin ($99.15\% \pm 0.079$). The results reveal that similar to the collagenase inhibition assay, the combination of the extracts did not improve the elastase inhibition activity of the extracts at both the lower (10 $\mu\text{g/ml}$) and the higher concentration (100 $\mu\text{g/ml}$). The pure compounds EGCg and ECg were screened for elastase inhibition activity and showed no activity (section 2.7.14). Thus, these compounds were not expected to improve the elastase inhibition activity of the FD:EGCg:ECg (10:0.1:0.1) mixture. Consequently, the FD:EGCg:ECg (10:0.1:0.1) mixture was not screened in the elastase inhibition assay.

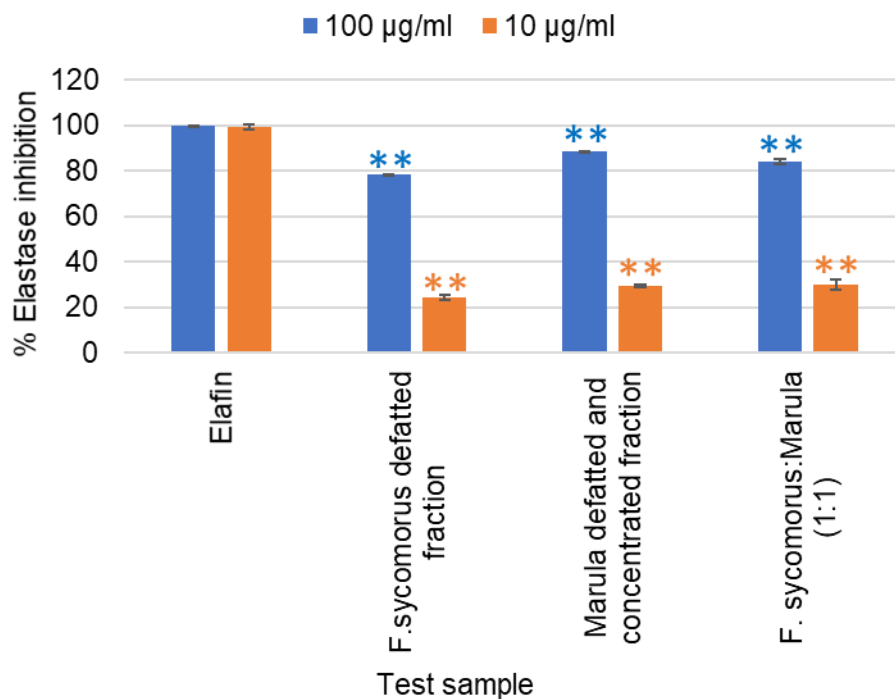


Figure 4.2. Elastase inhibition of combinations of defatted *F. sycomotorus* and Marula defatted and concentrated fractions screened at 100 and 10 µg/ml (Error bars represent SEM, with n=3). ** = P<0.01 represent a significant difference with EDTA at 10 µg/ml ** = P<0.01 represent a significant difference with EDTA at 100 µg/ml.

4.5.2 Anti-aging day cream-SPF 20

Bioassay results of the combined extracts revealed that the FD:MDC (1:1) mixture was in the same potency range as the FD extract while the MDC extract exhibited higher potency than the FD:MDC mixture in the collagenase assay. Consequently, formulation was done by adding more of the MDC extract than the FD extract to ensure higher anti-aging activity. Constant formulation improvements were carried out during prototype development. The dosage of Marula extract was increased from 0.50% to 1.0% and finally the dosage of *F. sycomotorus* extract was increased from 0.20% to 0.50% to produce a product with the desired consistency and to improve on the stability of the products. Marula fragrance was added at 0.50% in the final product. The changes resulted in better mixing technique in preparation for commercial scale batch production.

The product development process was initiated at lab scale. A light creamy texture was developed in anticipation for better moisturisation during and after application on face. This compared very well on product attributes (appearance, product feel during and after application). The final packaging for the anti-ageing day cream SPF 20 was a 250 ml chemically inert glass jar with cap (Figure 4.3). The approved prototype was prepared at kilogram scale for future evaluation of shelf life, compatibility, microbiological and dermal safety studies outside the scope of this study.



Figure 4.3. Anti-ageing day cream SPF-20 prototype

4.5.3 Nourishing night cream

The product development process evolved from prototype 1 – first generation to prototype 2- second generation prototype. Similar to the anti-aging day cream, formulation was done by adding more of the MDC extract than the FD extract to ensure higher anti-aging activity. As a result, the dosage of Marula extract (MDC extract) was at 1.0% throughout the product prototyping stages and finally the dosage of the *F. sycomorus* extract (FD) extract was

increased from 0.2% to 0.5% to produce the desired product consistency. The Marula fragrance was added at the level 0.25% in the final product. A light creamy texture was required for better moisturization during and after application on face. The nourishing cream compared very well on product attributes (appearance, product feel during and after application). Similar to the anti-aging day cream SPF-20, the final packaging for the nourishing night cream was also selected as 250 ml chemically inert glass jars with cap (Figure 4.4). The approved prototype 2 was prepared at kilogram scale for the evaluation of shelf life, compatibility, microbiological and dermal safety studies.



Figure 4.4. Nourishing night cream prototype

4.6 CONCLUSION

In the collagenase assay, at 100 $\mu\text{g/ml}$ the combinations of the FD extract : MDC extract (1:1) and the FD extract:EGCg:ECg (10:0.1:0.1) were as potent as ($p>0.05$) EDTA while at 10 $\mu\text{g/ml}$, both combinations exhibited lower activities ($p<0.01$) than the positive control. Similarly, the FD extract was as potent as ($p>0.05$) EDTA at 100 $\mu\text{g/ml}$ but exhibited lower potency ($p<0.01$) at 10 $\mu\text{g/ml}$. In contrast, the MDC extract was more potent ($0.01<p<0.05$) than EDTA at 100 $\mu\text{g/ml}$ but exhibited lower potency ($p<0.01$) to the positive control at 10 $\mu\text{g/ml}$. These

results revealed that in the collagenase assay, the FD:MDC (1:1) mixture and the FD extract:EGCg:ECg (10:0.1:0.1) had the same potency as the FD separate extract but were less potent than the MDC extract at 100 µg/ml. Further, combining the FD and the MDC extracts and the FD extract and the active compounds from Marula stems (EGCg and ECg) did not improve the collagenase inhibition activities of the extracts at 10 µg/ml but maintained equivalent levels of potency as EDTA at 100 µg/ml. In the elastase assay, the FD:MDC (1:1) mixture, the FD extract:EGCg:ECg (10:0.1:0.1) and the separate FD and MDC extracts were less potent ($p < 0.01$) than EDTA at both 10 and 100 µg/ml revealing that the combinations did not improve elastase inhibition activities of the extracts. Based on the higher potency of the MDC extract to the combinations in the collagenase assay, the prototypes were formulated by adding a higher proportion of the MDC extract than the FD extract in an appropriate combination producing a stable product. The prototypes were successfully developed for proof of concept, the project will proceed beyond the scope of these studies to evaluate the formulations for shelf life, compatibility, microbiology and dermal safety studies.

4.7 REFERENCES

1. Kraunsoe JA, Claridge TD, Lowe G: **Inhibition of human leukocyte and porcine pancreatic elastase by homologues of bovine pancreatic trypsin inhibitor.** *Biochemistry* 1996, **35**(28):9090-9096.
2. Moore S, Stein WH: **Photometric nin-hydrin method for use in the chromatography of amino acids.** *Journal of biological chemistry* 1948, **176**:367-388.
3. Mandl I, MacLennan JD, Howes EL, DeBellis RH, Sohler A: **Isolation and characterization of proteinase and collagenase from *Cl. histolyticum*.** *The Journal of Clinical Investigation* 1953, **32**(12):1323.

CHAPTER 5: METHODOLOGY

5.1 INTRODUCTION

This chapter gives a detailed methodology of all the work done in Chapters 2, 3 and 4.

5.2 CHAPTERS 2 AND 3

5.2.1 Chemicals and reagents

Elastase substrate N-Methoxysuccinyl-Ala-Ala-Pro-Val-*p*-nitroanilide (Sigma, M4765), human leukocyte elastase (Sigma, E8140), 0.1 M of 4-(2-hydroxyethyl)-1-piperazinethanesulfonic acid (HEPES, pH 7.5) (Sigma, H3375) with 0.5 M sodium chloride (Sigma, S5886), standard inhibitor, elafin (Sigma, E7280), Collagenase substrate N-[3-(2-Furyl)acryloyl]-Leu-Gly-Pro-Ala (FALGPA)(Sigma, F5135, tris(hydroxymethyl)-methyl-2-aminoethane sulfonate (TES) (Sigma, T1375) with calcium chloride dihydrate (Sigma, C3881), EDTA as the inhibitor (Sigma, E5134), Citric acid (Sigma, C0759) were procured from Sigma Aldrich. 9.8% DMSO (Sigma, D8418), 4% (w/v) Ninhydrin (Sigma, N4876), 0.16% (w/v) Tin (II) chloride (Sigma, 208256) and 50% 2-propanol (Sigma, I9616), 1% v/v 10 mg/ml BSA (Life Technologies, 30036578) were prepared in double distilled water.

Collagenase type 1 from *Clostridium histolyticum* (Life technologies, 17100-017) was purchased from Life Technologies. The pure standards epigallocatechin gallate (Sigma, E4143), epicatechin gallate (Sigma, E3893), epigallocatechin gallate (Sigma, 93894), epicatechin (Sigma, 68097), catechin (Sigma, 43412) and gallic acid (Sigma, 91215) were purchased from Sigma Aldrich. Quinic acid (Supelco, 46944-U) was purchased from Supelco. Extraction solvents were of analytical grade, ethyl acetate (Merck,1047748), acetone (Merck,1047256), dichloromethane (DCM) (Merck, 1047260), methanol (Merck, 1046862), ethanol absolute (Merck, 1048022), n-hexane (Merck, K47641967608) were procured from Merck. Methanol ultra LC (Romil, UN1230), acetonitrile ultra LC (Romil, UN1648) were

purchased from Microsep. Water with 0.1% formic acid LC-MS Ultra Chromasolv (Sigma,101719312) was purchased from Sigma Aldrich and filter paper Whatman number 1 (1001-50) was used. Triethanolamine (TEA 99%)(Serendipity Toiletries, 14h2185A9T1), Beeswax (Serendipity Toiletries,P14440005-001), Liponate NEB (Serendipity, P1525C16), Vitamin E Acetate (Serendipity Toiletries, UT14110326) were supplied by Serendipity Toiletries.

5.2.2 Extraction procedures

5.2.2.1 Extraction of plant material at CSIR

Dried and ground plant material (100 g) was placed in an Erlenmeyer flask (2 L), a mixture of methanol and dichloromethane (1 L) in a (1:1) ratio was added to the flask. The plant material was extracted by stirring using a magnetic stirrer continuously for 24 hours. At the end of the extraction period, filtration was carried out using a Buchner funnel connected to a vacuum pump and a filter paper. The plant residue was discarded, the organic extract was placed in a round bottomed flask and concentrated using a rotary evaporator. The concentrated plant extract was completely dried in a desiccator connected to a vacuum pump.

5.2.2.2 Separate extraction of plant material

Three portions of dried and ground plant material (100 g) were each measured in a separate Erlenmeyer flasks (2 L). To each of the three flasks was added one extraction solvent; ethanol (1 L) or acetone (1 L) or a mixture of methanol and dichloromethane (1 L) in a (1:1) ratio. The plant material was extracted by agitating each flask using a magnetic stirrer continuously for 3 hours. At the end of the extraction period, filtration was carried out using a Buchner funnel, a Buchner flask connected to a vacuum pump and a filter paper. The plant residue was discarded, the organic extract was placed in a pre-weighed round bottomed flask and concentrated using a rotary evaporator. The concentrated plant extract left in the fume hood overnight to allow for complete dryness and was stored in a cold room at 4 °C. The dried

extract was weighed, results of the dried extract and the ground plant material were used to calculate the percentage yield.

5.2.2.3 Sequential extraction of plant material

Dried and ground plant material (100 g) was measured into an Erlenmeyer flask (2 L). Hexane (1 L) was added to the flask and the mixture was continuously agitated for two hours using a magnetic stirrer. The residue and the hexane extract were separated by filtration using a Buchner funnel, a Buchner flask connected to a vacuum pump and a filter paper. The filtrate was placed in a round bottomed flask and evaporated to dryness on a rotary evaporator. After drying, the extract was weighed, and the results were used to calculate the extraction yield of the hexane extract. The residue from the hexane extract was placed in an Erlenmeyer flask (2 L) and dichloromethane (1 L) was added to the flask. The flask was continuously agitated using a magnetic stirrer bar for 2 hours. At the end of the extraction, filtration was carried out and the filtrate was placed in a pre-weighed round bottomed flask and evaporated on a rotary evaporator. The extract was then weighed, and the results used to calculate the percentage yield. The residue from the dichloromethane extraction was placed in an Erlenmeyer flask (2 L), ethyl acetate (1 L) was added to the flask. Extraction was carried out by continuous agitation using a magnetic stirrer for 2 hours. At the end of the extraction, the mixture was filtered using filter paper and Buchner funnel under vacuum. The filtrate was placed in a pre-weighed round bottomed flask and concentrated using a rotary evaporator. The extract was then weighed, and the result used to calculate the percentage extraction yield. Residue from the ethyl acetate extract was placed in an Erlenmeyer flask (2 L) and methanol (1 L) was added. Extraction was carried out by continuous agitation using a magnetic stirrer for 2 hours. At the end of the extraction, the mixture was filtered, and the plant residue was discarded. The filtrate was placed in a round bottomed flask and evaporated to dryness using a rotary evaporator. The extract was weighed, and the results were used to calculate percentage yield.

5.2.3 Defatting of extracts

The plant extract (500 mg) was weighed into an Erlenmeyer flask (100 ml), the extract was dissolved in ethanol (40 ml) and water (10 ml) by sonicating for 10 minutes on an ultrasonic bath at 25 °C. The dissolved extract was transferred to a separatory funnel (200 ml) and defatted by liquid-liquid partitioning using hexane (50 ml). The hexane fraction was separated from the water:ethanol fraction. Defatting was repeated twice and the hexane fractions were combined. The water:ethanol fraction was added to a round bottomed flask and evaporated to dryness and weighed, the results were used to calculate percentage yield.

5.2.4 Concentration of actives

Compounds responsible for activity in Marula were concentrated by modifying a method used by Row and Jin [1] to extract catechins from tea. The extract (1 g) was measured into an Erlenmeyer flask and distilled water (100 ml) at 80 °C was added and the mixture was sonicated for 10 minutes. The dissolved extract was partitioned using ethyl acetate (100 ml) in an Erlenmeyer flask (250 ml). The aqueous fraction was discarded, and the ethyl acetate fraction was placed into a round bottomed flask and evaporated to dryness using a rotary evaporator. The dried concentrated actives were weighed, and the results used to calculate the percentage yield.

5.2.5 Defatting-concentration of actives

Simultaneous defatting and concentration of the Marula extract was carried out by modifying the method used by Row and Jin [1] to extract catechins from tea. The extract (1 g) was added to an Erlenmeyer flask (200 ml) and distilled water at 80 °C was added. The mixture was sonicated for 10 minutes to dissolve the extract. The dissolved extract was transferred to separatory funnel (250 ml) and partitioned using hexane (100 ml). The hexane fraction was discarded, and the water fraction was returned to the separatory funnel and further partitioned using ethyl acetate (100 ml). The water fraction was discarded, and the ethyl acetate fraction

was evaporated to dryness using a rotary evaporator. The ethyl acetate fraction (defatted-concentrated fraction) was weighed and the results were used to calculate the percentage yield.

5.2.6 Determination of anti-elastase activity

The method according to Kraunsoe et al. [2] with a few modifications was used to determine anti-elastase inhibition activity. In 96 well plates, 25 µl of HEPES buffer, 25 µl of test samples (1.4 mg/ml) and 25 µl of elastase (1 µg/ml) (0.00125 enzyme units) were added. The blank contained 75 µl HEPES buffer and the control contained 25 µl elastase and 50 µl HEPES buffer. The positive controls contained 25 µl elastase, 25 µl HEPES buffer and 25 µl elafin (10 µg/ml) or 25 µl N-Methoxysuccinyl-Ala-Ala-Pro-Chloro (10 µg/ml). The inhibitors were added in their respective wells. The solvent controls contained 25 µl elastase, 25 µl HEPES buffer and 25 µl of 10% methanol (MeOH). The test samples were added in triplicate and the experiment was done in duplicate. Since extracts contain pigments, it is possible that these may react with the reagents to give false results. Therefore, the extract controls were prepared and contained no enzyme nor substrate but 150 µl HEPES buffer and 25 µl of the extract and were treated as the experimental tubes. These were added in triplicate as well. The plates were incubated at room temperature (25 °C) for 20 minutes. To all the wells 100 µl of N-Methoxysuccinyl-Ala-Ala-Pro-Val-*p*-nitroanilide (1 mM) was added and the plates incubated further for 40 minutes at 25 °C. The final concentration of the dried extract in the test samples was therefore 200 µg/ml. A similar procedure was followed for final concentrations of 100 µg/ml (starting concentration = 0.7 mg/ml), 25 µg/ml (starting concentration 0.175 mg/ml), 20 µg/ml (starting concentration = 0.14 mg/ml), 10 µg/ml (starting concentration = 0.07 mg/ml), 5 µg/ml (starting concentration = 0.035 mg/ml).

To analyse the results, all the extract controls were subtracted from their experimental results. The control wells (enzyme and substrate) turned yellow while the blank and the inhibitors showed no colour change. As such, the extracts which showed inhibition on elastase were

recognized by low yellow colour intensity or no colour change, which in turn determined the extent of inhibition. The absorbance was read at 405 nm on a Tecan-Infinite 500 spectrophotometer.

5.2.7 Determination of anti-collagenase activity

Anti-collagenase inhibition was determined according to Moore and Stein's method [3] and modifications by Mandl et al. [4] being incorporated. In 2 ml tubes, 25 µl of collagenase (1 mg/ml) (5.5 enzyme units), 25 µl TES buffer (50 mM) with 0.36 mM calcium chloride, pH 7.4 and 25 µl of test samples (1.4 mg/ml) were added. The blank contained 75 µl TES buffer and the control contained 25 µl collagenase and 50 µl TES buffer. The positive control contained 25 µl collagenase, 25 µl TES buffer and 25 µl ethylenediaminetetraacetic acid (EDTA)(2 mg/ml), the solvent control contained 25 µl collagenase, 25 µl TES buffer and 25 µl of either 10% methanol (MeOH), 10% dimethylsulfoxide (DMSO) or 30% DMSO. The tubes were incubated in a water bath at 37 °C for 20 minutes. To all the tubes 100 µl of FALGPA (1 mM) was added and the tubes were incubated further for 60 minutes at 37 °C. The final concentration of the test samples was therefore 200 µg/ml. A similar procedure was followed for final concentrations of 100 µg/ml (starting concentration = 0.7 mg/ml), 25 µg/ml (starting concentration 0.175 mg/ml), 20 µg/ml (starting concentration = 0.14 mg/ml) and 10 µg/ml (starting concentration = 0.07 mg/ml) and 5 µg/ml (starting concentration = 0.035 mg/ml).

Extract controls were prepared and contained no enzyme nor substrate but 150 µl TES buffer and 25 µl of the extract and were treated as the experimental tubes. For the calculation of results, the extract controls were subtracted from the experimentals.

Before use, equal volumes of citrate buffer (200 mM), pH 5.0 and ninhydrin solution were combined, 200 µl of the solution was added to all the tubes and the tubes were placed in a boiling water bath for 5 minutes. The control tubes (enzyme and substrate) turned blue and there was no colour change in the blank and positive control (EDTA) tubes. As a result, the

extracts which showed inhibition on collagenase were recognized by low blue colour intensity or no colour change, which in turn determined the extent of inhibition. The tubes were left to cool down and 200 μ l of 50% isopropanol was added to each tube. The contents in the tubes were then transferred to respective wells in 48 well plates (Corning, 3548) and the absorbance was read at 540 nm on a Tecan-Infinite 500 spectrophotometer. Each test sample was done in triplicate [3, 4].

5.2.8 Statistical Analysis

All enzyme assays were done in triplicate. MS Excel was used to analyse the enzyme assay results which were presented as percentage inhibition. Enzyme assay results were given in tables as mean \pm standard deviation (SD) and in Figures as mean \pm standard error of the mean (SEM). The Student's t-test function in Excel was used to compare the significance of the differences between the activity of the positive controls and the test samples.

5.2.9 UPLC-Q-TOF-MS analysis

UPLC was performed using a Waters Acquity UPLC system (Waters Corp., MA USA), equipped with a binary solvent delivery system and an autosampler. The dried ethanol extract was reconstituted in acetonitrile with 0.1% formic acid: water with 0.1% formic acid in a (80%:20%) ratio to a concentration of 1 mg/ml. The extract was centrifuged at 10 000 g for 10 minutes to remove particles. Separation was performed on a Waters BEH C18, (2.1 mm x 100 mm, 1.7 μ m column). The mobile phase consisted of solvent A: 0.1% formic acid in purified water and solvent B: acetonitrile with 0.1% formic acid. The gradient elution was optimized as follows: 5% B (0-0.1 minutes), 5-95% B (0.1-15 minutes), 95% B (15-16.50 minutes), 95-5% B (16.50-17.50 minutes), 5% B (17.50-20 minutes). The flow rate was 0.400 ml/minutes and the injection volume was 5 μ l. The column temperature was 40 $^{\circ}$ C. The extracts and standards were run using this method.

5.2.9.1 MS Conditions

A Waters Synapt G2 high definition QTOF mass spectrometer equipped with an ESI source was used to acquire negative and positive ion data. The system was driven by MassLynx V 4.1 software (Waters Inc., Milford, Massachusetts, USA) for data acquisition. MS calibration was performed by direct infusion of 5 mM sodium formate solution at a flow rate of 10 μ l/minute and using Intellistart functionality over the mass range of 50 - 1200 Da. The MS source parameters were set as follows for both the positive and negative mode: Source temperature 110 $^{\circ}$ C, sampling cone 25 V, extraction cone 4.0 V, desolvation temperature 300 $^{\circ}$ C, cone gas flow 10 L/hour, desolvation gas flow (500 L/hour). The capillary was 2.8 kV in the positive and 2.6 kV in the negative modes.

5.2.9.2 Acquisition

Throughout all acquisitions, a 2 ng/ μ l solution of leucine enkephalin was used as the lockspray solution that was constantly infused at a rate of 2 μ l/minute through a separate orthogonal ESI probe so as to compensate for experimental drift in mass accuracy. Trap collision energies were 30 V (high) and (10 V) for the low energy.

5.2.10 Column and thin layer chromatography

Column chromatography was performed on a column of length 107 cm long and 7 cm in diameter with a reservoir of 2 L capacity. The *F. sycamorus* ethanol extract (20 g) was loaded on to the column packed with 1500 g using Kieselgel 60 (0.063-0.2 mm/70-230 mesh). The initial solvent system EtOAc:MeOH:H₂O:formic acid (FA) in the ratio 10:0.3:0.3:0.3 was used while the polarity was later increased to EtOAc:MeOH:H₂O:FA in the ratio 8:1:1:1 for the elution of the more polar compounds. Thin layer chromatography (TLC) was performed on Merck aluminium silica gel plates (60 F₂₅₄) and visualised under UV light at 254 and 320 nm. The spots on TLC plates were also detected by dipping in a vanillin stain prepared by dissolving 0.1 g of vanillin in concentrated H₂SO₄ (1 ml) and heating with a heat gun to produce

coloured spots. Further, the plates were visualised in a tank with iodine granules or heating with a gun after dipping in a solution of phosphomolybdic acid dissolved in ethanol. A total of 72 fractions were collected, three of these fractions were selected for further purification on a prep HPLC-MS.

5.2.11 Purification of compounds 1, 2 and 3 using preparative HPLC-MS

Isolation of compounds 1, 2 and 3 (biflorin, isobiflorin and vicianin-2) from the *F. sycamoros* ethanol extract was performed on a Waters chromatographic system with Waters PDA (2998) and MS detector (Waters, Milford, MA, USA). The fraction (50 mg) was dissolved in DMSO (1 ml), and the solution was filtered through a 0.22 µm membrane (Millipore). The chromatographic conditions were optimised to achieve chromatograms with good resolution. Separation was achieved on an XBridge Preparative C18 column (19 × 250 mm, i.d., 5 µm particle size, Waters) maintained at 40 °C. The mobile phase consisted of 0.1% formic acid in water (solvent A) and acetonitrile (solvent B) at a flow rate of 20 mL/min; gradient elution was applied as follows: Initial ratio 95.0% A: 5.0% B, keeping for 1 min, maintained at 95.0% A: 5.0% B for 1 min, changed to 85.0% A: 15.0% B in 1 min, to 50% A: 50% B in 6 min, changed to 10% A:90% B in 3 minutes, maintained for 0.5 min and back to initial ratio in 0.5 min. The total run time was 12 min. The injection volume was 400 µL. Data were collected using MassLynx 4.1™ (Waters, USA) software. The Preparative HPLC system was interfaced with a QDa mass spectrometer. Negative ion mode was selected. The probe temperature was set at 500 °C. The source temperature was 120 °C. The capillary and cone voltages were set to 800 and 15 V, respectively. Data was collected between 100 and 650 *m/z*. The eluents were fractionated into 250 drops/tube (about 2.5 mL) using a fraction collector. The target compounds were collected in various fractions, subsequently combined, and concentrated to give residues, which were analysed by UPLC-MS.

5.2.12 NMR

The NMR spectra for compound 1 (isobiflorin) was obtained from a Bruker Avarice III 500 MHz spectrophotometer. The compound was dissolved in deuterated methanol ($\text{CD}_3\text{OD-}d4$) (Aldrich Chemistry, Sigma-Aldrich, USA). The ^1H NMR spectrum of compound 1 was also acquired on a Bruker Avarice III HD 500 MHz NMR spectrophotometer with Prodigy Probe, the compound dissolved in deuterated acetonitrile ($\text{CD}_3\text{CN-}d3$) (Aldrich Chemistry, Sigma-Aldrich, USA). NMR data for compound 2 (biflorin) was obtained from a Bruker Avarice III 400 MHz spectrophotometer. The compound was dissolved in deuterated methanol ($\text{CD}_3\text{OD-}d4$) (Aldrich Chemistry, Sigma-Aldrich, USA). The ^1H NMR spectrum of compound 2 was also acquired on a Bruker Avarice III HD 500 MHz NMR spectrophotometer with Prodigy Probe, the compound dissolved in deuterated acetonitrile ($\text{CD}_3\text{CN-}d3$) (Aldrich Chemistry, Sigma-Aldrich, USA) and its chemical shifts were referenced to ($\delta_{\text{H}} - 2.05$). Compound 3 (vicenin-2) was analysed on a Bruker Avarice III HD 500 MHz NMR spectrophotometer with Prodigy Probe, the compound dissolved in deuterated methanol ($\text{CD}_3\text{OD-}d4$) (Aldrich Chemistry, Sigma-Aldrich, USA). The ^1H NMR spectrum of compound 3 was also obtained in deuterated dimethyl sulfoxide ($\text{DMSO-}d6$) (Aldrich Chemistry, Sigma-Aldrich, USA) on the same instrument.

The chemical shifts for the solvents used were referenced as follows; $\text{CD}_3\text{OD-}d4$ ($\delta_{\text{H}} - 3.31$; $\delta_{\text{C}} - 49.01$), $\text{CD}_3\text{CN-}d3$ ($\delta_{\text{H}} - 2.05$) and $\text{DMSO-}d6$ ($\delta_{\text{H}} - 2.52$). The chemical shifts were reported in ppm, J coupling constants in hertz (Hz) and the multiplicity of ^1H peaks are denoted with corresponding letters in italics as follows *s*: singlet, *d*: doublet, *dd*: doublet of doublets, *t*: triplet, *m*: multiplet.

5.2.13 Chemical profiling

Compounds were tentatively identified by generating molecular formulas from MassLynx V 4.1 based on their iFit value, and by comparison of MS/MS fragmentation pattern with that of matching compounds from Metlin, Metfusion, ChemSpider and Massbank libraries. Additionally, acquired accurate masses were compared with those of known compounds in compound databases. Pure standards were used to confirm the presence of selected compounds.

5.2.14 Semi Prep HPLC fractionation

Samples (100 mg) of the ethanol extract of Marula ground stems and leaves of *F. sycomorus* were separately dissolved in DMSO (4 ml) and each sample was filtered using a 0.45 PTFE filter. Fractionation was done using an Agilent Technologies 1200 series Semi-prep HPLC on a Sunfire prep C18 10 µm, 10 x 150 mm column. A gradient method was used for both extracts with Solvent A water with 1% formic acid, solvent B was 100% Methanol and solvent D was 100% acetonitrile. The gradient method used for *F. sycomorus* extract was 0%-10% D in 2 minutes, 10%-15% D in 5 minutes, 15% to 20% D in 8 minutes, 20-22% D, 22%-50% D in 2 minutes, 50%-80% D in 5 minutes, 80%-90% D in 5 minutes, 90%-100% D in 3 minutes, 100%-100% D in 5 minutes, 100%-50% D in 2 minutes, 50%-5% D in 2 minutes, and 5%-5% D in 10 minutes. Marula extract was as follows; 0%-15% D in 0.50 minutes; 15%-16% D in 2.5 minutes; 16%-17% D in 1 minute; 17%-17.5% in 2 minutes; 17.5%-18 minutes in 1 minute; 18%-18% D in 2 minutes; 18%-19% D in 1 minute; 19%-19% D in 2 minutes; 19%-23% D in 2 minutes; 23%-23% D, 0%-1% in 2 minutes; 23%-25% D, 1%-2% B in 1 minute; 25%-25% D, 2%-2% B in 1 minute, 25%-25% D, 2%-2% B in 2 minutes; 25%-25% D, 2%-2% B in 2 minutes; 25%-30% D, 2%-2% D, in 3 minutes; 30%-35% D; 2%-2% B in 2 minutes, 35%-45% D, 2.0%-2.0% in 2 minutes; 45%-60% D, 2%-2% in 2 minutes. The injection volume was 250 µl per injection at a flow rate of 4 ml per minute at a pressure of 400 kPA.

5.3 CHAPTER 4

5.3.1 Combination studies

5.3.1.1 Combination of Marula and Sycamore extracts

F. sycomorus defatted extract (FD extract) 1.3 mg and the Marula defatted and concentrated extract (MDC extract) 1.3 mg were weighed into a 2.5 ml Eppendorf tube. Ethanol (1 ml) was added to the extracts to allow for even mixing of the extracts. The combination was mixed using a small glass rod. The ethanol was later evaporated using an Acid resistant Centrivap Concentrator (Labconco) at 50 °C for 20 minutes and then submitted for screening.

5.3.1.2 Combination of Sycamore extract and active compounds from Marula

Epigallocatechin gallate (1 mg) and epicatechin gallate (1 mg) were weighed into a 2.5 ml Eppendorf tube and ethanol (1 ml) was added. The compounds were dissolved in ethanol by stirring using a small glass rod to dissolve the pure compounds. *F. sycomorus* defatted extract (FD extract) 10 mg was weighed into a separate Eppendorf tube and the dissolved pure compounds were added to the tube with the FD extract. The ethanol was evaporated using an Acid resistant Centrivap Concentrator (Labconco) at 50 °C for 20 minutes and then submitted for screening.

5.3.2 Formulation studies

5.3.2.1 Formulation of the antiaging day cream (200.00g batch)

The required amounts of Part A components; deionised water (131.91 g), disodium EDTA (0.14 g) and xanthum gum (0.65 g) were placed in a beaker and heated to 75 °C. The mixture was stirred using an overhead stirrer and heated on a hot plate until all the ingredients had completely dissolved. In a separate beaker, the required amounts of Part B components; emulsifying wax (10.13 g), liponate NEB (10.42 g), Beeswax (3.16 g), Parsol MCX (20.16 g) and Cocoa butter(10.09 g) were mixed and heated to 75 °C in a similar manner to Part A,

using a hot plate while stirring at low speed using a mixer at 300 revolutions per minute (rpm). Part B mixture was then poured into the Part A mixture with the mixture being stirred and the batch was homogenised for 15 minutes. The mixture was cooled down to approximately 40 °C, while continuously stirring at 500 rpm. The required amounts of Part C components; titanium dioxide (5.03 g), dimethicone (4.21 g) and 99% TEA (2.21 g) were weighed, mixed and added into the main batch with mixing. The required amounts of Part D components; vitamin E Acetate (0.26 g), Marula extract (2.10 g), *F. sycomorus* extract (1.16 g), spearmint fragrance (1.26 g), Marula fragrance (1.14 g) and Euxyl k100 (0.22 g) was weighed in a separate beaker and added to the main batch with mixing. During the preliminary study, the pH was found to be 5.2-6.2, yielding light pink product.

5.3.2 Formulation of the nourishing night cream (200.00g batch)

The required amounts of Part A components; deionised water (134.92 g), disodium EDTA (0.11 g) and xanthum gum (0.62 g) were measured into a beaker and heated to 75 °C using a hot plate. The mixture was stirred using an overhead stirrer at 300 rpm. Heating was maintained until all the ingredients present had fully dissolved. In a separate beaker, the required amounts of Part B components emulsifying wax (10.04 g), Tegosoft TN (10.20 g), beeswax (3.05 g) and Cocoa butter (10.13 g) were mixed and heated to 75 °C in a similar manner to Part A, using a hot plate at 300 rpm, while stirring at low speed using a mixer at 300 rpm. Part B mixture was then poured into the Part A mixture with mixing and the batch was homogenised for 15 minutes. The mixture was cooled down to approximately 40 °C, while continuously stirring at 500 rpm. The required amounts of Part C components coconut oil (20.11 g), glycerine (6.25 g), vitamin E Acetate (0.22 g), Marula extract (2.02 g), *F. sycomorus* extract (1.21 g), spearmint fragrance (1.11 g) and Marula fragrance (1.21 g) were weighed and added into the main batch with mixing. The required amounts of Part D components Euxyl K100 (0.23 g) was weighed in a separate beaker and added to the main

batch with mixing. During the preliminary study, the pH was found to be 5.2-6.2, yielding a dark brown product.

5.3.3 Formulation of the antiaging day cream (2 kg batch)

The required amounts of Part A components; deionised water (1204.83 g), disodium EDTA (1.21 g) and xanthum gum (6.42 g) and 99% Triethanol amine (TEA) were placed in a beaker and heated to 75 °C. The mixture was stirred using an overhead stirrer at 300 rpm and heated on a hot plate until all the ingredients had completely dissolved. In a separate beaker, the required amounts of Part B components; emulsifying wax (100.44 g), liponate NEB (100.71 g), Beeswax (30.41 g), Parsol MCX (200.34 g), Parsol 1789 (100.72 g) and Cocoa butter (100.22 g) were mixed and heated to 75°C using a hot plate while stirring at low speed using a mixer at 300 rpm. Part B mixture was then poured into the Part A mixture with the mixture being stirred and the batch was homogenised for 15 minutes. The mixture was cooled down to approximately 40 °C, while continuously stirring at 500 rpm. The required amounts of Part C components; titanium dioxide (50.09 g) and dimethicone (40.46 g) were weighed, mixed and added into the main batch with mixing. The required amounts of Part D components; vitamin E Acetate (5.69 g), Marula extract (20.10 g), *F. sycomorus* extract (10.88 g), Marula fragrance (10.41 g) and Euxyl k100 (2.06 g) was weighed in a separate beaker and added to the main batch with mixing.

5.3.4 Formulation of the nourishing night cream (2 kg batch)

The required amounts of Part A components; deionised water (1342.10 g), disodium EDTA (1.07 g) and xanthum gum (6.49 g), TEA (22.43 g) were measured into a beaker and heated to 75 °C using a hot plate. The mixture was stirred using an overhead stirrer at 300 rpm. Heating was maintained until all the ingredients present had fully dissolved. In a separate beaker, the required amounts of Part B components emulsifying wax (100.15 g), Tegosoft TN

(100.35 g), beeswax (30.15 g) and Cocoa butter (100.72 g) were mixed and heated to 75 °C in a similar manner to Part A, using a hot plate at 300 rpm, while stirring at low speed using a mixer at 300 rpm. Part B mixture was then poured into the Part A mixture with mixing and the batch was homogenised for 15 minutes. The mixture was cooled down to approximately 40 °C, while continuously stirring at 500 rpm. The required amounts of Part C components coconut oil (200.71 g), glycerine (60.13 g), vitamin E Acetate (5.21 g), Marula extract (20.09 g), *F. sycomorus* extract (10.09 g), Marula fragrance (5.52 g) were weighed and added into the main batch with mixing. The required amounts of Part D components Euxyl K100 (2.05 g) was weighed in a separate beaker and added to the main batch with mixing.

5.4 REFERENCES

1. Row KH, Jin Y: **Recovery of catechin compounds from Korean tea by solvent extraction.** *Bioresource Technology* 2006, **97**(5):790-793.
2. Kraunsoe JA, Claridge TD, Lowe G: **Inhibition of human leukocyte and porcine pancreatic elastase by homologues of bovine pancreatic trypsin inhibitor.** *Biochemistry* 1996, **35**(28):9090-9096.
3. Moore S, Stein WH: **Photometric nin-hydrin method for use in the chromatography of amino acids.** *Journal of biological chemistry* 1948, **176**:367-388.
4. Mandl I, MacLennan JD, Howes EL, DeBellis RH, Sohler A: **Isolation and characterization of proteinase and collagenase from *Cl. histolyticum*.** *The Journal of Clinical Investigation* 1953, **32**(12):1323.

CHAPTER 6: CONCLUSIONS

This project started as a CSIR initiative to identify and develop new natural anti-aging ingredients with similar or better efficacy to existing synthetic ingredients on the market. The MeOH:DCM (1:1) extracts of Marula stems was shown to exhibit elastase activity comparable to that of elafin (>88%) and collagenase activity in the same range as EDTA (>76%). This was higher than the corresponding extracts of the leaves which exhibited moderate elastase inhibition activity of 54% but showed no activity in the collagenase assay. Fruits from the same plant had limited activity (<25%) in both assays. Additionally, organic extracts of the leaves of the Sycamore plant were shown to exhibit good elastase (93%) and collagenase (81%) inhibition activities. As a result, Marula stems and leaves of the Sycamore tree were selected for further investigations aimed at developing anti-aging ingredients. These initial effective screening results for the extracts of *S. birrea* plant and *F. sycomorus* plants provided the first scientific evidence substantiating the traditional use of the plants for anti-aging purposes and their potential for further development into commercial anti-aging ingredients.

Screening results for extracts from Marula stems prepared through sequential extraction revealed that the methanol sequential extract had the highest elastase inhibition activity of 99% and in the collagenase assay the methanol sequential extract and the ethyl acetate sequential extract had a >94% inhibition. In the Sycamore leaves the methanol sequential extract exhibited the highest inhibition activities of >89% in both assays. These results revealed that the active constituents were concentrated in the more polar extracts. In addition, sequential extraction using hexane, DCM, ethyl acetate and methanol successfully extracted compounds based on their polarity. This was confirmed through UPLC MS as constituents of extracts from polar solvents such as methanol were detected in the early retention times (0 to 6 minutes) while constituents of extracts from non-polar solvents that is DCM were concentrated in the later retention times (6 to 18 minutes).

Results from the separate extraction using ethanol, methanol:DCM (1:1) and acetone clearly showed that the methanol:DCM (1:1) combination had the highest extraction efficiency of >5% in both plants. In Marula stems the ethanol extract exhibited the highest inhibition activities with 93.35% anti-elastase activity and 99% anti-collagenase activity. Similarly, the Sycamore leaves exhibited the highest activities with 83% inhibition in the elastase assay and 102% inhibition in the collagenase assay. Based on screening results obtained and acceptability to the cosmetic industry, the ethanol extract of leaves of the Sycamore tree and Marula stems were selected as the most appropriate extracts for further research and development. The harvesting of stems is often seen as being destructive and non-sustainable. To circumvent this, our study utilized the soft wood side stems or twigs which will not result in destructive harvesting.

UPLC-QTOF-MS analysis of Marula stem ethanol extracts led to the tentative identification of eleven compounds which are quinic acid, gallo catechin, procyanidin B2, catechin, epicatechin-epicatechin-3'-O-gallate, epicatechin-3-gallate, epicatechin-3-O-gallate-epicatechin, procyanidin B2-3'3 di-O-gallate, epicatechin gallate, undecainedioc acid and 9,10,13 TriHOME. The presence of quinic acid, catechin, epigallocatechin gallate and epicatechin gallate was confirmed using pure standards on UPLC-QTOF-MS. Further, the compound 9,8,13 TriHOME has been tentatively identified for the first time in Marula stems. Identification of the compounds led to a unique chemical fingerprint of the ethanol extract of Marula stems which can be used for quality control and to show batch to batch reproducibility.

Analysis of the ethanol extract of leaves of the Sycamore tree using UPLC-QTOF-MS resulted in the tentative identification of eight compounds which are palatinose, quinic acid, isobiflorin, chlorogenic acid, biflorin, rutin, quercetin-3-glucoronide and isoquercetin. The presence of five of these palatinose, quinic acid, chlorogenic acid, rutin and isoquercetin was confirmed using

pure standards on UPLC-QTOF-MS. The presence of vicenin-2, biflorin and isobiflorin was confirmed through isolation, purification and structure elucidation using NMR and quercetin-3-glucuronide was tentatively identified. The chemical profiles for the ethanol extracts of Marula stems and leaves of *F. sycomorus* were developed for quality control purposes achieving the second objective of this chapter. This is the first report of the presence of palatinose, quinic acid, isobiflorin, chlorogenic acid, biflorin, vicenin 2, quercetin-3-glucuronide in the *F. sycomorus* plant. The chemical profile of the ethanol extract of leaves of the Sycamore extract active in the elastase and collagenase assays have thus been developed for the first time for quality control purposes.

Screening results from the collagenase assay at 100 µg/ml revealed that the crude extract and the defatted fraction had lower potency ($p < 0.01$) than EDTA, the concentrated fraction was as potent as ($p < 0.05$) EDTA and the defatted-concentrated fraction was significantly ($p < 0.01$) more potent than EDTA. These results revealed that the concentration and defatting-concentration steps improved the anti-aging activity of the Marula stem ethanol extract and further lowered the colour intensity of the extract. In addition, defatting the ethanol extract of the Sycamore leaves dissolved in a water/ethanol mixture using hexane lowered the colour intensity of the extract. For the first time in this study, Marula oil, although traded as a cosmetic ingredient was shown to have no anti-collagenase or anti-elastase activity contributing to anti-aging claims on products containing the oil. Its application in cosmetic formulations is therefore due to a different mode of action.

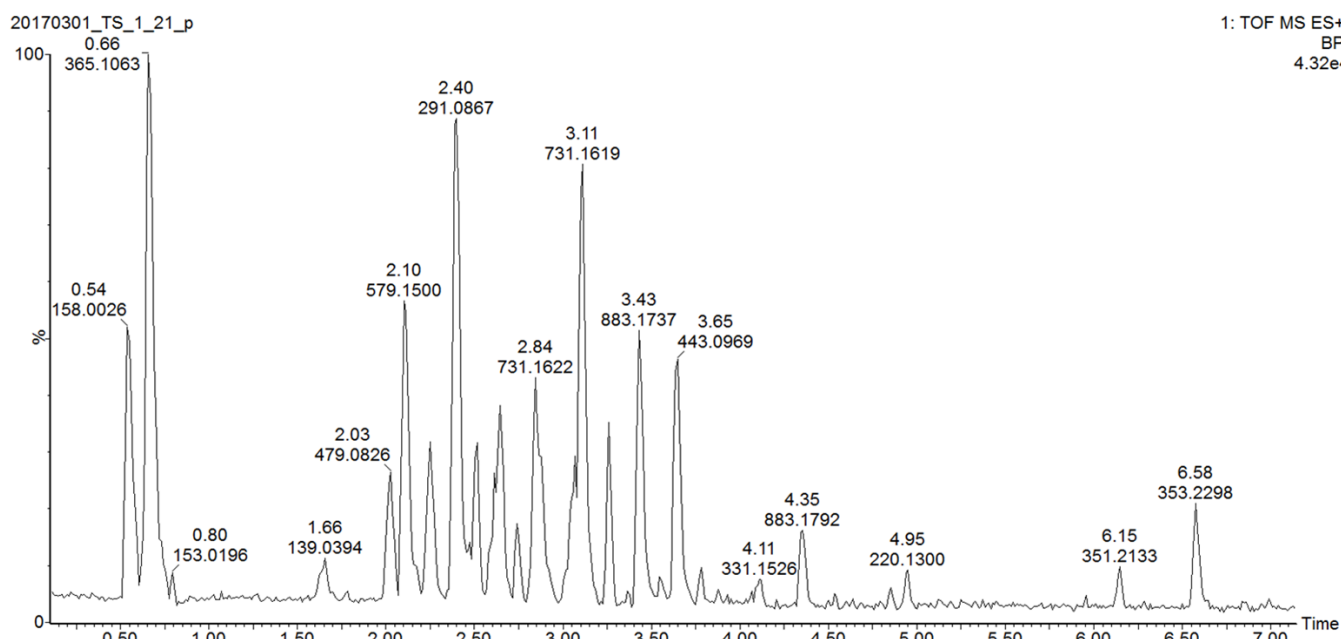
Bioassay guided fractionation resulted in the identification of the compounds epigallocatechin gallate and epicatechin gallate as the major compounds contributing to the collagenase inhibition activity of the Marula stem ethanol extract. Isoquercetin was identified as the major compound contributing to the collagenase inhibition activity of the Sycamore extract. Upon screening of the pure compounds in the collagenase assay, epigallocatechin gallate and

epicatechin gallate were found to be as potent as EDTA at 5 µg/ml and isoquercetin showed collagenase inhibition activity at a low concentration of 10 µg/ml. This confirms findings from previous studies in which epigallocatechin gallate and epicatechin gallate have been shown to exhibit collagenase inhibition activity. However, this is the first report of collagenase inhibition activity of these flavonoids in the Marula plant. In addition, this is the first report in which isoquercetin has been shown to exhibit collagenase inhibition activity and substantiates its potential for further development into anti-aging ingredients. In the elastase assay, the ethanol extract of Marula stems and leaves of the Sycamore tree and their fractions showed activity. However, upon screening of pure compounds, none of the compounds showed activity showing that activity in the extracts and the fractions was due to synergistic effects. As such, synergism may have been lost upon isolation of compounds, hence, the lack of activity upon screening pure compounds.

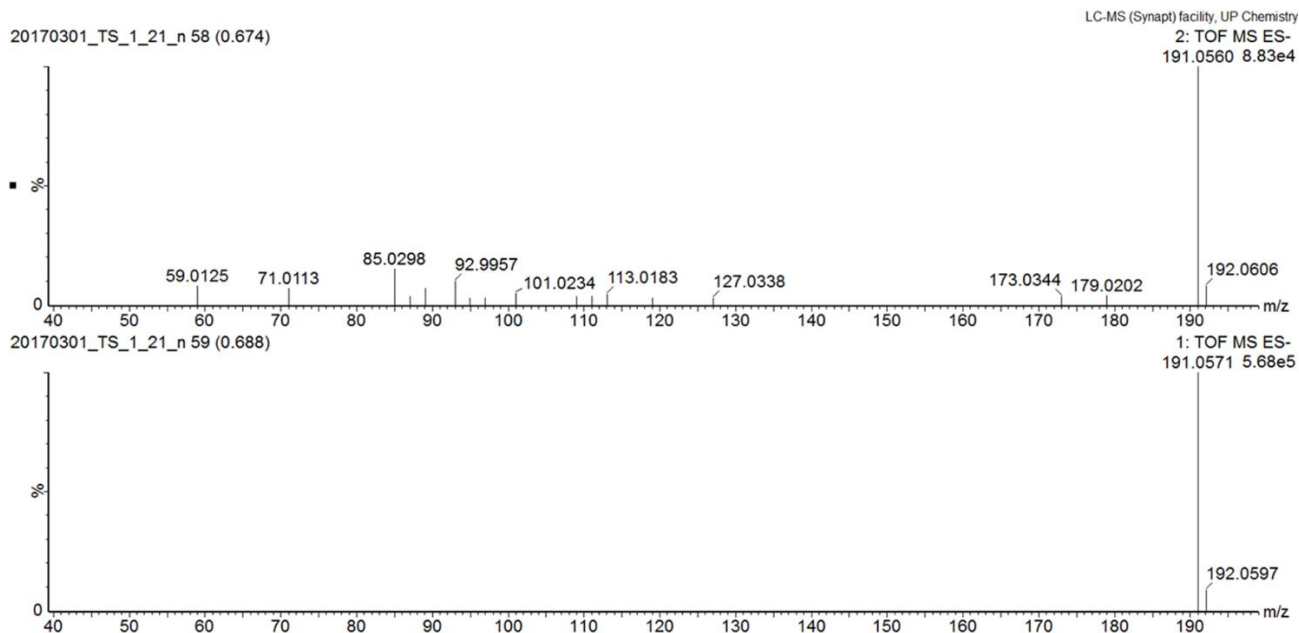
In the collagenase assay, at test concentration 100 µg/ml the combinations of the FD extract: MDC extract (1:1) and the FD extract:EGCg:ECg (10:0.1:0.1) were as potent as ($p>0.05$) EDTA while at 10 µg/ml, both combinations exhibited lower activities ($p<0.01$) than the positive control. Similarly, the FD extract was as potent as ($p>0.05$) EDTA at 100 µg/ml but exhibited lower potency ($p<0.01$) at 10 µg/ml. In contrast, the MDC extract was more potent ($0.01<p<0.05$) than EDTA at 100 µg/ml but exhibited lower potency ($p<0.01$) to the positive control at 10µg/ml. These results revealed that in the collagenase assay, the FD:MDC (1:1) mixture and the FD extract:EGCg:ECg (10:0.1:0.1) had the same potency as the FD separate extract but were less potent than the MDC extract at 100 µg/ml. Further, combining the FD and the MDC extracts and the FD extract and the active compounds from Marula stems (EGCg and ECg) did not improve the collagenase inhibition activities of the extracts at 10 µg/ml but maintained equivalent levels of potency as EDTA at 100 µg/ml. In the elastase assay, the FD:MDC (1:1) mixture, the FD extract:EGCg:ECg (10:0.1:0.1) and the separate FD and MDC extracts were less potent ($p<0.01$) than EDTA at both 10 and 100 µg/ml revealing that the

combinations did not improve elastase inhibition activities of the extracts. Based on the higher potency of the MDC extract to the combinations in the collagenase assay, the prototypes were formulated by adding a higher proportion of the MDC extract than the FD extract in an appropriate combination producing a stable product. The prototypes were successfully developed as part of proof of concept studies, and the project will proceed beyond the scope of these studies to evaluate the formulations for shelf life, compatibility, microbiology and dermal safety and efficacy studies.

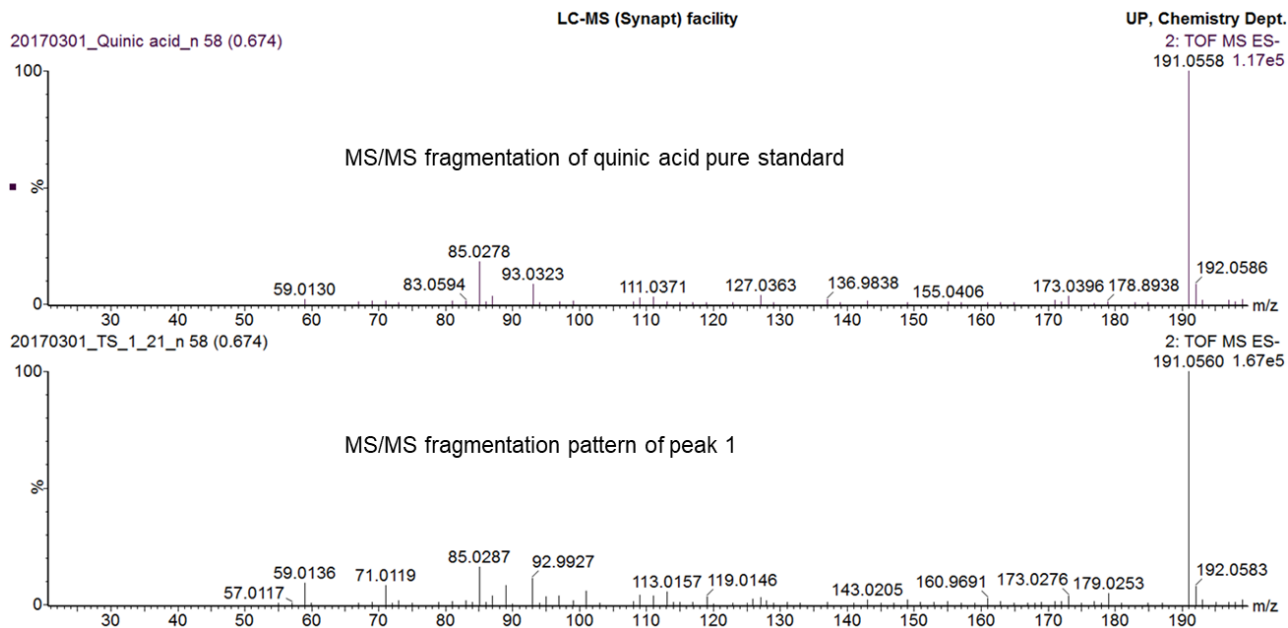
SUPPLEMENTARY DATA



Supplementary Data 1. ESI positive mode BPI chromatogram of crude ethanol extract of Marula stems.



Supplementary Data 2. MS/MS fragmentation pattern of peak 1 (quinic acid) in Marula stem ethanol extract



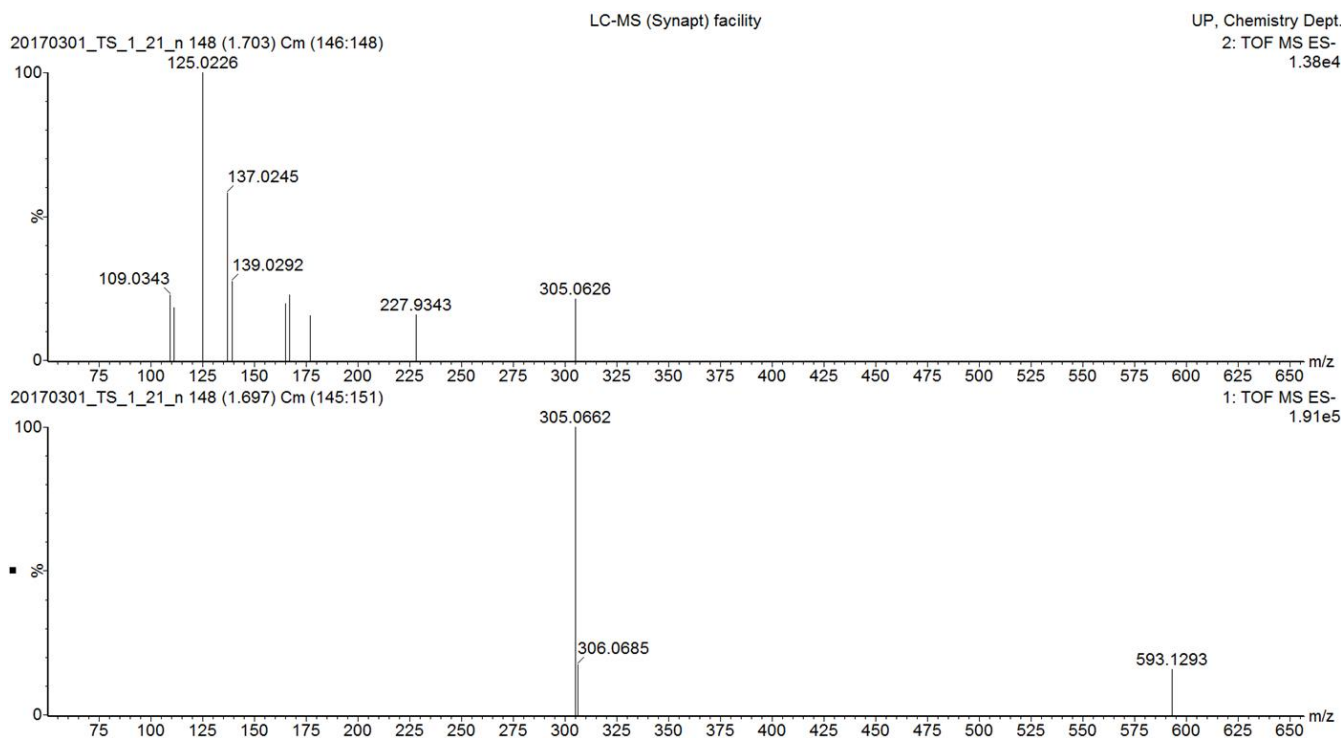
Supplementary Data 3. MS/MS fragmentation pattern of peak 1 (quinic acid) in Marula stems overlaid with MS/MS fragmentation pattern of quinic acid pure standard

File Edit View Process Help

Single Mass Analysis
Tolerance = 5.0 mDa / DBE: min = -1.5, max = 50.0
Element prediction: Off
Number of isotope peaks used for i-FIT = 3
Monoisotopic Mass, Even Electron Ions
50 formula(e) evaluated with 2 results within limits (up to 50 best isotopic matches for each mass)
Elements Used:

Mass	Calc. Mass	mDa	PPM	DBE	Formula	i-FIT	i-FIT Norm	Fit Conf %	C	H	O	F
191.0571	191.0556	1.5	7.9	2.5	C7 H11 O6	38.0	0.607	54.51	7	11	6	
	191.0567	0.4	2.1	-1.5	C4 H12 O7 F	38.2	0.788	45.49	4	12	7	1

Supplementary Data 4. iFit value quinic acid



Supplementary Data 5. MS/MS fragmentation pattern of peak 3 (galocatechin) in Marula stem ethanol extract.

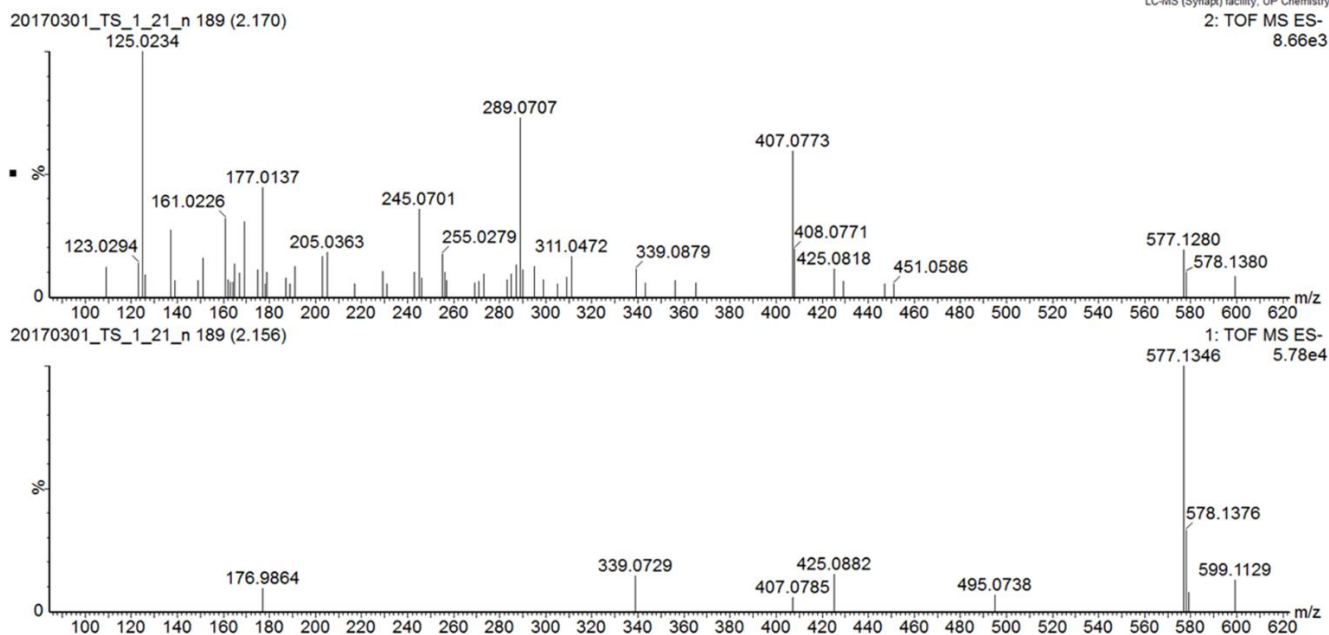
Elemental Composition

File Edit View Process Help

Single Mass Analysis
Tolerance = 5.0 mDa / DBE: min = -1.5, max = 50.0
Element prediction: Off
Number of isotope peaks used for i-FIT = 3
Monoisotopic Mass, Even Electron Ions
204 formula(e) evaluated with 4 results within limits (up to 50 best isotopic matches for each mass)
Elements Used:

Mass	Calc. Mass	mDa	PPM	DBE	Formula	i-FIT	i-FIT Norm	Fit Conf %	C	H	O	Cl
305.0662	305.0661	0.1	0.3	9.5	C15 H13 O7	38.9	0.163	84.94	15	13	7	
	305.0639	2.3	7.5	0.5	C9 H18 O9 Cl	41.3	2.589	7.51	9	18	9	1
	305.0631	3.1	10.2	4.5	C15 H20 Cl3	42.0	3.239	3.92	15	20		3
	305.0711	-4.9	-16.1	4.5	C14 H19 O3 Cl2	42.1	3.316	3.63	14	19	3	2

Supplementary Data 6. iFit value for peak 2 (galocatechin) in Marula stem ethanol extract



Supplementary Data 7. MS and MS/MS data of peak 3 (procyanidin B2)

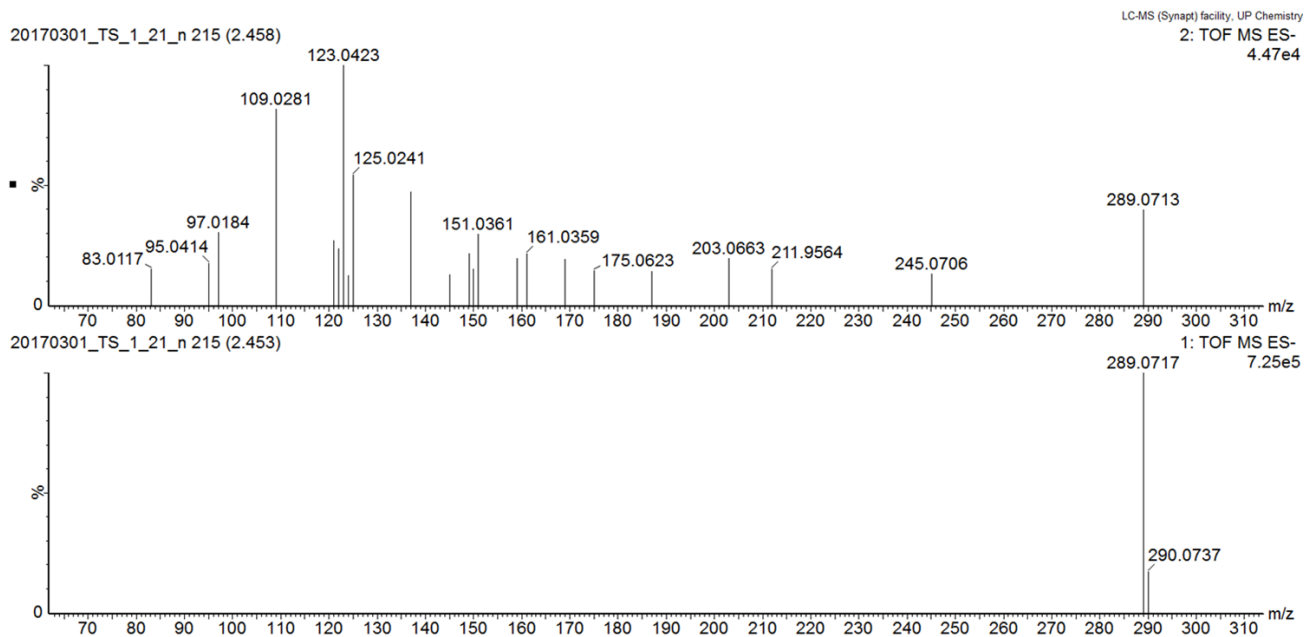
Elemental Composition

File Edit View Process Help

Single Mass Analysis
Tolerance = 5.0 mDa / DBE: min = -1.5, max = 50.0
Element prediction: Off
Number of isotope peaks used for i-FIT = 3
Monoisotopic Mass, Even Electron Ions
878 formula(e) evaluated with 11 results within limits (up to 50 best isotopic matches for each mass)
Elements Used:

Mass	Calc. Mass	mDa	PPM	DBE	Formula	i-FIT	i-FIT Norm	Fit Conf %	C	H	O	Cl
577.1346	577.1346	0.0	0.0	18.5	C30 H25 O12	32.7	0.545	58.01	30	25	12	
	577.1359	-1.3	-2.3	31.5	C42 H22 O Cl	34.4	2.294	10.09	42	22	1	1
	577.1337	0.9	1.6	22.5	C36 H27 O3 Cl2	34.5	2.397	9.10	36	27	3	2
	577.1324	2.2	3.8	9.5	C24 H30 O14 Cl	34.8	2.626	7.24	24	30	14	1
	577.1343	0.3	0.5	-0.5	C23 H43 O3 Cl6	35.1	2.944	5.26	23	43	3	6
	577.1365	-1.9	-3.3	8.5	C29 H38 O Cl5	35.7	3.602	2.73	29	38	1	5
	577.1315	3.1	5.4	13.5	C30 H32 O5 Cl3	35.9	3.818	2.20	30	32	5	3
	577.1374	-2.8	-4.9	4.5	C23 H36 O10 Cl3	36.1	3.961	1.90	23	36	10	3
	577.1383	-3.7	-6.4	0.5	C17 H34 O19 Cl	36.1	3.981	1.87	17	34	19	1
	577.1302	4.4	7.6	0.5	C18 H35 O16 Cl2	36.7	4.581	1.02	18	35	16	2
	577.1396	-5.0	-8.7	13.5	C29 H31 O8 Cl2	37.3	5.144	0.58	29	31	8	2

Supplementary Data 8. iFit value peak 4 (procyanidin B2)



Supplementary Data 9. MS and MS/MS data for peak 5 (catechin) in Marula stem ethanol extract

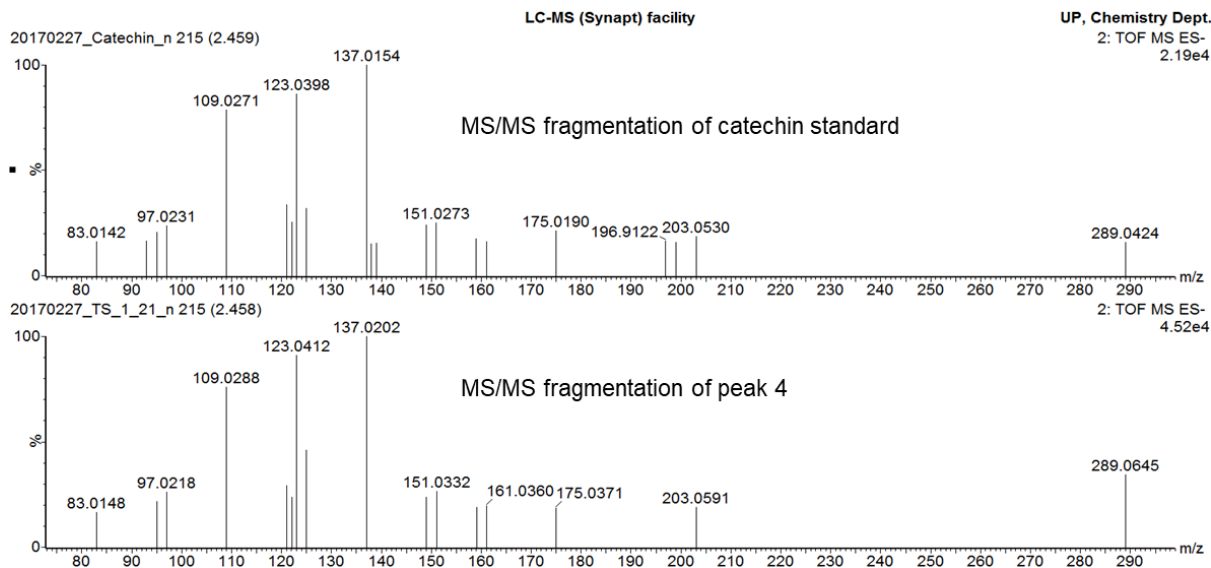
Elemental Composition

File Edit View Process Help

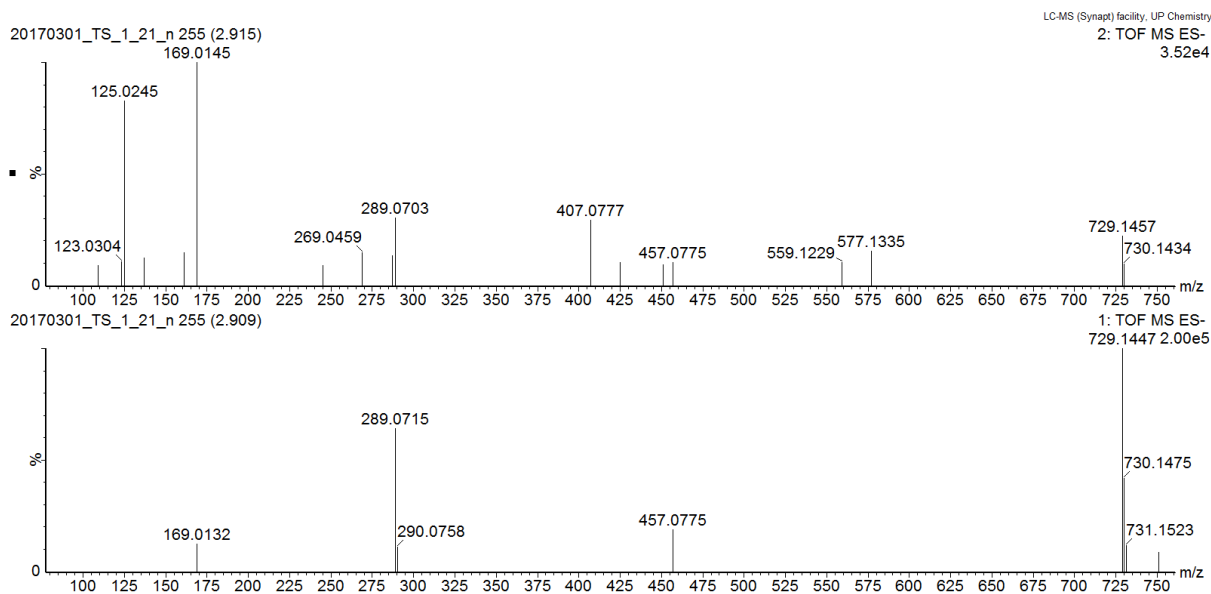
Single Mass Analysis
Tolerance = 5.0 mDa / DBE: min = -1.5, max = 50.0
Element prediction: Off
Number of isotope peaks used for i-FIT = 3
Monoisotopic Mass, Even Electron Ions
303 formula(e) evaluated with 3 results within limits (up to 50 best isotopic matches for each mass)
Elements Used:

Mass	Calc. Mass	mDa	PPM	DBE	Formula	i-FIT	i-FIT Norm	Fit Conf %	C	H	O	Cl	Br
289.0717	289.0712	0.5	1.7	9.5	C15 H13 O6	40.5	0.266	76.65	15	13	6		
	289.0690	2.7	9.3	0.5	C9 H18 O8 Cl	41.9	1.701	18.25	9	18	8	1	
	289.0762	-4.5	-15.6	4.5	C14 H19 O2 Cl2	43.2	2.975	5.10	14	19	2	2	

Supplementary Data 10. iFit value for peak 5 (catechin) in Marula stem ethanol extract



Supplementary Data 11. MS/MS fragmentation pattern of peak 4 (catechin) in Marula stems overlaid with MS/MS fragmentation pattern of quinic acid pure standard



Supplementary Data 12. MS and MS/MS data for peak 7 showing fragments for epicatechin-epicatechin-3'-O-gallate) in Marula stem ethanol extract

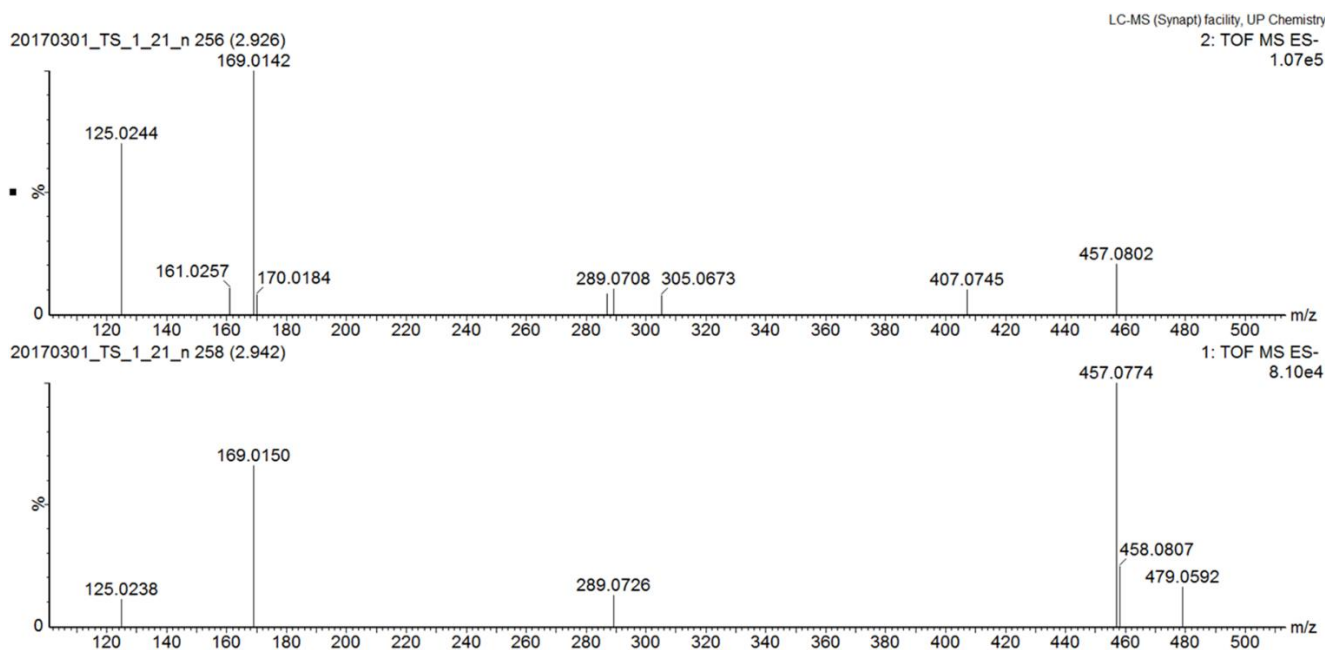
Elemental Composition

File Edit View Process Help

Single Mass Analysis
Tolerance = 5.0 mDa / DBE: min = -1.5, max = 50.0
Element prediction: Off
Number of isotope peaks used for i-FIT = 3
Monoisotopic Mass, Even Electron Ions
1474 formula(e) evaluated with 17 results within limits (up to 50 best isotopic matches for each mass)
Elements Used:

Mass	Calc. Mass	mDa	PPM	DBE	Formula	i-FIT	i-FIT Norm	Fit Conf %	C	H	O	Cl
729.1447	729.1456	-0.9	-1.2	23.5	C37 H29 O16	15.3	0.000	100.00	37	29	16	
	729.1491	-4.4	-6.0	45.5	C55 H21 O3	29.3	14.045	0.00	55	21	3	
	729.1421	2.6	3.6	1.5	C19 H37 O29	31.5	16.282	0.00	19	37	29	
	729.1469	-2.2	-3.0	36.5	C49 H26 O5 Cl	38.2	22.950	0.00	49	26	5	1
	729.1410	3.7	5.1	45.5	C56 H22 Cl	38.3	23.064	0.00	56	22		1
	729.1434	1.3	1.8	14.5	C31 H34 O18 Cl	38.8	23.556	0.00	31	34	18	1
	729.1492	-4.5	-6.2	5.5	C24 H38 O23 Cl	39.0	23.757	0.00	24	38	23	1
	729.1447	0.0	0.0	27.5	C43 H31 O7 Cl2	40.4	25.127	0.00	43	31	7	2
	729.1412	3.5	4.8	5.5	C25 H39 O20 Cl2	40.9	25.683	0.00	25	39	20	2
	729.1425	2.2	3.0	18.5	C37 H36 O9 Cl3	41.4	26.135	0.00	37	36	9	3
	729.1484	-3.7	-5.1	9.5	C30 H40 O14 Cl3	41.4	26.147	0.00	30	40	14	3
	729.1497	-5.0	-6.9	22.5	C42 H37 O3 Cl4	41.6	26.383	0.00	42	37	3	4
	729.1462	-1.5	-2.1	0.5	C24 H45 O16 Cl4	41.9	26.611	0.00	24	45	16	4
	729.1475	-2.8	-3.8	13.5	C36 H42 O5 Cl5	42.0	26.701	0.00	36	42	5	5
	729.1403	4.4	6.0	9.5	C31 H41 O11 Cl4	42.0	26.722	0.00	31	41	11	4
	729.1416	3.1	4.3	22.5	C43 H38 Cl5	42.0	26.761	0.00	43	38		5
	729.1453	-0.6	-0.8	4.5	C30 H47 O7 Cl6	42.2	26.977	0.00	30	47	7	6

Supplementary Data 13. iFit value for peak 6 (epicatechin-epicatechin-3'-gallate)



Supplementary Data 14. MS and MS/MS fragmentation pattern of peak 8 (epigallocatechin gallate) in Marula stem ethanol extract

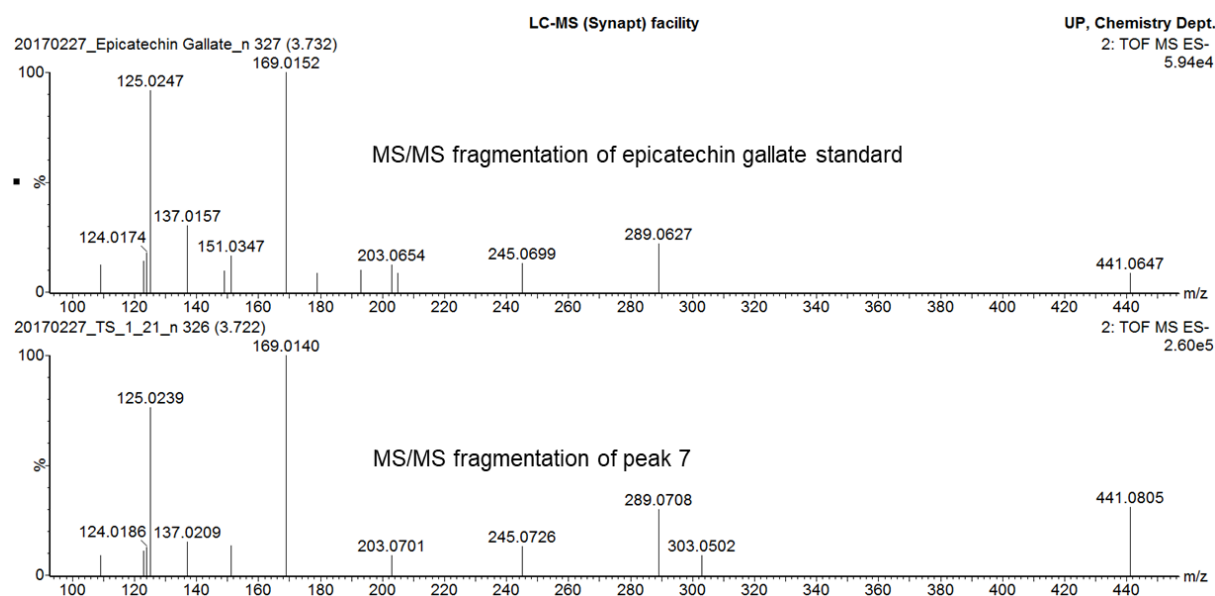
Elemental Composition

File Edit View Process Help

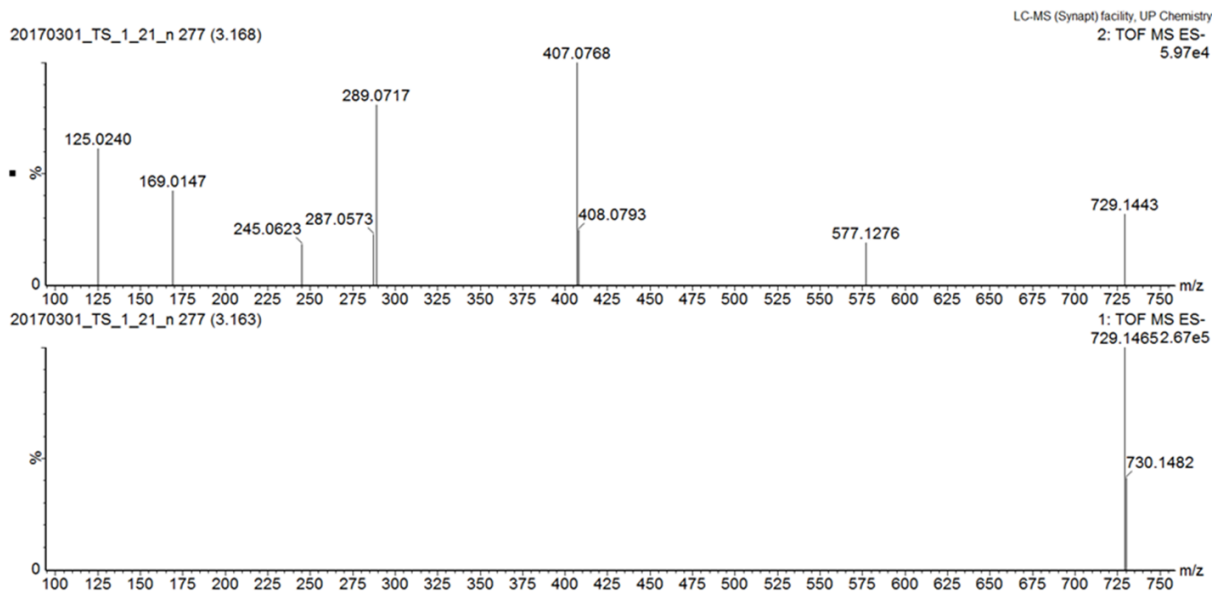
Single Mass Analysis
Tolerance = 5.0 mDa / DBE: min = -1.5, max = 50.0
Element prediction: Off
Number of isotope peaks used for i-FIT = 3
Monoisotopic Mass, Even Electron Ions
285 formula(e) evaluated with 4 results within limits (up to 50 best isotopic matches for each mass)
Elements Used:

Mass	Calc. Mass	mDa	PPM	DBE	Formula	i-FIT	i-FIT Norm	Fit Conf %	C	H	O	Br
457.0780	457.0771	0.9	2.0	14.5	C22 H17 O11	16.9	0.000	99.99	22	17	11	
	457.0830	-5.0	-10.9	5.5	C15 H21 O16	26.4	9.492	0.01	15	21	16	
	457.0803	-2.3	-5.0	16.5	C27 H22 O2 Br	39.2	22.285	0.00	27	22	2	1
	457.0742	3.8	8.3	5.5	C21 H31 O Br2	40.0	23.090	0.00	21	31	1	2

Supplementary Data 15. iFit value for peak 7 (epigallocatechin gallate) in Marula stem ethanol extract



Supplementary Data 16. MS/MS fragmentation pattern of peak 7 (epicatechin gallate) in Marula stems overlaid with MS/MS fragmentation pattern of epicatechin gallate pure standard



Supplementary Data 17. MS and MS/ MS data for peak 8 (epicatechin-3-O-gallate-epicatechin) in Marula stem ethanol extract

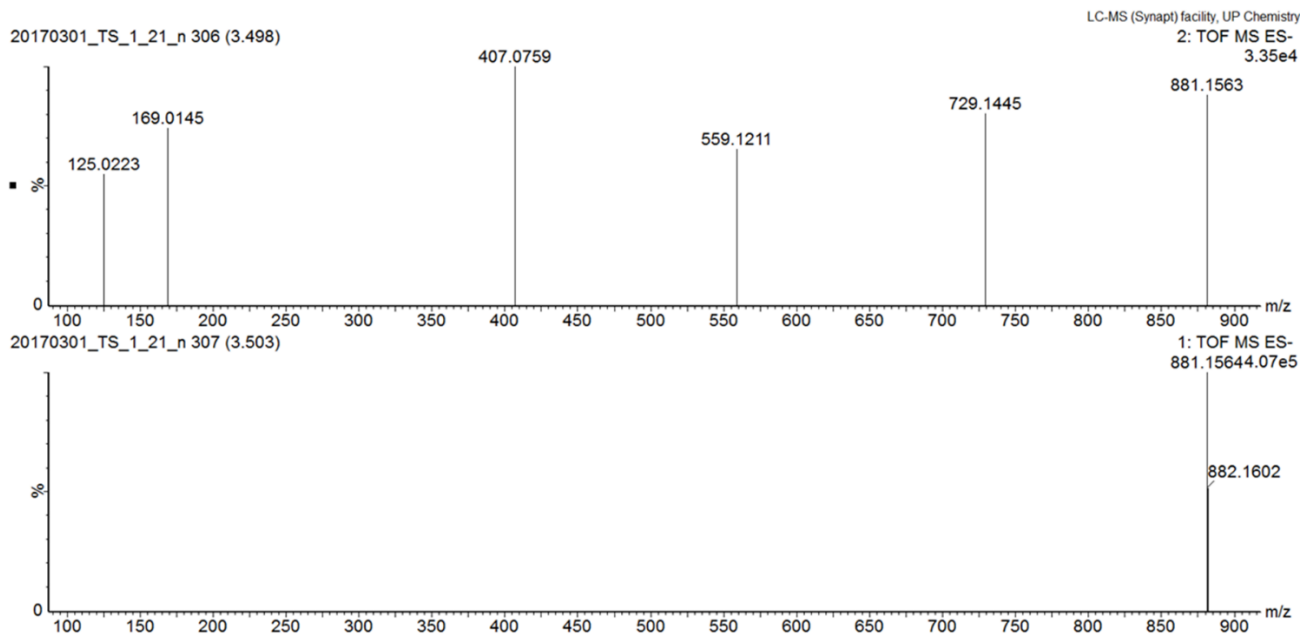
Elemental Composition

File Edit View Process Help

Single Mass Analysis
Tolerance = 5.0 mDa / DBE: min = -1.5, max = 50.0
Element prediction: Off
Number of isotope peaks used for i-FIT = 3
Monoisotopic Mass, Even Electron Ions
473 formula(e) evaluated with 5 results within limits (up to 50 best isotopic matches for each mass)
Elements Used:

Mass	Calc. Mass	mDa	PPM	DBE	Formula	i-FIT	i-FIT Norm	Fit Conf %	C	H	O	F
729.1462	729.1456	0.6	0.8	23.5	C37 H29 O16	17.4	0.009	99.06	37	29	16	
	729.1467	-0.5	-0.7	19.5	C34 H30 O17 F	22.1	4.674	0.93	34	30	17	1
	729.1502	-4.0	-5.5	41.5	C52 H22 O4 F	28.7	11.248	0.00	52	22	4	1
	729.1491	-2.9	-4.0	45.5	C55 H21 O3	28.7	11.320	0.00	55	21	3	
	729.1421	4.1	5.6	1.5	C19 H37 O29	30.6	13.226	0.00	19	37	29	

Supplementary Data 18. iFit value for peak 8 (epicatechin-3-O-gallate-epicatechin) in Marula stem ethanol extract



Supplementary Data 19. MS and MS/MS fragmentation pattern of peak 9 (procyanidin B2-3'3 di-O-gallate) in Marula stem ethanol extract

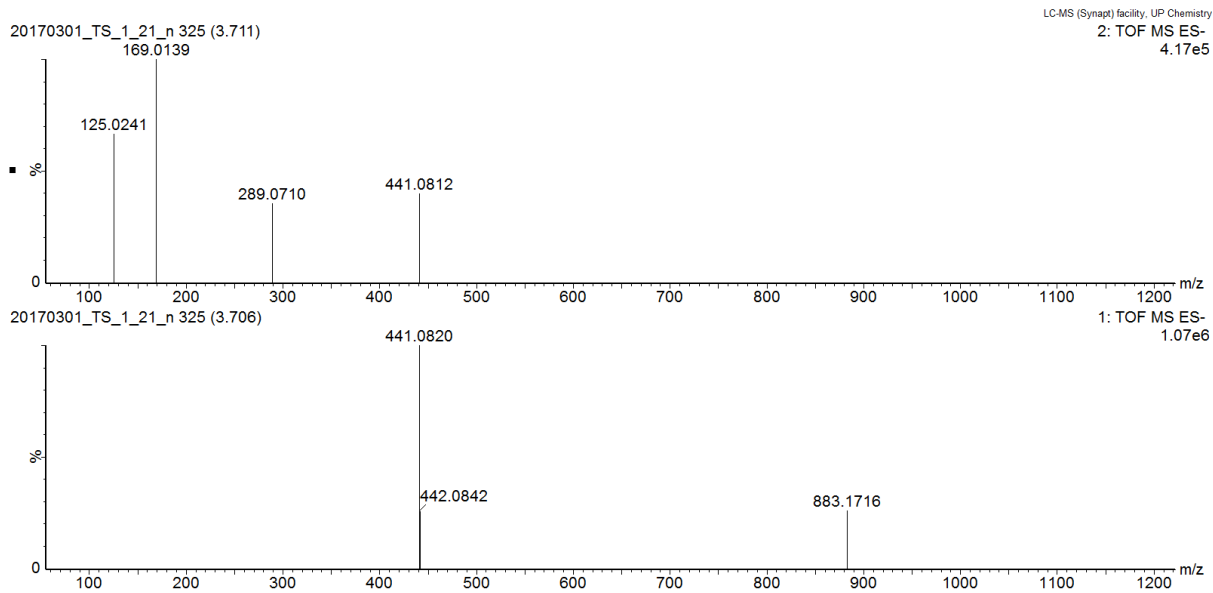
Elemental Composition

File Edit View Process Help

Single Mass Analysis
Tolerance = 5.0 mDa / DBE: min = -1.5, max = 50.0
Element prediction: Off
Number of isotope peaks used for i-FIT = 3
Monoisotopic Mass, Even Electron Ions
3807 formula(e) evaluated with 37 results within limits (up to 50 best isotopic matches for each mass)
Elements Used:

Mass	Calc. Mass	mDa	PPM	DBE	Formula	i-FIT	i-FIT Norm	Fit Conf %	C	H	O	Cl	I
881.1543	881.1565	-2.2	-2.5	28.5	C44 H33 O20	24.0	0.008	99.18	44	33	20		
	881.1506	3.7	4.2	37.5	C51 H29 O15	29.3	5.353	0.47	51	29	15		
	881.1553	-1.0	-1.1	39.5	C56 H34 O3 I	29.8	5.823	0.30	56	34	3		1
	881.1518	2.5	2.8	17.5	C38 H42 O16 I	31.7	7.747	0.04	38	42	16		1
	881.1576	-3.3	-3.7	8.5	C31 H46 O21 I	33.8	9.848	0.01	31	46	21		1
	881.1530	1.3	1.5	6.5	C26 H41 O33	35.2	11.207	0.00	26	41	33		
	881.1578	-3.5	-4.0	41.5	C56 H30 O9 Cl	40.8	16.779	0.00	56	30	9		1
	881.1531	1.2	1.4	30.5	C50 H39 O5 Cl I	40.9	16.897	0.00	50	39	5		1 1
	881.1589	-4.6	-5.2	21.5	C43 H43 O10 Cl I	40.9	16.920	0.00	43	43	10		1 1
	881.1543	0.0	0.0	19.5	C38 H38 O22 Cl	41.2	17.211	0.00	38	38	22		1
	881.1496	4.7	5.3	8.5	C32 H47 O18 Cl I	41.7	17.671	0.00	32	47	18		1 1
	881.1554	-1.1	-1.2	-0.5	C25 H51 O23 Cl I	41.7	17.719	0.00	25	51	23		1 1
	881.1556	-1.3	-1.5	32.5	C50 H35 O11 Cl2	43.1	19.118	0.00	50	35	11		2
	881.1498	4.5	5.1	41.5	C57 H31 O6 Cl2	43.3	19.309	0.00	57	31	6		2
	881.1568	-2.5	-2.8	12.5	C37 H48 O12 Cl2 I	43.4	19.398	0.00	37	48	12		2 1
	881.1509	3.4	3.9	21.5	C44 H44 O7 Cl2 I	43.4	19.459	0.00	44	44	7		2 1
	881.1580	-3.7	-4.2	1.5	C25 H47 O29 Cl2	43.7	19.690	0.00	25	47	29		2

Supplementary Data 20. iFit value peak 9 (procyanidin B2-3'3 di-O-gallate) in Marula stem ethanol extract



Supplementary Data 21. MS fragmentation pattern overlaid with MS/MS fragmentation pattern of peak 10 (epicatechin gallate) in Marula stem ethanol extract

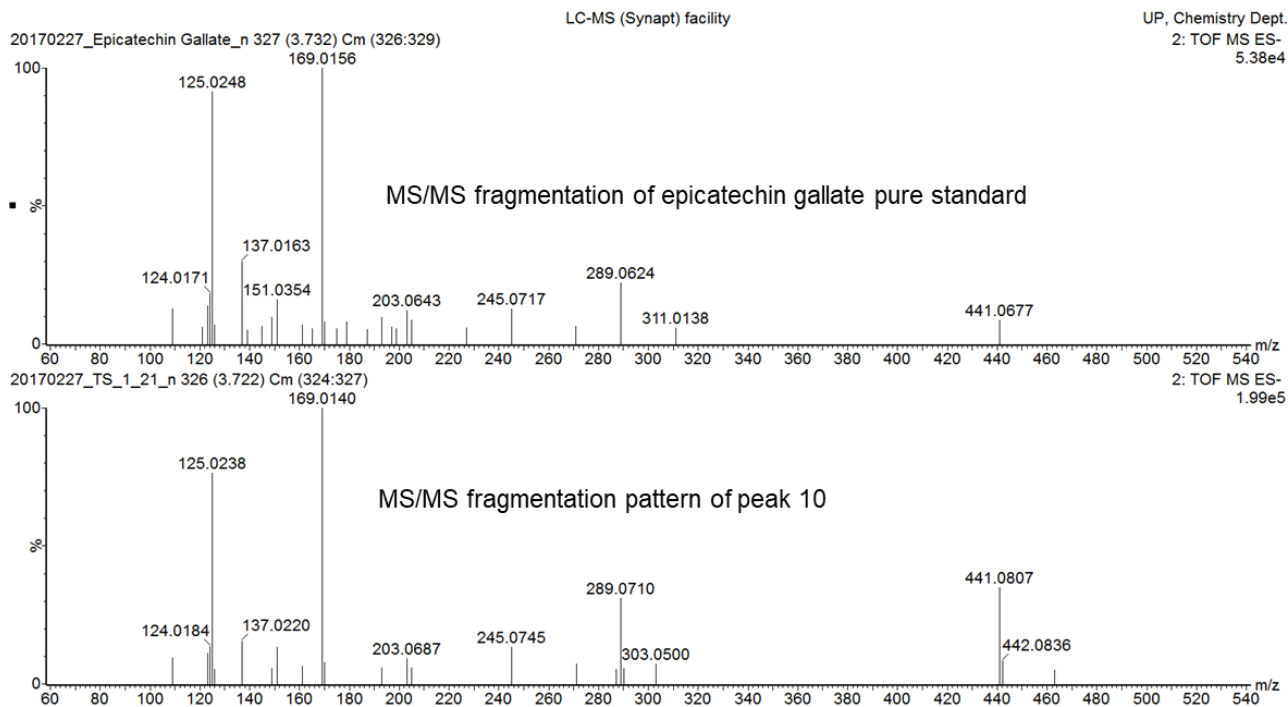
Elemental Composition

File Edit View Process Help

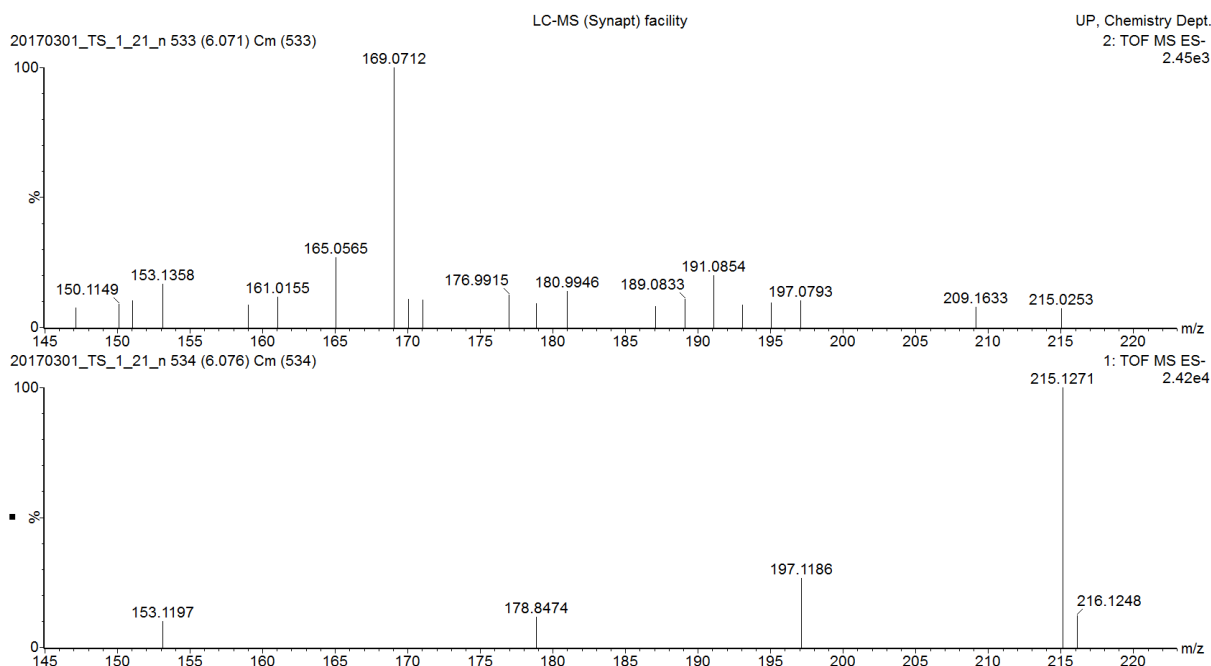
Single Mass Analysis
Tolerance = 5.0 mDa / DBE: min = -1.5, max = 50.0
Element prediction: Off
Number of isotope peaks used for i-FIT = 3
Monoisotopic Mass, Even Electron Ions
261 formula(e) evaluated with 3 results within limits (up to 50 best isotopic matches for each mass)
Elements Used:

Mass	Calc. Mass	mDa	PPM	DBE	Formula	i-FIT	i-FIT Norm	Fit Conf %	C	H	O	Br
441.0820	441.0822	-0.2	-0.5	14.5	C22 H17 O10	39.8	0.047	95.38	22	17	10	
	441.0793	2.7	6.1	5.5	C21 H31 Br2	43.3	3.577	2.80	21	31		2
	441.0854	-3.4	-7.7	16.5	C27 H22 O Br	43.8	4.005	1.82	27	22	1	1

Supplementary Data 22. iFit value epicatechin gallate peak 10 (epicatechin gallate) in Marula stem ethanol extract



Supplementary Data 23. MS/MS fragmentation pattern of peak 10 (epicatechin gallate) in Marula stems overlaid with MS/MS fragmentation pattern of epicatechin gallate pure standard



Supplementary Data 24. MS fragmentation pattern of peak 11 (undecanedioic acid) overlaid with MS/MS fragmentation pattern of peak 11 (undecanedioic acid) in Marula stem ethanol extract

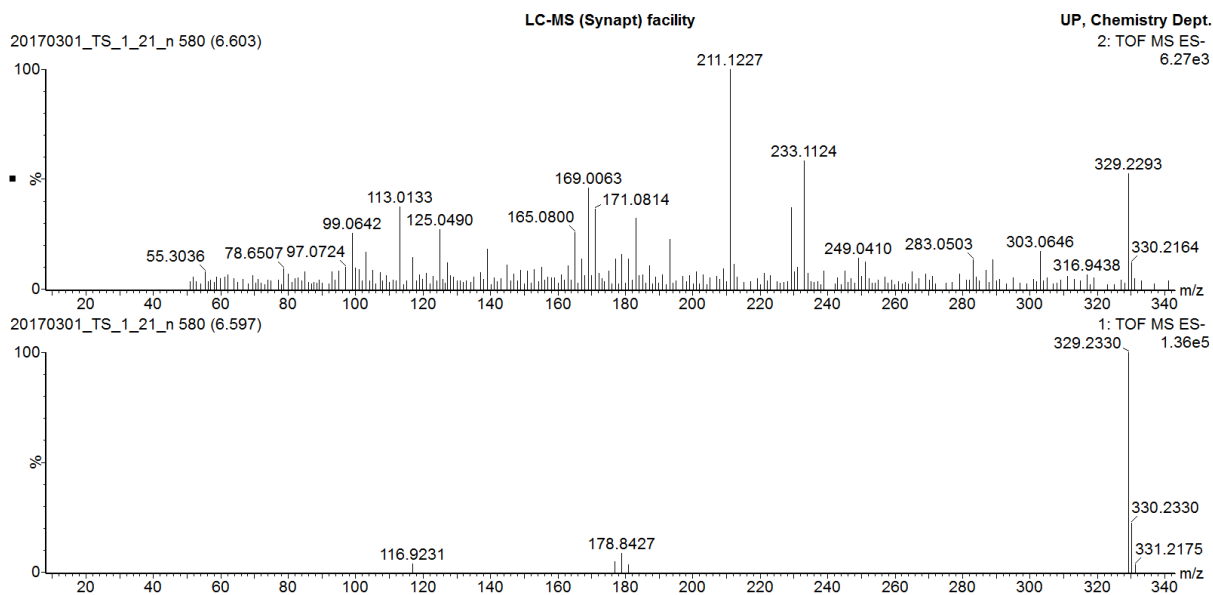
Elemental Composition

File Edit View Process Help

Single Mass Analysis
 Tolerance = 3.0 mDa / DBE: min = -1.5, max = 50.0
 Element prediction: Off
 Number of isotope peaks used for i-FIT = 3
 Monoisotopic Mass, Even Electron Ions
 305 formula(e) evaluated with 2 results within limits (up to 50 best isotopic matches for each mass)
 Elements Used:

Mass	Calc. Mass	mDa	PPM	DBE	Formula	i-FIT	i-FIT Norm	Fit Conf %	C	H	O	²³ Na	Cl
215.1276	215.1283	-0.7	-3.3	2.5	C11 H19 O4	23.9	0.076	92.67	11	19	4		
	215.1259	1.7	7.9	-0.5	C9 H20 O4 ²³ Na	26.4	2.614	7.33	9	20	4	1	

Supplementary Data 25. iFit value for undecanedioic acid



Supplementary Data 26. MS fragmentation pattern of 9,10,13 TriHOME (peak 12) overlaid with its MS/MS fragmentation pattern

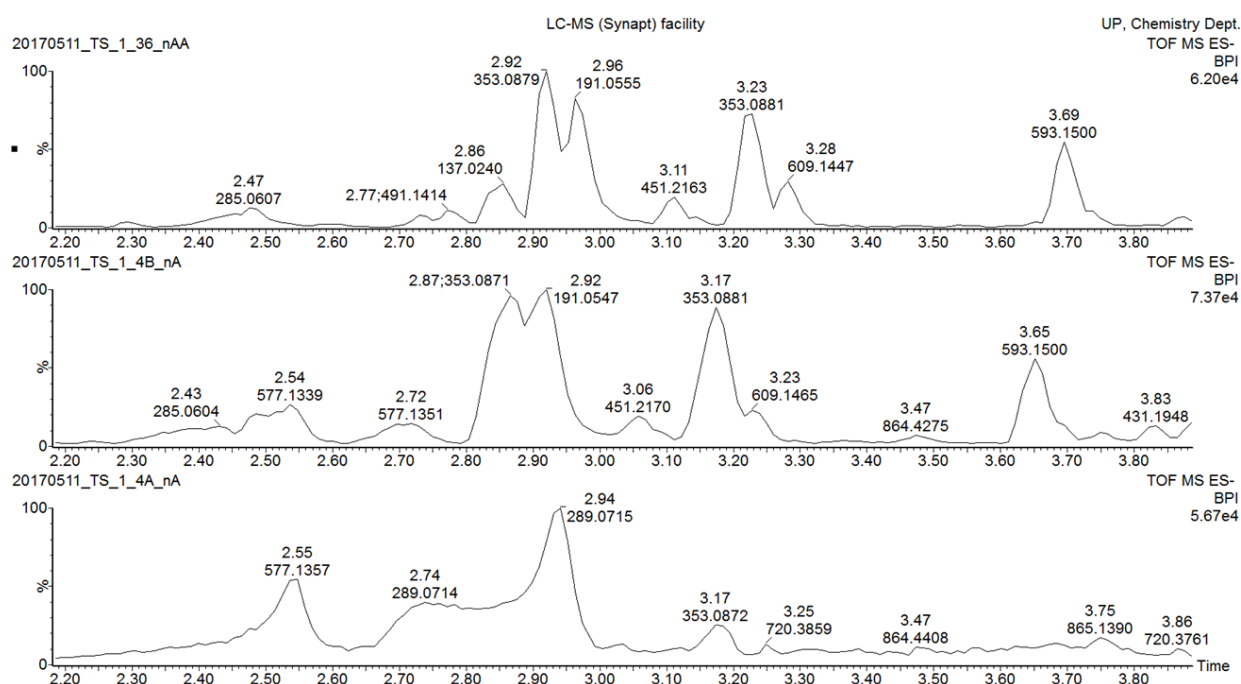
Elemental Composition

File Edit View Process Help

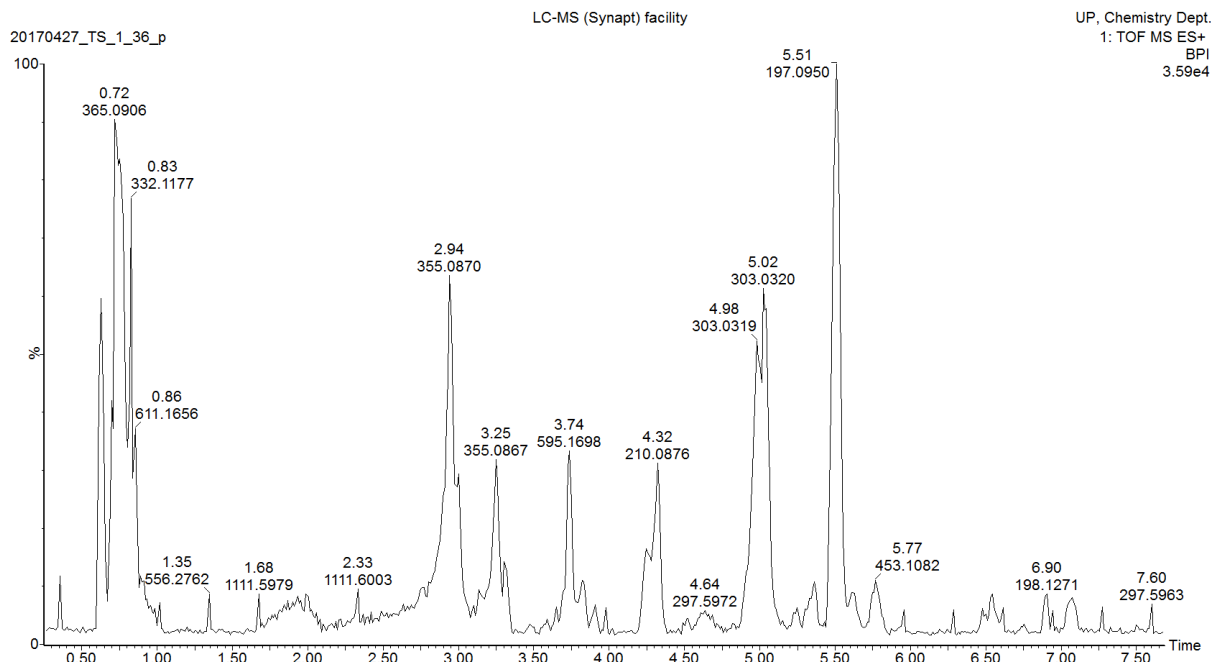
Single Mass Analysis
 Tolerance = 3.0 mDa / DBE: min = -1.5, max = 50.0
 Element prediction: Off
 Number of isotope peaks used for i-FIT = 3
 Monoisotopic Mass, Even Electron Ions
 985 formula(e) evaluated with 2 results within limits (up to 50 best isotopic matches for each mass)
 Elements Used:

Mass	Calc. Mass	mDa	PPM	DBE	Formula	i-FIT	i-FIT Norm	Fit Conf %	C	H	O	23Na	Cl
329.2328	329.2328	0.0	0.0	2.5	C18 H33 O5	32.0	0.053	94.85	18	33	5		
	329.2304	2.4	7.3	-0.5	C16 H34 O5 23Na	34.9	2.965	5.15	16	34	5	1	

Supplementary Data 27. iFit value of 9,10,13 TriHOME (peak 12).



Supplementary Data 28. Expansion of ESI negative mode BPI chromatograms of leaves of *F. sycomorus* extracted sequentially showing retention times 2.20 minutes to 3.80 minutes



Supplementary Data 29. ESI negative mode BPI chromatogram of crude ethanol extract of leaves of *F. sycomorus*.

Elemental Composition

File Edit View Process Help

Single Mass Analysis
Tolerance = 5.0 mDa / DBE: min = -1.5, max = 50.0
Element prediction: Off
Number of isotope peaks used for i-FIT = 3
Monoisotopic Mass, Even Electron Ions
7384 formula(e) evaluated with 55 results within limits (up to 50 best isotopic matches for each mass)
Elements Used:

Mass	Calc. Mass	mDa	PPM	DBE	Formula	i-FIT	i-FIT Norm	Fit Conf %	C	H	O	S	Cl	Br	F	Si
377.0836	377.0851	-1.5	-4.0	1.5	C12 H22 O11 Cl	25.6	0.023	97.76	12	22	11		1			
	377.0837	-0.1	-0.3	1.5	C13 H23 O7 S Cl F	29.7	4.128	1.61	13	23	7	1	1		1	
	377.0835	0.1	0.3	1.5	C12 H23 O8 Cl F Si	32.0	6.433	0.16	12	23	8		1		1	1
	377.0803	3.3	8.8	6.5	C16 H19 O7 Cl F	32.3	6.647	0.13	16	19	7		1		1	
	377.0859	-2.3	-6.1	0.5	C13 H26 O6 S2 Cl	32.8	7.169	0.08	13	26	6	2	1			
	377.0826	1.0	2.7	5.5	C16 H22 O6 S Cl	32.8	7.185	0.08	16	22	6	1	1			
	377.0857	-2.1	-5.6	0.5	C12 H26 O7 S Cl Si	33.2	7.568	0.05	12	26	7	1	1			1
	377.0823	1.3	3.4	5.5	C15 H22 O7 Cl Si	34.2	8.542	0.02	15	22	7		1			1
	377.0812	2.4	6.4	5.5	C17 H23 O2 S2 Cl F	34.3	8.650	0.02	17	23	2	2	1		1	
	377.0846	-1.0	-2.7	0.5	C14 H27 O2 S3 Cl F	34.3	8.689	0.02	14	27	2	3	1		1	
	377.0843	-0.7	-1.9	0.5	C13 H27 O3 S2 Cl F Si	34.3	8.729	0.02	13	27	3	2	1		1	1
	377.0792	4.4	11.7	10.5	C19 H18 O6 Cl	34.6	8.999	0.01	19	18	6		1			
	377.0810	2.6	6.9	5.5	C16 H23 O3 S Cl F Si	34.9	9.309	0.01	16	23	3	1	1		1	1
	377.0834	0.2	0.5	4.5	C17 H26 O S3 Cl	35.1	9.503	0.01	17	26	1	3	1			
	377.0866	-3.0	-8.0	-0.5	C13 H30 O2 S3 Cl Si	35.2	9.562	0.01	13	30	2	3	1			1
	377.0832	0.4	1.1	4.5	C16 H26 O2 S2 Cl Si	35.4	9.749	0.01	16	26	2	2	1			1
	377.0868	-3.2	-8.5	-0.5	C14 H30 O S4 Cl	35.4	9.756	0.01	14	30	1	4	1			
	377.0801	3.5	9.3	9.5	C20 H22 O S2 Cl	35.6	9.942	0.00	20	22	1	2	1			
	377.0798	3.8	10.1	9.5	C19 H22 O2 S Cl Si	36.0	10.384	0.00	19	22	2	1	1			1
	377.0875	-3.9	-10.3	10.5	C21 H20 O Cl2 F	38.0	12.346	0.00	21	20	1		2		1	
	377.0864	-2.8	-7.4	14.5	C24 H19 Cl2	38.1	12.468	0.00	24	19			2			
	377.0868	-3.2	-8.5	9.5	C20 H22 S3 F	38.3	12.666	0.00	20	22		3			1	
	377.0865	-2.9	-7.7	9.5	C19 H22 O S2 F Si	38.3	12.668	0.00	19	22	1	2			1	1
	377.0854	-1.8	-4.8	13.5	C22 H21 S2 Si	38.7	13.051	0.00	22	21		2				1
	377.0881	-4.5	-11.9	9.5	C19 H21 O4 S2	38.8	13.146	0.00	19	21	4	2				
	377.0879	-4.3	-11.4	9.5	C18 H21 O5 S Si	38.9	13.266	0.00	18	21	5	1				1
	377.0795	4.1	10.9	-0.5	C12 H27 O5 Br F Si	39.0	13.374	0.00	12	27	5			1	1	1

Supplementary Data 30. iFit value chloride adduct of palatinose

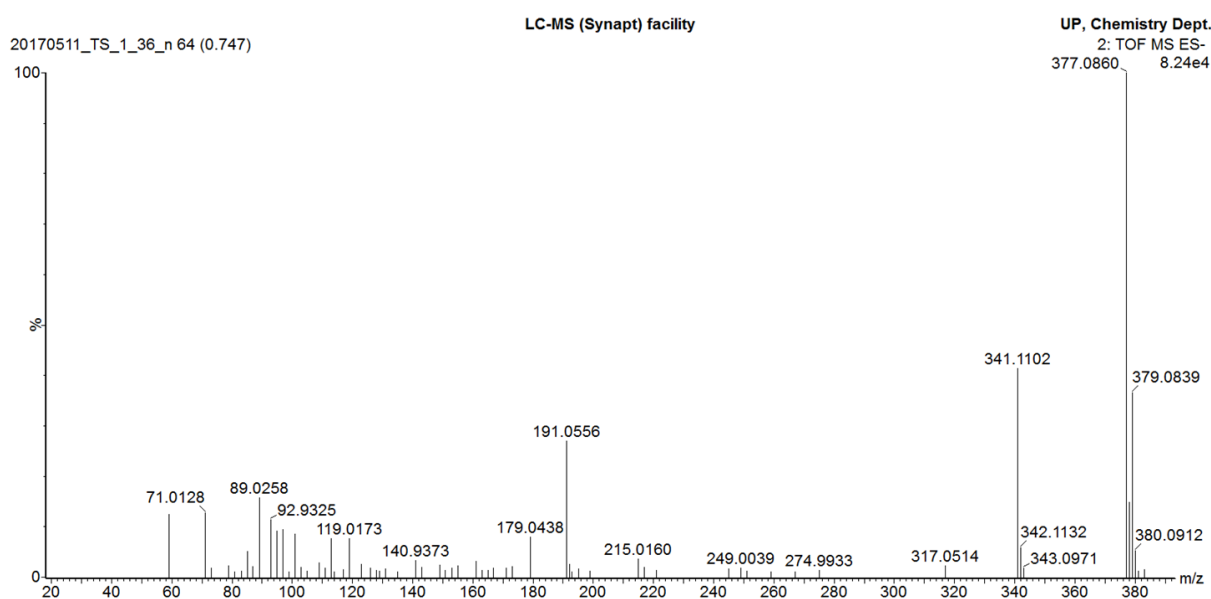
Elemental Composition

File Edit View Process Help

Single Mass Analysis
Tolerance = 5.0 mDa / DBE: min = -1.5, max = 50.0
Element prediction: Off
Number of isotope peaks used for i-FIT = 3
Monoisotopic Mass, Even Electron Ions
4053 formula(e) evaluated with 33 results within limits (up to 50 best isotopic matches for each mass)
Elements Used:

Mass	Calc. Mass	mDa	PPM	DBE	Formula	i-FIT	i-FIT Norm	Fit Conf %	C	H	N	O	Cl	Br
341.1098	341.1084	1.4	4.1	2.5	C12 H21 O11	24.6	0.022	97.82	12	21		11		
	341.1097	0.1	0.3	7.5	C13 H17 N4 O7	29.4	4.838	0.79	13	17	4	7		
	341.1070	2.8	8.2	8.5	C9 H13 N10 O5	29.7	5.194	0.56	9	13	10	5		
	341.1057	4.1	12.0	3.5	C8 H17 N6 O9	30.0	5.416	0.44	8	17	6	9		
	341.1084	1.4	4.1	13.5	C10 H9 N14 O	30.4	5.883	0.28	10	9	14	1		
	341.1111	-1.3	-3.8	12.5	C14 H13 N8 O3	31.8	7.241	0.07	14	13	8	3		
	341.1137	-3.9	-11.4	11.5	C18 H17 N2 O5	33.3	8.797	0.02	18	17	2	5		
	341.1142	-4.4	-12.9	4.5	C3 H13 N14 O6	33.4	8.830	0.01	3	13	14	6		
	341.1129	-3.1	-9.1	-0.5	C2 H17 N10 O10	34.6	10.077	0.00	2	17	10	10		
	341.1129	-3.1	-9.1	10.5	H5 N24	35.1	10.545	0.00		5	24			
	341.1079	1.9	5.6	20.5	C25 H13 N2	36.4	11.826	0.00	25	13	2			
	341.1102	-0.4	-1.2	8.5	C9 H14 N12 O Cl	37.8	13.223	0.00	9	14	12	1	1	
	341.1089	0.9	2.6	3.5	C8 H18 N8 O5 Cl	37.8	13.284	0.00	8	18	8	5	1	
	341.1097	0.1	0.3	15.5	C24 H18 Cl	38.0	13.497	0.00	24	18				1
	341.1129	-3.1	-9.1	7.5	C13 H18 N6 O3 Cl	38.1	13.539	0.00	13	18	6	3	1	
	341.1075	2.3	6.7	-1.5	C7 H22 N4 O9 Cl	38.2	13.624	0.00	7	22	4	9	1	
	341.1062	3.6	10.6	4.5	C4 H14 N14 O3 Cl	38.3	13.753	0.00	4	14	14	3	1	
	341.1048	5.0	14.7	-0.5	C3 H18 N10 O7 Cl	38.3	13.774	0.00	3	18	10	7	1	
	341.1057	4.1	12.0	11.5	C19 H18 N2 O2 Cl	38.4	13.820	0.00	19	18	2	2	1	
	341.1116	-1.8	-5.3	2.5	C12 H22 N2 O7 Cl	38.4	13.833	0.00	12	22	2	7	1	
	341.1089	0.9	2.6	5.5	C13 H22 N6 Br	38.6	14.088	0.00	13	22	6			1
	341.1049	4.9	14.4	1.5	C8 H22 N8 O2 Br	38.7	14.198	0.00	8	22	8	2		1
	341.1120	-2.2	-6.4	3.5	C8 H19 N10 O Cl2	39.0	14.492	0.00	8	19	10	1	2	
	341.1076	2.2	6.4	0.5	C12 H26 N2 O4 Br	39.1	14.607	0.00	12	26	2	4		1
	341.1107	-0.9	-2.6	-1.5	C7 H23 N6 O5 Cl2	39.2	14.622	0.00	7	23	6	5	2	
	341.1080	1.8	5.3	-0.5	C3 H19 N12 O3 Cl2	39.3	14.733	0.00	3	19	12	3	2	
	341.1116	-1.8	-5.3	4.5	C17 H26 O2 Br	39.3	14.793	0.00	17	26		2		1
	341.1108	-1.0	-2.9	0.5	C12 H27 N4 Cl Br	39.4	14.858	0.00	12	27	4		1	1
	341.1139	-4.1	-12.0	-1.5	C7 H24 N8 O Cl3	39.6	15.072	0.00	7	24	8	1	3	

Supplementary Data 31. iFit value of palatinose in *F. sycomorus* leaves extracted with ethanol.



Supplementary Data 32. MS/MS fragmentation pattern peak of 1 (palatinose and chlorogenic acid) in leaves of *F. sycomorus* extracted with ethanol.

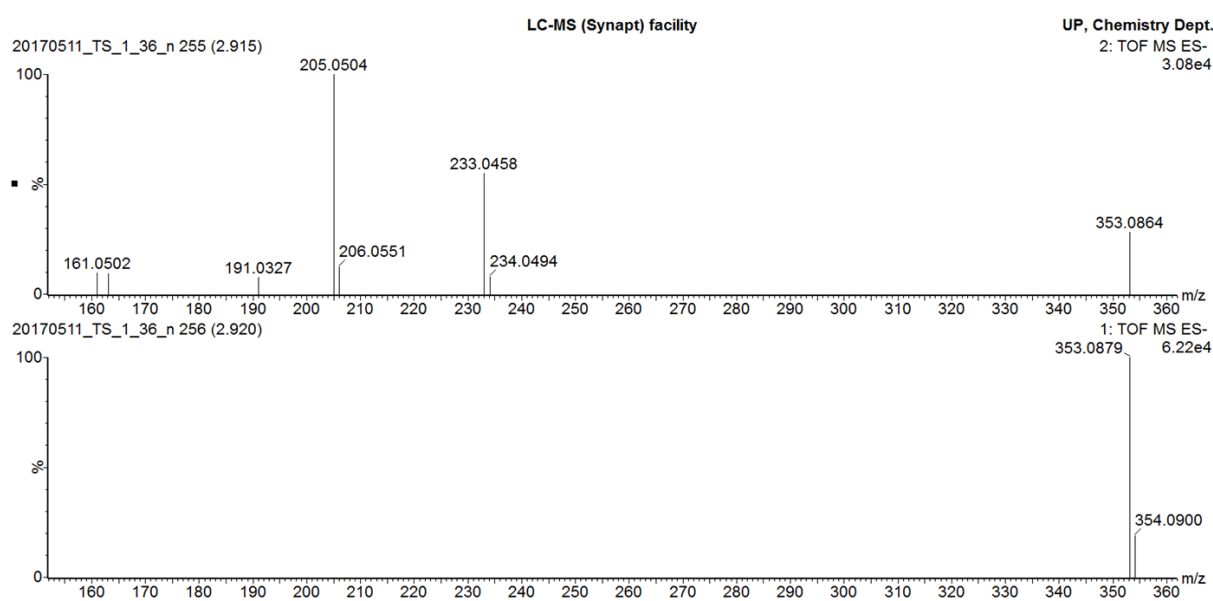
Elemental Composition

File Edit View Process Help

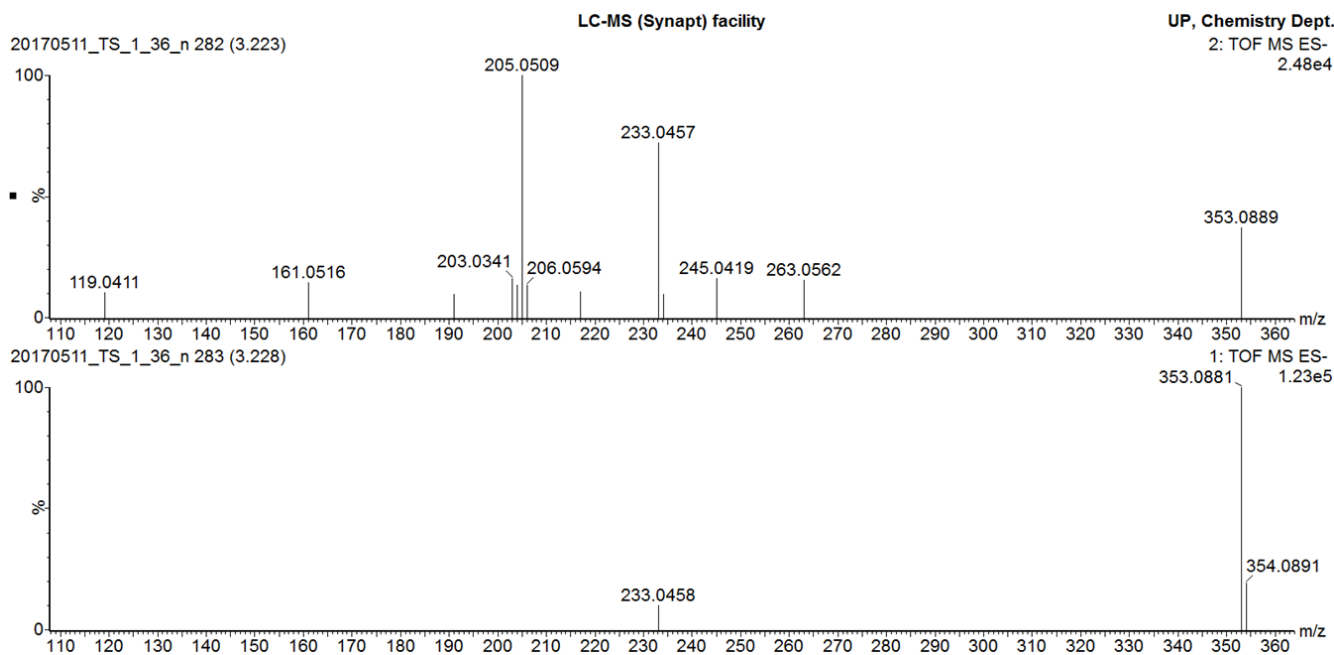
Single Mass Analysis
Tolerance = 5.0 mDa / DBE: min = -1.5, max = 50.0
Element prediction: Off
Number of isotope peaks used for i-FIT = 3
Monoisotopic Mass, Even Electron Ions
269 formula(e) evaluated with 6 results within limits (up to 10 closest results for each mass)
Elements Used:

Mass	Calc. Mass	mDa	PPM	DBE	Formula	i-FIT	i-FIT Norm	Fit Conf %	C	H	N	O	Br
191.0562	191.0556	0.6	3.1	2.5	C7 H11 O6	32.5	0.190	82.66	7	11		6	
	191.0569	-0.7	-3.7	7.5	C8 H7 N4 O2	35.3	3.048	4.74	8	7	4	2	
	191.0542	2.0	10.5	8.5	C4 H3 N10	36.4	4.085	1.68	4	3	10		
	191.0529	3.3	17.3	3.5	C3 H7 N6 O4	37.8	5.546	0.39	3	7	6	4	
	191.0609	-4.7	-24.6	11.5	C13 H7 N2	34.6	2.336	9.67	13	7	2		
	191.0515	4.7	24.6	-1.5	C2 H11 N2 O8	37.1	4.771	0.85	2	11	2	8	

Supplementary Data 33. iFit value for quinic acid



Supplementary Data 34. MS and MS/MS fragmentation pattern of peak 2 (Isobiflorin) in the ethanol extract of leaves of *F. sycamoros*.



Supplementary Data 35. MS and MS/MS fragmentation pattern for Biflorin (peak 4) in *F. sycomorus* ethanol extract

Elemental Composition

File Edit View Process Help

Single Mass Analysis
Tolerance = 5.0 mDa / DBE: min = -1.5, max = 50.0
Element prediction: Off
Number of isotope peaks used for i-FIT = 3
Monoisotopic Mass, Even Electron Ions
13194 formula(e) evaluated with 97 results within limits (up to 50 best isotopic matches for each mass)
Elements Used:

Mass	Calc. Mass	mDa	PPM	DBE	Formula	i-FIT	i-FIT Norm	Fit Conf %	C	H	N	O	S	Cl	B
353.0875	353.0873	0.2	0.6	8.5	C16 H17 O9	14.4	0.072	93.10	16	17		9			
	353.0859	1.6	4.5	14.5	C13 H9 N10 O3	17.5	3.185	4.14	13	9	10	3			
	353.0886	-1.1	-3.1	13.5	C17 H13 N4 O5	18.3	3.976	1.88	17	13	4	5			
	353.0846	2.9	8.2	9.5	C12 H13 N6 O7	19.3	4.930	0.72	12	13	6	7			
	353.0899	-2.4	-6.8	18.5	C18 H9 N8 O	20.9	6.608	0.13	18	9	8	1			
	353.0832	4.3	12.2	4.5	C11 H17 N2 O11	23.2	8.844	0.01	11	17	2	11			
	353.0904	-2.9	-8.2	0.5	C5 H17 N6 O12	23.8	9.455	0.01	5	17	6	12			
	353.0918	-4.3	-12.2	5.5	C6 H13 N10 O8	24.6	10.315	0.00	6	13	10	8			
	353.0832	4.3	12.2	15.5	C9 H5 N16 O	25.3	10.946	0.00	9	5	16	1			
	353.0827	4.8	13.6	22.5	C24 H9 N4	26.2	11.859	0.00	24	9	4				
	353.0891	-1.6	-4.5	6.5	C2 H9 N16 O6	29.2	14.882	0.00	2	9	16	6			
	353.0904	-2.9	-8.2	11.5	C3 H5 N20 O2	29.5	15.182	0.00	3	5	20	2			
	353.0878	-0.3	-0.8	1.5	C H13 N12 O10	30.3	15.932	0.00	1	13	12	10			
	353.0893	-1.8	-5.1	9.5	C10 H13 N10 O3 S	30.9	16.575	0.00	10	13	10	3	1		
	353.0920	-4.5	-12.7	8.5	C14 H17 N4 O5 S	31.0	16.727	0.00	14	17	4	5	1		

Supplementary Data 36. iFit value Peak 2 (isobiflorin) in leaves of *F. sycomorus* extracted with ethanol

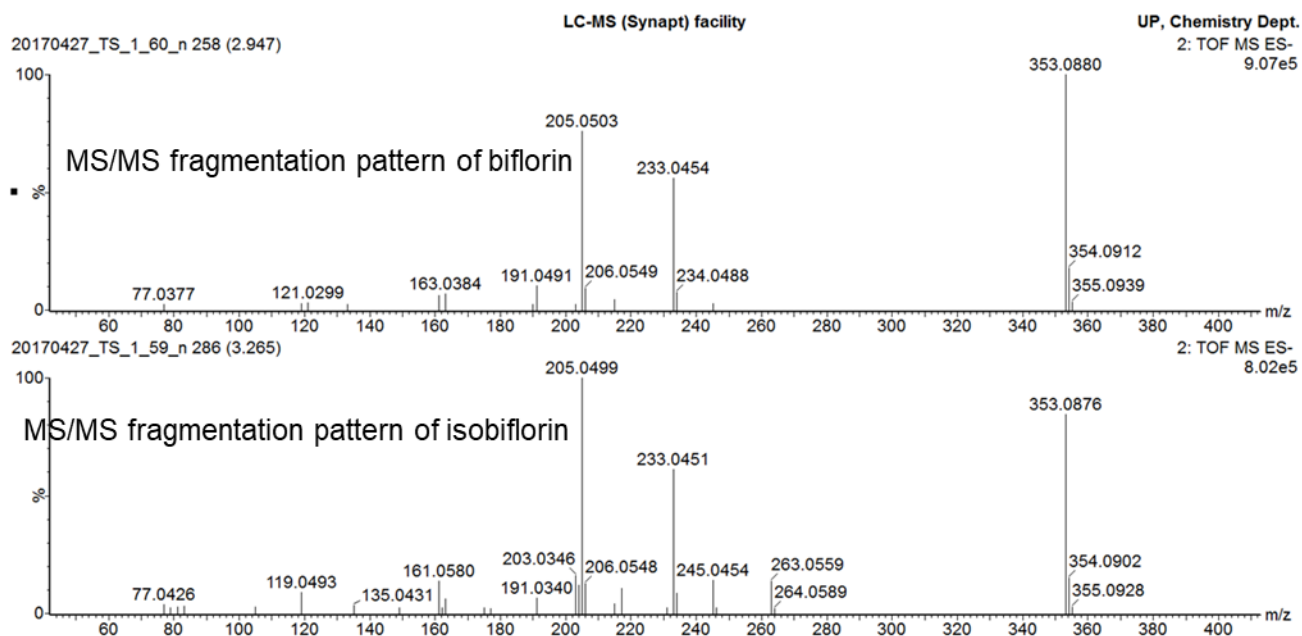
Elemental Composition

File Edit View Process Help

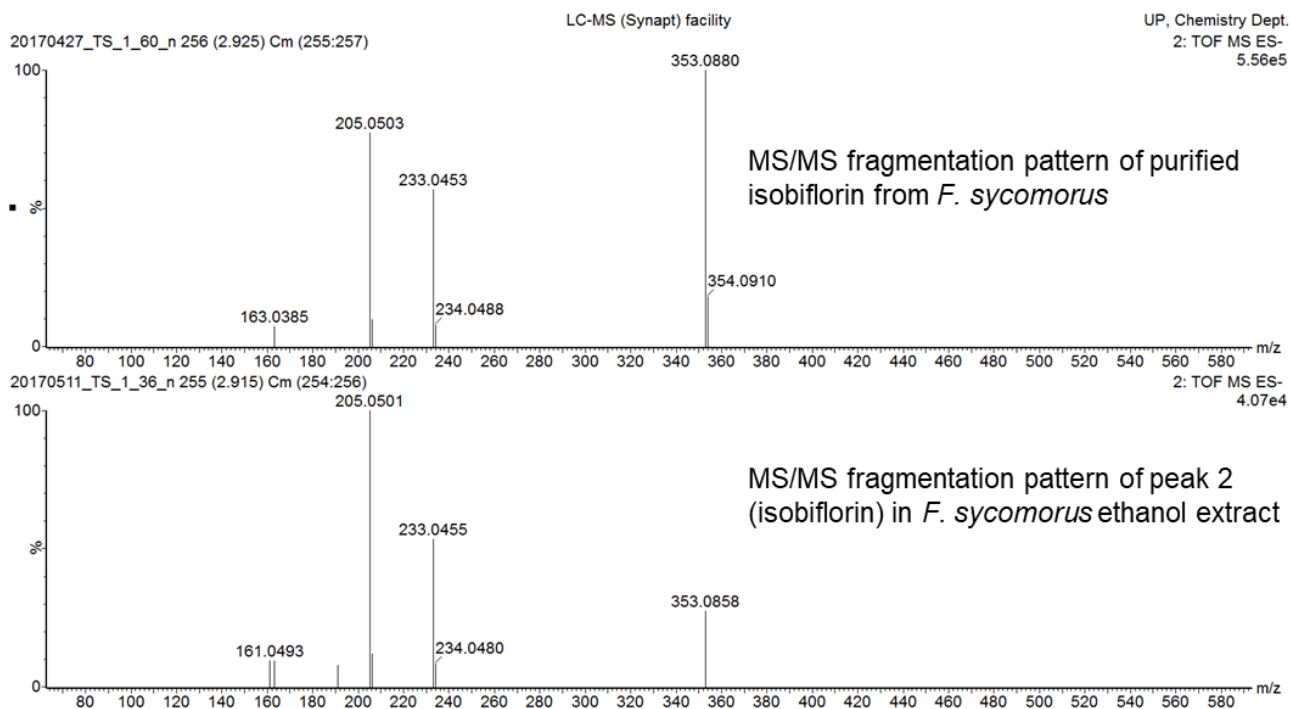
Single Mass Analysis
Tolerance = 5.0 mDa / DBE: min = -1.5, max = 50.0
Element prediction: Off
Number of isotope peaks used for i-FIT = 3
Monoisotopic Mass, Even Electron Ions
1783 formula(e) evaluated with 19 results within limits (up to 50 best isotopic matches for each mass)
Elements Used:

Mass	Calc. Mass	mDa	PPM	DBE	Formula	i-FIT	i-FIT Norm	Fit Conf %	C	H	O	Cl	Br	P	Si
353.0880	353.0873	0.7	2.0	8.5	C16 H17 O9	20.3	0.002	99.78	16	17	9				
	353.0849	3.1	8.8	-0.5	C9 H22 O12 P	26.8	6.517	0.15	9	22	12			1	
	353.0904	-2.4	-6.8	3.5	C12 H21 O10 Si	28.0	7.734	0.04	12	21	10				1
	353.0845	3.5	9.9	12.5	C19 H17 O5 Si	28.8	8.546	0.02	19	17	5				1
	353.0915	-3.5	-9.9	16.5	C23 H18 P Si	29.4	9.135	0.01	23	18				1	1
	353.0893	-1.3	-3.7	7.5	C17 H23 O2 Cl P Si	37.9	17.606	0.00	17	23	2	1		1	1
	353.0862	1.8	5.1	12.5	C21 H19 O Cl P	37.9	17.670	0.00	21	19	1	1		1	
	353.0921	-4.1	-11.6	3.5	C14 H23 O6 Cl P	38.1	17.881	0.00	14	23	6	1		1	
	353.0851	2.9	8.2	-0.5	C10 H22 O11 Cl	38.2	17.977	0.00	10	22	11	1			
	353.0895	-1.5	-4.2	7.5	C18 H23 O Cl2 Si	39.0	18.700	0.00	18	23	1	2			1
	353.0872	0.8	2.3	-1.5	C11 H28 O4 Cl2 P Si	39.0	18.725	0.00	11	28	4	2		1	1
	353.0864	1.6	4.5	12.5	C22 H19 Cl2	39.2	18.903	0.00	22	19		2			
	353.0905	-2.5	-7.1	10.5	C21 H22 Br	39.2	18.943	0.00	21	22				1	
	353.0881	-0.1	-0.3	1.5	C14 H27 O3 Br P	39.3	19.039	0.00	14	27	3		1	1	
	353.0923	-4.3	-12.2	3.5	C15 H23 O5 Cl2	39.3	19.048	0.00	15	23	5	2			
	353.0840	4.0	11.3	3.5	C15 H24 O3 Cl2 P	39.3	19.075	0.00	15	24	3	2		1	
	353.0873	0.7	2.0	-1.5	C12 H28 O3 Cl3 Si	39.4	19.140	0.00	12	28	3	3			1
	353.0883	-0.3	-0.8	1.5	C15 H27 O2 Cl Br	39.6	19.375	0.00	15	27	2	1	1		
	353.0842	3.8	10.8	3.5	C16 H24 O2 Cl3	39.8	19.490	0.00	16	24	2	3			

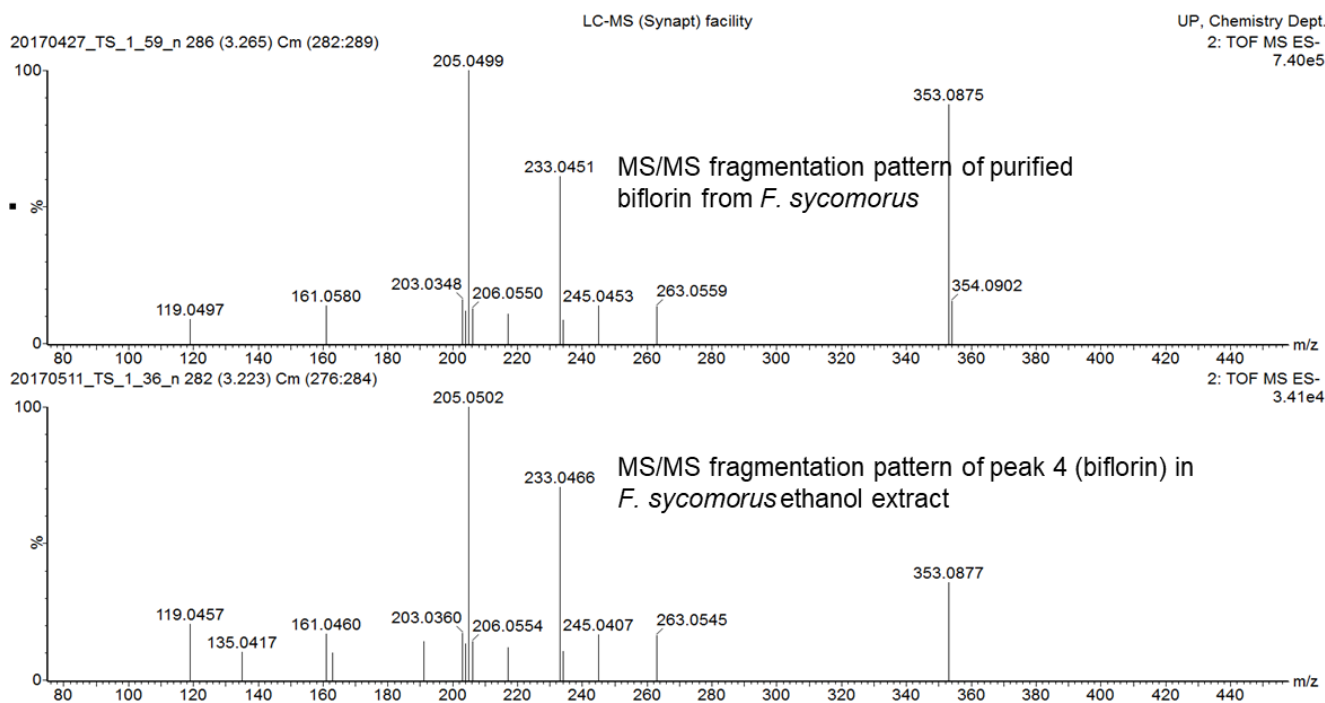
Supplementary Data 37. iFit value biflorin peak 5 in leaves of *F. sycomorus* extracted with ethanol



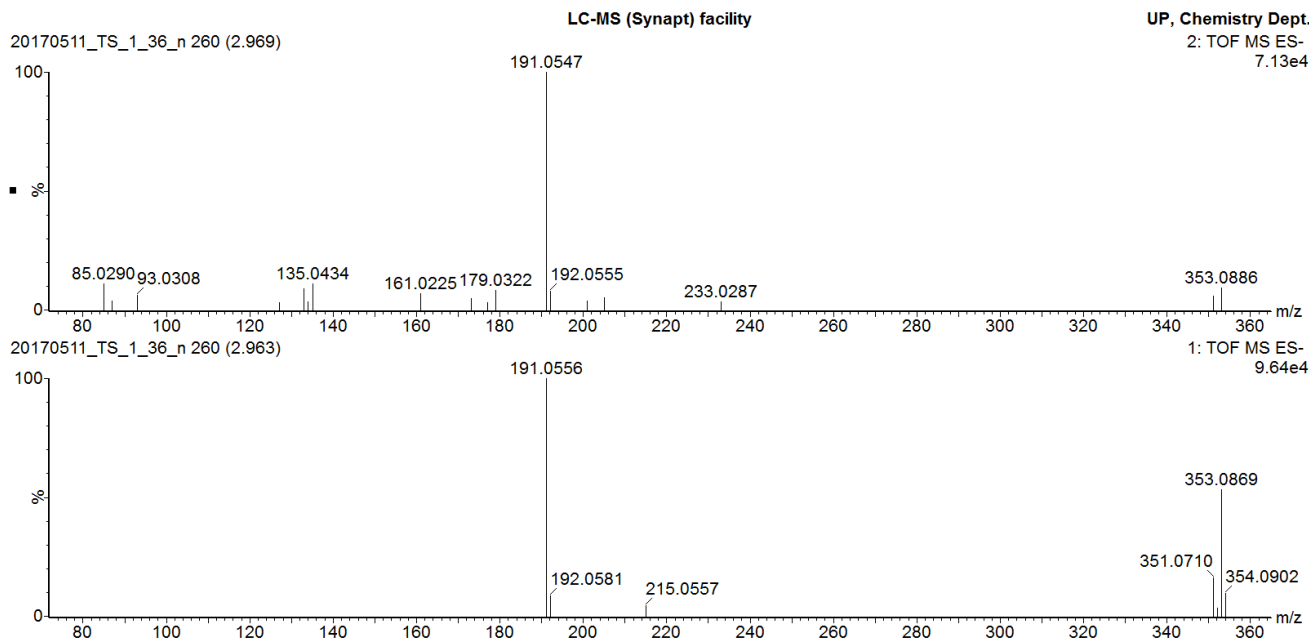
Supplementary Data 38. MS/MS fragmentation pattern of biflorin overlaid with MS/MS fragmentation pattern of isobiflorin



Supplementary Data 39. MS/MS fragmentation pattern of peak 2 (isobiflorin) in *F. sycomorus* ethanol extract overlaid with MS/MS fragmentation pattern of purified isobiflorin from *F. sycomorus*



Supplementary Data 40. MS/MS fragmentation pattern of peak 4 (biflorin) in *F. sycomorus* ethanol extract overlaid with MS/MS fragmentation pattern of purified biflorin from *F. sycomorus*.



Supplementary Data 41. MS and MS/MS data of peak 3 (chlorogenic acid) in the ethanol extract of leaves of *F. sycomorus*.

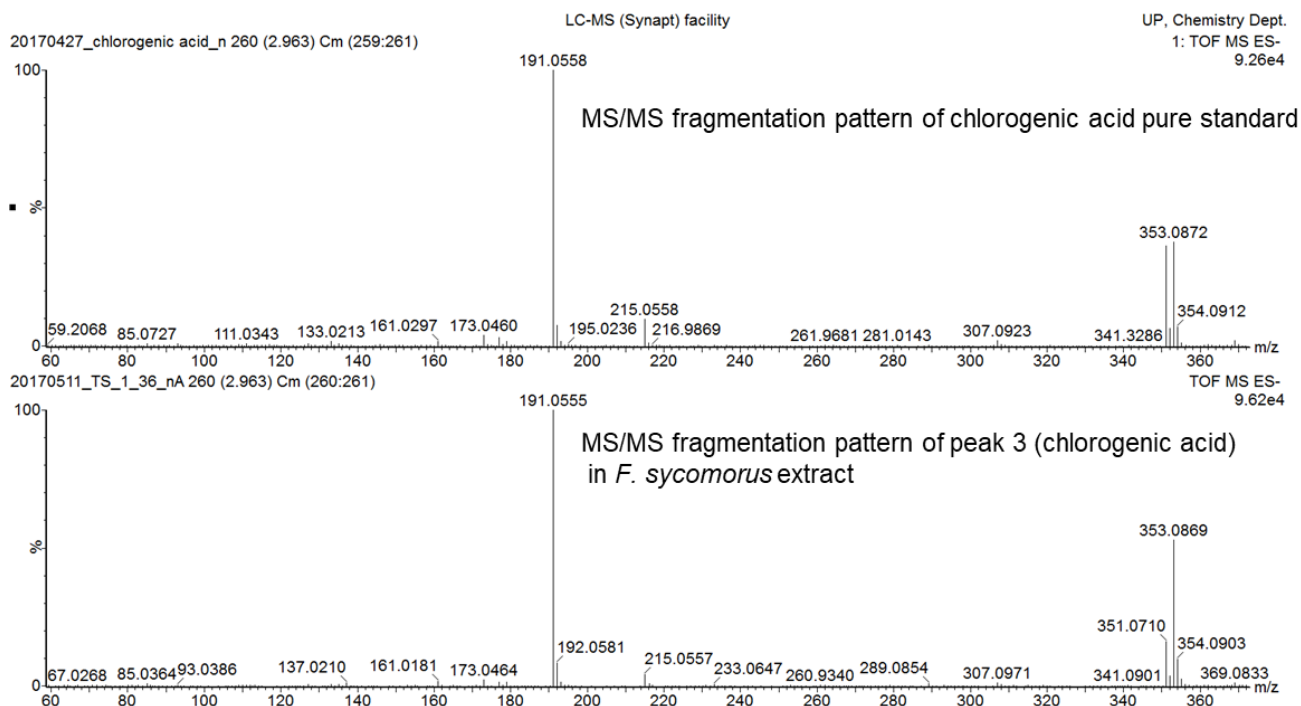
Elemental Composition

File Edit View Process Help

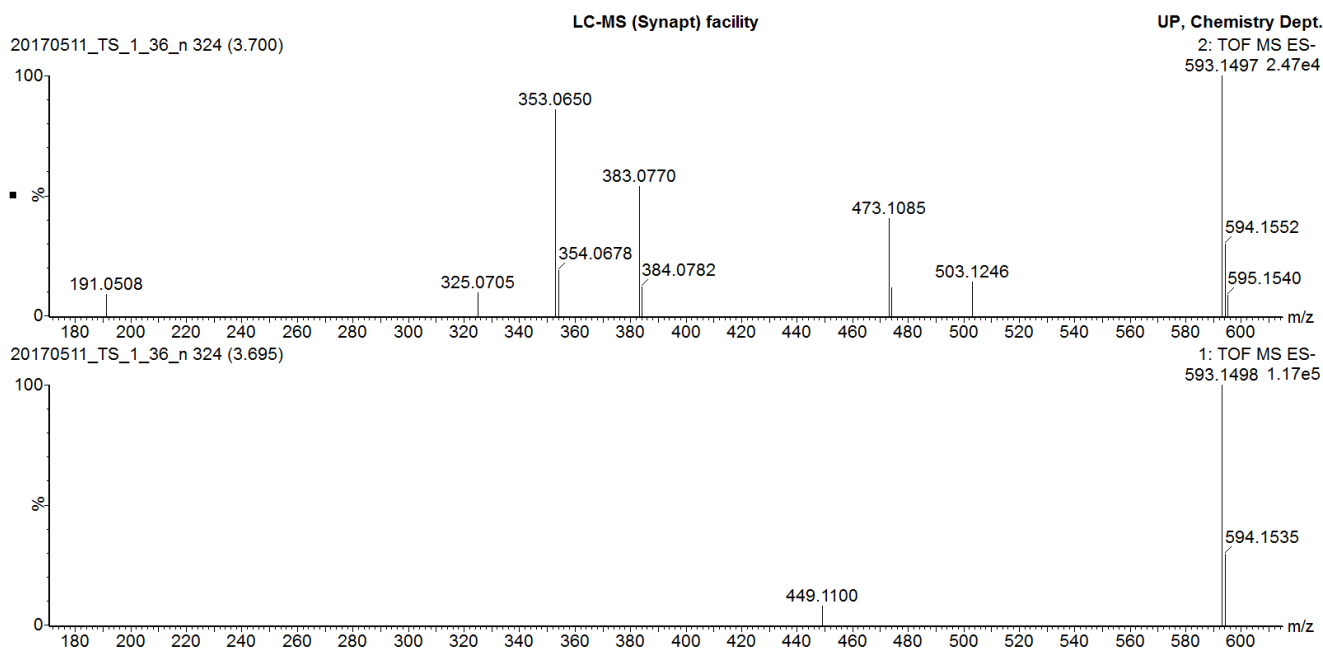
Single Mass Analysis
Tolerance = 5.0 mDa / DBE: min = -1.5, max = 50.0
Element prediction: Off
Number of isotope peaks used for i-FIT = 3
Monoisotopic Mass, Even Electron Ions
13194 formula(e) evaluated with 99 results within limits (up to 50 best isotopic matches for each mass)
Elements Used:

Mass	Calc. Mass	mDa	PPM	DBE	Formula	i-FIT	i-FIT Norm	Fit Conf %	C	H	N	O	S
353.0870	353.0873	-0.3	-0.8	8.5	C16 H17 O9	19.6	0.246	78.20	16	17		9	
	353.0886	-1.6	-4.5	13.5	C17 H13 N4 O5	21.1	1.756	17.27	17	13	4	5	
	353.0899	-2.9	-8.2	18.5	C18 H9 N8 O	23.5	4.156	1.57	18	9	8	1	
	353.0846	2.4	6.8	9.5	C12 H13 N6 O7	24.0	4.584	1.02	12	13	6	7	
	353.0859	1.1	3.1	14.5	C13 H9 N10 O3	24.2	4.796	0.83	13	9	10	3	
	353.0827	4.3	12.2	22.5	C24 H9 N4	24.5	5.063	0.63	24	9	4		
	353.0832	3.8	10.8	4.5	C11 H17 N2 O11	25.0	5.645	0.35	11	17	2	11	
	353.0832	3.8	10.8	15.5	C9 H5 N16 O	27.6	8.167	0.03	9	5	16	1	
	353.0918	-4.8	-13.6	5.5	C6 H13 N10 O8	27.6	8.196	0.03	6	13	10	8	
	353.0904	-3.4	-9.6	0.5	C5 H17 N6 O12	27.8	8.447	0.02	5	17	6	12	
	353.0821	4.9	13.9	13.5	C16 H13 N6 O2 S	28.7	9.352	0.01	16	13	6	2	1
	353.0920	-5.0	-14.2	8.5	C14 H17 N4 O5 S	29.0	9.571	0.01	14	17	4	5	1
	353.0893	-2.3	-6.5	9.5	C10 H13 N10 O3 S	29.0	9.597	0.01	10	13	10	3	1
	353.0848	2.2	6.2	12.5	C20 H17 O4 S	29.5	10.128	0.00	20	17		4	1
	353.0861	0.9	2.5	17.5	C21 H13 N4 S	29.8	10.378	0.00	21	13	4		1
	353.0891	-2.1	-5.9	6.5	C2 H9 N16 O6	29.8	10.439	0.00	2	9	16	6	
	353.0866	0.4	1.1	10.5	C6 H9 N16 O S	29.8	10.455	0.00	6	9	16	1	1
	353.0906	-3.6	-10.2	3.5	C13 H21 O9 S	29.9	10.488	0.00	13	21		9	1
	353.0878	-0.8	-2.3	1.5	C H13 N12 O10	30.1	10.742	0.00	1	13	12	10	
	353.0879	-0.9	-2.5	4.5	C9 H17 N6 O7 S	30.2	10.817	0.00	9	17	6	7	1
	353.0904	-3.4	-9.6	11.5	C3 H5 N20 O2	30.3	10.916	0.00	3	5	20	2	
	353.0853	1.7	4.8	5.5	C5 H13 N12 O5 S	31.0	11.560	0.00	5	13	12	5	1
	353.0866	0.4	1.1	-0.5	C8 H21 N2 O11 S	31.2	11.810	0.00	8	21	2	11	1
	353.0839	3.1	8.8	0.5	C4 H17 N8 O9 S	31.8	12.372	0.00	4	17	8	9	1
	353.0826	4.4	12.5	6.5	C H9 N18 O3 S	32.0	12.602	0.00	1	9	18	3	1

Supplementary Data 42. iFit value for peak 3 (Chlorogenic acid) in the ethanol extract of the leaves of *F. sycomorus*



Supplementary Data 43. MS/MS fragmentation pattern of peak 3 (chlorogenic acid) overlaid with MS/MS fragmentation pattern of chlorogenic acid pure standard



Supplementary Data 44. MS and MS/MS fragmentation pattern of peak 5 in the ethanol extract of leaves of *F. sycomorus*

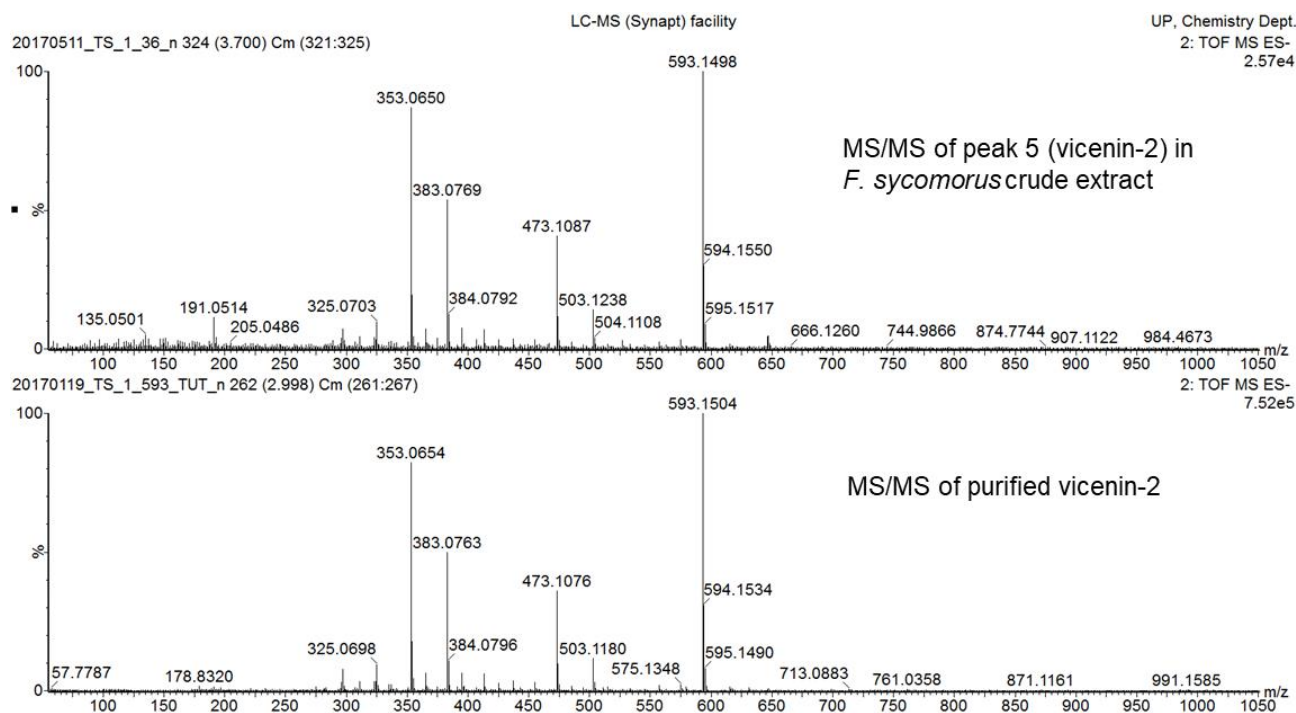
Elemental Composition

File Edit View Process Help

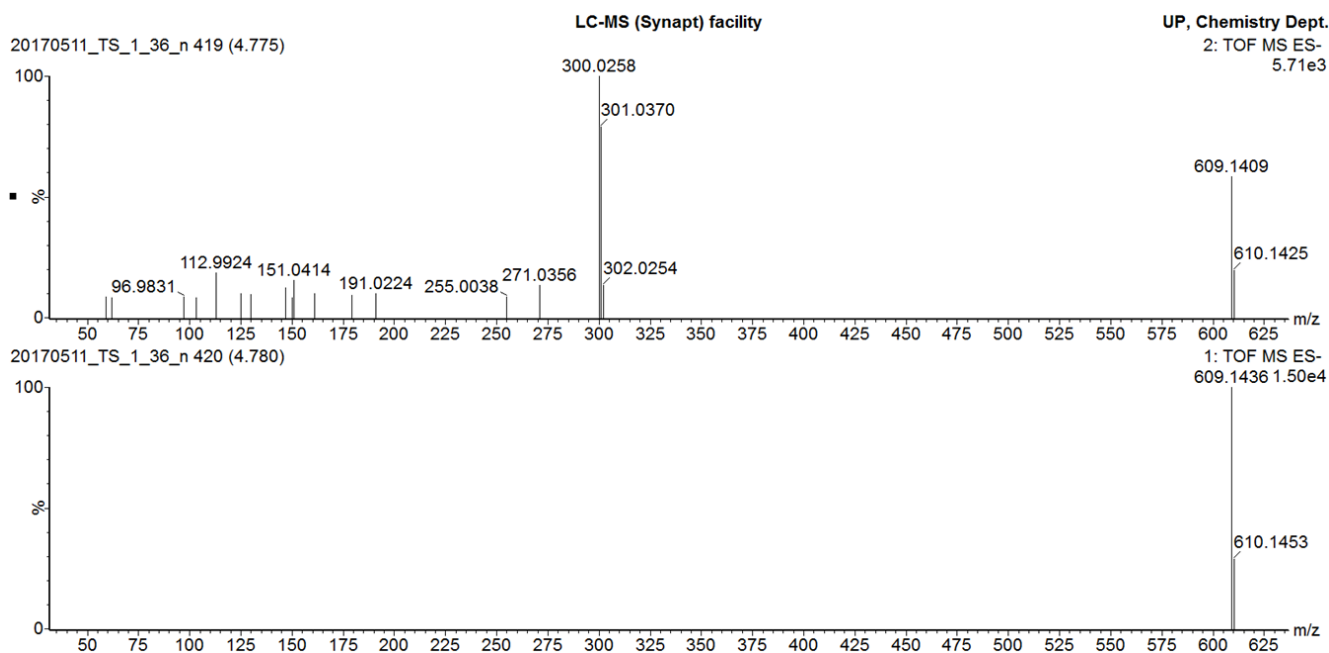
Single Mass Analysis
Tolerance = 5.0 mDa / DBE: min = -1.5, max = 50.0
Element prediction: Off
Number of isotope peaks used for i-FIT = 3
Monoisotopic Mass, Even Electron Ions
3605 formula(e) evaluated with 37 results within limits (up to 50 best isotopic matches for each mass)
Elements Used:

Mass	Calc. Mass	mDa	PPM	DBE	Formula	i-FIT	i-FIT Norm	Fit Conf %	C	H	N	O
593.1493	593.1506	-1.3	-2.2	13.5	C27 H29 O15	20.1	0.101	90.38	27	29		15
	593.1520	-2.7	-4.6	18.5	C28 H25 N4 O11	23.1	3.031	4.83	28	25	4	11
	593.1480	1.3	2.2	14.5	C23 H25 N6 O13	24.3	4.240	1.44	23	25	6	13
	593.1493	0.0	0.0	19.5	C24 H21 N10 O9	24.5	4.451	1.17	24	21	10	9
	593.1533	-4.0	-6.7	23.5	C29 H21 N8 O7	25.3	5.244	0.53	29	21	8	7
	593.1466	2.7	4.6	9.5	C22 H29 N2 O17	25.3	5.277	0.51	22	29	2	17
	593.1506	-1.3	-2.2	24.5	C25 H17 N14 O5	25.7	5.687	0.34	25	17	14	5
	593.1448	4.5	7.6	22.5	C34 H25 O10	26.4	6.319	0.18	34	25		10
	593.1520	-2.7	-4.6	29.5	C26 H13 N18 O	27.0	7.012	0.09	26	13	18	1
	593.1461	3.2	5.4	27.5	C35 H21 N4 O6	27.1	7.055	0.09	35	21	4	6
	593.1466	2.7	4.6	20.5	C20 H17 N16 O7	27.2	7.128	0.08	20	17	16	7
	593.1501	-0.8	-1.3	31.5	C40 H21 N2 O4	27.2	7.179	0.08	40	21	2	4
	593.1453	4.0	6.7	15.5	C19 H21 N12 O11	27.4	7.397	0.06	19	21	12	11
	593.1479	1.4	2.4	25.5	C21 H13 N20 O3	27.5	7.498	0.06	21	13	20	3
	593.1474	1.9	3.2	32.5	C36 H17 N8 O2	27.8	7.745	0.04	36	17	8	2
	593.1515	-2.2	-3.7	36.5	C41 H17 N6	28.1	8.066	0.03	41	17	6	
	593.1448	4.5	7.6	33.5	C32 H13 N14	28.4	8.374	0.02	32	13	14	
	593.1538	-4.5	-7.6	5.5	C16 H29 N6 O18	28.6	8.523	0.02	16	29	6	18
	593.1542	-4.9	-8.3	35.5	C45 H21 O2	28.6	8.592	0.02	45	21	2	2
	593.1525	-3.2	-5.4	0.5	C15 H33 N2 O22	29.2	9.137	0.01	15	33	2	22
	593.1538	-4.5	-7.6	16.5	C14 H17 N20 O8	29.5	9.507	0.01	14	17	20	8
	593.1525	-3.2	-5.4	11.5	C13 H21 N16 O12	29.6	9.566	0.01	13	21	16	12
	593.1453	4.0	6.7	26.5	C17 H9 N26 O	29.7	9.693	0.01	17	9	26	1
	593.1511	-1.8	-3.0	6.5	C12 H25 N12 O16	29.9	9.852	0.01	12	25	12	16
	593.1498	-0.5	-0.8	1.5	C11 H29 N8 O20	30.3	10.260	0.00	11	29	8	20

Supplementary Data 45. iFit value for peak 5 (vicenin-2) in the ethanol extract of leaves of *F. sycomorus*



Supplementary Data 46. MS/MS peak 5 (vicenin-2) in *F. sycomorus* crude extract overlaid with the MS/MS of vicenin-2 pure standard



Supplementary Data 47. MS and MS/MS fragmentation pattern of peak 6 (rutin) in the ethanol extract of leaves of *F. sycomorus*

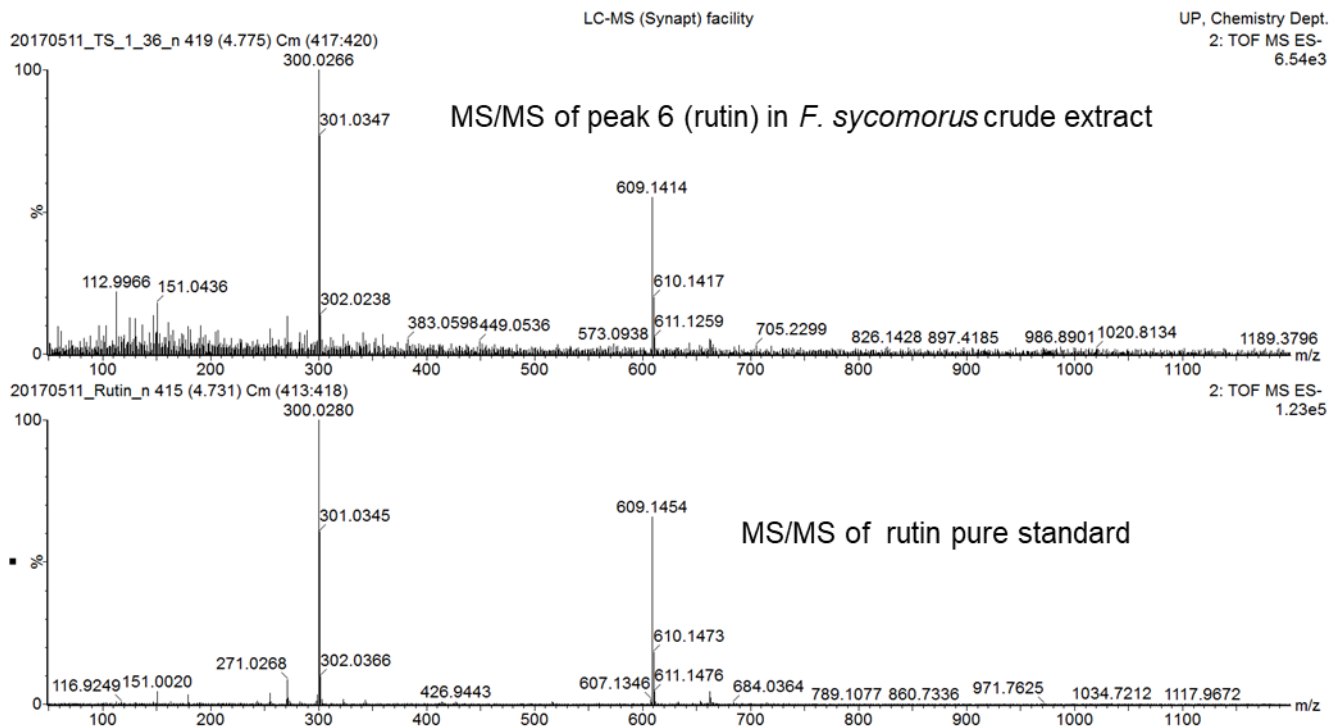
Elemental Composition

File Edit View Process Help

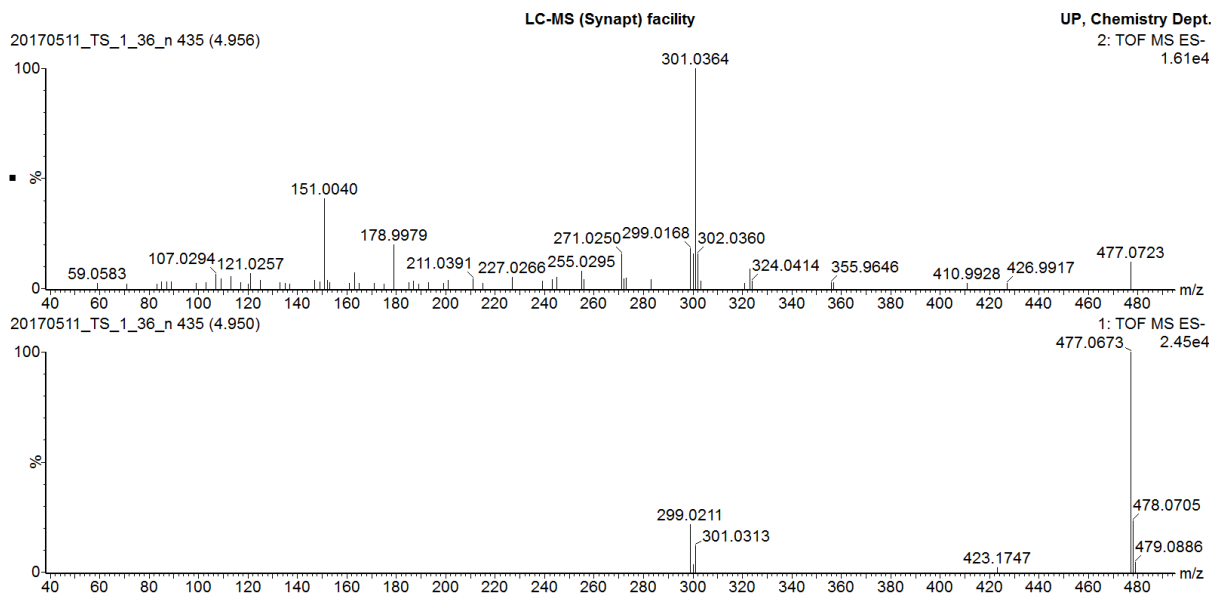
Single Mass Analysis
Tolerance = 5.0 mDa / DBE: min = -1.5, max = 50.0
Element prediction: Off
Number of isotope peaks used for i-FIT = 3
Monoisotopic Mass, Even Electron Ions
178 formula(e) evaluated with 2 results within limits (up to 50 best isotopic matches for each mass)
Elements Used:

Mass	Calc. Mass	mDa	PPM	DBE	Formula	i-FIT	i-FIT Norm	Fit Conf %	C	H	O
609.1447	609.1456	-0.9	-1.5	13.5	C ₂₇ H ₂₉ O ₁₆	27.3	0.022	97.79	27	29	16
	609.1491	-4.4	-7.2	35.5	C ₄₅ H ₂₁ O ₃	31.1	3.813	2.21	45	21	3

Supplementary Data 48. iFit value for peak 6 (rutin) in the ethanol extract of *F. sycomorus*.



Supplementary Data 49. MS/MS peak 6 (rutin) in *F. sycomorus* crude extract overlaid with the MS/MS of rutin pure standard



Supplementary Data 50. MS and MS/MS fragmentation pattern of peak 7 (quercetin 3 glucuronide) in the ethanol extract of leaves of *F. sycomorus*.

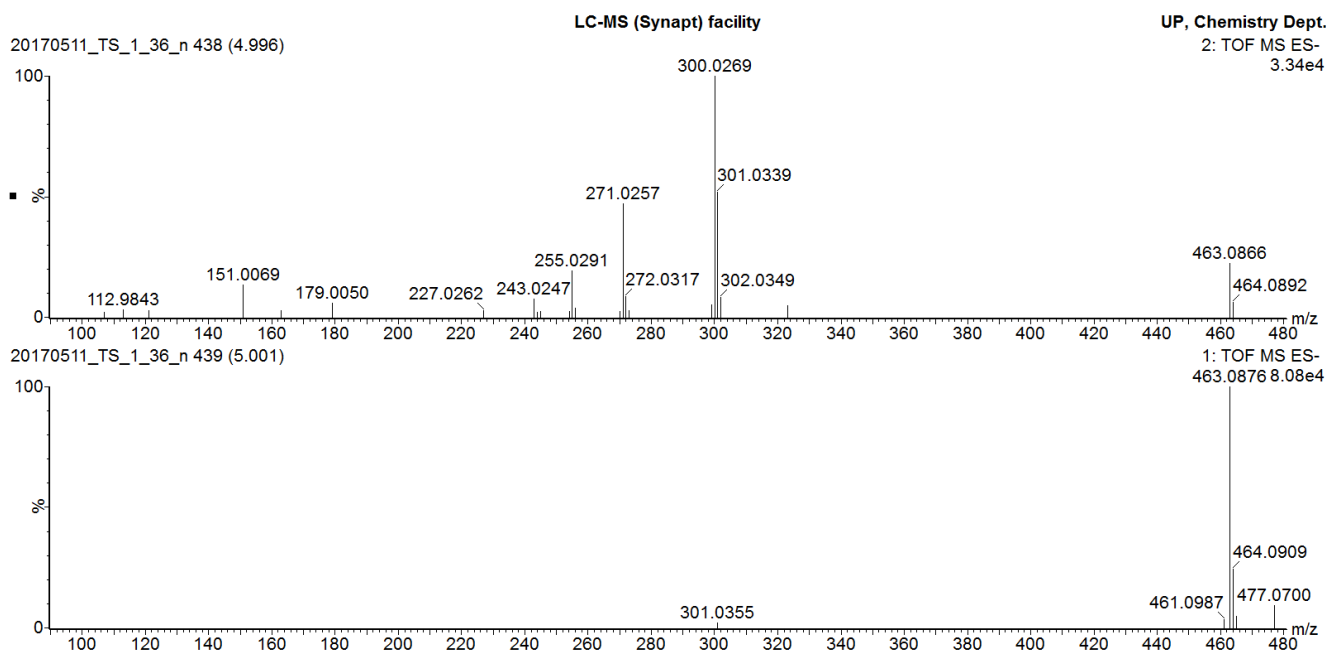
Elemental Composition

File Edit View Process Help

Single Mass Analysis
Tolerance = 5.0 mDa / DBE: min = -1.5, max = 50.0
Element prediction: Off
Number of isotope peaks used for i-FIT = 3
Monoisotopic Mass, Odd and Even Electron Ions
159782 formula(e) evaluated with 1979 results within limits (up to 50 best isotopic matches for each mass)
Elements Used:

Mass	Calc. Mass	mDa	PPM	DBE	Formula	i-FIT	i-FIT Norm	Fit Conf %	C	H	N	O	Si	P
477.0671	477.0669	0.2	0.4	13.5	C21 H17 O13	18.6	0.009	99.12	21	17		13		
	477.0656	1.5	3.1	14.0	C19 H15 N3 O12	24.4	5.807	0.30	19	15	3	12		
	477.0699	-2.8	-5.9	13.5	C20 H18 N2 O10 P	24.8	6.201	0.20	20	18	2	10		1
	477.0669	0.2	0.4	19.0	C20 H11 N7 O8	26.0	7.348	0.06	20	11	7	8		
	477.0647	2.4	5.0	21.5	C7 H N26 Si	26.1	7.479	0.06	7	1	26		1	
	477.0683	-1.2	-2.5	18.5	C22 H13 N4 O9	26.4	7.812	0.04	22	13	4	9		
	477.0660	1.1	2.3	21.0	C9 H3 N23 O Si	26.7	8.059	0.03	9	3	23	1	1	
	477.0656	1.5	3.1	19.5	C18 H9 N10 O7	27.1	8.443	0.02	18	9	10	7		
	477.0712	-4.1	-8.6	18.5	C21 H14 N6 O6 P	27.3	8.691	0.02	21	14	6	6		1
	477.0686	-1.5	-3.1	14.0	C18 H16 N5 O9 P	27.3	8.707	0.02	18	16	5	9		1
	477.0642	2.9	6.1	14.5	C17 H13 N6 O11	27.4	8.717	0.02	17	13	6	11		
	477.0696	-2.5	-5.2	18.0	C24 H15 N O10	27.7	9.087	0.01	24	15	1	10		
	477.0699	-2.8	-5.9	19.0	C19 H12 N9 O5 P	28.0	9.313	0.01	19	12	9	5		1
	477.0717	-4.6	-9.6	20.0	C12 H8 N19 Si P	28.1	9.464	0.01	12	8	19		1	1
	477.0690	-1.9	-4.0	15.5	C9 H10 N18 O3 Si P	28.2	9.577	0.01	9	10	18	3	1	1
	477.0674	-0.3	-0.6	20.5	C11 H5 N20 O2 Si	28.4	9.794	0.01	11	5	20	2	1	
	477.0704	-3.3	-6.9	15.0	C11 H12 N15 O4 Si P	28.5	9.897	0.01	11	12	15	4	1	1
	477.0642	2.9	6.1	20.0	C16 H7 N13 O6	28.6	9.929	0.00	16	7	13	6		
	477.0682	-1.1	-2.3	24.0	C21 H7 N11 O4	28.8	10.167	0.00	21	7	11	4		
	477.0672	-0.1	-0.2	9.0	C17 H20 N O13 P	28.9	10.219	0.00	17	20	1	13		1
	477.0677	-0.6	-1.3	16.0	C7 H8 N21 O2 Si P	28.9	10.242	0.00	7	8	21	2	1	1
	477.0669	0.2	0.4	24.5	C19 H5 N14 O3	28.9	10.257	0.00	19	5	14	3		
	477.0686	-1.5	-3.1	19.5	C17 H10 N12 O4 P	29.0	10.370	0.00	17	10	12	4		1
	477.0672	-0.1	-0.2	14.5	C16 H14 N8 O8 P	29.0	10.371	0.00	16	14	8	8		1
	477.0629	4.2	8.8	15.0	C15 H11 N9 O10	29.1	10.458	0.00	15	11	9	10		
	477.0696	-2.5	-5.2	23.5	C23 H9 N8 O5	29.1	10.506	0.00	23	9	8	5		

Supplementary Data 51. iFit value for peak 7 (quercetin 3 glucuronide) in the ethanol extract of leaves of *F. sycomorus*.



Supplementary Data 52. MS and MS MS data of peak 8 (isoquercetin) in the ethanol extract of leaves of *F. sycomorus*

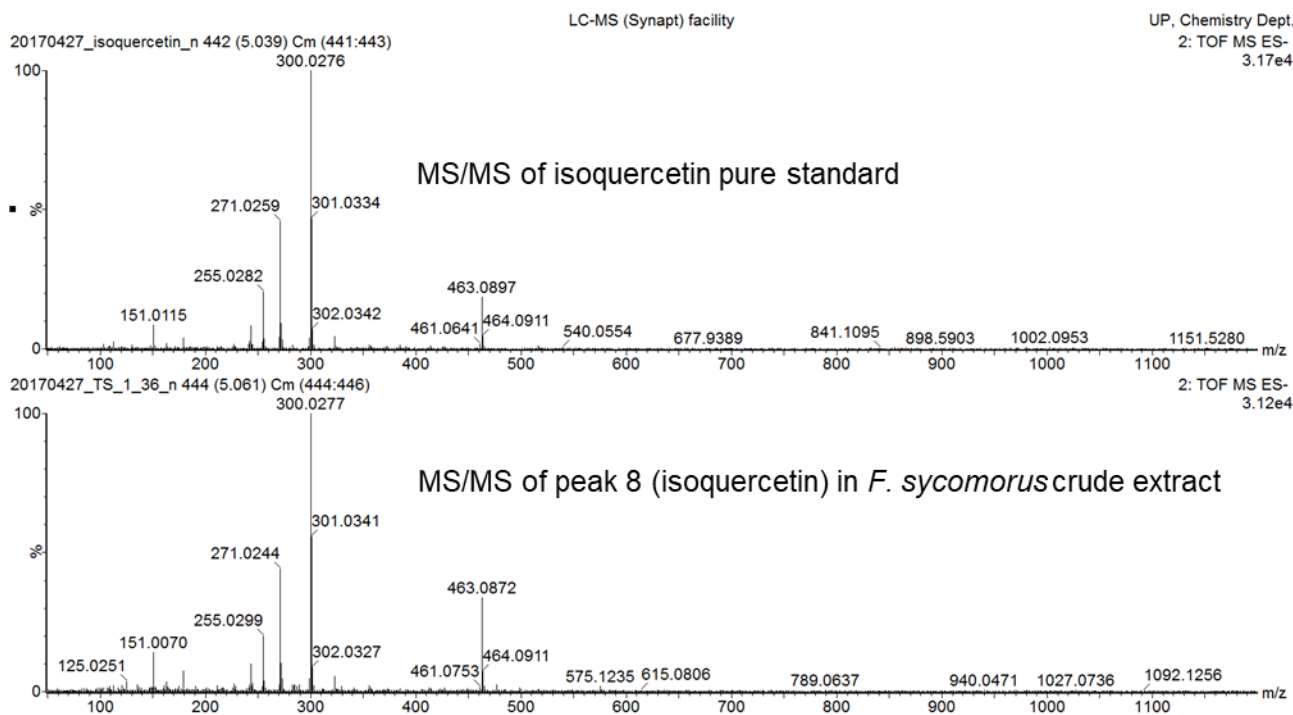
Elemental Composition

File Edit View Process Help

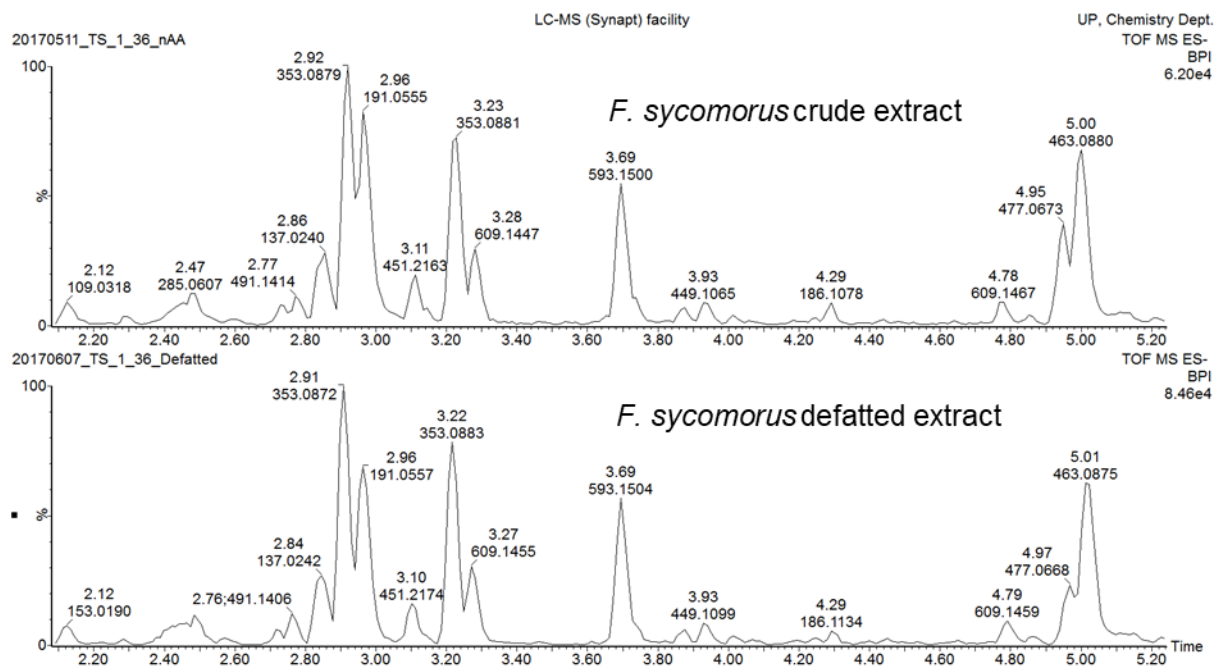
Single Mass Analysis
Tolerance = 5.0 mDa / DBE: min = -1.5, max = 50.0
Element prediction: Off
Number of isotope peaks used for i-FIT = 3
Monoisotopic Mass, Even Electron Ions
23659 formula(e) evaluated with 187 results within limits (up to 50 best isotopic matches for each mass)
Elements Used:

Mass	Calc. Mass	mDa	PPM	DBE	Formula	i-FIT	i-FIT Norm	Fit Conf %	C	H	N	O	P
463.0880	463.0877	0.3	0.6	12.5	C21 H19 O12	18.9	0.008	99.20	21	19		12	
	463.0906	-2.6	-5.6	12.5	C20 H20 N2 O9 P	24.1	5.216	0.54	20	20	2	9	1
	463.0890	-1.0	-2.2	17.5	C22 H15 N4 O8	26.2	7.276	0.07	22	15	4	8	
	463.0850	3.0	6.5	13.5	C17 H15 N6 O10	26.3	7.416	0.06	17	15	6	10	
	463.0863	1.7	3.7	18.5	C18 H11 N10 O6	26.7	7.739	0.04	18	11	10	6	
	463.0920	-4.0	-8.6	17.5	C21 H16 N6 O5 P	26.9	8.029	0.03	21	16	6	5	1
	463.0880	0.0	0.0	13.5	C16 H16 N8 O7 P	28.1	9.226	0.01	16	16	8	7	1
	463.0836	4.4	9.5	8.5	C16 H19 N2 O14	28.4	9.501	0.01	16	19	2	14	
	463.0893	-1.3	-2.8	18.5	C17 H12 N12 O3 P	28.5	9.571	0.01	17	12	12	3	1
	463.0903	-2.3	-5.0	22.5	C23 H11 N8 O4	28.6	9.681	0.01	23	11	8	4	
	463.0876	0.4	0.9	23.5	C19 H7 N14 O2	28.6	9.699	0.01	19	7	14	2	
	463.0866	1.4	3.0	8.5	C15 H20 N4 O11 P	29.1	10.214	0.00	15	20	4	11	1
	463.0848	3.2	6.9	21.5	C27 H16 N2 O4 P	29.4	10.484	0.00	27	16	2	4	1
	463.0836	4.4	9.5	19.5	C14 H7 N16 O4	29.5	10.604	0.00	14	7	16	4	
	463.0917	-3.7	-8.0	27.5	C24 H7 N12	30.2	11.240	0.00	24	7	12		
	463.0850	3.0	6.5	24.5	C15 H3 N20	30.3	11.345	0.00	15	3	20		
	463.0861	1.9	4.1	26.5	C28 H12 N6 P	30.4	11.514	0.00	28	12	6		1
	463.0853	2.7	5.8	3.5	C14 H24 O15 P	30.6	11.659	0.00	14	24		15	1
	463.0853	2.7	5.8	14.5	C12 H12 N14 O5 P	30.8	11.836	0.00	12	12	14	5	1
	463.0831	4.9	10.6	26.5	C29 H11 N4 O3	30.8	11.848	0.00	29	11	4	3	
	463.0888	-0.8	-1.7	25.5	C32 H16 O2 P	30.8	11.851	0.00	32	16		2	1

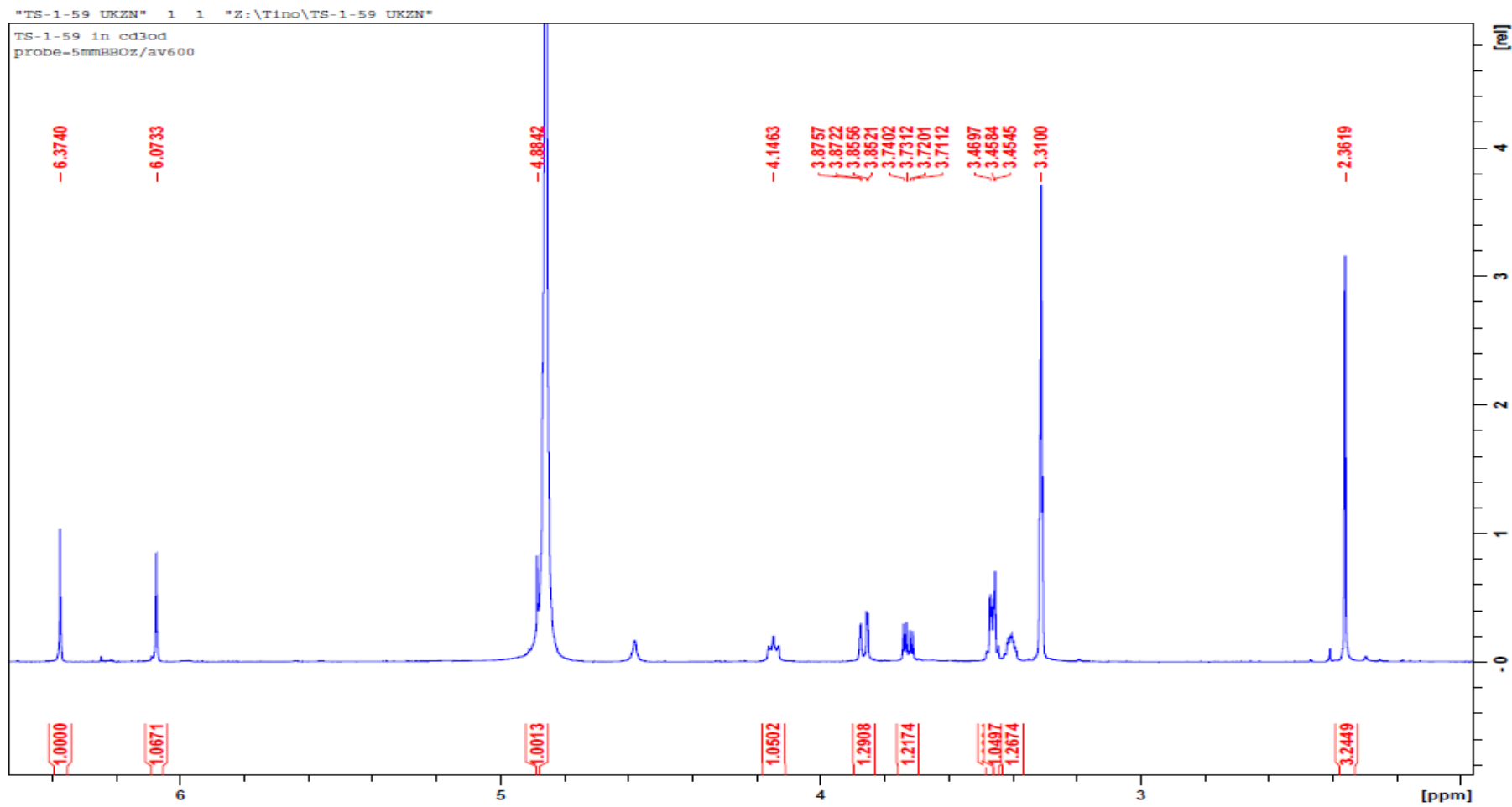
Supplementary Data 53. iFit value for peak 8 (isoquercetin) in the ethanol extract of leaves of *F. sycomorus*



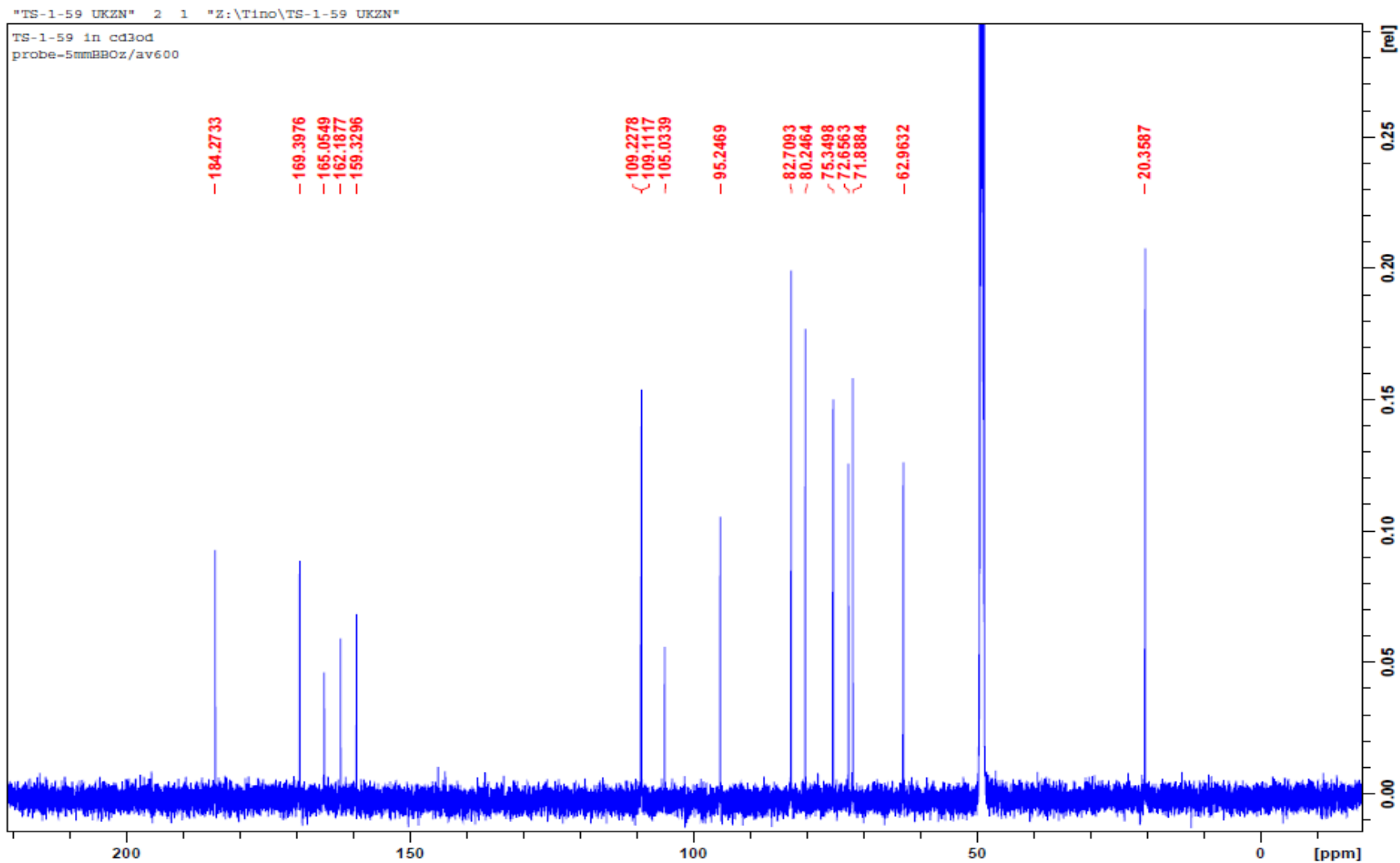
Supplementary Data 54. MS/MS peak 8 (isoquercetin) in *F. sycomorus* crude extract overlaid with the MS/MS of isoquercetin pure standard



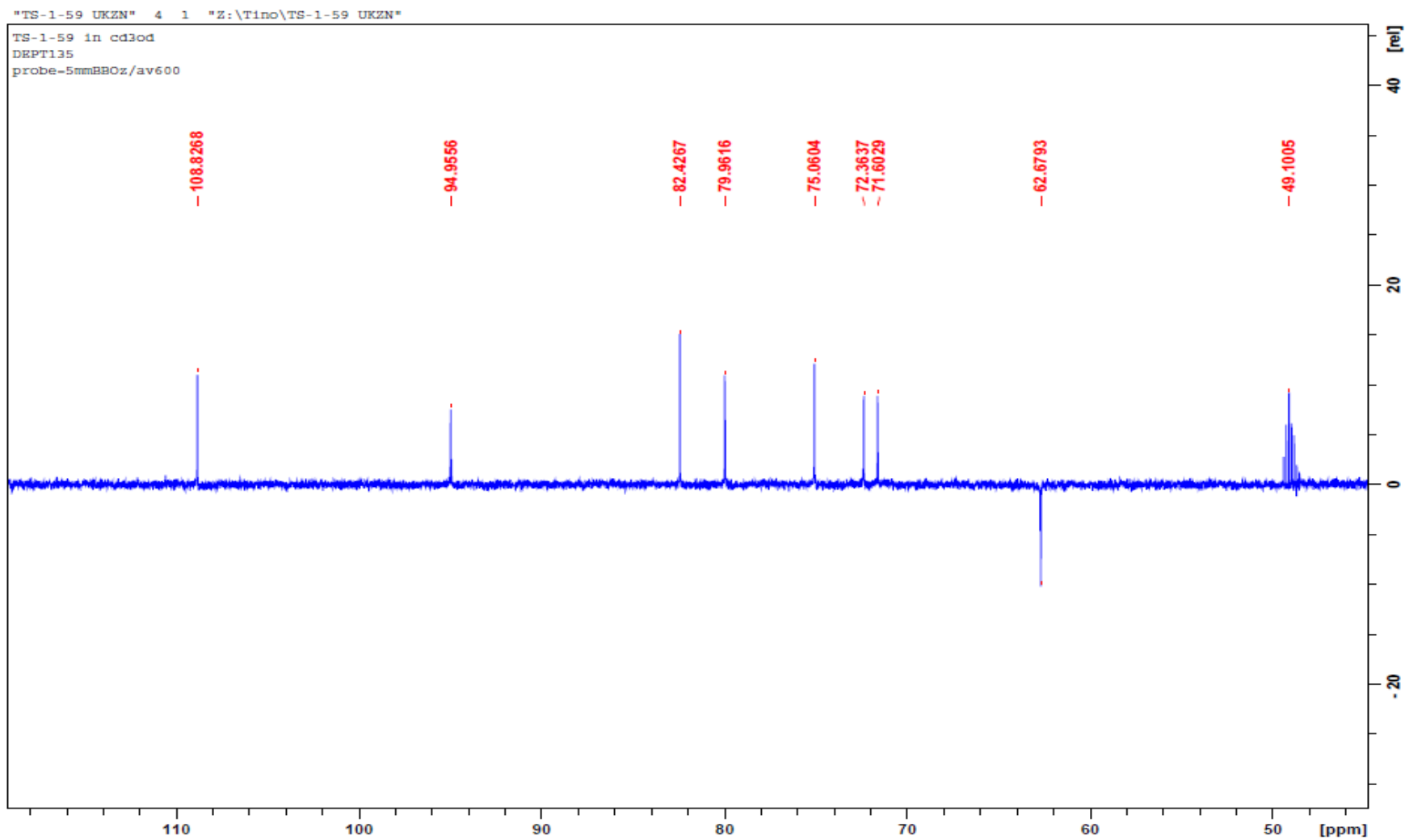
Supplementary Data 55. Expanded chromatograms of the *F. sycomorus* crude ethanol extract overlaid with the defatted fraction



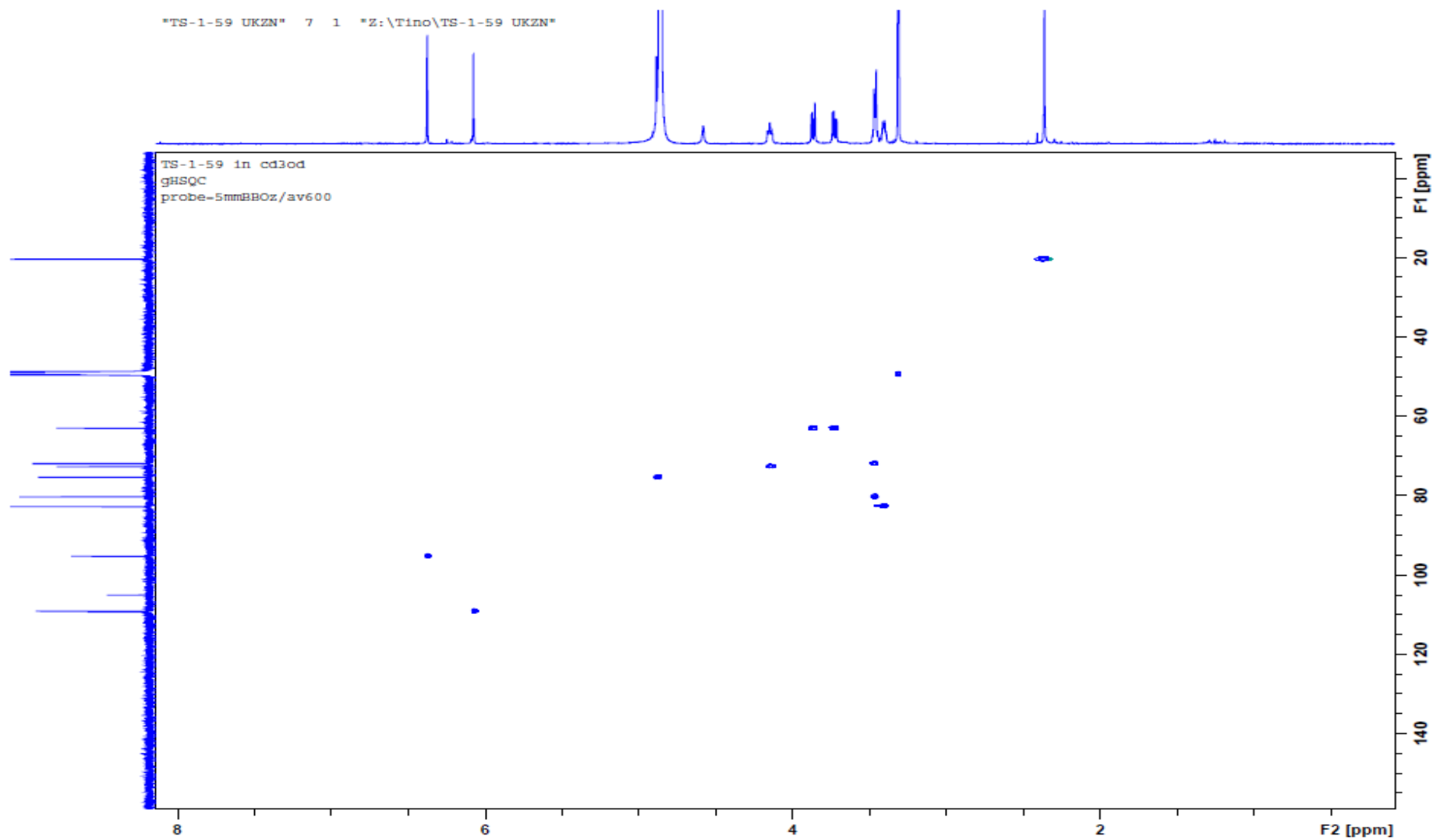
Supplementary Data 56. ^1H NMR of compound 1 (biflorin) in $\text{MeOD-}d_4$



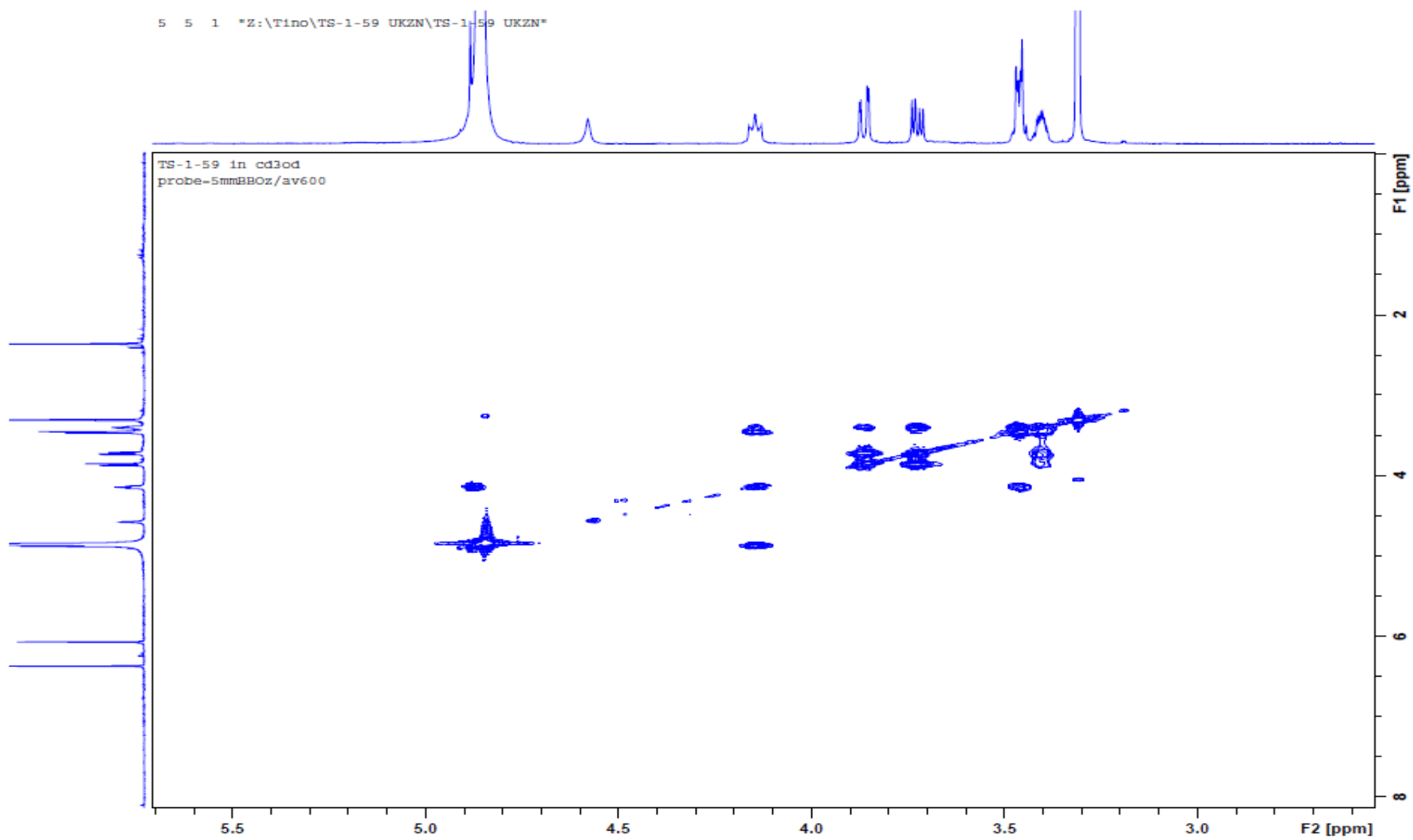
Supplementary Data 57. ¹³C NMR of compound 1 (biflorin) in MeOD-*d*₄



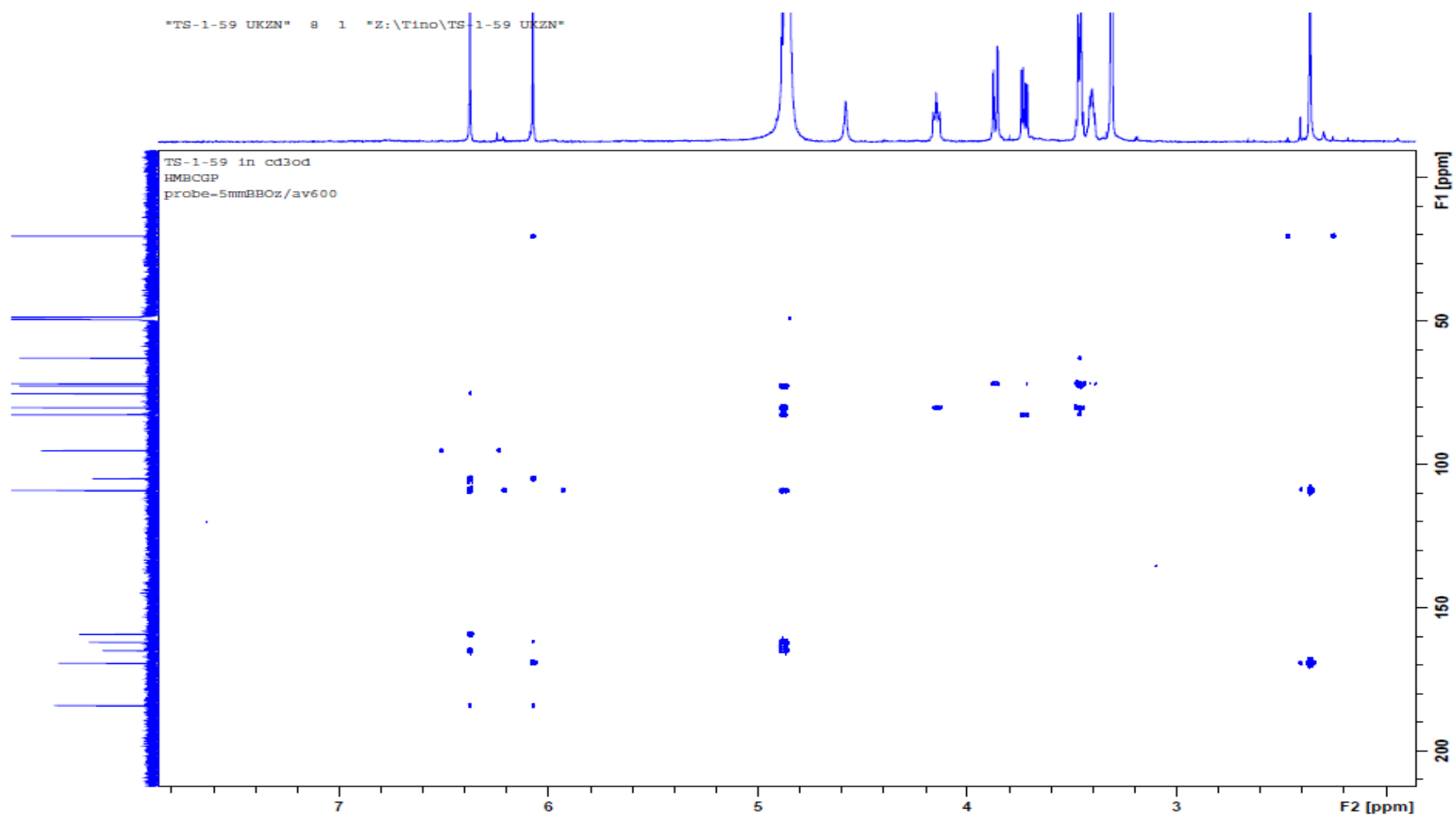
Supplementary Data 58. DEPT 135 for compound 1 (biflorin) in MeOD-*d*4



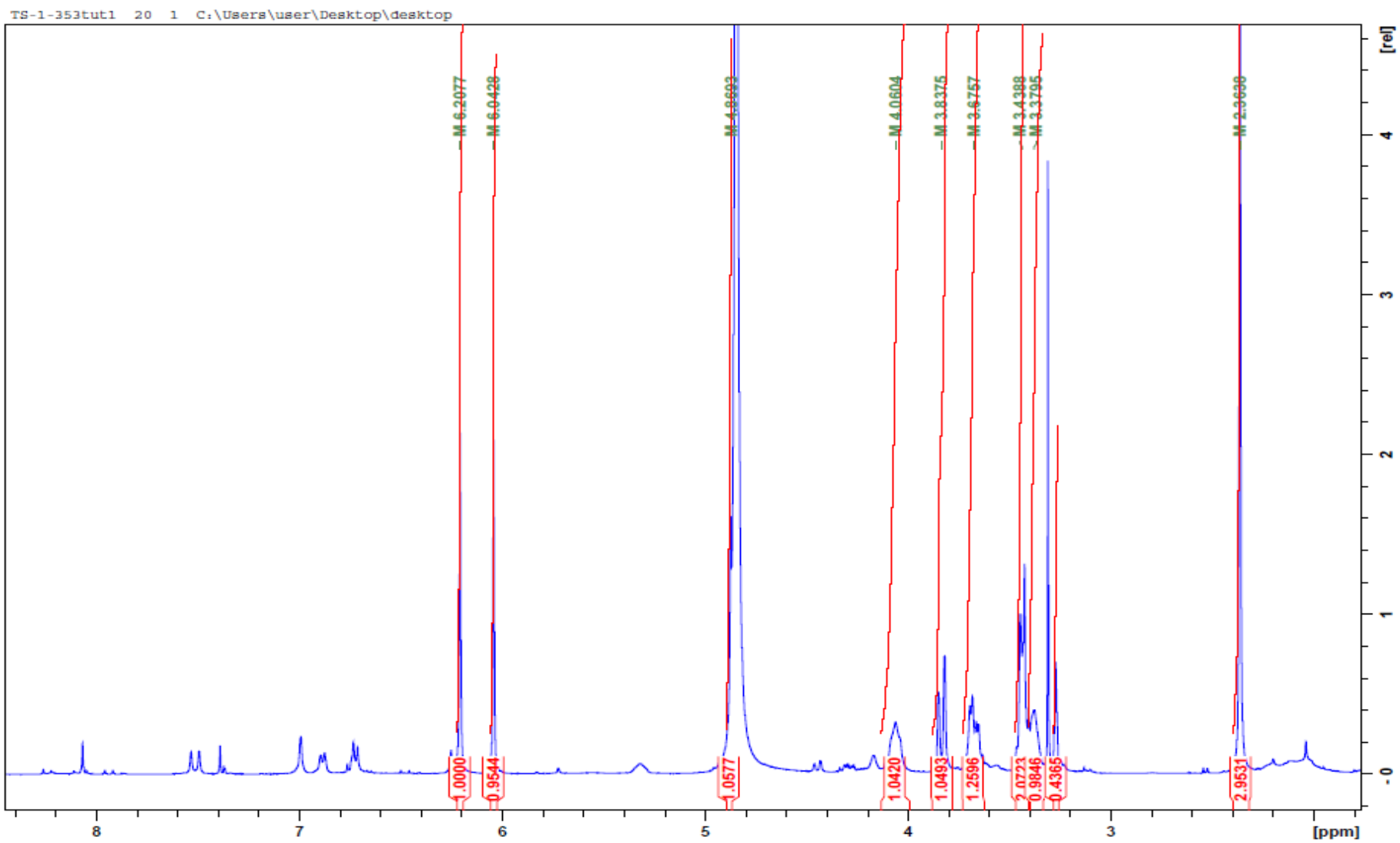
Supplementary Data 59. HSQC spectrum for compound 1 (biflorin) in MeOD-*d*4



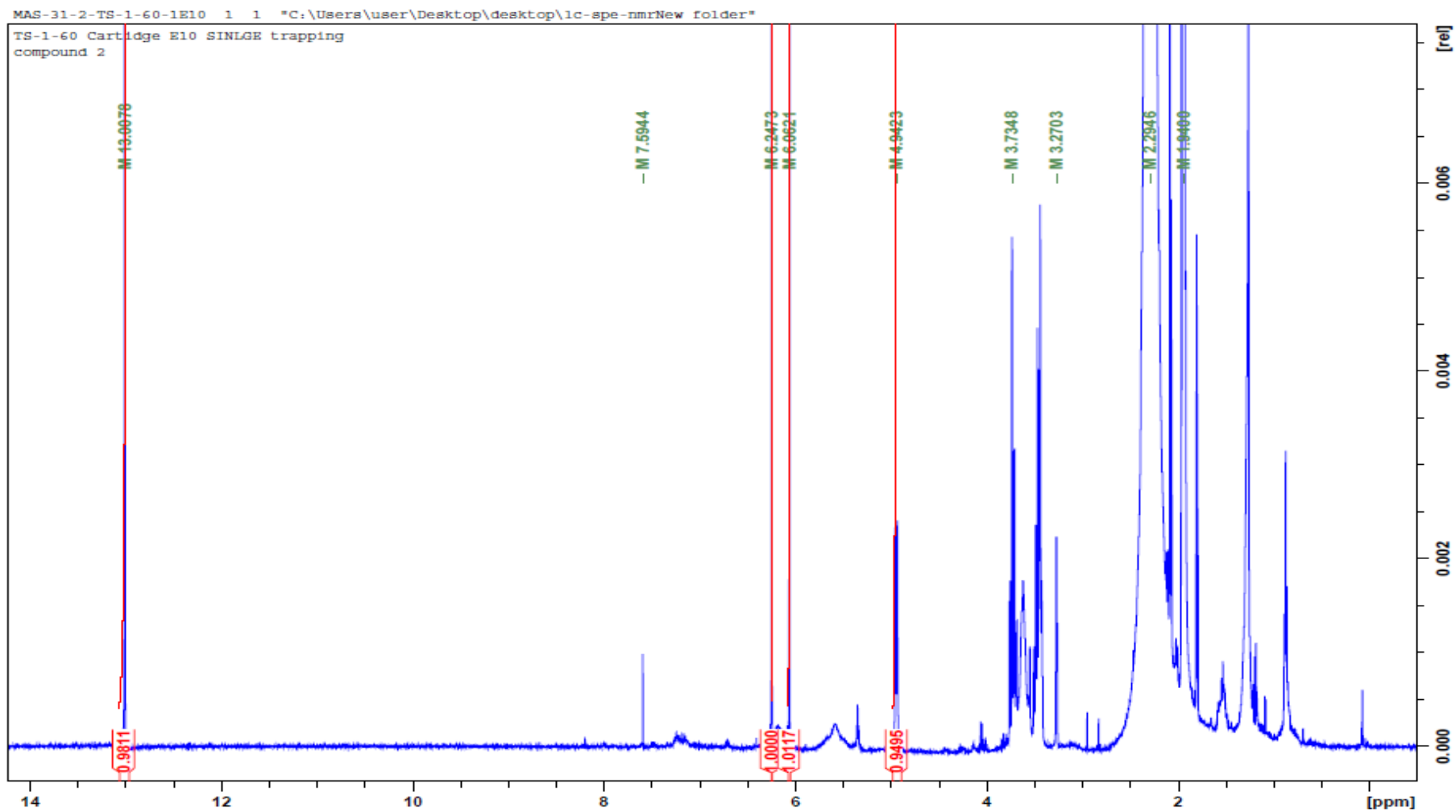
Supplementary Data 60. COSY spectrum for compound 1 (biflorin) in MeOD-*d*₄



Supplementary Data 61. HMBC spectrum of compound 1 (biflorin) in MeOD-*d*4

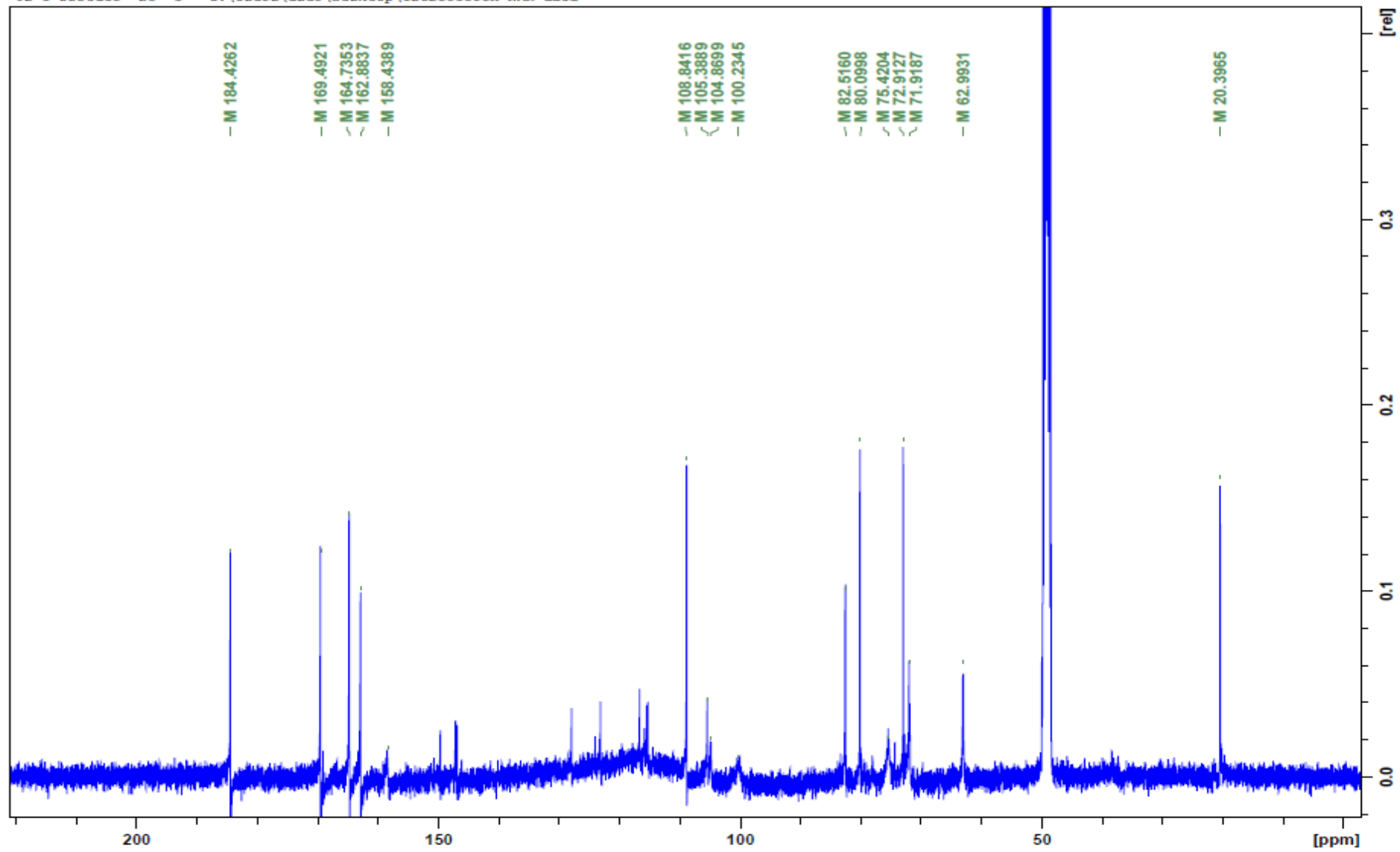


Supplementary Data 62. ^1H spectrum for compound 2 (isobiflorin) in $\text{MeOD-}d_4$



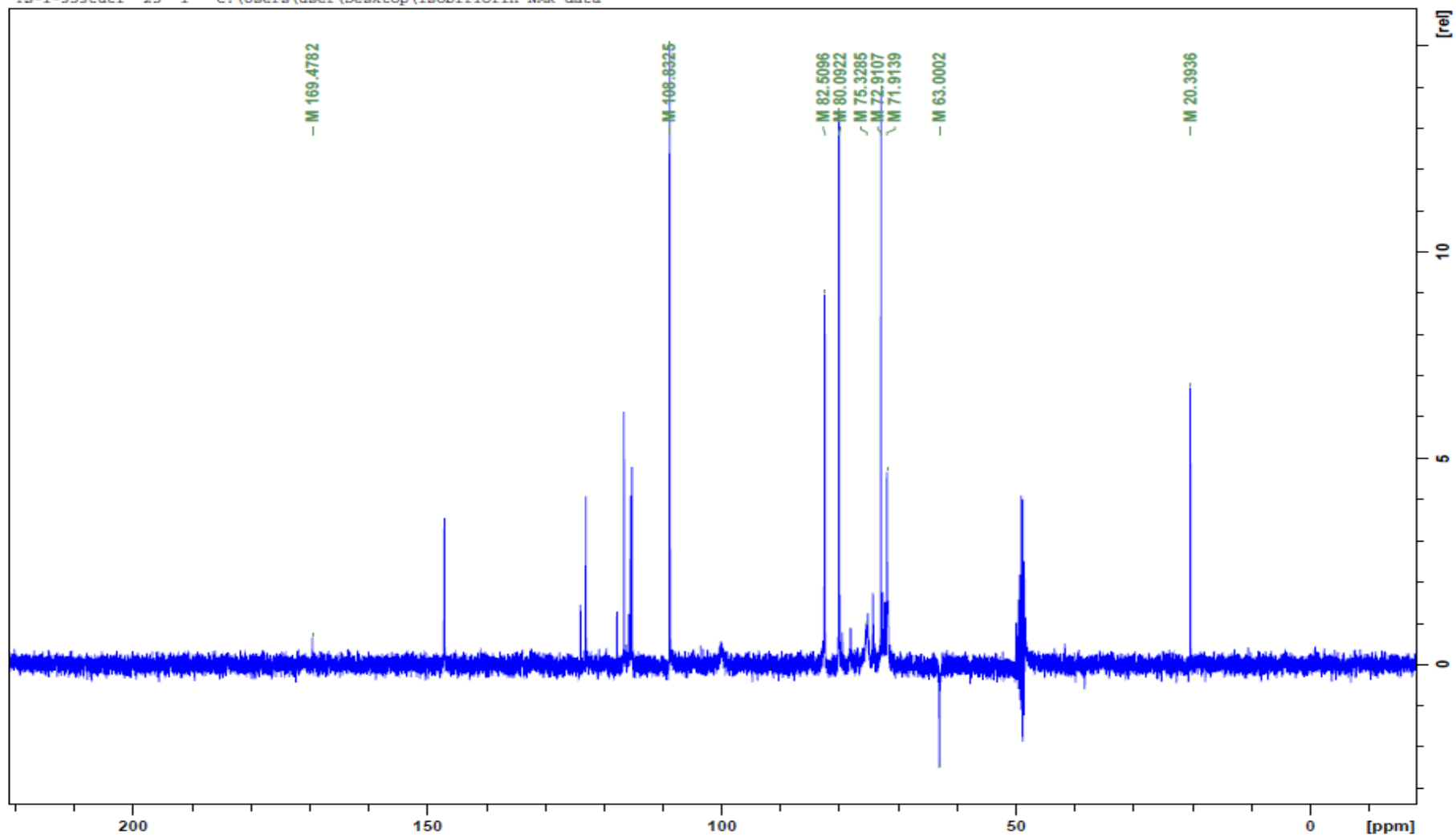
Supplementary Data 63. ^1H spectrum for compound 2 (isobiflorin) in $\text{CD}_3\text{CN-}d_3$

TS-1-353tut1 21 1 "C:\Users\user\Desktop\isobiflorin NMR data"

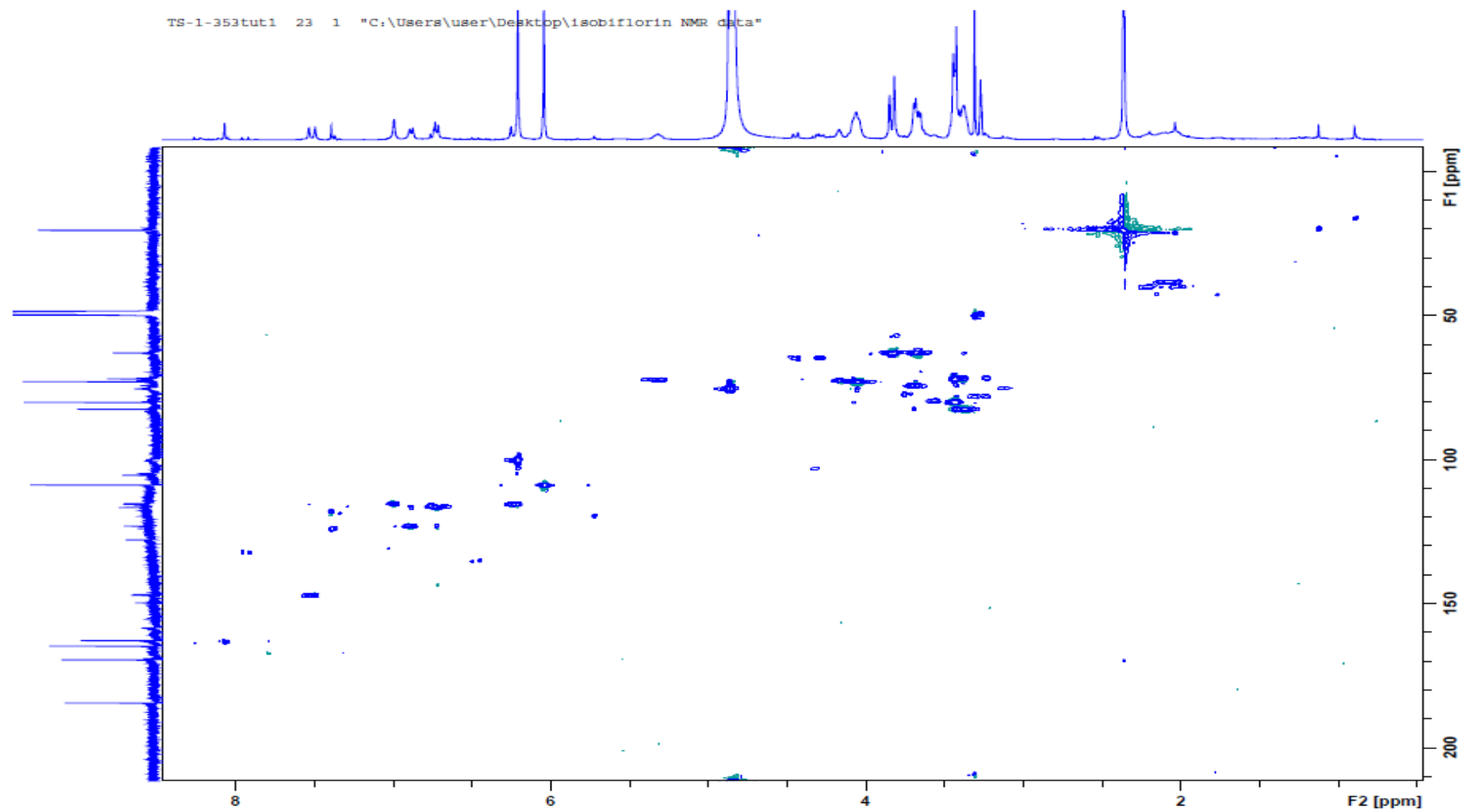


Supplementary Data 64. ¹³C spectrum for compound 2 (isobiflorin) in MeOD-*d*₄

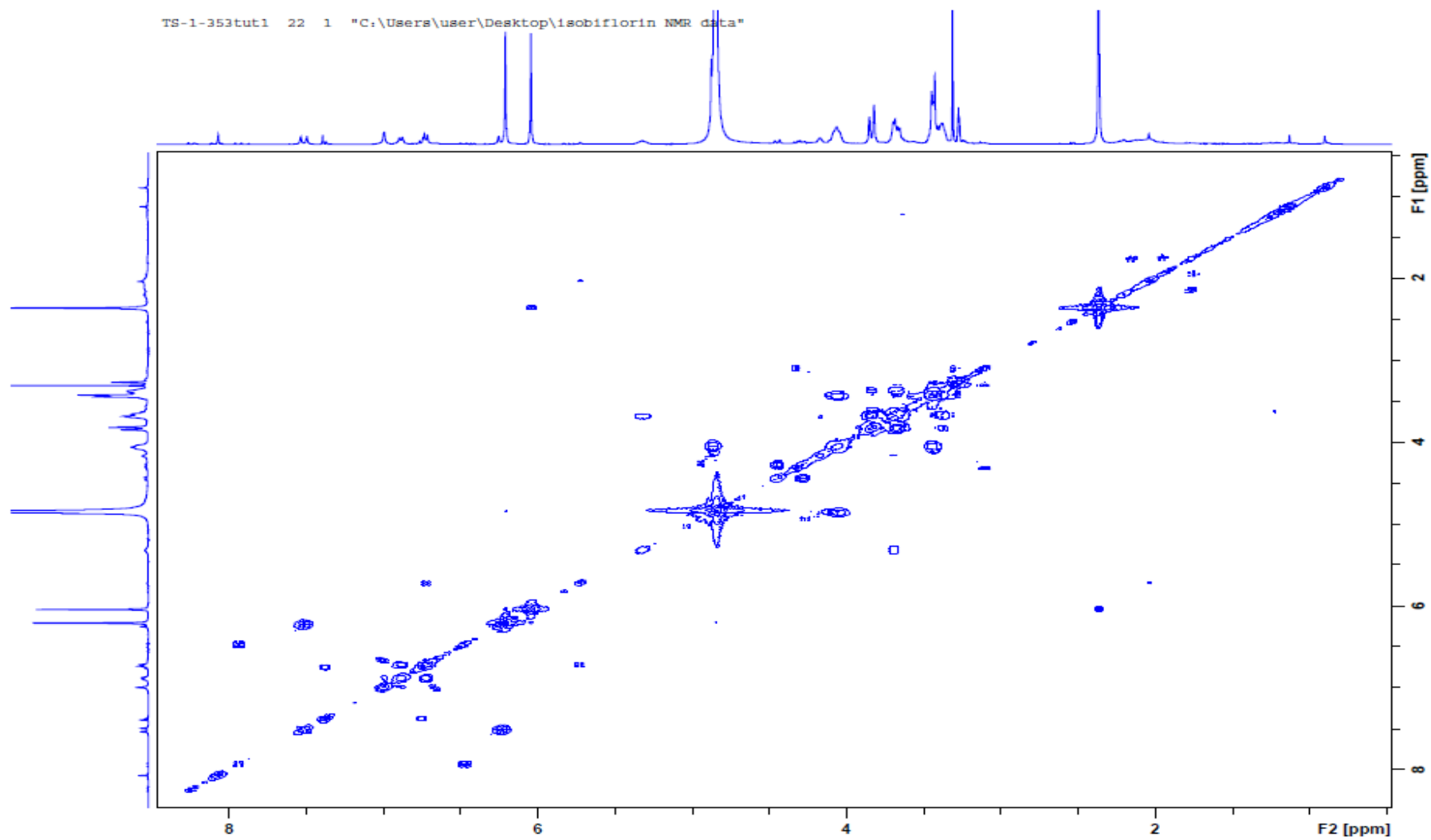
TS-1-353tut1 25 1 "C:\Users\user\Desktop\isobiflorin NMR data"



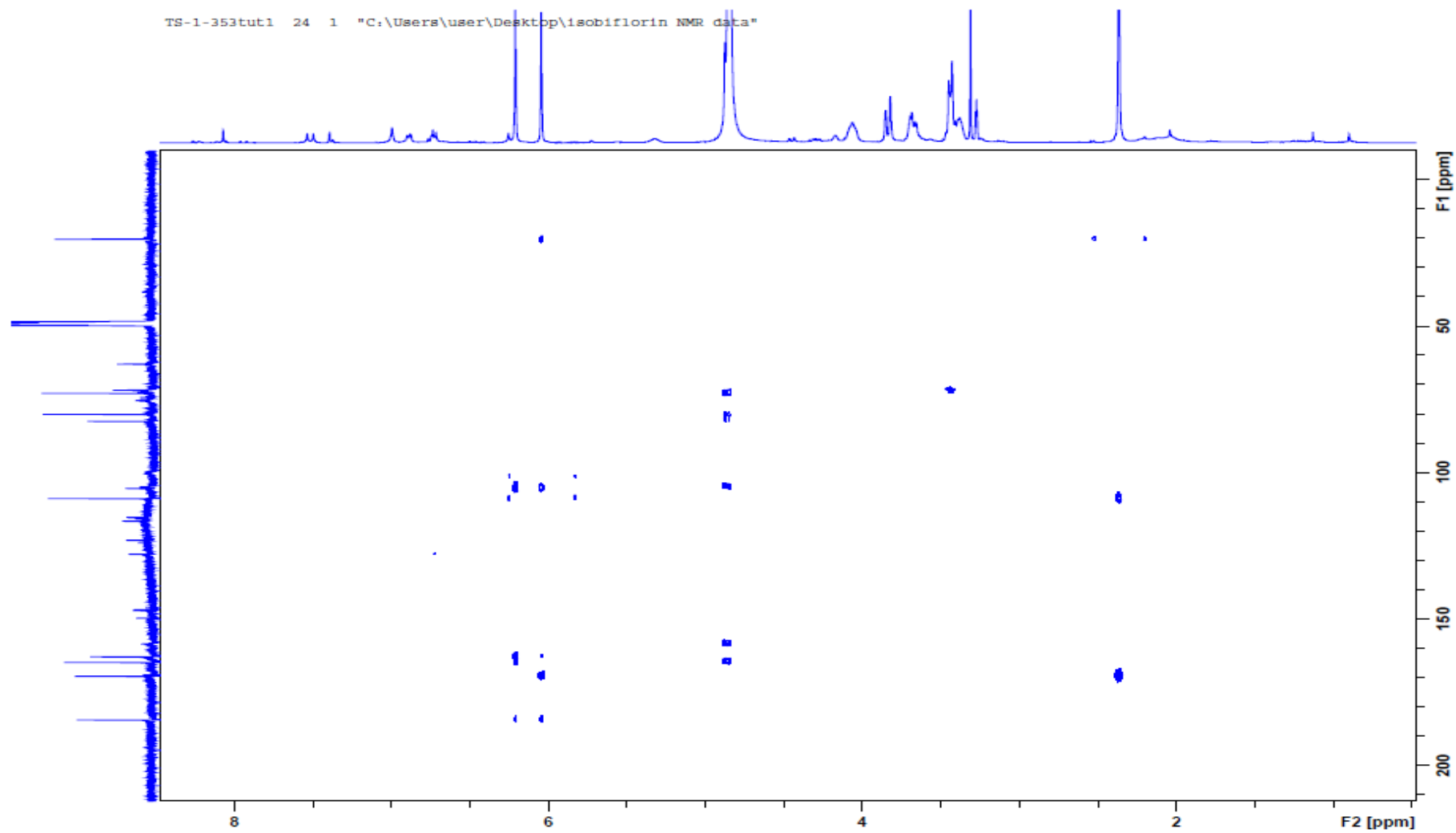
Supplementary Data 65. DEPT 135 spectrum for compound 2 (isobiflorin) in MeOD- *d*4.



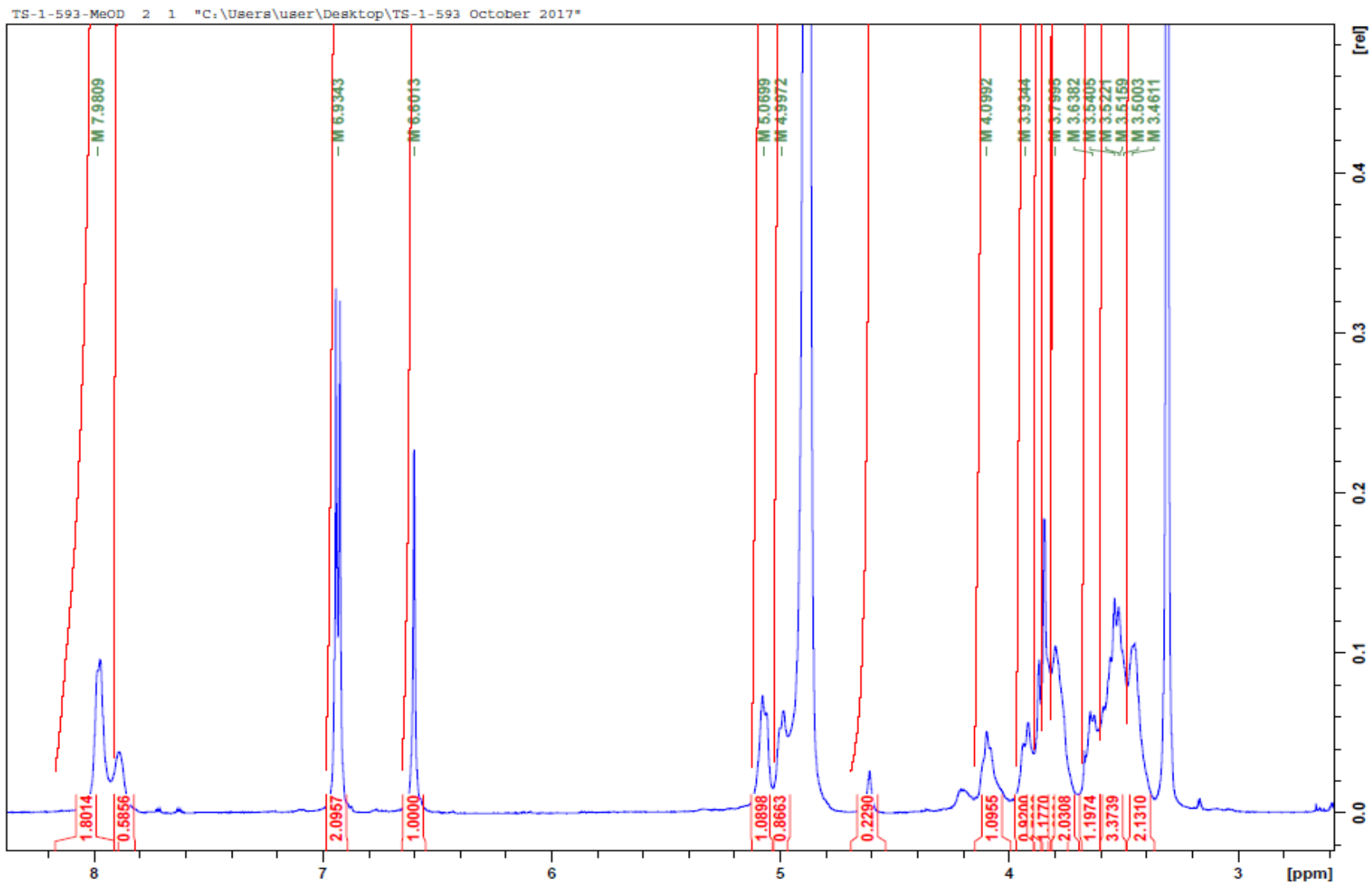
Supplementary Data 66. HSQC spectrum for compound 2 (isobiflorin) in MeOD-*d*₄.



Supplementary Data 67. COSY spectrum for compound 2 (isobiflorin) in MeOD-*d*₄.

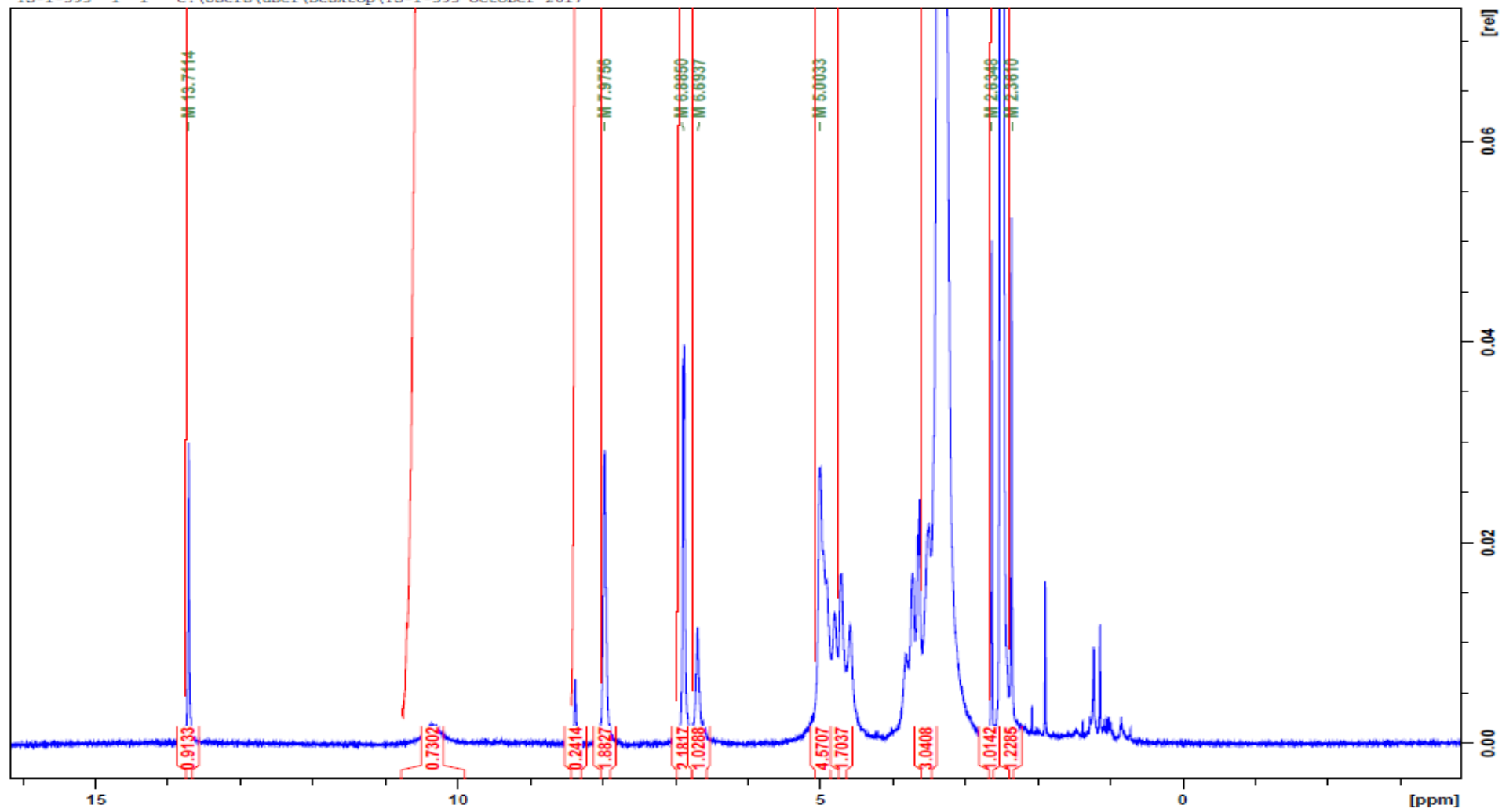


Supplementary Data 68. HMBC spectrum for compound 2 (isobiflorin) in MeOD-*d*₄.

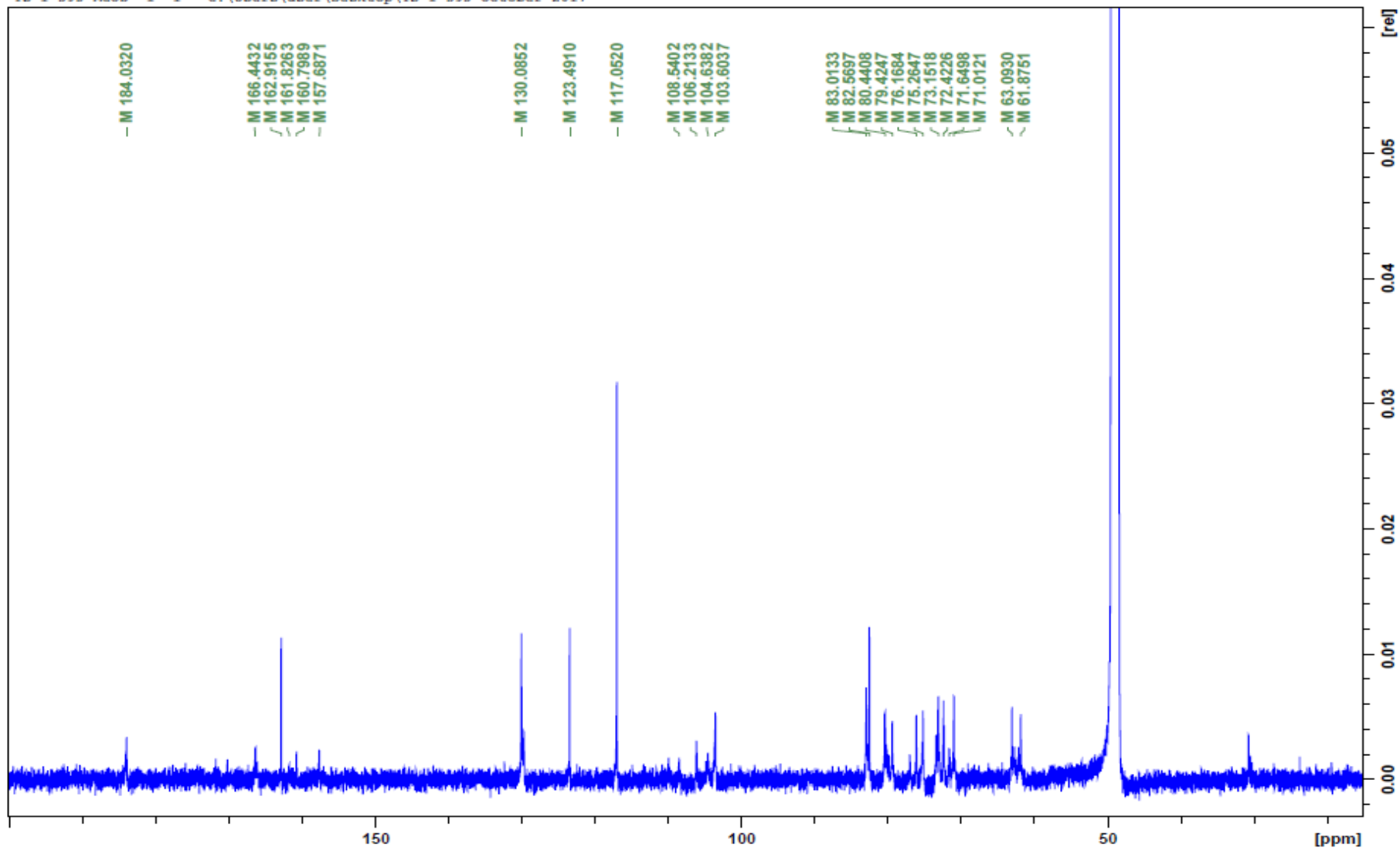


Supplementary Data 69. ^1H NMR spectrum for compound 3 (vicenin 2) in MeOD- d_6 .

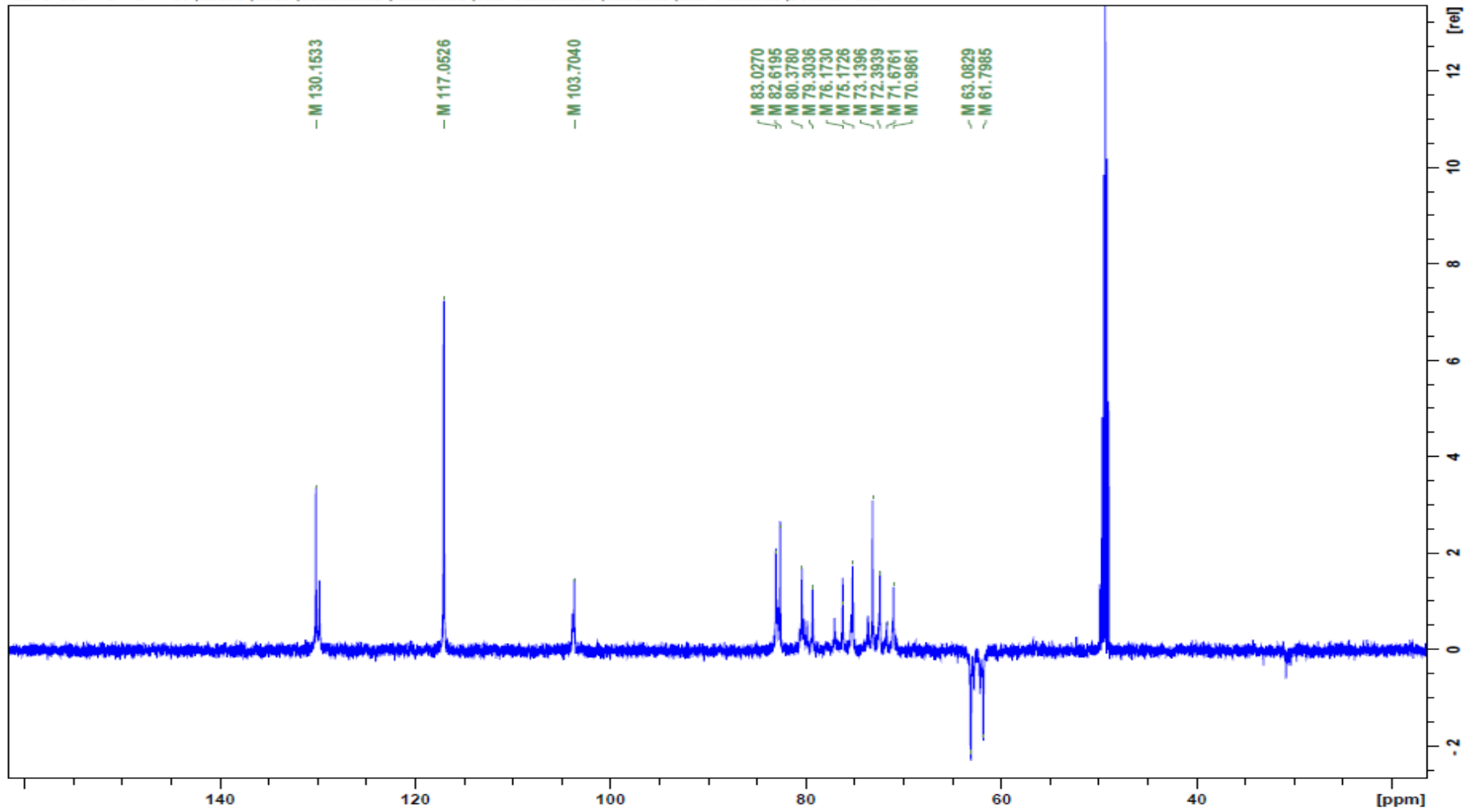
TS-1-593 1 1 "C:\Users\user\Desktop\TS-1-593 October 2017"



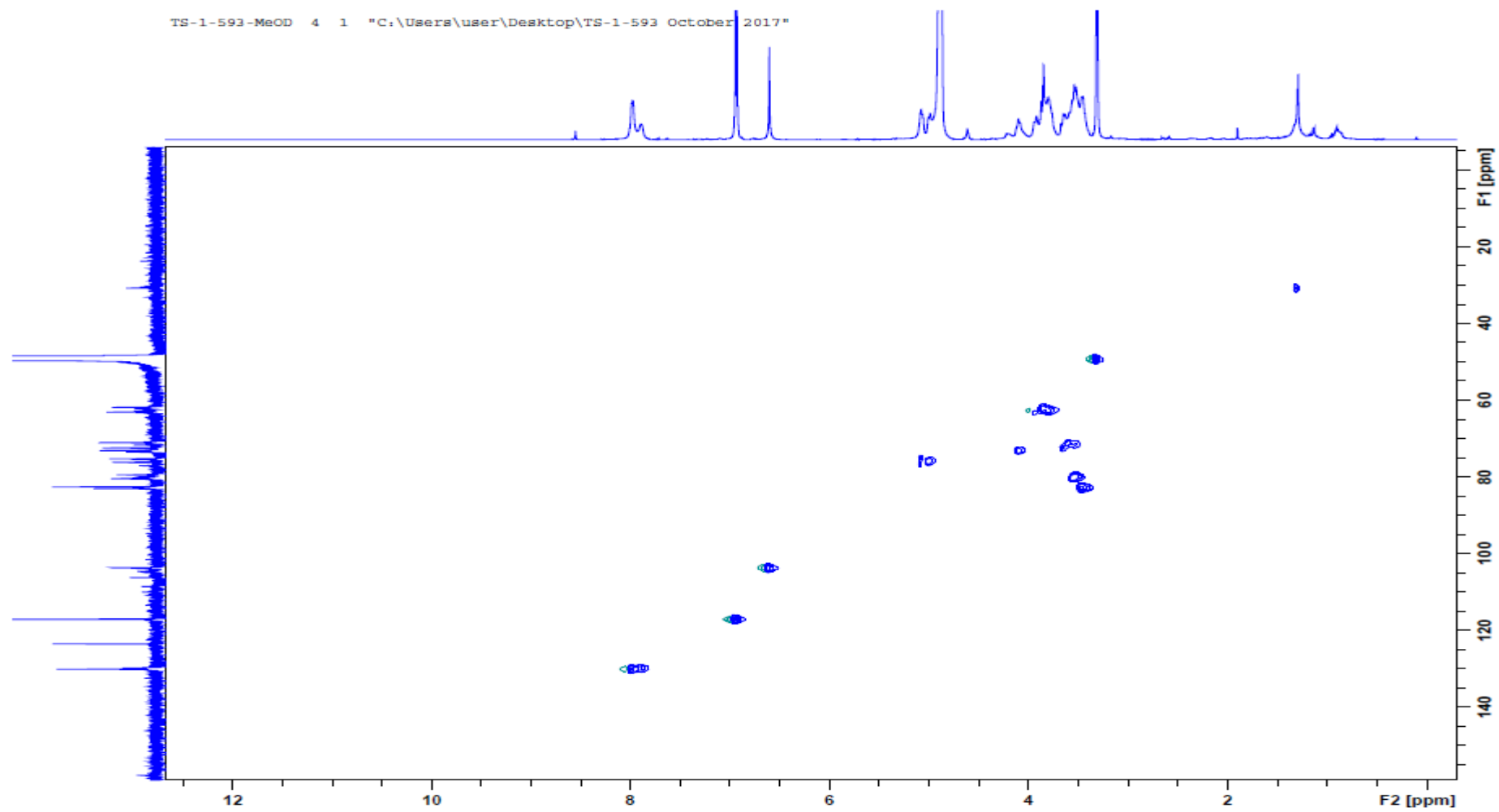
Supplementary Data 70. ¹H NMR of compound 2 (vicenin 2) in DMSO-d₆.



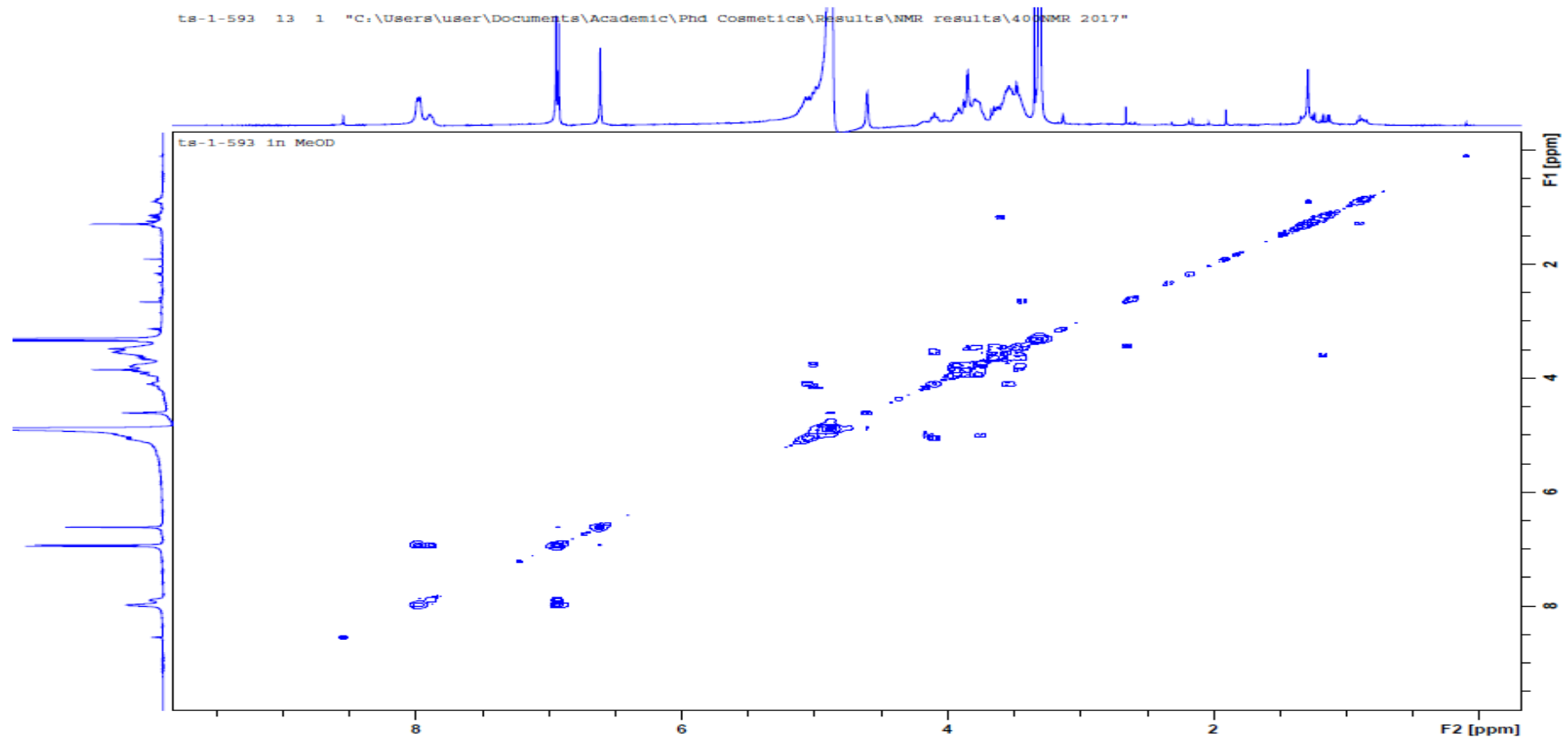
Supplementary Data 71. ¹³C NMR of compound 3 (vicenin 2) in MeOD *d*₄.



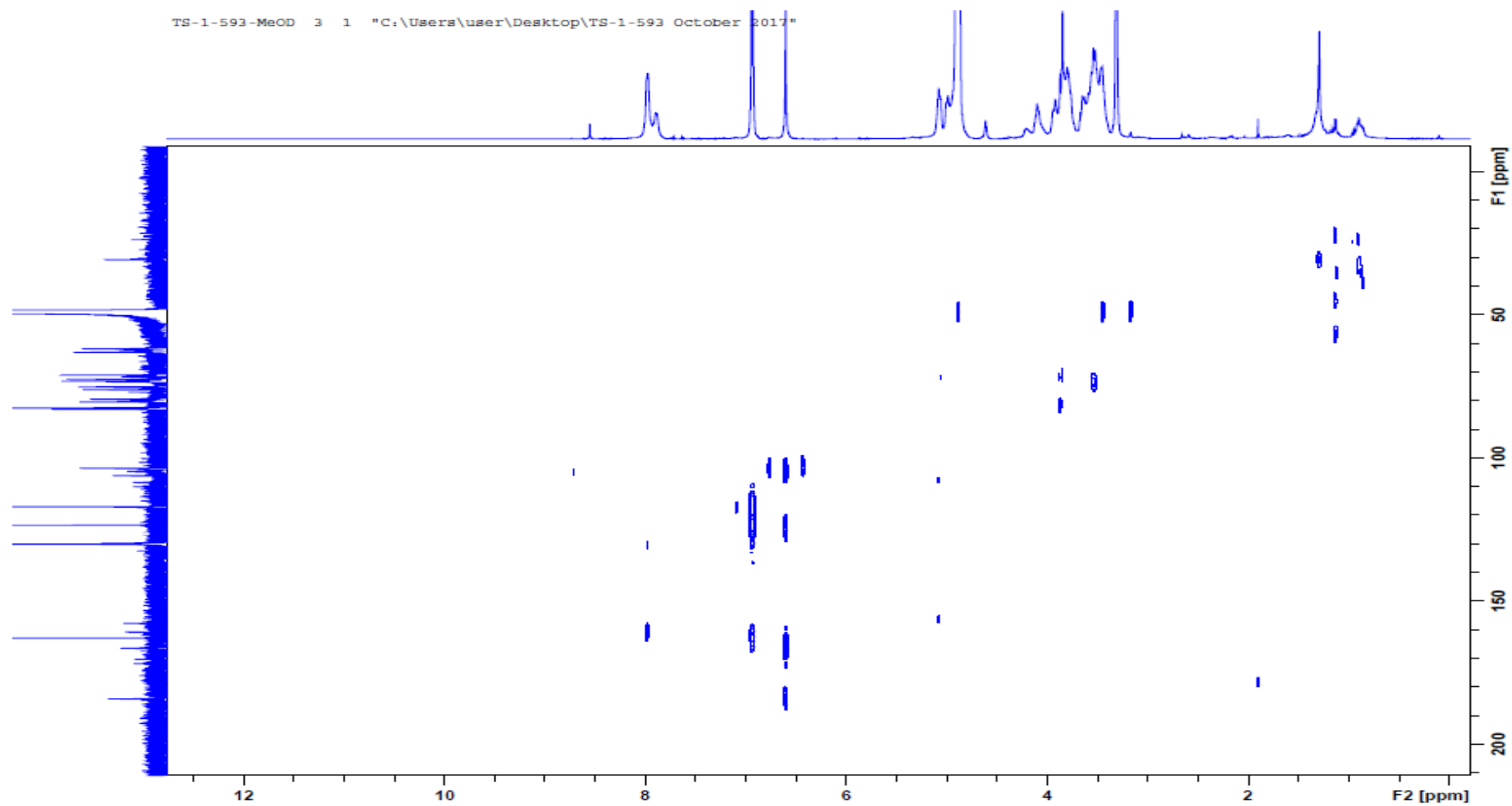
Supplementary Data 72. DEPT 135 spectrum for compound 3 (vicenin-2) in MeOD-d4.



Supplementary Data 73. HSQC spectrum of compound 3 (vicenin- 2) in MeOD *d*4.



Supplementary Data 74. COSY spectrum of compound 3 (vicenin-2) in MeOD *d*₄.



Supplementary Data 75. HMBC spectrum for compound 3 (vicenin 2) in MeOD *d*₄.